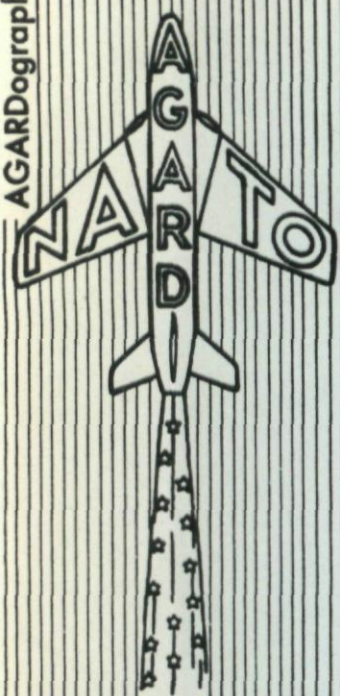


LIBRARY  
ROYAL AIRCRAFT ESTABLISHMENT  
BEDFORD. A



# AGARDograph

## THE USE OF RHEOELECTRICAL ANALOGIES IN AERODYNAMICS

by  
L. C. Malavard

- BELGIEUE
- +
- CANADA
- +
- DANMARK
- +
- DEUTSCHLAND
- +
- ELLÁS
- +
- FRANCE
- +
- ISLAND
- +
- ITALIA
- +
- LUXEMBOURG
- +
- NEDERLAND
- +
- NORGE
- +
- PORTUGAL
- +
- TURKIYE
- +
- UNITED KINGDOM
- +
- UNITED STATES
- +

AUGUST 1956



NORTH ATLANTIC TREATY ORGANIZATION  
ADVISORY GROUP FOR AERONAUTICAL RESEARCH AND DEVELOPMENT  
(ORGANISATION DU TRAITE DE L'ATLANTIQUE NORD)

THE USE OF RHEOELECTRICAL ANALOGIES  
IN AERODYNAMICS

By

L. C. Malavard

Professeur à la Faculté des Sciences de Paris  
(Chaire d'Aviation)

August 1956



This is one of a series of Wind Tunnel AGARDographs  
concerned with wind tunnel design, operation, and test techniques.  
Professor Wilbur C. Nelson of the University of Michigan is the editor.

This AGARDograph was prepared with the  
cooperation of the Air Force Office of Scientific Research  
of the Air Research and Development Command, U. S. Air Force.

## TABLE OF CONTENTS

	Page
SUMMARY	
I. INTRODUCTION	1
II. THE PRINCIPLE OF THE RHEOELECTRIC ANALOGIES	3
(a) Homogeneous Three-Dimensional Conductor	3
(b) Plane Conductors: The Two Types of Analogies	4
(c) Generalities on the Boundary Conditions	5
(d) Remarks on the Nature of the Conducting Medium	6
III. ANALOG REPRESENTATION OF PLANE FLOWS: EXPERIMENTAL METHODS	7
(a) Principle of the Analog Set-up for Plane Flows	7
(b) Plane Electric Tanks	8
(c) Electrical Apparatus	9
(d) Mechanical Apparatus for Recording the Location of Equipotential Points	13
(e) Automatic Tracing of Equipotential Lines	13
(f) Gradient Measurements: Tracing of Curves of Constant Velocity	14
(g) Use of Conducting Paper	17
IV. THE ANALOG STUDY OF WING SECTIONS	18
(a) Analog Representation of Circulation	18
(1) Analogy B	18
(2) Analogy A	20
(b) Study of Airfoil Sections with Analogy B	21
(c) Studies on Combinations of Airfoil Sections: Interaction Problems	22
(d) Examples	22
(1) Airfoils with Flap and Hinged Leading Edge	23
(2) Airfoils with Leading Edge Slots	23
(3) Airfoils with Double Slotted Flap	24
(e) Effects of Sources and Sinks on an Airfoil	24
V. RHEOELECTRIC CONFORMAL TRANSFORMATIONS	26
(a) Principle of the Method	26
(b) Conformal Transformation of an Airfoil onto a Circle	26
(c) Conformal Transformation of any Region onto a Rectangle or Circle	28

	Page
VI. ANALOG STUDY OF AIRFOIL CASCADES	30
(a) Direct Representation of the Flow in a Cascade	30
(b) Analog Set-up Based on the Periodicity of the Field	32
(c) Methods Based on Conformal Mapping	33
VII. ANALOG STUDY OF FLOWS OF REVOLUTION	36
(a) Principle of the Analogy	36
(b) Representation of the Velocity Potential: Inclined Tank	36
(c) Applications of the Inclined Tank	37
(d) Representation of the Stream Function, Tank with Hyperbolic Bottom	38
VIII. ANALOG REPRESENTATION OF THREE-DIMENSIONAL FLOWS	40
IX. ANALOG STUDY OF LIFTING LINE PROBLEMS	42
(a) Principle of Solving Prandtl's Equation by Electrical Analogy	42
(b) Description and Use of the Wing Calculator	45
(c) Examples of Use of the Wing Calculator	48
(d) Study of Various Lifting Systems	50
(e) Problems of Optimum Lifting Systems	53
(f) Determination of Wind Tunnel Wall Corrections	54
X. ANALOG STUDY OF PROPELLER THEORY	57
(a) Principles of the Propeller Calculator	57
(b) Examples	61
XI. ANALOG STUDY OF LIFTING SURFACE PROBLEMS	62
(a) Study of Two-Dimensional Problems	62
(b) Principles of the Rheoelectric Analogy for Lifting Surfaces	67
(1) Statement of the Problem	67
(2) Principles of the Analogy for the Velocity Potential $\varphi(x,y,z)$	69
(3) Description and Operation of an Analog Installation	69
(4) Examples	72
(5) Analog Study of Plane Wings	74
(6) Principles of the Acceleration Potential Analogy	75
(c) Analog Study of Thin Wings (Symmetric Problem)	77
XII. ANALOG STUDY OF COMPRESSIBLE FLOWS	78
(a) Representation of Subsonic Compressible Flow Fields	78

	Page
(b) Hodograph Tank	79
(c) Study of Certain Linearized Supersonic Flows	82
(1) Analog Representation of Conical Flows	82
(2) Calculation of the Supersonic Drag of a Thin Body	86
XIII. CONCLUSION	87
REFERENCES	89
CLASSIFICATION OF THE BIBLIOGRAPHY BY SUBJECT MATTER	94
ILLUSTRATIONS	97

## SUMMARY

The rheoelectric analogy method is based on the identity between the equations which govern certain fluid flows and those for the distribution of electric potential in a continuous conducting medium (electric tank, conducting paper, etc.).

After a review of the principle of this method, the study describes the equipment and experimental techniques used in model construction, in the physical realization of the given problem data, in the exploration of the potential fields, and in carrying out the necessary adjustments and measurements.

Next the different aerodynamic applications are examined: representations of plane flows, studies of airfoil sections and turbine blade lattices, practical accomplishment of conformal mappings, and studies of axially symmetric and three-dimensional flows. Detailed descriptions are given of the analog methods and set-ups used for the solution of lifting line, propeller, lifting surface, and compressible flow problems.

## SOMMAIRE

La méthode d'analogie rhéoélectrique est basée sur l'identité des équations qui régissent d'une part certains écoulements fluides et d'autre part, la distribution du potentiel électrique dans un milieu conducteur continu (bassin électrique, papier conducteur graphité, etc.).

Après avoir rappelé le principe de la méthode, on décrit l'équipement et le mode expérimental utilisé pour la construction des modèles, l'établissement des données, l'exploration des champs et les diverses opérations de réglages et de mesures.

On examine ensuite les différents domaines d'applications aérodynamiques: représentation des écoulements plans, étude des profils d'ailes et des grilles, réalisation pratique de transformations conformes, étude des écoulements de révolution et tridimensionnels, et on décrit en détail les méthodes et installations analogiques employées pour la résolution des problèmes de la ligne portante, des hélices, des surfaces portantes, des fluides compressibles.

## I. INTRODUCTION

The electric analogy method, based on experimental analysis of the distribution of electric potential in a continuous electrical conductor (in the electric tank or by other procedures) has now become classic, and its use for solving various aerodynamic problems has become widespread in the course of the last twenty years. Yet, certain of its aspects are still relatively little known and remain, therefore, unexploited. This method presents advantages, however, which are comparable with those of other transposition techniques for which important analog computers have been built: electronic differential analyzers, flight simulators, etc.

The earliest applications go back over thirty years. In 1924, Relf (Ref. 1) had already presented the traces of streamlines, obtained in an electric tank, about an airfoil section. In 1927, Hahn (Ref. 2) considered the representation of the flow about turbine blades, and a year later, G. I. Taylor and C. F. Sharman (Ref. 3) published their well-known paper on the analog determination of compressible flows.

In Italy Ferrari (Ref. 6) in 1930 constructed a deep tank for wing studies; while in France, as early as 1931, J. Peres set up the first of several laboratories specializing in the systematic exploitation of this method. This exploitation was directed toward problems not only in fluid mechanics and aerodynamics but also toward various problems in mathematical physics. At the International Congress of Mechanics in 1938, Peres gave a brief review of the work carried out under his direction (Ref. 10). Since that time several analog installations have been made in different countries where they operate in the service of research organizations or aircraft builders.

It is commonly considered that the rheo-electric\* analogy is a convenient procedure for exploring a theoretical field and more particularly for tracing the graphical image of a given flow. Though this is a classic application, both easy to conceive of and interesting in itself, it must not be thought that this is the only type of result which can be hoped for from this method. In this regard, it is perhaps useful to emphasize certain other aspects, consideration of which may considerably broaden the field of application of the technique. To view the various possibilities as a group it is often necessary to consider the electric tank as one of the special elements of an analog machine, the other parts of which are electrical devices which fulfill some of the conditions necessary to the solution of the problem. This viewpoint leads one quite naturally to seek the advantages to be gained from the measurement of electrical quantities found inside the field under study, or on its boundaries, or at points of the other electrical apparatus of the machine.

In numerous electric set-ups exploited in this way, it is not unusual for the graphical trace of the field to be considered of only accessory interest. It will further be seen that in the construction of certain rheoelectric analogy machines (wing and propeller calculators, lifting surface calculators) it has even been found unnecessary to trace out the equipotential lines of the flows involved, except on rare occasions. Also, the role which the rheoelectric method can play as an auxiliary to analytic calculation should be emphasized. In this case, there is

---

\*To avoid confusion with other electrical analog techniques we will adopt in this text the expression "rheoelectric analogy" (analogie rhéoelectrique) which has come into common use in French-speaking countries.

no "image" correspondence between the electric set-up used and the physical form of the phenomenon analyzed. A typical example of this is the carrying out in the electric tank of conformal transformations used to solve certain fluid flow problems the "direct" representations of which are considered either of little value or very difficult.

This AGARDograph has been written with the following double objective:

1. To give the aerodynamicist a fairly wide view of the possibilities offered by the rheoelectric analogy method so that he may be lead to try out new applications in his field.

2. To indicate to those who would like to exploit this method with their own equipment, the principal facts concerning the experimental technique (model construction, methods of adjustment and measurement, how to conduct experiments, reduction of test results) as well as how to approach certain problems through appropriate transformations of their original theoretical form, the aim being to obtain simpler and more practical analog set-ups.

Section II of the text reviews briefly the principle of the rheoelectric analogy. The two ensuing sections deal with representations of plane flows and with applications to airfoil section problems. Section V discusses methods for carrying out rheoelectric conformal mappings. In Section VI, various applications to cascades of airfoils are examined. Sections VII and VIII treat the analog representation of three-dimensional flows, either flows of revolution or otherwise. Sections IX, X, and XI treat the experimental set-ups used in those analog machines dealing with the vortex theories of the lifting line, the propeller, and the lifting surface. Finally, the last chapter groups together those applications which are of interest in compressible flow studies.

In order not to overburden the text, the experimental techniques and descriptions of installations are given in connection with each individual application; only the essentials are presented, the reader being referred to specific publications for details. Practical examples are cited in many cases in order to emphasize the interest of the analog work described and to suggest further possibilities.

The rheoelectric analog method can render useful service when it is used in conjunction with the wind tunnel. Although many of the problems treated deal only with perfect fluid flows, the comparison of the results obtained in the electric tank with those measured in flight and in the wind tunnel is often very instructive for the experienced aerodynamics engineer who is able to interpret these data appropriately.

Theoretical formulations are often neglected due to lack of a convenient means for obtaining numerical solutions. The electric tank constitutes one of these means; its advantage lies in the simplicity of the models used, the ease and rapidity with which the forms, models, or data of the problem can be changed, and the modest cost of the experimental work compared to that of wind tunnel tests.

The electric analogy method can serve as a guide and a method of first approximation. It often enables the engineer to predict from its results, at what stage the physical phenomenon may be likely to cease to be comparable with the theoretical flow, or, on other occasions, it may yield the explanation of certain anomalies. Correctly exploited, it may spare numerous wind tunnel tests.

This method can also aid the theoretician by furnishing a concrete backing for his theoretical analysis. Finally, its use in engineering offices may be extremely useful, either at the preliminary design stage of an

airplane to help determine performance for various configurations, or at the time when, for detailed stress analysis purposes, the calculations of aerodynamic loads, which must be defined as well as possible, are undertaken.

## II. THE PRINCIPLE OF THE RHEOELECTRIC ANALOGIES

The principle of the rheoelectric analogies is based on the identity between the equations which govern, on the one hand, the distribution of electrical potential in a conductor in which current is flowing, and, on the other hand, fluid flows. Before giving the details of the different aspects of this correspondence, it will not be out of place to recall the laws of electrical conduction in two- and three-dimensional conductors.

Supposing the steady state to be already established, let us consider the distribution of electric current in a three-dimensional conductor. Let  $V$  be the electrical potential at the point  $M(x,y,z)$  and  $\sigma(x,y,z)$  the conductivity, which may vary from one point to another. The electric current vector is, under these conditions,  $-\sigma \text{grad } V$ , and the element of current intensity,  $di$ , which crosses a surface element,  $dS$ , is given by Ohm's Law:

$$di = -\sigma \frac{dV}{dn} dS \tag{1}$$

where  $n$  is the surface normal to  $dS$ .

By expressing the fact that, in the absence of interior sources within the conductor, this flux is conservative, there is obtained the partial differential equation satisfied by the electric potential,  $\text{div}(\sigma \text{grad } V) = 0$  or, in rectangular coordinates

$$\frac{\partial}{\partial x} (\sigma \frac{\partial V}{\partial x}) + \frac{\partial}{\partial y} (\sigma \frac{\partial V}{\partial y}) + \frac{\partial}{\partial z} (\sigma \frac{\partial V}{\partial z}) = 0. \tag{2}$$

Expressed in its most general form, then, the principle of the rheoelectrical analogy is as follows. Any function,  $\varphi(x,y,z)$ , concerning a fluid flow defined in a certain domain,  $D$ , and satisfying an equation like Eq. (2), may be identified with the electrical potential  $V(x,y,z)$  of a conducting model having the same geometric form as  $D$ . This electrical representation will give an image of the function sought, and the measurement of the electrical potential,  $V$ , wherever necessary will constitute the numerical solution of the given problem, i.e., the solution of the equation governing  $\varphi(x,y,z)$  together with the additional conditions, which are usually the boundary conditions for  $D$  (and which must be properly satisfied at the boundaries of the conducting model).

### (a) Homogeneous Three-Dimensional Conductor

The creation of a three-dimensional conductor, the internal conductivity of which varies from point to point according to a given distribution  $\sigma(x,y,z)$ , is difficult. Therefore, three-dimensional rheoelectric models are practically all made up of homogeneous conductors ( $\sigma = \text{constant}$ ). Eq. (2) then reduces to the Laplacian

$$\frac{\partial^2 V}{\partial x^2} + \frac{\partial^2 V}{\partial y^2} + \frac{\partial^2 V}{\partial z^2} = 0 \tag{3}$$

Any fluid flow problem having a harmonic potential  $\varphi(x,y,z)$ :

$$\frac{\partial^2 \varphi}{\partial x^2} + \frac{\partial^2 \varphi}{\partial y^2} + \frac{\partial^2 \varphi}{\partial z^2} = 0 \tag{3'}$$

may then be treated experimentally by means of a rheoelectric model,  $\varphi$  being identified, up to a constant factor, with the electrical

potential,  $V$ . This will be the case, for example, for the velocity potential of a perfect incompressible fluid.

(b) Plane Conductors: The Two Types of Analogies

In the case of plane models, it is possible to represent variable conductivity by the creation of a model having variable thickness. For example, let us consider a homogeneous conductor having the form of a plate in the  $xy$  plane and having a thickness,  $h(x,y)$ , which varies slowly. In this case the potential,  $V$ , will depend hardly at all on the thickness coordinate,  $z$ , and the current intensity,  $di$ , crossing the surface element,  $dS$ , described by the perpendiculars along the arc,  $ds$ , in the  $x,y$  plane, is

$$di = -\sigma h(x,y) \frac{dV}{dn} ds. \quad (4)$$

Since the conductivity,  $\sigma$ , is constant, the fact that the divergence of  $(h \text{ grad } V)$  is zero leads to the partial differential equation

$$\frac{\partial}{\partial x} (h \frac{\partial V}{\partial x}) + \frac{\partial}{\partial y} (h \frac{\partial V}{\partial y}) = 0 \quad (5)$$

which is the analog of Eq. (2). In this result only two variables,  $x, y$ , remain, and  $h(x,y)$  takes on the role formerly played by  $\sigma$ .

There exists, moreover, a current function,  $W$ , associated with  $V$ , for which the element  $dW$  represents the current intensity,  $di$ , across  $dS$ , and which, consequently, can be defined by

$$dW = -\sigma h \left( \frac{\partial V}{\partial x} \alpha + \frac{\partial V}{\partial y} \beta \right) ds \quad (6)$$

where  $\alpha$  and  $\beta$  are the direction cosines of the normal  $n$  (which makes an angle of  $\pi/2$  with the positive tangent to  $ds$  in the direction shown in Fig. II-1). Here,  $\alpha = -dy/ds$  and  $\beta = dx/ds$  so that Eq. (6) becomes

$$dW = -\sigma h \left( \frac{\partial V}{\partial y} dx - \frac{\partial V}{\partial x} dy \right). \quad (7)$$

The current function,  $W$ , then satisfies the equation

$$\frac{\partial}{\partial x} \left( \frac{1}{h} \frac{\partial W}{\partial x} \right) + \frac{\partial}{\partial y} \left( \frac{1}{h} \frac{\partial W}{\partial y} \right) = 0 \quad (8)$$

which has the same form as Eq. (5).

The two associated functions  $V$  and  $W$  are linked by the relations

$$\begin{aligned} \frac{\partial V}{\partial x} &= \frac{1}{\sigma h} \frac{\partial W}{\partial y} \\ \frac{\partial V}{\partial y} &= -\frac{1}{\sigma h} \frac{\partial W}{\partial x} \end{aligned} \quad (9)$$

through use of which Eq. (5) or Eq. (8) may be derived, by elimination of  $W$  or of  $V$ .

In aerodynamics, numerous two-dimensional problems make use of associated functions  $\varphi$  and  $\psi$  (this is the case, for example, for the velocity potential,  $\varphi(x,y)$ , and the stream function,  $\psi(x,y)$ , of a plane compressible or incompressible flow). In general, a plane rheoelectric model of variable thickness,  $h(x,y)$ , can be used for any problem requiring determination of a function,  $\varphi$ , which is the solution of

$$\frac{\partial}{\partial x} \left( \lambda \frac{\partial \varphi}{\partial x} \right) + \frac{\partial}{\partial y} \left( \lambda \frac{\partial \varphi}{\partial y} \right) = 0 \quad (5')$$

where  $\lambda(x,y)$  is a given function having always the same sign which may be taken positive.

The analog representation may be made in two ways according to whether  $\varphi$  be identified (up to a factor) with the potential,  $V$ , or with the current function,  $W$ . To every solution,  $\varphi$ , of Eq. (5') there corresponds the associated function,  $\psi$ , defined by the relations

$$\begin{aligned} \frac{\partial \varphi}{\partial x} &= \frac{1}{\lambda} \frac{\partial \psi}{\partial y} \\ \frac{\partial \varphi}{\partial y} &= -\frac{1}{\lambda} \frac{\partial \psi}{\partial x} \end{aligned} \tag{9'}$$

which satisfies the partial differential equation

$$\frac{\partial}{\partial x} \left( \frac{1}{\lambda} \frac{\partial \psi}{\partial x} \right) + \frac{\partial}{\partial y} \left( \frac{1}{\lambda} \frac{\partial \psi}{\partial y} \right) = 0. \tag{8'}$$

The identification may be made as follows:

Analogy A

$$\varphi = mV \quad \psi = nW \quad h = \frac{m\lambda}{n\sigma} \tag{10}$$

Analogy B

$$\varphi = m'W \quad \psi = -n'V \quad h = \frac{n'}{m'\lambda\sigma} \tag{11}$$

$m, n, m', n'$  being constants.

It is clear that, according to the analogy chosen, the thickness of the conductor should be either proportional or inversely proportional to  $\lambda$ . In the most common applications, where  $\varphi$  and  $\psi$  represent, respectively, the velocity potential and stream function of a plane flow, the function  $\lambda(x,y)$  corresponds to the fluid density  $\rho(x,y)$ . If the fluid is incompressible, the model thickness should

be constant. In the case of compressible flow, as G. I. Taylor (Ref. 3) has shown, the thickness,  $h(x,y)$ , of the conductor must either be proportional or inversely proportional at each point to  $\rho(x,y)$ , according to whether  $\varphi$  or  $\psi$  is to be determined.

The fact that there exist two analogies, A and B, in the plane case, merits additional comment. From the experimental standpoint, the simpler operation is the measurement of the electrical potential,  $V(x,y)$ . Plotting the electrical equipotentials readily gives, in the analogy A, the potential lines  $\varphi = \text{constant}$ ; in a model for analogy B, the streamlines  $\psi = \text{constant}$  are obtained.

The use of two models thus gives a very complete picture of the field (orthogonal network of lines  $\varphi$  and  $\psi$  constant). It should be remarked, however, that it is rarely necessary to use both models; usually a single model suffices, type A or B being used according to the problem. The thickness,  $h(x,y)$ , must vary slowly enough that the model give correct results; this is one factor, as will be seen later in particular applications, which can determine the choice of A or B. Other considerations also can affect this choice; for example, when one of the functions  $\varphi$  or  $\psi$  is not single-valued in its domain of definition, the analogies in which it is identified with the electric potential,  $V$ , are not so desirable because they introduce special difficulties (cuts must be provided in the conductor in order to make the potential,  $V$ , single-valued).

### (c) Generalities on the Boundary Conditions

From what has been discussed above, it is evident that experimentation by rheoelectric analogy may be applied to any phenomenon of fluid flow depending on an equation of type (3') in three dimensions or type (5') in two dimensions. However, the partial differential

equation, (3') or (5'), is not sufficient in itself to determine the function  $\varphi$ . Supplementary conditions must be included, and these vary with the problem under consideration; they usually have to do with the values of  $\varphi$  or of its derivatives on the boundary of the region. The rheoelectric model must of course assure the corresponding conditions for  $V$ .

The usual boundary conditions are the following:

- (1) Dirichlet condition: the function,  $\varphi$ , is given on the boundary.
- (2) Neumann condition: the normal derivative,  $d\varphi/dn$ , is given.
- (3) Fourier (mixed) condition: a relation of the form

$$\varphi - a \frac{d\varphi}{dn} = b \tag{12}$$

is given;  $a$  and  $b$  may be given functions of the point under consideration on the boundary,  $a$  being positive when the boundary normal is directed toward the interior of the region.

The Dirichlet and Neumann conditions are particularly simple to reproduce in the electrical model when they happen to reduce to the forms  $\varphi = \text{constant}$  and  $d\varphi/dn = 0$  on a portion of the boundary. In the former case the whole boundary is covered with an electrode which is raised to the potential  $V = \text{constant}$ ; in the latter case the boundary is insulating (no electric current crosses the boundary and hence, according to Eq. (1), it is clear that  $dV/dn = 0$ ).

In the general case where  $\varphi$  or  $d\varphi/dn$  is given at each point of the boundary but variable from point to point, the analog representation of these boundary conditions is somewhat more complicated. The boundary of the model may be covered by a large number of small electrodes which are insulated from each other. Each one of these

electrodes then represents an element of the contour of area  $S$  (necessarily finite). In the case of Dirichlet conditions, each electrode is raised to a potential having the same value as that which  $\varphi$  must have at the midpoint of this electrode; the given distribution of boundary potentials, which is generally continuous, is thus replaced by an approximate stepwise distribution, each step corresponding to an electrode.

The same set-up may be used for Neumann conditions. The normal derivative of  $\varphi$  at a point on the contour corresponds, in the electrical model, to the current flux density at this point, as is indicated by Eq. (1); therefore each electrode must allow a known current,  $i$ , to pass, equal to

$$i = -\sigma S \left( \frac{dV}{dn} \right)_{av} \tag{13}$$

where  $(dV/dn)_{av}$  is the average value of the normal derivative over the surface,  $S$ , of the electrode (as a general rule, the value of  $dV/dn$  used is that calculated at the midpoint of the electrode).

In the applications to be considered later, numerous examples of such representations will be given; in each case all technical construction details of the small electrodes, as well as for the electrical set-ups used to establish the potentials and the current flux intensities, will be given. It will also be seen how these set-ups can be used to satisfy Fourier conditions as well without special difficulty.

(d) Remarks on the Nature of the Conducting Medium

It should be stated that in most of these analog set-ups, the conducting medium is a liquid. It is usually a weak electrolyte contained in a tank the form of which defines

the field in which the function is to be represented. For this reason the rheoelectric analogy method is often called the "electric tank" or "electrolytic basin" technique. However, other than liquid conductors are occasionally used; for example, metallic plates having high resistivity or semiconducting solids obtained by mixing powders with greater or less conductivity or insulating quality (graphite and cement, for example, or graphite and bakelite, or again, damp plaster) (Ref. 18). For rapid set-ups concerning plane regions, a new procedure can be employed based on the use of special conducting paper, as will be discussed later.

Although different conducting materials have been discussed, the corresponding analog set-ups are based on the same principle, the distribution of electrical current in a continuous medium. In what follows, the now habitual term "rheoelectric analogy" will be retained so as to avoid possible confusion with other electrical analogy methods (resistance networks, for example). It will also be noticed that the greater part of the analog methods which will be described for the electric tank are immediately transposable to the other analogy methods. This will be true in particular for the set-ups used to establish the boundary conditions. Examples of such carryover will be seen in connection with the use of conducting paper.

### III. ANALOG REPRESENTATION OF PLANE FLOWS: EXPERIMENTAL METHODS

#### (a) Principle of the Analog Set-up for Plane Flows

In the case of plane incompressible flows, the velocity potential,  $\varphi(x,y)$ , and the stream function,  $\psi(x,y)$ , are conjugate and satisfy the Laplace equation. Either one of these

functions may be identified with the electrical potential,  $V(x,y)$ , in a conducting model of constant thickness such as a conducting plate or electric tank with a flat, horizontal bottom wherein the liquid is of constant depth,  $h$ .

The essentials of the experimental method may be described in conjunction with a simple application. The example taken will be that of the representation in the electric tank of a uniform flow disturbed by the presence of a body (c). The flow will first be considered in the absence of circulation. Far from the body, the lines  $\varphi$  and  $\psi$  constant are straight lines respectively parallel to the axes  $y$  and  $x$ , if the velocity,  $U$ , is taken as being in the  $x$ -direction.

Let us first consider the case of analogy A (Fig. III-1a). The two sides of the tank which are parallel to the  $y$  axis may be taken as corresponding to two straight potential lines,  $\varphi_0$  and  $\varphi_1$ , provided that each be covered by one of two electrodes  $E_0, E_1$  raised respectively to the potentials  $V_0$  and  $V_1$ . The potential difference  $V_1 - V_0$ , furnished by an electric current generator,  $G$ , will correspond to the difference  $\varphi_1 - \varphi_0$ . The body will be represented near the center of the tank by a cylindrical model, the cross section of which will be geometrically similar to the contour (c). The dimensions of the model should be quite small compared to those of the electric tank so that the disturbance it causes in the uniform fluid will be negligible along the boundaries of the region represented. The contour of (c) is a streamline (where  $d\psi/dn = 0$ ); therefore, in analogy A, the contour should be built of insulating material ( $dV/dn = 0$ ).

A diagram of the electrical set-up is given in Fig. III-1a. The electrodes  $E_0$  and  $E_1$  of the electric tank are connected respectively to the terminals of the generator,

G, in parallel with a potentiometer bridge, P, the readings of which serve to define an arbitrary scale convention for the electrical potential (for example 0 and 100 at the generator terminals  $V_1 - V_0 = 100$ ). Here then,  $m$  is defined by  $m = (\varphi_1 - \varphi_0)/100$ .

The measurement of electrical potential,  $V$ , at a point of the tank is taken by a balance or opposition method. An exploring probe,  $p$ , made of a fine metallic wire pointing down into the liquid, is brought to this point. It is connected through a null indicator,  $0$ , to the movable contact,  $C$  of  $P$ . When, by adjustment of  $C$ , the condition of no-current flow through  $0$  is obtained, the value of the potential sought is read off on the scale of  $P$ . The value of  $\varphi$  is then given by:

$$\varphi = \varphi_0 + \frac{\varphi_1 - \varphi_0}{100} V. \tag{14}$$

By moving  $p$  along in the tank while keeping  $0$  at zero and the movable contact of  $P$  always at the same position, one may define the corresponding equipotential line point by point in the tank. Of course some means must be provided for carrying over the positions of  $p$  thus determined onto a permanent record.

Analogy B is carried out in much the same way. In this case the feed electrodes  $E_0^I$  and  $E_1^I$  are placed along the tank sides parallel to the  $x$ -axis (Fig. III-1b). The body,  $c$ , forming a streamline, must be represented in this analogy by an electrical equipotential line. The model,  $c$ , will therefore be made of a perfectly conducting material like that used in making up the electrodes  $E_0^I$  and  $E_1^I$ . The electrical set-up is identical to that used in analogy A. Reading off the equipotential lines in this case gives the streamlines around the body.

The use of the two analogies A and B enables one to draw up the entire flow field by means of the orthogonal network of lines  $\varphi$  and  $\psi$  constant. It will be observed that the change from one analog representation to the other is made by interchanging the positions of the insulating and conducting boundaries.

### (b) Plane Electric Tanks

Detailed description of experimental installations has already been given in various papers (see in particular Ref. 18). It will suffice here to give a few general indications concerning the experimental equipment with emphasis on certain recent improvements.

Electric tanks may have quite different forms. Occasionally a tank is built just for a certain model. In this case its walls correspond to the boundaries of the region studied. Most commonly, models are set up in a tank of parallelepiped form, limiting the size of the useful field as may be necessary. Square or rectangular tanks of shallow depth are used for studying plane phenomena; here the liquid depth is not over a few centimeters (between 1 and 10).

The tank dimensions vary with the applications and depend on the scale factor adopted in the given problem; in general, it is better to choose a larger scale. Often, the region represented is theoretically infinite, and in this case the model dimensions are governed by the necessity of reducing the interference due to the presence of the walls; the case cited above is an example. Tanks 2 meters long and from 1.5 to 2 meters wide are currently used. These tanks are generally built of insulating glass or marble slabs, or, more cheaply, of slate, which may be lined with relatively thin glass plates when very high quality insulation is desired.

In most applications it is necessary to have quite flat walls which are strictly parallel or perpendicular to each other and have well-defined corners. In plane tanks particularly the bottom should be perfectly smooth, an obvious necessity in view of maintaining a constant thickness of electrolyte. For the same reason it is necessary to level the bottom of the plane tank. To accomplish this the tank may be set up on a metal framework provided with jack screws. Leveling up is done with a precision level. It is easy to confirm the establishment of a correct level condition by analyzing the uniform fields obtained between two electrodes applied along the two opposite sides of the tank; occasionally this procedure also helps in the final stages of leveling-up the tank bottom.

Weak electrolytes are used as liquid conductors. In order to avoid annoying polarization phenomena, a very weak solution of a salt of the same metal as that composing the electrodes may be used (for example, copper sulfate with electrodes of electrolytic copper). In fact, the most commonly used electrolyte is ordinary tap water, the convenience of which is evident. The resistivity of city water usually lies between 2000 and 10,000 ohm/cm. The conductivity of ordinary water is almost always very homogeneous; for this reason its use gives results which are at least as satisfactory as those obtained with chemical solutions carefully selected but having one particular disadvantage, that of requiring a long and difficult preparation.

The material which makes up the feed electrodes or the conducting models is usually a metal. Copper, brass, dural, stainless steel, etc., are used. The choice depends on various factors: cost, machining problems of the models, risk of polarization, frequency and nature of the feed current used, etc.

Later, in connection with applications, the choice of material in each case will be given.

The main requirement is that the electrode not undergo any deterioration either through contact with the liquid in which it is plunged or through the effects of the current passed through it. In particular, electrodes should be sanded or at least carefully cleaned and degreased before every experiment. Occasionally carbon electrodes are used (Ref. 29). These provide complete protection against unwanted polarization phenomena. To accomplish the same purpose it has been recommended to cover metallic electrodes with a thin layer of specially prepared solution of graphite in colloidal suspension (Ref. 18).

#### (c) Electrical Apparatus

The electrical feed for a tank is always provided by alternating current in order to avoid electrolysis. Usually a sinusoidal current having a frequency between 500 and 2000 cycles per second is used. In this case, the current source is the well-known audio-frequency generator. The power required depends on the impedance of the analogy models under study and on the external series or parallel circuits used. It is selected so that the maximum voltage applied to the tank electrodes does not, on the one hand, fall below a few volts (so as not to diminish excessively the sensitivity of the measurements) and, on the other, does not exceed some tens of volts (in order to avoid heating up the liquid).

Sometimes the sinusoidal line or main current of 60 cycles per second is used, the voltage being reduced by a transformer to some tens of volts. For simple set-ups in which there is no reason to fear important local current densities in the neighborhood

of the electrodes, this kind of electrical feed can give satisfactory results, but, in general, the frequency of 60 cycles is too low and therefore only partially eliminates polarization phenomena.

The measuring potentiometer, P, is usually made up of carefully calibrated resistances placed on either side of the contact, C; a standard set-up automatically insures a total resistance of 1000 ohms, as it is usually taken. The whole consists as a rule of four double decades of resistances for which the control knobs allow readings to within 1/10,000 of the voltage applied at the terminals.

The most convenient and most frequently used zero indicator is the cathode ray oscillograph used in such a way as to provide a Lissajous figure. On the vertical plates of the tube there is imposed, by way of an amplifier having a gain of from 3000 to 10,000, the potential difference between p and C which is to be brought to zero. On the other set of plates there is applied the alternating voltage of the generator itself.

If the signals are not out of phase, the result observed on the screen is a straight line inclined one way or the other. The zero is obtained by bringing this line horizontal. This set-up shows up immediately on the screen any source of error due to the entrance of an unwanted signal which is out of phase, such as might be caused by accidental capacitive or inductive effects, or by polarization. The anomaly is made visible by the opening out of the straight line oscilloscope figure to form an ellipse.

A standard electrical set-up for tank experiments is shown in Fig. III-2. There may be observed the electric tank, B, its

electrodes,  $E_0$  and  $E_1$ , the current generator, G, the measuring bridge, P, the exploring probe, p, the cathode-ray tube, O, with its horizontal and vertical plates, as well as its amplifier, A, and the horizontal sweep transformer,  $T_1$ .

A transformer,  $T_2$ , may also be seen between the source and the rest of the set-up. This is a shielded transformer such as is habitually used in alternating current bridge measurements to avoid parasitic coupling as much as possible. It serves to establish a fixed, small value of capacity with respect to ground. A similar transformer,  $T_3$ , may be used between the amplifier, A, and the circuit which opposes the bridge contact, C, to the probe, p. A Wagner grounding system, a method for making the potential to be measured coincide with the ground potential, may also be used. As is known, this kind of adjustment requires a supplementary operation for each measurement.

In order to compensate for the internal capacitive effects of the electric tank, two variable condensers,  $C_1$  and  $C_2$ , are occasionally employed between the probe and the electrodes (their value ranges from 0 to 1 microfarad). The electrolyte, used with alternating current, never constitutes a pure resistance; moreover, the residual polarization of the electrodes shows up as a phase shift which can quite considerably affect the zero readings when, for high amplifications, increased measuring sensitivity is being sought. For example, it is observed that on the oscilloscope screen, the ellipse grows round out of normal proportions. It may be useful in this case to introduce into one of the bridge arms, constituted by the tank and the potentiometer, P, certain impedances which tend to reduce the out-of-phase component; this is the role played by the two condensers,  $C_1$  and  $C_2$ .

Pursuing the same question, Sander and Yates (Ref. 52) suggest the use of square wave alternating current for the electric tank feed. This system eliminates parasitic reaction voltages while measurements are being taken. The presence in an essentially resistive bridge of unwanted capacity slightly modifies the form of the square wave by introducing, at the onset of each change of sign of the current, a fairly sharp maximum followed by an exponential decay. In the electric tank, the polarization phenomenon between electrode and electrolyte produces an effect similar to that of a resistance and a capacity in parallel followed by a capacity in series.

From this there results a new distortion of the square wave, and the signal existing between the exploratory probe,  $p$ , and the point,  $C$ , of the potentiometer,  $P$ , shows up on the oscilloscope as the trace sketched in Fig. III-3b. The step  $AB$  of the initial excitation takes on a certain slope; however, this slope does not affect the height  $BA_1$ , which represents the real value of the potential difference between  $p$  and  $P$ .

In order to reduce this potential difference to zero, it is then only necessary to adjust the point  $C$  of the bridge thus bringing the points  $B$  and  $A_1$  into coincidence as Fig. III-3c shows. The use of square waves enables one to avoid the double manipulation required in establishing equilibrium when one of the bridge arms contains the two capacities,  $C_1$  and  $C_2$ , of the previous set-up.

The choice of the electrolyte, the nature of the conductor used for the electrodes, and the frequency of the supply current have been the subjects of various recommendations on the part of users of the electric tank. These recommendations deal with a great variety of questions, and a nonspecialized reader

may be confused by what appear to be conflicting opinions. It should be remarked in this connection that the difficulties encountered in rheoelectric experimentation vary to a great extent with the type of study made. It is not surprising therefore that emphasis is placed upon one or another precaution to be taken, according to the type of analog application under consideration.

It is clear, for example, that the precautions will not be the same in the case of a tank containing only a few liters of liquid as for a tank containing several cubic meters. Certain causes of error have a completely different level of importance according to whether the tank is plane, inclined, or deep. Those set-ups in which only two large electrodes are used, connected directly to the terminals of the current generator, do not present the same kind of difficulty as a model employing perhaps a hundred small electrodes, each one held at a different potential.

Generally, great importance is attached to the precautions to be observed in order to avoid troubles due to polarization of the electrodes. Each experimenter has his more favored electrolyte, associated with a given metal used for the electrodes. Actually, the errors due to residual polarization vary considerably from one experiment to another, since the polarization phenomenon depends to a great extent on the local current density, and this density is itself a function of the shape of the electrodes and of the field under study.

It is easy to see that under these conditions it is difficult to set up rules which hold for all cases. A certain amount of practical rheoelectric experience is necessary in order to be able to foresee and remedy the causes of error. In each case, close study of the model is necessary, and this occasionally leads to the utilization of another type of analog model having a more

complicated technical aspect but insuring better precision in the case under consideration. Very often, a good way to ascertain the difficulties to be encountered is to use the tank at first to treat a theoretically calculable case which lies as near as possible to the practical case to be studied.

It may, even under the above conditions, be worthwhile to give some very general recommendations, as summarized below.

(1) Avoid using an electrolyte in which, in the course of time, certain deposits may form which locally modify the tank conductivity. In certain cities the tap water, depending on its origin, may contain salt solutions which deposit out on the tank bottom within a few hours. In all cases, the renewal of the tank liquid every day or two is recommended, since, except if special precautions be taken, dust and bacteria of all sorts accumulate within a week and interfere with the homogeneity of the medium.

(2) Stir the liquid while the tank is being filled.

(3) Before starting an experiment, wait until the liquid has taken on a constant temperature. In this connection, the filling of the tank several hours before the experiment is recommended.

(4) Avoid local heating and temperature variations in the room where the tank is located. The conductivity of the liquid varies considerably with the temperature. A heat source (ray of sunlight, radiator, lamp) near the tank may modify the conductivity locally and falsify the experimental field.

(5) Always use electrodes which are very clean, carefully scoured, and degreased. It has already been remarked that the electrode must not be affected in any way by the liquid in which it stands, nor by the

passage of current through it. A few preliminary tests will tell whether or not these requirements have been met. Certain tap waters contain salts which attack the metal or alloy used for the electrode.

(6) Avoid placing the tank on a floor subject to vibrations. Shocks or vibrations transmitted to the tank supports give rise to small wavelets at the liquid surface and this causes potential variations and measurement difficulties.

(7) Carefully verify the horizontal level of plane tanks and double check this by experiments on uniform fields. The same precautions hold also for inclined tanks.

(8) Avoid placing a rheoelectric analogy tank near a supply line carrying considerable current. This gives rise to induction and capacity effects.

(9) Verify the correct functioning of the external circuits used in conjunction with the tank by tentatively replacing the tank electrically by an equivalent ohmic resistance. Some out-of-phase signals often attributed to polarization in the tank are really due to poorly set up external circuits (undesired capacities or inductions, bad transformers, accidental grounding, etc.).

(10) Avoid resistive voltage drops in the wires which bring current to the tank; the resistance of several meters of small diameter copper wire is not always negligible with respect to that of a deep tank, and the resistances of the two vary in opposite directions with the ambient temperature. If this changes, a change may then be observed in the field under study.

(11) In constructing analog models, avoid all risk of leaks and lack of watertightness where insulating frontiers are involved. Avoid infiltration under the model and deformation or porosity of those materials which are sensitive to humidity.

The above recommendations will give an idea of the elementary precautions to be observed if suitable precision is to be obtained. These precautions involve about the same difficulty as does any electrical set-up wherein magnitudes are to be measured to within a few tenths of a percent.

(d) Mechanical Apparatus for Recording the Location of Equipotential Points

When, by suitably locating the probe and establishing equilibrium, a point of a given equipotential line is located, there remains the necessity of accurately recording this position on paper. Numerous systems exist for carrying out this recording operation. The mechanism which serves to carry the probe can be used for this purpose. This mechanism is usually made up of two carriages, one superimposed on the other to form a set of rectangular cross-slides (Fig. III-4). The larger of the two rolls above the tank on rails fixed along two parallel sides of the tank. The smaller carriage, placed upon the larger, is free to move perpendicularly to the motion of the larger.

On this smaller carriage is placed the exploring probe and a long arm, the extremity of which, cantilevered out over a drawing board, is equipped with a recording point (a pencil or a fine needle point, operated by a solenoid, which punches a fine hole in the paper to mark the point). Handles placed on one side facilitate the movement of the two carriages and thus enable the operator to bring the probe and its rigidly attached point scriber to any part of the field to be explored.

These recording items should be carefully constructed since the reading off of the equipotential lines should be done to within about a tenth of a millimeter if it is desired

to retain the advantages of sensitivity inherent in the electrical part of the apparatus, which latter permits voltages to be read off to within one or two ten-thousandths of the feed voltage.

For exploring plane fields the probe is usually made of a fine conducting wire plunged vertically into the liquid. This wire is fairly rigid, a diameter of around one-tenth of a millimeter being used. The metals commonly employed for it are copper, nickel, stainless steel, or what is best, platinum, to avoid any oxidation.

When the probe is adjusted to a strictly vertical position, which is, incidentally, important, the depth to which it is plunged into the liquid has little importance. The results obtained do not vary for different depths of plunge of the order of a few millimeters more or less. However, just grazing the water surface with the probe should be avoided because the meniscus surrounding the probe causes a slight local change of depth and the measurement can be falsified by this, particularly if one is working near a wall.

It is convenient in general to support the exploring probe wire by means of a probe holder which permits variation of the height of the probe and measurement of its vertical position. This device is useful when it is necessary to know the depth,  $h$ , of the liquid in the tank. A drawing of such a device is given in Fig. III-5.

(e) Automatic Tracing of Equipotential Lines

Various types of automatic apparatus have been built for the continuous tracing of equipotential lines. In this case, the movement of the probe is governed by a servomotor to the terminals of which is applied

the voltage, appropriately amplified, of the error signal between the probe and the bridge, P. The servomotor always operates to bring the probe back to a point on the equipotential curve. While a second motor pulls the probe along in one direction, the servomotor maintains it constantly on the equipotential. It is then only necessary to hook up the probe to a recording stylus to record its movements on a drawing board and thus plot the curve being sought.

With the automatic tracer constructed at ONERA by J. Miroux, the speed of tracing may attain several centimeters per second while maintaining a precision of from one- to two-tenths of a millimeter. A complete field of about 100 equipotential lines occupying an area of 100 x 50 cm can be traced off directly in ink in this way in two hours. An automatic device changes the reference potential when each line has been traced and reverses the direction of carriage displacement as well as raising and lowering the tracing stylus for passage from one equipotential to the next.

Another device automatically varies the speed of that motor which is not servocontrolled, according to the curvature of the equipotential being traced. This insures at all times a practically constant accuracy of trace, which allows the average speed of the whole operation to be increased. Finally, a memory device which automatically interchanges the roles of the two motors at the right moment, makes possible the tracing of curves of any form at all, including closed curves.

(f) Gradient Measurements: Tracing of Curves of Constant Velocity

When a fluid flow is represented in the electric tank by identifying the electric potential,  $V$ , with either the velocity potential,

$\varphi$ , or with the stream function,  $\psi$ , the measurement of the gradient  $dV/dn$  at a point of the tank gives the corresponding value of the velocity. In order to determine then the velocity field of a flow, it is worthwhile to have available a direct means of measuring this gradient.

The principle of this measurement is based on the identification of  $dV/dn$  with the finite difference quantity  $\Delta V/\Delta n$  obtained in the tank by measuring the potential difference  $\Delta V = V_1 - V_2$  between two probes, A and B, placed very close together at a fixed distance  $\Delta n$  (Fig. III-6), when the direction of  $\Delta n$  is normal to the line bearing the potential  $(V_1 + V_2)/2$  and passing through the midpoint M of AB. The approximation thus made in determining the gradient is the more accurate when the separation  $\Delta n$  is small and when the gradient to be measured varies slowly in the region under investigation.

In the most common device for this purpose, the two exploring probes, A and B, are held in a vertical position by a mechanical system which permits their rotation around a vertical axis passing through M. The direction  $n$ , which is generally unknown beforehand, is determined in the following way. The device is turned until the two probes, connected to the zero indicator, show the same potential. They are then in positions A and B on the equipotential passing through M. Next a rotation of the whole through  $\pi/2$  is accomplished so as to bring the probes to A and B on the normal  $n$ . In this position the potential difference  $\Delta V$  is measured. The value of the gradient at M is deduced therefrom, taking into account the separation distance  $\Delta n$ .

In the devices used the two probes, A and B, generally have a diameter of from one- to two-tenths of a millimeter, and their separation,  $\Delta n$ , is taken around one or two millimeters. It is obvious that in order to obtain a precise estimate of the gradient, this distance,  $\Delta n$ , should be as small as

possible, but in this case the potential difference,  $\Delta V$ , is itself very small and its measurement becomes rather difficult as a result. Without taking special pains, and in relatively simple cases, it is possible to obtain an accuracy of a few percent. To improve this figure and achieve, for example, a few thousandths, particularly careful electrical set-ups must be undertaken.

Detailed analysis of such set-ups has been given in various papers. The present discussion will be confined to a brief enumeration of facts of a general nature with reference more particularly to the apparatus built at ONERA by J. Miroux (Ref. 49). A diagram of the apparatus is given in Fig. III-7. The measurement of the potential difference,  $\Delta V$ , is made by a balancing method. The tank being fed electrically by a transformer,  $T_1$ , the potential difference,  $\Delta V$ , is brought to the primary of a transformer,  $T_2$ , and opposed by the fraction  $R_1/(R + R_1 + R_2)$  of the total potential. The difference between the two voltages is applied to the vertical amplifier of a cathode ray oscilloscope,  $O_1$ , which serves as a zero reader. The resistances  $R_1$  and  $R_2$  are twinned and have a total, fixed value (200 ohms, for example).  $R$  is a tare adjustment resistance having a value between 20,000 and 200,000 ohms according to the particular apparatus and the distance between the two probes.

To avoid the necessity of direct measurement of the separation of the probes, an operation which is always difficult and inaccurate, a known reference gradient at a particular point of the field is taken, or a uniform field in a small auxiliary tank in parallel with the main tank is used. The adjustment of  $R$  is then accomplished in the following way: The double probe is placed at the particular point where the gradient is known, and  $R_1$  is made zero. The device is then oriented so as to obtain zero on the oscilloscope. Next, it

is turned through 90 degrees, at which time a particular  $R_{10}$  is imposed on  $R_1$  (for example, 100 or any other value judged convenient). This value represents the reference gradient  $(dV/dn)_0$ . Next  $R$  is adjusted until zero is obtained. Thus  $R$  is fixed at its tare value for the particular analog set-up being studied.

To determine the gradient,  $dV/dn$ , at any point of the field it then suffices to bring the double probe up to the point in question, to perform the orientation operations which determine the direction,  $n$ , and, finally, to readjust the resistance,  $R_1$ , to that value which gives zero on the oscilloscope. The gradient sought is then given by

$$\frac{dV}{dn} = \left( \frac{dV}{dn} \right)_0 \frac{R_1}{R_{10}}$$

The adjustment of the tare value of  $R$  depends, in general, on the depth to which the probes are plunged into the liquid. It is therefore important to maintain a rigorously constant depth of probe once this adjustment has been effected.

The transformers,  $T_1$  and  $T_2$ , are doubly shielded. They should be of excellent quality and should have a very low capacity between primary and secondary. It will be noticed that in the diagram of Fig. III-7 the secondary of the transformer  $T_2$  is practically shorted to ground through the resistance  $R_1$  (which varies from 0 to a few hundred ohms) and that, also, the tank, fed by the transformer  $T_1$ , can take on an arbitrary average potential which will be brought on by various effects (small leaks, capacity of the liquid with respect to metallic masses, etc.) which may vary with the tanks and models studied.

Now, it is obvious that if there is to be no danger of disturbing the field in the neighborhood of the point where the measurement is being taken, the average potential of

the double probe must be that of the equipotential line already in existence at the point in question prior to plunging in the probes. In order to avoid all parasitic coupling, things must be so arranged that the potential at this point be equal to ground potential. To satisfy this condition a potentiometer,  $P$ , is connected to the terminals of the tank, its variable point being connected to ground, and the position of this variable point is adjusted to bring the average potential of the two probes, taken at the midpoint of the transformer  $T_2$ , to ground potential, this being verified by means of a second oscillograph,  $O_2$ .

The importance of maintaining the probes at constant depth has already been mentioned. It should also be mentioned that, for a given depth, there exists a particular frequency of the feed current which produces a perfectly straight line Lissajous figure on the oscilloscope screen. For this particular frequency (taken as a rule between 500 and 1200 cycles per second) there exists a compensation between the residual reactive elements, for example, between the low capacity of the double probes and the inductance of the transformer  $T_2$ . It is clearly advantageous to set the feed generator,  $G$ , at that particular frequency, for this remains the same during the study of the whole field, and, moreover, it permits the operator to increase the sensitivity of the measurements by increasing the amplification of the potential which is to be brought to zero.

The measurement of the gradient at a point of the tank requires several successive operations: finding of the direction,  $n$ , through correct orientation of the probes, then rotating through 90 degrees, bringing the average potential to the ground potential through adjustment of the potentiometer,  $P$ , and, finally, measuring the gradient by opposition through adjustment of  $R_1$ .

The task of the operator can be facilitated by making some of these manipulations automatic. In the apparatus build by J. Miroux, a simple switch replaces  $P$  by a servo-controlled potentiometer,  $P_1$ , so that for any position of the probes, the error signal is made zero as viewed on the oscilloscope  $O_2$ . This potentiometer,  $P_1$ , is driven by a motor which is controlled by a discriminating circuit according to the error voltage.

A second servomechanism serves to orient the probes automatically in the direction,  $n$ , of the maximum gradient. This latter device is particularly useful for tracing the equipotential lines, an operation required when the curves of constant velocity of a flow are sought.

It is then only necessary to adjust the resistance,  $R_1$ , to the desired value, then to move the double probe in the field until the zero is obtained on the oscilloscope  $O_1$ . The points of the lines of constant velocity can thus be read off with the same ease as in reading off equipotential lines. For this purpose the double probe, equipped with its motor device for automatic orientation, can be mounted in place of the simple exploring probe on the small carriage (cross-slide) of the mechanical system already described.

In numerous studies, all that is desired is knowledge of the local velocity distribution around the contour of the obstacle, which requires the measurement of the electrical gradient along either an insulating surface as in analogy A, or along a conducting surface as in analogy B. A simpler means than the double probe can then be employed because in these cases the direction of  $n$  is known. For example, in the case of the insulating surface, the operator can use a simple probe to obtain very fine readings

of the potential,  $V$ , along the contour, then draw up the curve of  $V$  versus contour arc length and differentiate this curve by well-known graphical or numerical methods.

When dealing with a conducting surface, the operator must move the probe perpendicularly to the contour and carefully measure the distances. For this purpose, a micrometric device may be used (Ref. 38), but evaluation of the derivative is always difficult.

Again, a small element,  $\delta s$ , may be isolated from the rest of the contour and, while it is kept at the original potential, the current,  $\delta i$ , being passed by that element may be measured. According to Eq. (13), it is possible to obtain an average value of the gradient  $(dV/dn)_{av} = \delta i / \delta s \cdot \sigma h$  in this way.

#### (g) Use of Conducting Paper

To obtain quick and cheap representations of plane harmonic fields, a new procedure based on the use of a special conducting paper may be used. This paper, called "Teledeltos" is manufactured by the Western Union Telegraph Company (Ref. 42). With this paper, the accuracy of measurements and the reading off of equipotential lines is usually somewhat inferior to that obtained by using the electric tank; it is, however, quite satisfactory in numerous cases. The principal advantage of the procedure lies in the extreme simplicity with which it may be put into use and the ease of model construction. This is a procedure which is exceptionally useful in obtaining rough preliminary results.

The electrical conductivity of Teledeltos paper is homogeneous enough for most applications (as can be seen by tracing uniform fields), and its sensitiveness to atmospheric

conditions (temperature and humidity) is relatively low. In "type L" paper the resistance of a square sheet, taken between parallel sides, is of the order of 3000 ohms, i.e. about five or six times more than that between electrodes of a square plane tank having a liquid depth of several centimeters.

The procedure utilized to insure contact between the electrodes and the paper is very simple. It is only necessary to glue a thin sheet of copper or tin foil to the graphited surface of the Teledeltos, using aquadag solution. Another method is to cover the electrode region with a silver base conducting paint which is applied directly by brush, or better still, by spray gun using suitable masking forms. The model thus prepared is stuck to a drawing board or heavy cardboard sheet with adhesive tape. The connecting wires are soldered directly to the metallic foil. The electrical feed may be provided by direct current of a few volts from either a flashlight battery for simple set-ups, or a multi-cell battery, or finally by using the alternating current line voltage reduced by transformer and rectified.

Tracing the equipotential lines is once more accomplished by a balancing method, using a microammeter as zero indicator. The measuring potentiometer is identical to that used in the electric tank experiments. The exploring point is made of a metal conducting stick with the end sharpened to a slightly rounded stylus point. Contact is obtained by slight pressure of the point on the paper. Once the zero is found, it is only necessary to push down a little harder on the paper to mark the equipotential point located. This determination is easily carried out to within half a millimeter. A general view of such a set-up is given by the photograph of Fig. III-8. The apparatus shown therein groups together the electrical feed, the measuring bridge, the microammeter, and the switches required for adjusting the applied voltage and the sensitivity.

Most of the analog representations carried out in the electric tank can also be carried over to the Teledeltos paper technique. Included in this are the set-ups for problems of the Dirichlet, Neumann, and Fourier types, as will be seen in what follows. It will also be seen that the two procedures of paper and tank can complement each other advantageously. Also, the use of conducting paper is particularly convenient when the shape of the field boundaries is unknown a priori and where successive approximations are used to determine them.

As an example, there may be cited the determination of flows having a free surface wherein the shape of the jet line is unknown. All that is supposed known is that this frontier must correspond to a streamline which forms an extension of the surface of the body placed in the flow and along which the velocity (i.e. the potential gradient  $d\varphi/ds$ ) is constant. When conducting paper is used for the analog representation of such a flow, the exact shape of the jet line may be sought by starting from an approximate form and then successively cutting the paper in such a way as to obtain the condition  $d\varphi/ds = \text{constant}$ .

This procedure was used by Marchet (Ref. 61) to determine the jet lines of a Riabouchinsky wake (dead-water region contained between two obstacles having the form of a plate or forming a dihedral angle and oriented symmetrically in a flow which is uniform at infinity). Seeking out the correct jet line by successive trials, cutting the paper model more or less as necessary, is evidently much easier than determining this line in the electric tank, where each approximation requires adjustment of the insulating boundary representing the jet line, this boundary requiring strict watertightness in each new position if the experimental errors that are always brought on by leaks are to be eliminated.

Other examples of the same sort in fluid mechanics can be mentioned: determination of the free surfaces in problems of water infiltration through permeable masses (Ref. 42) and in dam overflows, etc., where the effect of gravity is a factor.

In conclusion, it may also be mentioned that the use of conducting paper is very convenient for representing Riemann surfaces consisting of several sheets. The superposed sheets are separated and represented by distinct sheets of Teledeltos paper electrically connected in appropriate fashion. An example of this is given (Ref. 56) in a study dealing with the flow about a cascade of turbine blade profiles.

#### IV. THE ANALOG STUDY OF WING SECTIONS

##### (a) Analog Representation of Circulation

The electric tank study of flow around section profiles of wings requires an appropriate analog interpretation of the circulation. We will first examine the general use of a contour of any shape, (c). It is clearly possible to use one or the other of the two analogies, but it should be noticed that, the velocity potential,  $\varphi$ , being no longer single-valued when the circulation is not zero, the physical realization of analogy A, wherein  $\varphi$  is identified with the electrical potential, introduces a few auxiliary complications.

##### (1) Analogy B

As a result, analogy B will be the first to be examined because its representation is the simpler and more immediate. Let us consider once more the example shown in Section III (a), assuming this time that

the circulation around (c) has a given value  $\Gamma$ . The analog model arrangement remains the same. Electrodes  $E_0^1$  and  $E_1^1$  are on the sides parallel to the x axis and the model of the contour is a conducting one.

According to Eqs. (11) of analogy B, the following hold here (for  $\lambda = 1$ ):

$$\psi = -n'V \quad \varphi = \frac{n'}{\sigma h} W \tag{15}$$

Hence, the analog representation of the circulation is given by:

$$\Gamma = \int_{(c)} d\varphi = \frac{n'}{\sigma h} \int_{(c)} dW = \frac{n'}{\sigma h} I \tag{16}$$

where I represents the total intensity of the electric current which passes into the tank from the conducting model (c).

If this model is not electrically fed, the circulation is necessarily zero; therefore, to give the circulation a prescribed value the model must function as an extra electrode. Hence it must be connected through an adjustable resistance, R, to one of the poles (conveniently chosen to obtain the correct sign for  $\Gamma$ ) of the general electrical feed.

The diagram of Fig. IV-1 gives the set-up usually used: the resistance, R, is connected to an auxiliary potentiometer,  $P_1$ , which in turn is connected in parallel with the electrodes,  $E_0^1$ ,  $E_1^1$ , of the tank. The current intensity, I, can thus be adjusted to any desired value by varying R or by varying the position of the variable point,  $P_1$ , of the potentiometer which controls the voltage,  $V_2$ . As a rule this current is measured by means of the potential drop  $\Delta V = V_2 - V_2$  between the terminals of R.

If  $L^1$  is the width of the tank between  $E_0^1$  and  $E_1^1$ , the stream function of the uniform flow,  $\psi = Uy$ , increases by the value  $UL^1$  in passing from  $E_0^1$  to  $E_1^1$ , whence, in view of the fact that the corresponding variation of the electrical potential, V, is equal to  $V_1 - V_0$ , there is obtained

$$n' = \frac{-UL^1}{V_1 - V_0} \tag{17}$$

and the circulation,  $\Gamma$ , if the difference  $V_1 - V_0$  is conventionally taken as equal to 100, is given by

$$\frac{\Gamma}{U} = \frac{-L^1 I}{100\sigma h} = -L^1 \frac{\Delta V}{100} \frac{1}{\sigma h R} \tag{18}$$

$\Delta V$  being measured within the scale 0-100.

The liquid depth, h, can be measured by using the exploring probe and the graduated probe holder as was indicated in Section III (d). The measurement of conductivity,  $\sigma$ , can be made by plunging into the liquid a standard measuring cell such as is commonly used to measure the resistivity of electrolytes.

Fig. IV-2 shows one of these cells consisting of a glass tube 1.5 cm in diameter containing two platinum electrodes having surface areas about 1 square cm and separation 1 cm. When this cell is placed in the tank the electrolyte enters it by small side and bottom orifices, and the resistance between electrodes is then measured by means of a Wheatstone bridge. The cell having been previously calibrated, use of its calibration factor permits immediate calculation of the desired resistivity.

Another means for taking this measurement is that shown in Fig. IV-3, where the device is placed on the tank bottom. The

apparatus consists of two concentric conducting cylinders of radii  $\rho$  and  $\rho_2$ . Measurement of the resistance,  $r$ , of the liquid ring caught between them gives directly the product,  $\sigma h$ , needed in Eq. (18). The necessary relation is given by

$$\sigma h = \frac{1}{2\pi r} \log \rho_1/\rho_2. \quad (19)$$

A still easier method of measurement for the set-up of Fig. IV-2 is the determination of the product,  $\sigma h$ , by measuring the resistance,  $R'$ , of the liquid between the electrodes,  $E_0'$  and  $E_1'$ , after having removed the model, (c). There is then obtained the following practically useful formula for the circulation:

$$\frac{\Gamma}{U} = -L \frac{R'}{R} \frac{\Delta V}{100} \quad (20)$$

where  $L$  is the tank length.

## (2) Analogy A

In order to represent correctly the velocity potential,  $\varphi$ , in the electric tank, the condition imposed on the circulation,  $\Gamma$ , must be taken into account: when a complete circuit is described around the contour of the body the potential,  $\varphi$ , undergoes a variation equal to the magnitude of  $\Gamma$ ; this must hold also for the electrical potential,  $V$ . Therefore it is necessary to establish a "cut" in the field, which can be chosen along an equipotential line,  $MN$ , extending outward from the contour (c) (Fig. IV-4a). This cut is represented in the electric tank by two auxiliary electrodes,  $E_2$  and  $E_3$ , separated by a thin insulating strip.

The potential difference,  $\Delta V$ , to be established between these two electrodes corresponds to the value of the circulation ( $\Gamma = m \Delta V$ ). This potential difference is

imposed by means of a potentiometer,  $P_1$ , fed through a transformer,  $T$ , so that the current entering one of the electrodes,  $E_2$  for example, flows out of the other,  $E_3$ . This coincides with the hydrodynamic necessity that the flux crossing  $MN$  be conservative.

In practice the cut is constructed from an insulating strip of ebonite or plexiglass about 1 mm thick on the faces of which the electrodes  $E_2'$  and  $E_3'$  are glued, these latter being cut from copper foil. They can also be made by painting the faces of the insulator with a conducting paint.

Another practical set-up is occasionally used when the streamline,  $PQ$ , leaving the body is known (if such a streamline exists). In this case an insulating cut is established along this line. Under these conditions the tank is fed by three electrodes (Fig. IV-4b),  $E_0$ ,  $E_1$ , and  $E_2$ , in such a way that between  $E_1$  and  $E_2$ , which are separated by the cut, the potential difference,  $\Delta V$ , which corresponds to the circulation, is maintained.

The employment of analogy A according to the two schemes outlined above requires, in practice, knowledge of the streamlines ( $\psi = \text{constant}$ ) obtained from analogy B. Indeed, there must be known either the streamline,  $PQ$ , or the equipotential line,  $MN$ , determination of which can only be made by establishing the normals to the streamlines. The only exception arises in the case of bodies having the  $y$  axis as axis of symmetry.

However, knowledge of the streamlines is not indispensable if a third, more complex type of experimental set-up can be undertaken (Fig. IV-4c). In this system, the "cut" can be made along a straight line; however, on the two boundary faces the potential difference,  $\Delta V$ , must be established for each opposed pair of points, such as  $A, A'$ .

In order to achieve this condition, the insulating strip making up the cut is covered with a large number of small paired electrodes, such as  $e, e'$ , which are electrically insulated from one another and fed in pairs by means of transformers like T. Thus, the potential difference,  $\Delta V$ , can be established between any two paired electrodes. Obviously, the experiment requires as many transformers, T, as there are pairs of electrodes ( $e, e'$ ) on the cut. The experimental equipment is therefore considerable. This will be described in Section IX in connection with other analog installations.

(b) Study of Airfoil Sections  
 with Analogy B

Most practical studies of flow around wing sections are carried out by means of analogy B. To satisfy the Joukowski condition, the circulation,  $\Gamma$ , must be adjusted so that the streamline, to which the section profile belongs, leaves the contour exactly at the trailing edge and, at the same time, takes off along the prolongation of the point making up the trailing edge (i.e. along the tangent to the contour in the case of a trailing edge which forms a cusp or along the bisector of the tangents in the case of an angular trailing edge).

In the electrical tank this streamline corresponds to the equipotential line to which the model belongs. To adjust it a fine metallic point,  $t$ , is plunged into the tank parallel to the vertical edge of the trailing point of the model and a short distance behind it so as to define, in conjunction with the trailing point, the direction of the equipotential in question (Fig. IV-5). The oscilloscope is connected between the model and the point,  $t$ , and the current,  $I$ , is adjusted, by means of the resistance,  $R$ , or the auxiliary potentiometer,  $P_1$ , to bring the two potentials to the same value.

It is convenient in practice to fasten the point to the section model so that it follows the model throughout any changes of incidence and remains always in the same relative position. For this purpose the point,  $t$ , is mounted on an insulating support fixed to the model and having the desired orientation (Fig. IV-6).

It is interesting to notice that, once the adjustment is made, the measurement of the current,  $I$ , that is, of the potential difference,  $\Delta V$ , at the terminals of the resistance,  $R$ , gives, the value, a priori unknown, of the circulation,  $\Gamma$  (by Eq. (20)). By obtaining this result for different angles of attack of the profile, the electric tank makes it easy to define the aerodynamic characteristics of any airfoil section whatsoever.

The circulation is usually expressed in the form

$$\Gamma = -k l U \sin(\alpha - \alpha_0) \quad (21)$$

where  $l$  is the reference chord of the airfoil,  $\alpha$  the angle of attack,  $\alpha_0$  the angle of zero lift and  $k$  a coefficient characteristic of the section. The direction,  $\alpha_0$ , may be determined directly by leaving the model without electrical feed ( $R = \infty$ , whence  $I = \Gamma = 0$ ) and by turning it until the Joukowski condition is fulfilled.

It is then easy to determine the coefficient,  $k$ , by placing the model at any given angle of incidence,  $\alpha$ :

$$k = \frac{L}{l} \frac{R'}{R} \frac{\Delta V}{100} \frac{1}{\sin(\alpha - \alpha_0)} \quad (22)$$

The value,  $k$ , thus obtained is generally accurate to within one percent. Several experiments should of course be run off

with different angles  $\alpha$  to verify this result. In connection with such experiments the following represent the orders of magnitude of some experimentally measured quantities (we consider the concrete case of a section profile of chord 30 cm, placed in the plane tank of dimensions 2 x 1.5 meters):  $\lambda = 30$ ,  $L = 200$ ,  $L' = 150$ , water depth,  $h = 5$  cm,  $R'$  is measured to be  $R' = 375$  ohms (water resistivity  $1/\sigma = 2500$  ohm x cm), and the potential drop across  $R = 3000$  ohms is  $\Delta V = 48.75$  for an angle  $\alpha - \alpha_0 = 10^\circ$ . The value of  $k$  thus found is  $k = 3.5$ .

For a given angle of attack, with the Joukowsky condition fulfilled, the tracing of the aerodynamic streamlines is accomplished by reading off the electrical equipotentials in the manner indicated in Section III. The same holds for the velocities which are obtained by one of the previously described methods.

(c) Studies on Combinations of Airfoil Sections: Interaction Problems

The method just outlined is regularly used to define the aerodynamic characteristics of empirically designed airfoils of any form whatsoever and to analyze the forms of corresponding flows. This method can easily be generalized to deal with combinations such as biplane or multiplane airfoils, slotted or slatted airfoils, ailerons with open hinge gaps, etc. Of course in each case the Joukowsky condition must be satisfied at the trailing edge of each separate one of the airfoil elements present. This is accomplished by adjusting, as has already been described, the values of the currents  $I_1, I_2, I_3, \dots$  which flow into the different parts of the model. The measurement of these currents gives the corresponding values  $\Gamma_1, \Gamma_2, \Gamma_3, \dots$  of circulation about the

element and, finally, the lift coefficient,  $C_L$ , of the combination:

$$C_L = 2 \sum_{i=1}^n (\Gamma_i / U l).$$

Fig. IV-7 gives the electric circuits of an analog representation for an airfoil with a double slotted flap. By means of a switch, the zero-reading oscilloscope may be connected between any of the airfoil elements and its corresponding trailing edge probing point. Adjustments of the Joukowsky condition are made by trial and error, the adjustment for one airfoil element being subsequently more or less upset by that for another; however, these manipulations, accomplished with the potentiometers,  $P_1, P_2, P_3$ , are very rapid.

The same kind of experiment can be used to study the effect of a wall placed near an airfoil or combination of airfoils. The most common application is the study of the ground effect on the characteristics of a given airfoil. In analogy B the ground becomes a straight electrode. The airfoil then need only be placed in the attitude chosen near one of the feed electrodes of the tank, say  $E_0$ . The electrical circuits are not modified, and the circulation can be determined or the flow field traced out as has been described earlier (Ref. 11).

(d) Examples

Knowledge of the theoretical characteristics of an airfoil (lift, velocity and pressure distributions, plot of the surrounding flow field) may be effectively used in the course of certain experimental aerodynamics studies.

When certain wind tunnel results on forms similar to those to be studied are available, the following method can be utilized. Those contours which offer the best aerodynamic properties are selected from the experimental results. These contours are then studied

theoretically in the electric tank. The detailed analysis of the fields thus obtained often explains the reason for the good qualities observed in the wind tunnel results. It is thus possible to deduce certain criteria of good performance which, when carried over to new forms, aid in designing them.

Later, it is obviously advantageous to study the newly chosen airfoil forms in the electric tank first, before trying them in the wind tunnel (the electric tank necessitating only inexpensive models which are easily built and modified), for in the analog experiments the experimental modifications needed for bringing out the criteria sought after are both simple and rapid. It is thus easily possible to define beforehand the range of set-ups which are presumed optimal, thus reducing the number of required wind tunnel tests.

#### (1) Airfoils with Flap and Hinged Leading Edge

In the course of examination of a certain modern airfoil having a small radius of curvature at the leading edge and carrying a flap, it was possible to show, from a few wind tunnel and electric tank tests, that the agreement between theoretical and experimental pressure distributions was very satisfactory in all the cases considered.

It was also noticed from the wind tunnel results that the maximum lift coefficients,  $C_{L_{max}}$ , which corresponded to different flap deflection angles, were always reached when a certain fixed value of maximum negative pressure appeared at the airfoil leading edge. The conclusion was therefore drawn that the appearance of this negative pressure peak might serve to predict the  $C_{L_{max}}$  for other cases of flap deflection or arrangement.

The agreement which had been shown to exist between theoretical and experimental pressure distributions enabled the study to

be continued using only the results of the electrical tank. Thus, it was possible to use the analogy to study a great number of special configurations involving this airfoil (double break in the flap, curvature of the leading edge, etc.) and in each case to estimate the  $C_{L_{max}}$  with reasonable accuracy. In this way the number of wind tunnel studies was considerably cut down, for the electric tank experiments eliminated the obviously unfavorable combinations and kept only those few which appeared good, as was confirmed later in the tunnel. For the details concerning this study, see Ref. 27.

Occasionally, a very rapid tracing of only a few streamlines provides valuable information. Thus the influence of a hinged leading edge can be approximately estimated (Fig. IV-8). The mechanical hinge linkage of the nose reduces the negative pressure point by bringing the stagnation point into the neighborhood of the leading edge, but when the angle  $\eta$  exceeds a certain value a new velocity peak appears at the break and can cause separation. It may thus be hoped to determine in advance the value of the angle which  $\eta$  should not exceed, or again, the chord location where it will be necessary to undertake aspiration of the boundary layer, for example.

#### (2) Airfoils with Leading Edge Slots

The examination of theoretical fields is useful in analyzing the effect of a leading edge slot. It may be seen even at an early stage of the investigation (Fig. IV-9) that the difference between the flows around the original airfoil and around that with slot is much greater than would be thought at first. For the best slot locations (those giving high  $C_{L_{max}}$  in the wind tunnel), the stagnation points are located near the leading edge of the primary and secondary airfoils, and on the whole the pressure peaks are not

greatly accentuated, thus explaining the delay observed in the flow separation. Other interesting observations can be made on the basis of the form taken by the aerodynamic field: the way in which the nose of the auxiliary airfoil is attacked by the flow, the velocity distribution in the slot, and, particularly, the flow through the slot and its exit velocity.

It may be remarked in passing that the flow through the slot is measured in the electrical analogy by the difference between the potentials of the primary and secondary airfoils. It is thus easy to obtain the desired slot flow by moving the auxiliary airfoil slightly in the tank. For a certain slot shown to be ineffective in the wind tunnel, the electric tank showed that the theoretical slot flow was quite feeble. In this case it was relatively easy to find a better configuration through use of the tank.

### (3) Airfoils with Double Slotted Flap

Determination of aerodynamic forces is necessary for structural analysis. In the case of a complicated device like a double slotted flap, a wind tunnel model for pressure distribution surveys is a costly undertaking. In many cases theoretical estimates of these distributions are sufficient.

Consider the example given in Fig. IV-10, which gives an opportunity to illustrate certain methods for which the principle has already been given. The field of streamlines was obtained in the standard way in a tank by using analogy B. Starting with this field the contour velocities can be determined precisely enough by using conducting paper, as follows: In the field of Fig. IV-10 two streamlines, AB and CD, are chosen to include the airfoil, and two equipotential lines, AD and BC, are traced normally to the

streamlines. This curvilinear quadrilateral is obtained experimentally by cutting it out of a sheet of conducting paper (Fig. IV-11). The forms of the airfoils are also cut out of the paper so as to use analogy A this time (set-up number 2).

The cuts are made by slitting the paper along the three streamlines,  $P'Q'$ ,  $P''Q''$ ,  $P'''Q'''$ , which emerge from the trailing edge of each contour. The electrical feed is obtained by an electrode,  $E_0$ , placed along the equipotential, AD, and by the electrodes,  $E_1, E_2, E_3, E_4$ , located along BC. The potentials of these electrodes are adjusted so as to obtain the correct values of the circulations as found in the tank. Next the potential distribution,  $\varphi(s)$ , is precisely read off along the contours, and the velocity and pressure distributions are obtained therefrom by numerical differentiation along both the airfoil and its flaps. Fig. IV-12 gives the results obtained by this procedure.

### (e) Effects of Sources and Sinks on an Airfoil

The action of aspiration or blowing on a wing section affects not only the boundary layer, but also disturbs the whole of the flow in the neighborhood of the section (at least if the inflow or outflow is large enough). In effect, a modification of the potential flow is caused by a sink effect (or source effect in the case of relatively slow and diffuse blowing).

This sink effect changes the value of the circulation as well as the pressure distribution over the contour. The calculation of these modifications is easy when the conformal transformation of the airfoil onto the circle is known, and the method of conformal transformation by rheoelectric analogy described in the next chapter may be

used for this purpose. However, it may be worthwhile to examine the direct analog representation of the sink effect and to try to define the form of the flow.

Consider analogy B; the airfoil is then a conducting model. Let  $F$  be the aspiration slot the effect of which is approximated by a sink-type singularity. On either side of  $F$  the stream function,  $\psi$ , takes on distinct values the difference,  $\delta\psi$ , of which represents the flow toward the sink. A potential difference,  $\delta V$ , across the slot must be associated with the above variation of  $\psi$ . The airfoil model must therefore be made up of two electrodes,  $e$  and  $e'$ , which must be raised to two distinct potentials,  $V$  and  $V'$ , which differ by  $\delta V$ .

The presence of the singularity makes the stream function,  $\psi$ , multivalued in the region outside the airfoil; hence, a cut must be made somewhere to make this region simply connected. This cut will be chosen along a hydrodynamic equipotential line emerging from the lower side of the profile. It will therefore be made from a thin insulating strip.

The general aspect of the experiment is shown in Fig. IV-13a. The tank is fed by means of three electrodes,  $E_0$ ,  $E'_0$ , and  $E_1$ .  $E_0$  and  $E'_0$  are applied on the same boundary of the tank but separated by the insulating cut, MN. The electrodes  $E_0$  and  $E_1$ , raised respectively to the potentials 0 and 100, are connected directly to the terminals of the current generator.  $E'_0$  is raised to a potential distinct from  $E_0$  by means of an adjustable potentiometer so as to set up between these two electrodes the potential difference,  $\delta V$ , which must exist between  $e$  and  $e'$ . The magnitude of this difference is calculated from the flow coefficient

$$C_Q = Q/lU$$

( $Q$  = flow quantity,  $l$  = reference chord,

$U$  = velocity at infinity) which is to be represented.

It may be seen from the formulas of the analogy that

$$\delta V = (l/L')(100)C_Q \quad (23)$$

within the conventional scale (0-100) of the potential.  $L'$  again represents the width of the tank.

The Joukowski condition for flow off the trailing edge is fulfilled by regulating the potential of  $e'$  to the right value while maintaining the potential difference,  $\delta V$ , between  $e$  and  $e'$ .

The form to be given to the cut, MN, is not known at the outset since it depends on the flow field to be established; however, it may be verified that this curve is practically a straight line except very near the airfoil, which it must approach at right angles. It may be constructed approximately, using as a guide the field of streamlines around the airfoil with zero sink flow. The introduction of the sink effect only slightly modifies the form of this field, and if it is necessary, the final placement of the sink may be made after a couple of approximations by taking into account the shape of the streamlines on either side of the cut.

In certain experiments it may be required to represent on the same airfoil an aspiration,  $F_A$ , and a blowing,  $F_S$ , having the same flow. The experimental realization is then simplified. The equivalence of the outflow and inflow allow the cut, MN, to be eliminated since the function,  $\psi$ , becomes single-valued once more (the two singularities being of opposite intensities). The section is still represented by two electrodes,  $e$  and  $e'$  (Fig. IV-13b) separated by two narrow insulating spaces,  $F_A$  and  $F_S$ , and raised to potentials

which again differ by the amount  $\delta V$ . According as the potential of  $e'$  is greater or smaller than that of  $e$ , there is obtained the effect of an aspiration either followed or preceded by a blowing. Finally, it must be remarked that only a single electrode,  $E_0$ , is required.

In these experiments the airfoil model is made of insulating material and covered with copper foil or conducting paint to represent the electrodes  $e$  and  $e'$ . The potentials of  $E'$ ,  $e$  and  $e'$  are adjusted by means of potentiometers,  $P_{E'}$ ,  $P_e$  and  $P_{e'}$ .

## V. RHEOELECTRIC CONFORMAL TRANSFORMATIONS

### (a) Principle of the Method

The solution of numerous problems in fluid mechanics is based on the use of conformal transformations. It is therefore interesting to see what profit can be drawn from the rheoelectric analogy method in this regard. In these kinds of experimental realizations, which may be called indirect since they no longer involve direct definition of the image of the flow studied, the electric tank appears as a practical auxiliary aid to theoretical calculations at a particular step in the general analytical development.

The principle of the method is simple. Suppose the conformal transformation between two regions,  $D$  and  $d$ , is to be determined, these regions being respectively described in the complex planes of  $Z$  and  $z$ . To accomplish this, suppose a complex potential function  $f(Z)$  or  $f(z) = \varphi + i\psi$  defined inside  $D$  and hence, by the conformal transformation, also inside  $d$ . If it is possible to determine, either experimentally or by calculation, the two networks of lines,  $\varphi$  and  $\psi$ , constant in the two planes,  $Z$  and  $z$ , the conformal representation sought will practically be attained, for two homologous

points,  $Z$  and  $z$ , will be characterized by the same values of  $\varphi$  and  $\psi$ .

Theoretically, the choice of the complex potential function,  $f$ , makes little difference, but practically, it is chosen so as to satisfy the following two conditions:

(1) That  $f$  be easily calculable at every point of the  $Z$  plane.

(2) That  $f$  provide, on the boundaries of  $d$ , simple boundary conditions (for example,  $\varphi$  or  $\psi$  constant) in order that  $f(z)$  may be defined in the  $z$  plane by the simplest possible rheoelectric analogy.

### (b) Conformal Transformation of an Airfoil onto a Circle

To illustrate these considerations the classical aerodynamics problem may be evoked by the correspondence between the exterior of an arbitrary contour ( $c$ ) in the  $z$  plane and the exterior of a circle ( $C$ ) defined by  $|Z| = a$ , transformation preserving the point at infinity and the relation  $(dz/dZ)_{\infty} = 1$ . Various functions,  $f$ , are available with a view to satisfying the two conditions cited above.

For example,  $f = \text{Log } Z$  might be used. In this case, the experimental realizations in the  $z$  plane require, for  $\varphi$ , that the contour ( $c$ ) function as a source in an electric tank of large dimensions, and, for  $\psi$ , a fluid circulation around ( $c$ ). However, in the  $\psi$  experiment, a cut must be made in the tank since  $\psi$  is multivalued; the two sides of the cut must carry feed electrodes and the cut must follow a particular line,  $\psi$ , known a priori. Moreover, the question of scale, in particular that of the relation between the scales of  $\psi$  and  $\varphi$  in the two experiments (magnitude of  $a$ ), is relatively delicate.

More practical set-ups can be obtained by taking  $f = Z + a^2/Z$  which corresponds to the complex potential of the uniform flow without circulation about (C) or (c). A point  $Z = Re^{i\theta}$  located in the circle plane may be characterized by the value of the functions  $\varphi$  and  $\psi$  at this point:

$$\begin{aligned}\varphi &= R \cos \theta \left(1 + \frac{a^2}{R^2}\right) \\ \psi &= R \sin \theta \left(1 - \frac{a^2}{R^2}\right)\end{aligned}\quad (24)$$

To determine the homologous point  $z$  defined by these values of  $\varphi$  and  $\psi$  in the plane of the contour (c), the two analog representations A and B are successively used. Therefore the two experiments described in Section III (a) are carried out. One defines  $\varphi$  (with the contour (c) insulating); the other, the function  $\psi$  (contour (c) conducting).

Let  $V$  and  $V'$  be the electrical potentials observed in the tank in the first and second cases respectively, the potentials being measured on the conventional scale of values (0-100) between one electrode and the other. In the first set-up (Fig. V-1) the extreme equipotential lines terminating on (c) at points  $\alpha$  and  $\beta$  (which correspond, in the conformal transformation, to points A and B of the circle (C)) have potentials  $V_\alpha$  and  $V_\beta$ . In the second set-up, the conducting model (c) takes on the potential  $V'_0$ .

It can then be shown that

$$\varphi = \left(V - \frac{V_\alpha + V_\beta}{2}\right) \frac{L}{100}\quad (25)$$

and

$$\psi = (V' - V'_0) \frac{L'}{100}\quad (26)$$

$L$  and  $L'$  being the respective distances between electrodes in the first and second experiments.

The magnitude of  $a$ , radius of the circle (C), is thus obtained. To the points  $X = \pm a$  of (C) there correspond according to Eq. (24),  $\varphi = \pm 2a$  and  $V = V_\alpha$  or  $V_\beta$  whence

$$a = (V_\alpha - V_\beta) \frac{L}{400}\quad (27)$$

The precision of the correspondence ( $z|Z$ ) which is thus obtained is generally excellent. For example, the radius,  $a$ , can be determined in this way to within a relative error of less than 3/1000.

In those problems wherein it is sufficient to find the correspondence between the points of the contours (c) and (C), the first experiment, with insulating model, is all that is necessary. The distribution of the potential,  $V$ , about the contour of the model gives the corresponding values of  $\varphi$  whence are obtained the angles  $\theta$  since  $\varphi = 2a \cos \theta$ ,  $a$  being given by Eq. (27).

When it is desired to know, in addition, the modulus of the transformation  $\mu = |dZ/dz|$  for two homologous points ( $Z|z$ ), it is necessary to calculate  $|df/dZ|$  for the point  $Z$  and to determine  $|df/dz|$  in the tank at the point  $z$ . This latter determination requires measuring the gradient of the potential,  $V$  (or  $V'$ ), in one or the other of the preceding experiments. To accomplish this the procedures described in Section III (f) are used.

Most of the practical applications of this method of rheoelectric conformal transformation are concerned with studies of airfoils wherein the contour pressure distributions are later to be determined by calculation. For this, models of 30 to 50 cm chord length are placed in plane tanks of dimensions 200 cm x 150 cm. Generally, the airfoil is

placed at zero lift angle of attack in order to make the point  $\alpha$  coincide with the trailing edge (Fig. V-1b).

Thus, with the insulating model alone, there are determined the value of the radius,  $a$ , and the correspondence between the points of the two contours. This correspondence being known, the modulus,  $\mu$ , of the transformation is obtained from it by graphical or numerical differentiation. This is used to pass from the velocities on (C) to those on the airfoil. When the double probe apparatus described in Section III (f) is available, the contour gradient can be directly measured for use in calculating  $\mu$ .

It is interesting to note that the analogy allows determination of the aerodynamic center of the airfoil, as follows. When the airfoil is without circulation, this point is common to the respective asymptotes, D and  $\Delta$ , of the potential line  $(V_\alpha + V_\beta)/2$  of the first analog set-up and  $V_0'$  of the second. It is the values of  $(V_\alpha + V_\beta)/2$  and  $V_0'$  themselves which define the positions of D and  $\Delta$  in the tank.

This experimental method for conformally transforming an airfoil onto a circle has the advantage of being applicable to absolutely any form whatsoever, no matter how irregular it may be. Thus can be studied in rapid fashion the effects of the modification of airfoil forms by flap deformations, by thickening or thinning of certain regions, by articulating the nose region, etc.

(c) Conformal Transformation  
 of any Region onto a Rectangle  
 or Circle

There often arises the problem of defining the conformal transformation of a simply connected region, bounded by a closed curve (c) of arbitrary form, onto the inside of a rectangle or of a circle.

Let us first examine the case of the rectangle. We consider the analytic function  $f(z) = \varphi + i\psi$  defined in the  $z$ -plane of the contour (c) by the following boundary conditions (Fig. V-2),  $\varphi = \varphi_0$  on the arc AB and  $\varphi = \varphi_1$  on arc CD. The normal derivative,  $d\varphi/dn$ , is zero on arcs AC and BD (the points A, B, C, D being arbitrarily chosen).

The analog representation of the function  $\varphi$ , the real part of  $f(z)$ , is immediate. A plane electric tank the horizontal section of which represents the form of the contour (c) is fed by the two electrodes  $E_0$  and  $E_1$ ; the voltage applied to the terminals of these electrodes represents the difference  $\varphi_1 - \varphi_0$ . The electrical potential measured in the tank gives the value of  $\varphi$  at each point.

The other analogy represents  $\psi$ , the imaginary part of  $f(z)$ . In a second experiment the tank is fed by the electrodes  $E_0'$  and  $E_1'$  placed in this case along the arcs AC and BD. The potential read off at a point gives the corresponding value of  $\psi$ .

Let us now pass from the  $z$ -plane (where  $z = x + iy$ ) to the plane of  $f = \varphi + i\psi$ ; in this new plane the lines  $\varphi$  and  $\psi$  constant are parallel to the axes. A point  $m(x,y)$  of the domain (c) may be defined by the values  $\varphi(m)$  and  $\psi(m)$  taken by the functions at this point and measured during the two preceding experiments. The point M which corresponds to it in the rectangle is therefore the point having abscissa  $\varphi(m)$  and ordinate  $\psi(m)$  in the plane of  $f$ .

To complete the transformation, it remains necessary to link the scales of potential in the two experiments, or, which amounts to the same thing, to define the ratio of the sides,  $a$  and  $b$ , of the rectangle. The analogy formulas give  $a/b = R\circ h$  where  $R$  represents the electrical resistance measured in the first experiment between the electrodes  $E_0$

and  $E_1$ . The second experiment would give likewise,  $b/a = R'\sigma'h'$ ,  $R'$  being the resistance measured between  $E'_0$  and  $E'_1$ .

If it is desired to preserve the same scale of potential in the two experiments, it is necessary that the potential differences,  $\Delta V$  and  $\Delta V'$ , (applied respectively between electrode pairs  $E_0, E_1$  and  $E'_0, E'_1$ ) bear the ratio  $\Delta V/\Delta V' = a/b$ . By tracing out the equipotentials of the same value in arithmetic progression in the two experiments, the quadrangular orthogonal network is obtained.

This type of conformal representation is very useful in problems of wind tunnel wall correction. The contour (c) corresponds in this case to the cross section of the tunnel (Ref. 21). As is known, what is then necessary is to determine the effects due to the images, with respect to the walls, of the free vortices. The problem is treated easily in the plane of the rectangle because the effect of these images, taken with respect to straight line walls, is easy to determine.

In these rheoelectric realizations it is often advantageous to replace the tank by a conducting paper model. Fig. V-3 shows a model of this type which was utilized to calculate wind tunnel wall corrections in an elliptic tunnel with a floor. In the photograph are shown the two Teledeltos models which were needed to represent the functions  $\varphi$  and  $\psi$ .

It will be noticed that the two models are here placed in series so as to be experimentally examined simultaneously. It is interesting to note, in this regard, that the measurement of the common potential,  $V_m$ , of the two electrodes which are joined gives directly the ratio  $a/b$  of the sides of the rectangle. It is easily shown, in fact, that

$$a/b = \sqrt{\frac{V_m}{100 - V_m}}$$

( $V_m$  being measured in the usual 0-100 scale; in this experiment the value  $V_m = 68$  was obtained). (The trace of the upper field was superposed on the lower model.)

The preceding rheoelectric set-ups can also serve to define the conformal transformation of the interior of (c) on a circle (C). Let C, A, B be three arbitrary points of (c) which are made to correspond to the three points  $\gamma, \alpha, \beta$  of the circumference which differ by arguments of  $\pi/2$  (Fig. V-4). Let  $\delta$  be the fourth point similarly defined on the circumference and D its homologue on (c).

The position of D is at first unknown, and it must be determined. Let us suppose for an instant, that the problem is already solved, and let us imagine that it be attempted to apply the region interior to (c) onto a rectangle by using the method described above. In this case a square would be found, the corners  $A_1, B_1, C_1, D_1$  of which would be the points corresponding to A, B, C, D.

This supposed operation indicates the procedure to be followed in the actual problem at hand. The contour (c) is fed by electrodes  $E_0, E_1$ , placed along the arc AB and the arc  $CD'$ , the point  $D'$  being fixed at first and chosen where it is presumed that D will fall. The electrical resistance between these two electrodes is measured. If it is smaller than that of a square, the arc  $CD'$  is too long, and the electrode  $E_1$  must be shortened somewhat. (By the resistance of a square must of course be understood the resistance measured between opposite electrodes placed on two parallel sides of a square conductor of the same nature as the model for (c), i.e. a model having the same h and  $\sigma$ .)

After a few trials the correct length of the electrodes is found and the point D is precisely defined. It remains to trace the

lines  $\varphi = \text{constant}$ , then using the second analogy, to define the conjugate function  $\psi$ . The complex potential  $f = \varphi + i\psi$  is also easily determined in the plane of the circle.

## VI. ANALOG STUDY OF AIRFOIL CASCADES

The study by rheoelectric analogy of cascades of airfoils may be undertaken in various ways according to the objective of the problem. If the complete form of the flow about the blades of a given cascade system is desired, for example, by definition of the streamlines or lines of constant velocity for the whole field, it is evidently necessary to use an analog model which gives the direct picture of the phenomenon in the tank. But when a systematic analysis of the contour velocity and pressure distributions on the blades is sought, with variations of different parameters such as the blade angle, the blade pitch (blade separation), the angle of attack, etc., it is often advantageous to use the mixed process of analog and analytic calculation, using the electric tank to accomplish the appropriate conformal transformations.

In the following sections these different aspects of the problem will be examined and some of the methods and experimental set-ups used will be considered.

### (a) Direct Representation of the Flow in a Cascade

In brief review, it may be recalled that a cascade may be defined by the form of the airfoil section used, the reduced pitch,  $\delta = a/l$ , (ratio of the distance of separation  $a$  between the airfoils to the chord  $l$  of the airfoil), and the blade angle,  $\omega$ , (angle between the airfoil chord and the perpendicular  $Ox$  drawn to the translation vector

which serves to generate the cascade). Usually the upstream current is identified in terms of its velocity,  $U_1$ , and its direction  $\alpha$ . The first problem to solve is the determination of the downstream current velocity,  $U_2$ , and its direction,  $\beta$ .

The most immediate electrical analogy procedure consists in making a set-up according to analogy B, identification of the stream function,  $\psi$ , with the electric potential and use of conducting models. As it is clearly impossible to represent an infinite number of airfoils in the electric tank, the field is limited to that fraction of the flow comprising five to seven airfoils. The corresponding boundaries are taken along the two streamlines which touch the outermost airfoils. The shape of these streamlines is obviously unknown; however, without much error, and at least as a first approximation, they may be taken as straight lines.

The analog set-up is then as shown in Fig. VI-1. The straight streamlines are represented by the electrodes  $E_0, E'_0$  and  $E_1, E'_1$  located so that  $E_0, E_1$  and  $E'_0, E'_1$  are parallel two by two. These electrodes are connected and hinged ahead and behind the outermost electrodes. The airfoil models, made of conducting material, are electrically fed, to satisfy the Joukowski condition, by the potentiometers,  $p_1, p_2, \dots, p_n$ . Since the field of streamlines is periodic, the corresponding potentials are adjusted in arithmetic progression. If, for example, five airfoils are used, and if the outermost airfoils are raised to 0 and to 100 respectively, then the intermediate airfoil sections must be raised respectively to the potentials 25, 50, and 75.

Once these adjustments are made, it must be verified that the Joukowski condition be satisfied for the middle airfoil, and, as well, for the two adjacent airfoils at least.

If not, the orientation of the downstream electrodes,  $E'_1$  and  $E'_0$ , must be changed in order to obtain the correct departure of the trailing edge streamlines. In practice, it is known that the direction of the downstream flow is little influenced by the upstream angle of attack. This property is therefore utilized to adjust the electrodes properly.

The analog representation is better when the hinge points,  $A_0$ ,  $A_1$ , are chosen near the stagnation point,  $A$ , on the profile because the streamline which touches an airfoil there is close to a straight line. The current flowing from each of the middle airfoil models can also be measured. From this is deduced the magnitude of the circulation,  $\Gamma$ , (which must be the same for each airfoil). It thus can be ascertained whether or not its value corresponds to the angular deflection,  $\alpha - \beta$ , according to the known formula,  $\Gamma = (U_1 \sin \alpha - U_2 \sin \beta)a$ .

A good experimental set-up demands that the tank field be limited far enough upstream and downstream from the airfoil by insulating walls,  $I_0I_1$ ,  $I'_0I'_1$ , which are perpendicular to the electrodes.

The streamlines may be obtained by reading off the electrical equipotentials. An example is presented in Fig. VI-2. The field of constant velocity lines can be obtained by means of the device of J. Miroux described in Section III(f) (Fig. VI-3). It may also be sufficient to measure the velocities on the contour of an airfoil by means of the Hargest device for displacing a single probe (Ref. 38).

It is unusual in these problems to try to represent the velocity potential,  $\varphi$ , (analogy A). It may be noted however, that knowledge of the streamline which ends on the middle blade (which can be accurately ascertained

in the preceding experiment) can lead to a simple model in analogy A. This analog model is then bounded by two of these same lines which are represented by two insulating walls. It is fed by two electrodes,  $E_0$  and  $E_1$ , placed upstream and downstream (Fig. VI-4).

Use of conducting paper is often convenient for representing one or another of the two analogies. The two procedures can also be used together. For example, the Teledeltos paper can be used to represent the streamline from the central airfoil, in conjunction with a model similar to that of Fig. VI-1; the electric tank, reduced to contain only a single conducting airfoil model and the electrodes  $E_0$ ,  $E_1$ , curved as needed, is employed. In this way the fairly difficult construction of several blade models can be avoided, and, at the same time, the benefit of the precision of the electric tank can be retained for the second experiment. This precision is always better than that of the conducting paper, particularly for velocity determinations through gradient measurements.

It is clear that the analog models described above need not be limited to infinite cascades. In practice, it is often required to analyse the flow through turns equipped with vanes. In this case the analogy methods can serve as a convenient guide to finding the most effective arrangement of these vanes. An example of this kind is represented in Fig. VI-5. There the problem was to conduct off a partial flow of variable amount from a turn located in extension of a jet engine intake channel. By successive displacements of the turning vane models, a satisfactory division of the flow was accomplished. The flow fields obtained led to the prediction of operation without separation in the real fluid. In the analog model the right hand wall was

at potential 0, the left hand wall at 100. The third wall was raised to the potential corresponding to the percentage of flow to be tapped off, the potentials of the guide vanes being adjusted so that the Joukowsky condition was satisfied.

(b) Analog Set-up Based on the Periodicity of the Field

It is possible to create an analog set-up which is based on the periodic character of the flow field through a cascade of airfoils or blades. Although the corresponding electric equipment may appear complicated, it is worth examining here, if only for the generalizations which can be made therefrom with a view to dealing with other problems of periodic flows.

Let us consider a straight band  $MM'NN'$  (Fig. VI-6) containing a single airfoil of a cascade and having as width, parallel to the y-axis, the pitch length,  $a$ , of the cascade. In passing from any point  $A'$  of  $M'N'$  to another point  $A$  of  $MN$  on a line parallel to the y-axis, the stream function,  $\psi$ , increases by a constant amount the value of which may be calculated at infinity upstream or downstream of the field, thus:

$$\delta\psi = U_1 a \cos \alpha = U_2 a \cos \beta. \quad (28)$$

Similarly, the velocity vector is the same at  $A$  and  $A'$  and the flux entering across an element of arc  $ds'$  surrounding  $A'$  is the same as the flux leaving across an identical element  $ds$  surrounding  $A$ .

If the stream function,  $\psi$ , is identified with the electric potential,  $V$ , of a tank which represents the band  $MNM'N'$ , the conditions to be fulfilled at the boundaries

are the following:

(1) For any pair of opposite points, like  $A$  and  $A'$ , the potential difference is constant and of known value according to Eq. (28).

(2) The electric current which enters through  $ds'$  at  $A'$  is the same as that leaving through  $ds$  at  $A$ .

To satisfy these conditions, the segments  $MN$  and  $M'N'$  can be covered with a series of small paired electrodes ( $e, e'$ ) which represent the elements of the arcs  $ds, ds'$ . Each pair of electrodes is fed by a transformer,  $T$ , which produces the desired potential difference at its terminals and automatically satisfies the second condition above.

The upstream and downstream conditions must also be examined. Sufficiently far from the airfoil, the fields being uniform, the function,  $\psi$ , varies linearly along  $MM'$  and  $NN'$  and a corresponding distribution of the electrical potential must be assured. To accomplish this there can be used once more a series of small electrodes the potentials of which are adjusted according to the necessary linear distribution. Also, according to the analogy, the electric current traversing  $MM'$  must be equal to  $\sigma hU_1 a \sin \alpha$ ; likewise, the current which traverses  $NN'$  must equal  $\sigma h U_2 a \sin \beta$ . The difference between these two values corresponds to the circulation,  $\Gamma$ , of the airfoil, i.e. to the electrical current flowing out of the electrode which materializes it.

The electrical set-up is shown in Fig. VI-6. In order to adjust in an easy manner the potential difference between  $e$  and  $e'$ , it is convenient to install, between the electrodes and the transformer secondary, a small potentiometer,  $p$ . The potentials of

the electrodes situated along MM' and NN' are adjusted by means of variable resistances,  $r_M$  and  $r_N$ . The potentiometer,  $\pi$ , serves to feed the airfoil. The correct values of current through MM' and NN' are obtained by means of the potentiometers  $\pi_M$  and  $\pi_N$ . To sum up, after the potential difference between each pair of electrodes (e,e') has been established, the potentiometers  $\pi_M$ ,  $\pi_N$ , and  $\pi$  are adjusted so as to satisfy the Joukowski condition and obtain simultaneously the desired direction,  $\alpha$ , of the upstream flow.

The reading off of the streamlines is carried out by the usual process, and the complete field is restored by drawing in the lines cut off by the boundaries MN and M'N'.

Once the electrode-carrying boundary elements are made and the electrical set-up required by the transformers is provided (40 or 50 are needed), exploitation of this analog procedure is convenient. Construction of only a single model is necessary. Finally, this analog representation is the only one which may be used to represent the picture of a compressible flow, for in this latter case the tank bottom must be modeled by successive approximations (see Section XII). This operation is relatively easy to carry out in a narrow band around a single airfoil, while it would be extremely long and difficult with the set-up of Section VI (a).

#### (c) Methods Based on Conformal Mapping

For the solution of problems of cascades of turbine or compressor blades by the mixed process of analogy and analysis, there exists a choice among various types of conformal transformations (Refs 20, 26, 33, 29). This choice depends on several factors. An analog representation which is simple and easy to carry out may be chosen,

leaving, on the other hand, a greater volume of analytic calculations; it may also be desired to consider only a single cascade arrangement, or, contrariwise, to require a systematic study of the influence of fundamental parameters like the pitch and the blade angle setting. To make these points clear, certain of the set-ups which have been used will be described.

The first method to be described starts from the well-known transformation

$$Z = e^{2\pi \frac{z}{\alpha}} \quad (29)$$

which establishes a correspondence between the z-plane of the cascade and the Z-plane in which all airfoils (c) of the cascade have a single homologue (C) (Fig. VI-7).

The points at infinity in the second and third quadrants of the z-plane have the origin  $Z = 0$  as image in the new plane. The point  $Z_\infty$  corresponds to the points at infinity located in the first and fourth quadrants of the z-plane. As a result, the complex potential of the flow through the cascade, which behaves, for  $(z_\infty, x < 0)$ , like  $U_1 e^{-i\alpha} z$ , must be equivalent in the neighborhood of  $Z = 0$  to

$$\frac{aU_1}{2\pi} e^{-i\alpha} \log Z \quad (30)$$

and therefore has the same singularity as a point source-vortex of intensity  $aU_1 e^{-i\alpha}$  placed at this point.

It can also be seen that when  $|Z|$  increases indefinitely the complex potential of the Z-plane has the same singularity as a point vortex-sink of intensity  $aU_2 e^{-i\beta}$  located at infinity. It may also be verified that this sink absorbs the outflow from the

source, and that the difference of intensity between the vortices is in fact equal to the circulation existing about the airfoil (c).

The flow about (C), together with the vortex-sources and vortex-sinks which have just been examined, is known when there has been determined the conformal representation  $\zeta = f(Z)$  which maps the exterior of (C) onto the exterior of the unit circle ( $|\zeta| = 1$ ) ( $\gamma$ ) of the  $\zeta$ -plane, the points at infinity of the two planes being made to correspond. If  $M_0(\zeta_0)$  is the point in the  $\zeta$ -plane corresponding to the origin  $Z = 0$  of the plane of (C), then there will be a source of strength  $\alpha U \cos \alpha$  and a vortex of strength  $\alpha U \sin \alpha$ .

Use of the method of images places analogous singularities of proper sign at the point inverse to  $M_0$  with respect to ( $\gamma$ ) and at the origin  $\zeta = 0$ . The expression for the potential  $\Phi(\zeta)$  in the  $\zeta$ -plane is then easily obtained, and the condition which determines the circulation about the airfoil is that the complex velocity  $d\phi/d\zeta$  be zero at the point  $\pi$  which is the homologue on ( $\gamma$ ) of the point P on the airfoil (C).

In this problem the rheoelectric method is used only to define the conformal transformation  $\zeta = f(Z)$ . For this the procedure indicated in Section V (b) is used. This procedure defines the correspondence between the exterior of (C) and the exterior of the circle ( $\gamma$ ) and properly locates, in particular, the point  $M_0$ , homologue in the  $\zeta$ -plane of the origin  $Z = 0$ .

This method for studying cascades has been applied in various practical cases. It is easy to use except in the case where the cascade is closely spaced, for in the case of a low value of pitch, the point  $M_0$  falls very near the circle. This fact brings about certain difficulties in the velocity determinations. There is also another disadvantage in that it is necessary to employ as many

different models (C) as there are values of  $\epsilon$  and  $\omega$ , even if the airfoil (c) of the cascade studied remains unchanged.

Other conformal transformations, in which the preceding exponential function  $Z$  plays a different role, may be conceived of. In particular, certain internal problems can be treated (Fig. VI-8). Consider, for example, the transformation  $Z' = 1/(Z + 1)$  wherein the source and sink (or vortex) singularities are located at the points  $Z' = 0$  and  $Z' = 1$ . The flow field occupies the interior of the single contour (C') which corresponds to (c).

The solution of such a problem is immediate if there be known the conformal mapping of the inside of (C') onto the inside of a contour with respect to which the images of the singularities may be taken. Now, it is known, from Section V (c), that the mapping of the inside of C' on the surface of a rectangle is an operation easily accomplished in the electric tank.

To avoid, on the one hand, the construction of the numerous models required by the two preceding methods, and to avoid, on the other, the difficulties of calculation of cascades having a low pitch value, another mixed method, convenient and of quite general nature, has been developed (Ref. 33).

The notion of equivalent lattice or cascade is used. This concept employs the definition, for each pair of values ( $\omega, \epsilon$ ) of the real cascade, of a pair ( $\omega_1, \epsilon_1$ ) which has the property that the cascade made up of straight line segments having pitch  $\epsilon_1$  and blade angle  $\omega_1$ , possesses the same circulation as the real cascade, at all angles of attack.

The electric analogy is used to define the equivalent lattice, i.e. ( $\omega_1, \epsilon_1$ ), from

knowledge of  $(\omega, \epsilon)$ , as well as to define the correspondence between contours of the real blade sections and the equivalent segment. To carry this out the flow at zero lift incidence about the real cascade is studied in the electric tank.

First, analogy B is used. A group or stick of five or seven conducting models of blade sections representing a portion of the cascade in question is placed as shown in Fig. VI-9, in a plane tank fed by two straight electrodes,  $E'_0, E'_1$ . The whole is movable and can pivot about the midpoint. There is thus determined the orientation to be given to the stick of airfoils in order to satisfy the Joukowski condition without passing current through them (condition of zero circulation). The electrical equipotentials then represent the streamlines through the cascade for zero lift incidence. The inclination of the lattice with respect to the electrodes,  $E'_0$  and  $E'_1$ , defines zero lift incidence and thus the blade angle,  $\omega_1$ , of the equivalent lattice.

The complex potential,  $f(z)$ , the imaginary part,  $\psi$ , of which was determined in the preceding experiment, represents the function which maps the proposed cascade on the equivalent lattice. The preceding flow field mapped onto the plane of  $f = \varphi + i\psi$  becomes a uniform flow at zero lift about a lattice of straight line segments. As a result, any potential difference read off in the tank can be represented in terms of a length in the plane of these segments.

Thus, in order to obtain the chord length,  $l_1$ , of the segment equivalent to a given blade section of the cascade, it is only necessary to use analogy A. Here the models of blade sections are insulating and placed at the zero lift incidence, known from analogy B. Let  $\delta V$  be the potential difference measured between the trailing edge, P, and the stagnation point, A, at the leading edge of

the airfoil section. The chord  $l_1$  of the equivalent segment is given by

$$l_1 = \frac{\delta V}{100} L$$

where L is the distance between the two electrodes  $E_0$  and  $E_1$ . The pitch,  $\epsilon_1$ , of the equivalent lattice is then given by

$$\epsilon_1 = \frac{\bar{a}}{l_1 \cos \omega_1}$$

Knowledge of the characteristics  $(\epsilon_1, \omega_1)$  of the lattice of equivalent segments is all that is necessary for determining the operation of the given cascade; hence it is sufficient to measure  $\omega_1$  in analogy B and thereafter  $\delta V$  in analogy A.

If the mapping between an airfoil of the cascade and a segment of the equivalent lattice is desired, the electric potential, V, (analogy A) must also be read off along the contour of the model. The homologue of a point, M, on the blade section having potential, V, is the point,  $\mu$ , on the equivalent segment located at the relative distance  $x/l_1$  from the leading edge as given by

$$x/l_1 = \frac{V - V_A}{\delta V}$$

where  $V_A$  is the potential of the stagnation point A of the blade.

The distribution,  $V(s)$ , along the blade contour can give, through differentiation, the modulus of the conformal transformation. It is then easy, from a knowledge of the velocity distribution on a line segment of the equivalent lattice for a given angle of incidence, to derive the corresponding distribution over the blade section of the given cascade. This type of calculation is well known.

The reading off of the potential, V, must be done along the central blade section model of the analogy in order to reduce to a minimum the errors due to the limited number

of blades and to the approximation made at the boundaries by taking the streamlines straight (electrodes  $E'_0$  and  $E'_1$ ). It may be remarked that this latter approximation is legitimate in the case of flow at zero lift, as here.

In conclusion there will be mentioned an interesting method conceived by R. Legendre and carried out experimentally by J. Revuz (Refs. 50, 56). This method determines the flow in a cascade taking compressibility effects into account. The study is carried out in the hodograph plane starting with a given velocity distribution. The form of the airfoil or turbine blade section involved is obtained by subsequent calculations. To shorten the work, the electrical analogy is used to determine the field distribution of an auxiliary analytic function defined on a Riemann surface. The Teledeltos paper method is used for this purpose. It should be pointed out that this method serves to obtain, from a single analog experiment, a family of blade sections depending on several parameters.

## VII. ANALOG STUDY OF FLOWS OF REVOLUTION

### (a) Principle of the Analogy

It is known that the velocity potential,  $\varphi$ , and the stream function,  $\psi$ , of an axially symmetric flow can be defined in a meridian half-plane defined by taking the x-axis as axis of revolution and y-axis directed outward in the meridian plane. These functions satisfy the following equations

$$\frac{\partial}{\partial x} \left( y \frac{\partial \varphi}{\partial x} \right) + \frac{\partial}{\partial y} \left( y \frac{\partial \varphi}{\partial y} \right) = 0 \tag{31}$$

$$\frac{\partial}{\partial x} \left( \frac{1}{y} \frac{\partial \psi}{\partial x} \right) + \frac{\partial}{\partial y} \left( \frac{1}{y} \frac{\partial \psi}{\partial y} \right) = 0 \tag{32}$$

It is natural to compare these equations with those governing the electrical potential,  $V$ , in a conducting medium of slowly varying thickness,  $h$ , (Eq. (5)). Depending on whether it is desired to represent the velocity potential,  $\varphi$ , or the stream function,  $\psi$ , by electrical analogy, there must be used an electric tank in which the liquid depth,  $h$ , is proportional, or inversely proportional to the distance,  $y$ , from the axis of symmetry (x-axis).

### (b) Representation of the Velocity Potential: Inclined Tank

The most direct analog representation is that for the velocity potential,  $\varphi$  (analogy A). A tank having a flat, inclined bottom is used. It may be remarked that in this way there is represented a slice of the three-dimensional flow which is contained between two meridian planes, one of which is the tank bottom and the other the free liquid surface. The edge of the liquid dihedral thus formed corresponds to the axis of revolution  $x$ . The slope of the bottom may therefore be chosen arbitrarily. It is generally taken rather small, from 3 to 12 degrees, in order to simplify the model construction.

Inclined tanks are built of the same materials as plane tanks. Typical dimensions are 150 cm x 100 cm (Fig. VII-1). In order to define the axis of symmetry precisely, a fine horizontal line may be scribed on the inclined bottom, and the quantity of liquid may be regulated so as to bring the liquid surface just to the scribed line. Since the free surface should be perfectly plane in the neighborhood of the axis, the formation of a convex or concave meniscus should be avoided at the line. To reduce capillarity effects, a thin layer of detergent "teepol" may be spread along the axis. Finally, it is important to construct the bottom of the tank of a perfectly insulating material, for the slightest conductivity, even

superficial, can introduce errors in the region near the axis where the liquid is not very deep.

In the case of small slope of the bottom, the models of objects to be studied are cylindrical having vertical generating lines; the right section of the cylinder reproduces the meridian contour of the obstacle. The reading off of the potential is done on the free surface by an exploring probe penetrating relatively little into the liquid. The experimental procedure is the same as that utilized in plane tanks to trace the equipotential lines, to measure gradients, and to determine the curves of constant velocity.

### (c) Applications of the Inclined Tank

The simplest application is to flows about streamlined bodies of revolution. The inclined tank is electrically fed in this case by two electrodes,  $E_0$  and  $E_1$ , placed along the lateral boundaries. The insulating model is placed in the central region near the axis (Fig. VII-2). There is thus pictured a uniform field, parallel to the x-axis, disturbed by the presence of the streamlined body. The object of the experiment is generally to determine the local velocity distribution on the contour of the body.

The inclined tank has often been used for the study of convergent wind tunnel ducts, for finding the best location of entrance filters, for improving the form of a conduit having circular ring section, or to modify the contour of the convergent duct in the region of the test section with the purpose of attenuating an unfavorable gradient and assuring a velocity distribution as uniform as possible (Ref. 43).

The most recent applications have been to flows in axially symmetric air intakes with or without central body (Ref. 28). The

ratio of the entering velocity,  $U_e$ , to the velocity at infinity,  $U_\infty$ , varies according to the operating regime of the axial-flow machine in question, and it must be ascertained whether or not for typical values of this ratio the design of the intake causes locally unfavorable velocity peaks.

The analog model is easy to construct. In addition to the two electrodes at the tank ends there must be provided one auxiliary electrode  $e$  at the inner end of the air intake model (Fig. VII-3). Its potential must be adjusted to obtain the desired value of the ratio  $U_e/U_\infty$ . The current,  $I$ , flowing through this electrode corresponds (to within a scale fact or easily determined) to the intake flow.

The velocity distribution at the intake entrance can thus be studied, and the form of the entrance can be modified to obtain a good adaptation to all the operating regimes of the machine. For this purpose, a part of the model is often made of paraffin or any other material which can be cut or modeled. In this way, a few simple trial experiments in the electric tank often have given rise to notable improvements in an initially poor air intake design.

To conclude, there will be cited an example of an inclined tank experiment in which circulation was represented. The practical problem was as follows. A radiator surrounds a streamlined body of revolution. In order to improve the airflow around the body and through the radiator, the latter was covered by an annular fairing having an airfoil section contour. The presence of the radiator causes a head loss in the flow between the fairing and the body of revolution, this head loss being exactly compensated by the pressure rise created by a fan placed behind the radiator. Under these conditions, the flow takes place as if the group consisting of the radiator and fan did not exist,

and there remains only the problem of determining the aerodynamic flow field around an annular fairing in the presence of a body of revolution (Fig. VII-4).

As a result, it is necessary to represent in the tank the circulation around the airfoil composing the fairing. Since analogy A is used, a cut must be made in the field. This cut can be made along an equipotential line running between the fairing and the body. The separation of these two elements being small, the unknown form of the equipotential line can be well approximated by a straight line segment normal to the two contours. This cut is made in the tank of a thin insulating strip carrying two electrodes,  $E_2$ ,  $E_3$ , on its two faces.

The potential difference applied to these electrodes corresponds to the value of the circulation (see Section IV (a)). The electrical circuits are standard ones - the potential difference is obtained by means of a potentiometer,  $p$ , connected to the secondary of a transformer,  $T$ . Its value is adjusted so as to satisfy the Joukowsky condition at the trailing edge of the fairing. For this purpose, two probes,  $t_1$ ,  $t_2$ , are placed so that the direction  $t_1, t_2$  is perpendicular to the bisector of the trailing edge angle. The potential adjustment is correct when the two probes take on the same potential (Fig. VII-4c).

The fluid flow in the channel formed by the fairing and the streamlined body (flow which is therefore that through the radiator) corresponds in the analogy to the electric current,  $I$ , flowing through the electrodes of the cut. The measurement of this current thus gives the value of the flow. This current is directly linked to the value of the voltage between  $E_2$  and  $E_3$ . The electric circuit shows clearly the mutual dependence of the flow through the radiator and the circulation about the fairing. To obtain

the desired flow it was then necessary to provide a means of regulating the circulation, which could not be accomplished without modifying the contour of the fairing and in particular the position of the trailing edge (by means of a curved flap, for example).

(d) Representation of the Stream Function. Tank with Hyperbolic Bottom

The analog representation of the stream function,  $\psi$ , of an axially symmetric flow requires, according to Eq. (32), construction of a tank wherein the liquid depth varies as  $1/y$ . It is therefore necessary to form the bottom so that a vertical section represents a hyperbola. A difficulty arises immediately. In the neighborhood of the edge which represents the x-axis, the depth will increase very rapidly, becoming infinite on the axis of revolution. This condition is in flagrant contradiction with the hypothesis used to write Eq. (5) wherein a slow variation of  $h$  was supposed, the electrical potential being supposed independent of the vertical coordinate  $z$ .

It appears that use of analogy B for axially symmetric flow has been avoided because of this difficulty. This analogy still remains interesting, however, because it is useful for obtaining the direct traces of the aerodynamic streamlines (which are often more intuitively helpful than the field of velocity potential). Moreover, it can be used easily to represent the circulation in the case of a ring-shaped object having a meridian contour in the shape of an airfoil.

The above difficulty can be avoided by finding an analog representation which, while giving an adequate approximation in the axis region, depicts the stream function  $\psi(x,y)$  by a suitable distribution of the electrical potential  $V(x,y)$  at the free surface of the liquid.

Note first that in the immediate neighborhood of the axis of revolution, which is the streamline  $\psi = 0$ , the derivative  $\partial\psi/\partial x$  is usually negligible with respect to  $\partial\psi/\partial y$ , so that it can be legitimately supposed that, near this axis,  $\psi$  is proportional to  $y^2$ , the square of the radial distance from the axis.

More explicitly, let us consider the case of a uniform flow for which this distribution of  $\psi$  is rigorously correct. If the velocity parallel to the x-axis is  $U$ , the stream function is given by

$$\psi = Uy^2/2. \tag{33}$$

The streamlines are obviously parallel to the axis of revolution in this case.

The equivalent electrical picture of such a flow may be obtained by passing current into the tank with hyperbolic equilateral bottom through two plane electrodes,  $E_0, E_1$ , placed as follows (Fig. VII-5). Electrode  $E_0$  passes through the axis of revolution and is inclined at 45 degrees; the other,  $E_1$ , lies vertically against the edge of the tank opposite the x-axis.

The special location of the axis electrode, inclined at 45 degrees, makes it possible to limit the depth of the tank in the region where it would tend toward infinity, thus assuring an electrical potential distribution at the free surface of the liquid which satisfies Eq. (33). It can easily be verified that this is so by studying the distribution of electrical potential,  $v$ , in any vertical section of the tank (yz-plane).

If the complex function  $f = v + iw = \zeta^2$  be considered, where  $\zeta = y + iz$ , the potential,  $v$ , and its conjugate,  $w$ , are given by:

$$v = y^2 - z^2 \qquad w = 2yz \tag{34}$$

At the free surface of the tank ( $z = 0$ ) it may be verified that the distribution of electrical potential,  $V$ , ( $V \equiv (v)_{z=0}$ ) is proportional to  $y^2$ . The inclined electrode  $00_1$  having constant potential, corresponds to the line  $v = 0$ . The electrode  $MM_1$ , placed at the other extremity, represents a small arc of a certain hyperbola  $y^2 - z^2 = \text{constant}$ . This small arc may be taken as identical with a vertical straight-line segment.

The line  $w = 0$  corresponds to the free surface, and a particular line ( $w = \text{constant} = 2k$ ) may be identified with the hyperbolic contour,  $O, M_1$ , of the tank bottom:

$$z = \frac{W_1}{2y} = \frac{k}{y}. \tag{35}$$

Finally, it may be verified that the electrical resistance measured between the electrodes  $E_0$  and  $E_1$  actually corresponds to the resistance of a conductor having resistance inversely proportional to the distance from one of its edges. This resistance is equal to

$$R' = \frac{L'^2}{2k\sigma L} \tag{36}$$

where  $L$  and  $L'$  represent the dimensions of the tank in the x- and y-directions, respectively;  $\sigma$  is the conductivity of the liquid; and  $k$  is the factor of proportionality in Eq. (35).

The analog representation, rigorously correct in the case of a uniform field, may be used for most axially symmetric fields. Analysis of particular theoretical cases (flow about a sphere, flow in a theoretical converging conduit) has shown that the proposed approximation is legitimate even in the case of an object placed on the axis, provided that a sufficiently large scale be taken to represent the model (for example, in the case of the

sphere, the radius had to be about twice as large as the projection of  $OO_1$  on  $Oy$ ).

With this set-up it is easy to represent a circulation,  $\Gamma$ , about a meridian section of an annular object and fulfill the trailing edge Joukowski condition as need arises. The section contour is represented in the tank by a conducting model which acts like an auxiliary electrode.

It is also easy to link the value of electric current which flows with the magnitude of the circulation. It can easily be shown that

$$\Gamma = - I/k\sigma. \quad (37)$$

If use is made of the flow far from the object ( $\psi = Uy^2/2$ ) there is obtained  $U = 200/L^2$ . If the usual value 100 is taken to represent the potential difference between electrodes, the relation

$$\frac{\Gamma}{U} = - \frac{\Delta V}{200} \frac{L^2}{Rk\sigma} \quad (38)$$

is obtained, where  $\Delta V$  represents the potential drop across the terminals of the resistance,  $R$ , which conducts the current,  $I$ .

If the value  $R'$  of the tank resistance is introduced into this expression from Eq. (36), there is obtained:

$$\frac{R}{U} = - L \frac{R'}{R} \frac{\Delta V}{100} \quad (39)$$

a formula analogous to that used to measure the circulation about a plane object (see Eq. (20), Section IV (a)).

Various applications of analogy B have been carried out, studying flows about annular

objects and comparing the results thus obtained with those obtained in the corresponding plane fields. Fig. VII-6 gives, as an example, the streamlines of an axially symmetric flow about a meridian section having the form of an airfoil. Fig. VII-7 gives, for the same case, the lines of constant velocity about the airfoil according as the axially symmetric or the two-dimensional flow motion be considered (airfoil near the ground in the latter case).

### VIII. ANALOG REPRESENTATION OF THREE-DIMENSIONAL FLOWS

The analog representation of three-dimensional flows of a perfect, incompressible fluid is immediate insofar as its principle is concerned. The velocity potential  $\varphi(x,y,z)$  is a harmonic function of the three rectangular space coordinates  $(x,y,z)$  and can therefore be identified with the electric potential  $V(x,y,z)$  in a deep tank wherein the boundaries represent those of the field to be studied.

With the exception of lifting problems, certain of which will be considered in a subsequent chapter (Chapter XI), the conditions defining  $\varphi(x,y,z)$  are generally quite simple. The objects placed in the flow and the physical boundaries of the fluid, are materialized in the electric tank by insulating models. The flux, which corresponds to the electric current, can be represented by the correct electrical feeding of certain electrodes the forms of which reproduce the known surfaces  $\varphi = \text{constant}$ .

As far as the experimental technique is concerned, there is little that needs to be added to the descriptions and indications given in the preceding chapters. The deep electric tanks are usually constructed of insulating material, slate slabs or glass plates, for example. Their dimensions may

vary according to the applications envisaged. Tanks as large as 2 x 1.5 x 1.5 meters have been built, but generally, smaller dimensions of the order of one cubic meter are used.

The only special item to be noted is the construction of the exploratory probe and its use in determining the field. The probe is usually made of a glass tube, of very small diameter but nevertheless sufficiently rigid, the tip being drawn out as a capillary tube. A fine platinum wire, imbedded and sealed in the capillary tube, has a projecting tip which serves as a conducting electrode. The platinum tip is connected, by means of a wire passing through the tube, to a zero indicator. At its upper end, the glass tube is held vertically in a rigid metallic cylinder which serves as a guide. The whole is carried by the small cross-slide of the mechanical carriage described in Section III (d).

In addition to the two right-angle horizontal displacements given by the cross-slide and the large carriage, a vertical probe displacement must of course be provided. To accomplish this a rack-and-pinion device is fastened to the cross-slide to facilitate raising and lowering the probe or to hold it at a fixed depth. This device should also contain a positioning graduation for measuring the probe level.

The determination of the equipotential surfaces is carried out by defining their isopotentials, i.e. by tracing the equipotential curves in successive horizontal planes taken at fixed separations. For each horizontal plane, the experiment is carried out in the same way as in the two-dimensional tank, and use can be made of an automatic equipotential tracer. It should be remarked, however, that these experiments are considerably less simple than in the flat or inclined tanks, and often the form of the objects placed in the flow requires the use of curved probes in order to reach certain regions of the field.

The simplest application concerns the flow about an object placed in a stream which is uniform at infinity. The tank is fed electrically by two parallel electrodes applied against two opposite vertical sides of the tank and directly connected to the terminals of the generator. The model of the object, made of insulating material, is placed in the middle of the tank.

In general, the flow and the object are both symmetric with respect to one or two planes which should be used to best advantage to reduce the analog field to a half- or quarter-space. For example, in the case of a symmetry about the  $xz$ -plane, a half-model can be built which is applied either to one of the vertical walls or to the bottom of the tank. In the same way, the free surface of the liquid may also be identified with the plane of symmetry.

This type of representation has been used by R. Duquenne and C. Grandjean for studying thick delta or sweptback wings having symmetrical airfoil sections at zero lift. The half-model was placed over the tank, and the potential measurements were carried out using fine probes made up of metallic wire buried in the plexiglass model beforehand so as to emerge just flush with the wing surface.

In this way flows over streamlined bodies and nonlifting fuselages may be analyzed. Interesting studies have even been carried out on complete airplane models. At the Swedish company, SAAB, L. Stenstrom (Ref. 46) utilized a special set-up to evaluate the three components of velocity at arbitrary points of the flow field. He determined them by measuring the components of the electric field by means of a small auxiliary tank ( $e_0, e_1$ ) (Fig. VIII-1).

The operations are carried out as follows. The main probe,  $p$ , being brought to the point

where it is desired to take a reading, its potential is matched by that of the auxiliary probe,  $p_A$ , by adjusting the potentiometer,  $p_i$ . Then the main probe is displaced a small distance (known and constant), 1mm. for example, in one of the  $x$ ,  $y$ , or  $z$ -directions. To reestablish the equality between the potentials of  $p$  and  $p_A$ , the auxiliary probe must be displaced by a certain quantity  $\delta X$  which is then precisely measured by means of a micrometer. When this operation has been carried out for the three directions  $x$ ,  $y$ ,  $z$ , the three velocity components are obtained.

L. Stenstrom has used this method to study systematic shape changes undertaken on a single model. He cites the example of an airplane empennage study the purpose of which was to reduce the sharp velocity peaks around the fairings between horizontal stabilizer and vertical fin. The tank experiments were carried out as in the wind tunnel. The vertical location of the horizontal stabilizer was studied, shapes were modified by application of modeling clay to the model, etc. This example of the use of the electric tank, even though it does not take lifting phenomena into account, is a suggestive illustration of what may be obtained by electric analogy using simple and easy means.

The equipotential lines over the surface of the model may furnish useful information on the shape of the fluid filaments surrounding the object studied. If the orthogonal trajectories of these equipotential curves be constructed graphically, the streamlines over the surfaces of the object are obtained. The examination of the latter is often very instructive.

It may finally be mentioned that there is no difficulty to be encountered in representing an air intake on such models and in providing it with a variable inflow. It

is only necessary to fix, at the inner end of the air intake of the analog model, an auxiliary electrode, the potential of which may be adjusted to any convenient value in order that the current through it provide the correct image of the entering airflow.

Aside from these applications dealing with a uniform flow disturbed by the presence of an object, other analog representations of three-dimensional fields of interest to aeronautics can be envisaged. There is no special difficulty to be encountered, for example, in representing the theoretical flow through a closed tube. The model of the latter, constructed of insulating material, constitutes a special tank in which the same measurements as those described earlier can be carried out. Although this kind of model has not been extensively exploited, it appears that the electric analogy method might well make a certain contribution to the theoretical analysis of such internal aerodynamics problems.

#### IX. ANALOG STUDY OF LIFTING LINE PROBLEMS

##### (a) Principle of Solving Prandtl's Equation by Electrical Analogy

Numerous problems concerning the theory of the lifting line can be solved by the electrical analogy method. The simplest and best known application, for which the principle was laid down in 1932 (Ref. 7), is the numerical solution of Prandtl's integro-differential equation which defines the spanwise lift distribution along a straight wing. Various papers have been published on this subject (Refs. 8, 10, 11). A device called the "Wing Calculator," several examples of which have been built according to the above principle, has served aeronautical engineering designers for the past twenty years.

Although problems for straight wings evoke somewhat less interest today than formerly, the analog method to be explained will be begun with this simple case. Later will be described the various developments and generalizations which can be envisaged.

We begin with a brief review of the usual problem. Consider a straight wing placed in a uniform airstream having velocity,  $U$ , parallel to the  $x$ -axis. Let the wing have span  $2L$  along the  $y$ -axis. This wing is defined by:

(1) The variation of chord length,  $l(y)$ , along the span.

(2) The variation of the angle of attack,  $\alpha(y)$ , along the span (i.e. angle between the zero lift incidence of the local airfoil section and the wind direction).

(3) The variation along the span of the coefficients  $k(y)$  which characterize the lift characteristics of the airfoils ( $2k$  is taken as the slope  $dC_L/d\alpha$  for infinite aspect ratio).

The distribution of circulation,  $\Gamma(y)$ , along the span is given by the Prandtl equation

$$\Gamma = k l U (\alpha - \frac{w}{U}) \tag{40}$$

where

$$w = \frac{1}{4\pi} \int_{-L}^{+L} \frac{d\Gamma(\eta)}{y - \eta} \tag{41}$$

represents the induced downwash velocity at the point  $y$  of the span due to the free vortices.

To solve Prandtl's equation by electric analogy, the field of these free vortices is considered at infinity downstream (Trefftz plane). The properties of this flow are well known and will be only briefly recalled here. This is a plane flow field and can therefore be defined in the  $yz$ -plane (plane  $P$  of Fig. IX-1) where the complex variable  $\mu = y + iz$  will be taken.

The corresponding complex potential is expressed as follows:

$$f(\mu) = \varphi + i\psi = \frac{1}{2\pi} \int_{-L}^{+L} \log(\mu - \eta) d\Gamma(\eta). \tag{42}$$

It is single-valued if, as is the case in the wing problem, the function  $\Gamma$  becomes zero for  $y = \pm L$ , so that

$$\int_{-L}^{+L} d\Gamma(\eta) = 0.$$

The preceding expression also shows that passing from a point  $(y, z)$  to the point  $(y, -z)$ , symmetrically located with respect to the  $y$ -axis, causes  $\psi$  to take on again its same value, whereas  $\varphi$  changes to  $-\varphi$ .

Consider the values taken on by the function  $\varphi$  on the  $y$ -axis. Outside the lifting segment  $(-L, +L)$   $\varphi$  is clearly zero. At a point  $x$  of this segment  $\varphi$  takes on the respective values  $\varphi(y)$  or  $-\varphi(y)$  on the upper and lower sides of the  $y$ -axis. The segment  $(-L, +L)$  is therefore a line of discontinuity for  $\varphi$ . For an element  $dy$  of this segment, the circulation is clearly  $-2d\varphi = -d\Gamma$  whence, in view of the fact that  $\varphi$  and  $\Gamma$  become zero at the ends  $\pm L$ :

$$\varphi = \frac{1}{2} \Gamma. \tag{43}$$

Moreover, it is seen that the normal derivative is continuous across this segment. Its value at a point  $y$  of this segment is

easily calculated from  $df/d\mu$  and it can thus be verified, in view of Eq. (41), that

$$w = -\frac{1}{2} \frac{\partial \varphi}{\partial z} \quad (44)$$

It is now possible to specify the boundary conditions which define the function,  $\varphi$ . In view of the above discussion,  $\varphi$  need only be considered in a half-plane (for example, the side where  $z$  is positive), with the following  $y$ -axis boundary conditions:

(1)  $\varphi$  is zero outside  $(-L, +L)$ .

(2) At each point of the segment  $(-L, +L)$  there exists a linear relation between  $\varphi$  and  $\partial\varphi/\partial z$  which states the fundamental relation Eq. (40), as can be seen by putting Eq. (43) (for  $\varphi$ ) and Eq. (44) (for  $\partial\varphi/\partial z$ ) into Eq. (40) which yields

$$\varphi = \frac{k\ell U}{2} \left( \alpha + \frac{1}{2U} \frac{\partial \varphi}{\partial z} \right) \quad (45)$$

It is then natural to attempt to identify the velocity potential,  $\varphi$ , with the potential of a plane tank of large dimensions which represents the half-plane  $y, z$  (for  $z > 0$ ), and wherein one of the edges is chosen as the  $y$ -axis.

The electric feed of the tank along this edge ( $y$ -axis) must then satisfy the preceding conditions (1) and (2). The first condition is the simpler. Since  $\varphi$  must be zero, it is only necessary to place two electrodes,  $E_0, E_0'$ , on either side of the segment  $(-L, +L)$  these electrodes being held at zero potential (on the usual 0-100 scale).

Condition (2), defined by Eq. (45) corresponds to a mixed type boundary condition (see Section II (c), Eq. (12)). It can be satisfied with good approximation in the following way. The segment  $(-L, +L)$  of

the tank side is divided into small intervals of width  $\epsilon$  which are occupied by electrodes  $e_1, e_2, \dots, e_n, \dots$  separated from each other by narrow insulating bands (Fig. IX-2.) These electrodes may be placed so that the middle of each of the intervals  $\epsilon$  coincides with a particular spanwise position, for example

$$y/L = 0, \pm 0.1, \pm 0.2, \pm 0.3, \dots, \text{etc.}$$

Suppose finally that these electrodes pass currents  $i_1, i_2, i_3, \dots$ , etc. into the tank. These currents can be conducted through resistances  $R_1, R_2, R_3, \dots$ , which are connected to potentiometers  $p_1, p_2, p_3, \dots$ . Let us designate by  $\varphi_1, \varphi_2, \varphi_3, \dots$ , the potentials taken eventually by these electrodes in the tank, and designate by  $\bar{\varphi}_1, \bar{\varphi}_2, \bar{\varphi}_3, \dots$ , those potentials which are controlled directly by the potentiometers  $p_1, p_2, p_3, \dots$ . Each current,  $i$ , flowing out of an electrode,  $e$ , may be measured by means of its voltage drop  $\bar{\varphi} - \varphi$  across the corresponding resistance,  $R$ :

$$Ri = \bar{\varphi} - \varphi \quad (46)$$

Now, according to Eq. (13), the current passing through the electrode is, if its surface area be  $h\epsilon$ :

$$i = -\sigma h\epsilon \left[ \frac{\partial \varphi}{\partial z} \right]_{av} \quad (47)$$

where  $(\partial\varphi/\partial z)_{av}$  is the average value of the normal derivative of the electrical potential, which may in practice be taken to be the value of  $\partial\varphi/\partial z$  at the midpoint of the electrode,  $e$ , if  $\epsilon$  is small enough.

Using Eq. (47) in Eq. (46) gives

$$-R\sigma h\epsilon \left( \frac{\partial \varphi}{\partial z} \right) = \bar{\varphi} - \varphi \quad (48)$$

a relation which may be identified with Eq. (45) provided that the following choice be made for the resistances,  $R$ , and the potentials,  $\bar{\varphi}$ , for each electrode:

$$R = \frac{k l}{4 \sigma h \epsilon} \quad (49)$$

$$\bar{\varphi} = \frac{k l U \alpha}{2} \quad (50)$$

The current distribution in the tank is then automatically such as to satisfy Eq. (45) which links the electrode potentials to the corresponding normal derivatives. Measurement of these potentials,  $\varphi$  is what gives the spanwise distribution of circulation,  $\Gamma$ , as defined by discrete values at those particular points which are the midpoints of the intervals  $\epsilon$ ,  $\Gamma(y/L) = 2 \varphi(y/L)$ .

(b) Description and Use of the Wing Calculator

The wing calculator apparatus (Fig. IX-2) based on the principles given above, consists essentially of the following parts:

- (1) An electric tank.
- (2) A device for holding electrodes ( $E_0$ ,  $E_0'$ ,  $e_1$ ,  $e_2, \dots$ ) which is placed against one of the sides of the tank.
- (3) The panel of feed circuit elements (resistances,  $R$ , and potentiometers,  $p$ ).
- (4) Adjusting and measuring apparatus.

Little need be said about the electric tank. Any tank of constant depth can be

used, either square or rectangular. It is necessary, however, to adjust the dimensions of the tank and the length chosen along one side to represent the segment  $(-L, +L)$  so as to assure that the effect of the other sides be negligible. In the tanks presently in use,  $2L$  is about 10 to 20 cm and the tanks are from 100 to 150 cm on a side.

One of the tank sides ( $y$ -axis in the theory) carries the feed electrodes, two large electrodes,  $E_0$  and  $E_0'$ , which are placed on both sides of the electrodes,  $e$ , of the segment  $(-L, +L)$ . These latter are in general composed of small flat strips of brass or stainless steel set into an insulating plate of ebonite or plexiglass which is the electrode-carrying plate. The number of electrodes,  $e$ , depends on the accuracy sought. Usually 20 to 40 elements are taken, placed in spanwise locations so that their midpoints correspond to simple values of the reduced spanwise distance  $y/L$ .

The electrode plate, a drawing of which is shown in Fig. IX-3, contains 11 electrodes distributed throughout the semispan  $L$  at the following locations:

$$y/L = 0, 0.1, 0.2, \dots, 0.8, 0.9, 0.975$$

It should also be remarked that in the majority of cases the distribution,  $k(y)$ , is an even function of  $y$  (symmetric wing). It is natural to use this symmetry to reduce the analog representation to a quarter of the  $y, z$ -plane. The  $z$ -axis is then fixed along the side of the tank perpendicular to the electrode carrying plate. If the given distribution for  $\alpha(y)$  is even, this side of the tank is left insulating; if  $\alpha(y)$  is odd, it is covered with an electrode  $E_0''$  kept at zero potential.

It is thus easy, through use of only a half-plate placed in the corner of the tank,

to treat cases of symmetric or anti-symmetric twist distributions, flap or aileron deflections. Finally, it may be noted that any arbitrary distribution,  $\alpha(y)$ , can always be decomposed into an even and an odd part.

The electrode-carrying plate of Fig. IX-3 is placed in the corner of a tank one meter square. It will be noticed that the ratio,  $\rho$ , between the width,  $e$ , of the electrode and that of the fraction of insulating strip on either side of it is  $3/4$ . This proportion, the justification of which cannot be undertaken in the present discussion, is the most favorable for obtaining good results. It is better not to increase it too much nor to drop below a value of  $2/3$ . The interval,  $\epsilon$ , which is used in Eqs. (47) and (49) is taken as the real width of the electrode increased by the fraction of insulating strips which border it, as calculated by use of the ratio  $\rho$  (see Fig. IX-3).

The electrode plate described above gives 21 points throughout the span for the determination of the spanwise circulation distribution. This is sufficient in most cases but should be increased when the parameters vary rapidly in certain regions of the span (wing tips, wing-aileron or wing-fuselage junctions, sharp cut-backs in the plan form, etc.). There is obviously no difficulty encountered in increasing the number of electrodes except insofar as it increases the number of electric circuits. It may be noted also that the number of electrodes can be locally increased by narrowing them down in the region of interest and in taking  $\epsilon$  locally as required.

It may be mentioned in this regard that such special electrode plates may be very simply constructed. Taking a plexiglass plate, narrow bands of paper are pasted on it at those places which correspond to the insulating intervals. The whole is then

covered with a silver base conducting paint (for example, a paint such as is used on radio tubes). The paper bands are then taken off, thus baring the insulating intervals between electrodes. This process is fast and economical and gives good results.

The resistances,  $R$ , and the potentiometers,  $p$ , are grouped on the electrical feed panel. To each electrode there corresponds a calibrated resistance box composed of five decades (10, 100, 1000, 10,000, 100,000 ohms) which enables the operator to adjust the resistance,  $R$ , to the desired value. The potentiometers,  $p$ , are wire-wound, of 200 ohms each. They are mounted in parallel and connected across a feed generator (10 to 20 volts AC). The control knob of each potentiometer has graduations of 0 to 100 which help to establish, to a first approximation, the known potential,  $\varphi$ . The precise adjustment of this potential is carried out by using the measuring potentiometer,  $P$ , (usual measurement by a balance method). The necessary readjustments are very rapid because the currents passing through the resistances,  $R$ , and the tank are very small compared to those flowing through these potentiometers, which have low resistance.

The measuring instruments used are well known, potentiometer bridge,  $P$ , cathode-ray oscillograph used as a zero reader, etc. A Wheatstone bridge is also used to measure the resistance,  $R'$ , of the tank liquid between the  $y$ -axis and the opposite side. For this, a switch short-circuits all the electrodes along the  $y$ -axis; then another large electrode is placed on the opposite side. Finally, various control apparatus, grouped before the operator, permit adjustment of the parameters and the measurement of unknowns without touching the tank directly.

The wing calculator apparatus and equipment have been described here in some

detail because many of these same items can be used in other rheoelectric analogies. In the description of other analog set-ups, for example, the use of small electrodes has been mentioned. This procedure is quite general and is used, with variations, every time it is necessary to satisfy Fourier, Dirichlet, or Neumann boundary conditions.

For the same reason it may be useful to discuss how electrical magnitudes are linked to the magnitude of the elements of data of the problem, and how questions of scale are treated in establishing the data and in reduction of the experimental results.

Let us first consider the calculation of  $R$ . It is convenient to eliminate  $\sigma$ , the conductivity of the tank liquid, from this calculation, by introducing  $R'$ , the resistance of the same liquid, measured, as was indicated above, between two opposite tank sides.

Designating by  $D_1$  and  $D_2$  the dimensions of the tank perpendicular and parallel to these electrodes, and by  $h$  the depth of the liquid, the following relation holds:

$$R' = \frac{D_1}{\sigma h D_2} \quad (51)$$

so that Eq. (49) may be written:

$$R = \frac{k l}{4 \epsilon} \frac{D_2}{D_1} R' \quad (52)$$

that is

$$R = X \cdot k l \quad (53)$$

where

$$X = \frac{1}{4 \epsilon} \frac{D_2}{D_1} R' \quad (54)$$

The quantity  $X$  is a constant of the set-up consisting of the electrode holder and the electric tank. Its value may be calculated once and for all. The liquid depth can always be adjusted to maintain  $R'$  at a constant value, for example, 400 ohms. If, in the construction of the electrode holder,  $\epsilon$ , is taken at the value  $L/10$ , it may be seen that for a square tank ( $D_1 = D_2$ )  $X$  will be equal to  $1000/L$  ohms and each resistance,  $R$ , will be taken equal to  $1000 k/L$  ohms.

Consider now the formula for the potentials,  $\bar{\varphi}$ , and let us limit the discussion to the case (to which others can always be reduced) where the angles of attack,  $\alpha$ , are positive throughout the span. The corresponding potentials,  $\bar{\varphi}$ , given by Eq. (50), are all positive. The large electrodes,  $E_o, E_o'$ , being connected, as has been already mentioned, to the one of the generator terminals taken conventionally as zero, it is natural to take the maximum of  $\bar{\varphi}$  at 100 in order to benefit from the scale of 0 to 100 used with the potentiometers.

If  $(k l \alpha)_{\max}$  designates the maximum of this quantity the electric potential to be defined for  $k l \alpha$  will then be:

$$\bar{\varphi} = \frac{k l \alpha}{(k l \alpha)_{\max}} \quad (100) \quad (55)$$

which replaces Eq. (50).

Let us now sum up the necessary operations for determination of the spanwise distribution of circulation with the analog apparatus.

(1) Preliminary Calculations. Use being made of the wing characteristics  $l(y)/L$ ,  $\alpha(y)$  and  $k(y)$ , the values of the resistances,  $R$ , are calculated using Eq. (53), and those of the potentials,  $\bar{\varphi}$ , using Eq. (55).

(2) Adjustment of the Resistances. On the electrical feed panel the resistances,  $R$ , are set at the calculated values. The liquid depth is adjusted to obtain the value of  $R'$  desired.

(3) Adjustment of the Potentiometers. The potentials,  $\bar{\varphi}$ , are established first by using the graduations on the knobs of the potentiometers,  $p$ , and later, the fine adjustments are made using the potentiometer bridge,  $P$ .

(4) Measurement of  $\varphi$ . Finally the potential,  $\varphi$ , of each electrode is measured, using the bridge,  $P$ , by the usual balance method.

The experiment is then terminated. From the measurement of  $\varphi$  in the scale 0-100 there is immediately obtained the value of the corresponding circulation,  $\Gamma$ , or, what is more convenient, a nondimensional value  $\gamma = \Gamma/UL$ . The relation for this is

$$\gamma = (k \frac{l}{L} a)_{\max} \frac{\varphi}{100} \quad (56)$$

It can easily be verified also that the induced angle of attack,  $w/U$ , is then given by,

$$\frac{w}{U} = a \left( 1 - \frac{\varphi}{\bar{\varphi}} \right) \quad (57)$$

where  $\varphi$  and  $\bar{\varphi}$  are measured, as usual, in the 0-100 scale.

(c) Examples of Use of the Wing Calculator

The accuracy obtained with this analog set-up is quite satisfactory for practical

purposes. With 20 electrodes in the span, the error does not exceed a few thousandths of the maximum value of the circulation.

The time required for calculation of the spanwise lift distribution does not exceed 10 or 15 minutes. This time can, moreover, be considerably reduced in numerous cases. At the time when adjustment of the resistances,  $R$ , is done, the plan form of the wing and the airfoil characteristics (products  $k/l$ ) are, so to speak, recorded in the apparatus. Therefore, any twist distribution,  $\alpha(y)$ , can very rapidly be analyzed, since only the potentiometers,  $p$ , need be adjusted.

A particularly interesting application of this last statement concerns the calculation of the effect of flaps or ailerons which occupy variable portions of the span. It is known that to calculate these effects  $\alpha$  is taken constant and equal to unity in that part of the span occupied by the flap, and zero elsewhere. In the analog experiment, the potentials,  $\bar{\varphi}$ , are fixed proportional to  $k/l$ —(since  $\alpha = 1$ ), along the whole span. An untwisted wing, or, what is the same thing, a full span flap can be handled in this way.

As the span of the flap is thereafter shortened,  $\bar{\varphi}$  is set equal to zero over that part of the wing outside the flap, this being a very rapid operation since it is only necessary to turn the corresponding potentiometers,  $p$ , all the way over to zero. The lift distribution due to as many flaps or ailerons as there are electrodes can thus be obtained in a very rapid manner.

The determination of the matrix of influence coefficients is effected in the same way. For a single electrode, the potential,  $\bar{\varphi}$ , is taken proportional to the local  $k/l$  while for all other electrodes  $\bar{\varphi}$  is zero. The corresponding lift distribution is read

off, then the same thing is begun again with another electrode. Approximately 30 to 60 minutes are required to fill out the table of coefficients. The numerical tables of Ref. 13 were obtained in this way.

It is clear that the wing calculator can be used to solve the inverse problem, finding the twist distribution required on a given wing to obtain a lift distribution which is fixed beforehand. In this case, the potentials,  $\varphi$ , being known, the potentiometers,  $p$ , are adjusted by trial and error so as to establish these  $\varphi$  values at the electrodes. When this operation has been carried out, the potentials,  $\bar{\varphi}$ , are measured. These give the twist distribution,  $\alpha(y)$ .

As a general rule, the analog set-up permits rapid determination of the distribution of induced angles corresponding to a given lift distribution. The potentials,  $\varphi = \Gamma/2$ , are established at the electrodes, and the currents,  $i$ , flowing through them are measured. According to Eqs. (44) and (47):

$$w = -\frac{1}{2} \frac{\partial \varphi}{\partial z} = \frac{i}{2\sigma h \epsilon}$$

The flexibility and ease of this analog set-up have greatly facilitated the practical application of the theory of the wing of finite span. Aeronautical engineers have used this apparatus to predict the aerodynamic characteristics of wings as well as to determine wing loading distributions needed in stress analysis.

The wing calculator has often been used in close cooperation with the wind tunnel to provide theoretical calculations of the effects of slight changes in twist, flap or aileron deflection, changes in spoiler position, etc., prior to new tunnel investigations.

As another example there may be cited the study of a schematic representation of

a fuselage or streamlined body mounted on the wing (Ref. 12). The region occupied by the streamlined body was replaced by a fictitious wing section the chord and angular setting of which were determined from simple wind tunnel tests. It was then possible to use this device either to determine lift distributions for all flight conditions, or to choose a better angle of attack setting for the streamlined body and thus diminish undesirable interaction effects. Notable improvements were thus made in initially faulty configurations.

The problems of wing deformation under aerodynamic loads are easily handled on the wing calculator. Either the influence coefficients can be used as has already been suggested, or successive approximations can be carried out on the calculator, taking the elastic properties of the wing structure into account, to obtain the final wing deformation. It is amusing, in this connection, to relate that this procedure was once employed by users of the wing calculator to prove to wind tunnel experimenters that curious results obtained on a certain wing were not due to the special characteristics of the latter but rather to a simple deformation of the tunnel model under the effects of the wind.

It will also be noted that since the vortex field described by the free vortices of a wing is identified with the electric potential field in the tank of the wing calculator, there is absolutely no difficulty in obtaining the equipotential lines thereof by the standard process described in Section III. Thus, in this way a graphical plot is obtained which gives a complete notion of the field in question and which can be useful in many practical problems. Again, if the double probe Section III (f) is used, the field of constant velocity lines induced by the free vortices far behind the wing can be determined, and this can be used, in particular, to analyze the effects of the downwash of the wing on the tail surfaces of the aircraft.

It is interesting to remark also that non-linear wing problems can easily be treated by the electrical analogy (Ref. 23). Such problems arise when the curve of lift coefficient,  $C_L$  vs.  $\alpha$ , for infinite aspect ratio is no longer a straight line. This is the case, in particular, in the neighborhood of maximum lift.

The linear equation of Prandtl which was written for the local lift coefficient  $C_L(y)$  at section  $y$  as

$$C_L(y) = 2k(y) \left\{ \alpha(y) - \frac{w(y)}{U} \right\} \quad (58)$$

now must be replaced by the nonlinear equation:

$$C_L(y) = f \left[ y, \alpha(y) - \frac{w(y)}{U} \right] \quad (59)$$

where  $f$  gives the relation between the lift coefficient for infinite aspect ratio of the section considered and the angle of attack ( $C_{L\infty} = f(\alpha)$ ), (instead of  $C_{L\infty} = 2k\alpha$  as in the linear case).

The analog set-up of the wing calculator allows solution of the nonlinear equation Eq. (59) through use of successive approximations which follow identical manipulative operations (Ref. 23). It was thus possible to determine the spanwise lift distributions on rectangular or other wings in the neighborhood of their maximum lift.

Most of the analog representations which have been discussed can also be obtained through use of Teledeltos conducting paper. The accuracy is clearly less, but the experimental work can be simplified, for the resistances,  $R$ , can be dispensed with by prolonging the paper in the region  $(-L, +L)$  with bands whose lengths are equal to  $k\ell/4$ . (For details of this process, see Ref. 42.)

#### (d) Study of Various Lifting Systems

The discussion thus far has been limited to the case of the straight lifting line; however, the electric tank can be used to study, without great additional complication, the case of a lifting line of any shape contained in a plane parallel to the  $y,z$ -plane or even a lifting system formed of several lines of any shape, provided, of course, that these lines lie in planes perpendicular to the velocity,  $U$ .

This extension of the possibilities of the analog method is interesting because it permits treatment of new practical applications such as wings with dihedral, wings with lateral fins, wings in the neighborhood of a fuselage, wing with strut, annular wing, etc. For these cases the usual analytic methods of calculation are often difficult.

The theoretical bases are analogous to those developed for a straight wing. It is assumed once more that the free vortices remain parallel to the velocity,  $U$ , of the uniform stream so that at infinity downstream, the trace of the vortex sheet on a plane perpendicular to  $U$  (Trefftz plane) reproduces the front view of the lifting system (Fig. IX-4).

Interest centers as before on this vortex distribution in the vertical plane. Let  $\psi$  be the corresponding velocity potential. It is known that the trace ( $C_1$ ) of the vortices constitutes a cut with a discontinuity in the potential. On the two opposite sides of this cut the potential takes on different values which will be called  $\psi^+$  and  $\psi^-$ . Moreover, this potential difference,  $\psi^+ - \psi^-$ , is equal to the circulation,  $\Gamma$ .

On the other hand, the normal derivative,  $d\psi/dn$ , remains continuous across the cut:

$$\left( \frac{d\psi}{dn} \right)_+ = \left( \frac{d\psi}{dn} \right)_- \quad (60)$$

( $n$  is the direction of the normal to the cut (C), directed outward). As in the case of the straight lifting line (Eq. (44)) this normal derivative,  $d\varphi/dn$ , is equal, except for sign, to twice the induced velocity,  $w_n$ , normal to the corresponding point of the wing.

If again the assumption be made that each wing section acts as if its local section were at infinite aspect ratio but at an effective angle of attack,  $\alpha - (w_n/U)$ , where  $\alpha$  is the geometric angle of attack (angle between the axis of zero lift of the right section of (C) and the wind direction U), there may be written

$$\Gamma = k l U (\alpha - \frac{w_n}{U}). \quad (61)$$

Here, after what has been said above,

$$\varphi_+ - \varphi_- = k l U (\alpha + \frac{1}{2U} \frac{d\varphi}{dn}). \quad (62)$$

The determination of the circulation  $\Gamma$  (s) along a lifting line (C) can therefore be reduced to finding the difference between the values taken by a harmonic function,  $\varphi$ , defined in a plane in which the curve (C<sub>1</sub>) describes a cut and where conditions (60) and (62) are to be satisfied at each point of the boundary.

The rheoelectric solution of the problem is easy to imagine (Ref. 11). The field of the tank represents the Trefftz plane. The cut is easily represented. It is made of a thin insulating strip (about 1 mm thick) bent or formed so as to create a portion of a cylindrical surface which will rest on the plane bottom of the tank and reproduce the shape of the cut (C<sub>1</sub>). This strip is covered with conducting paint on its two faces, insulating strips parallel to the generators of the cylindrical surface dividing

the conducting paint up into numerous electrodes. These electrodes ( $e^+$ ,  $e^-$ ) are made identical on the two faces of the strip and can then be grouped in pairs consisting of a given electrode and the one just opposite it. These paired electrodes play the same role as the small electrodes of the electrode-carrying plate of the wing calculator. In the problem to be considered, the cut (or the cuts, if it is a question of a multiplane lifting system) is then represented by one (or several) electrode-carrying strips.

The electrical feed of the tank is accomplished by these electrodes so as to satisfy the conditions imposed (Eqs. (60) and (62)). It should be noted first of all that the current,  $i$ , entering the tank through an electrode,  $e$ , is given by

$$i^+ = - \sigma h \epsilon \left( \frac{d\varphi}{dn} \right)_+$$

or

$$i^- = + \sigma h \epsilon \left( \frac{d\varphi}{dn} \right)_- \quad (63)$$

according to whether it is an electrode,  $e^+$ , situated on the positive side of the cut or an electrode,  $e^-$ , just opposite it on the negative side. Thus condition (60) requires that

$$i^+ = - i^- \quad (64)$$

Equality must be established between the current entering the tank through an electrode on one side and the current leaving through the opposite electrode.

Consider now condition (62). Use of (63) leads to

$$\varphi_+ - \varphi_- = k l U \alpha - \frac{k l}{2 \sigma h \epsilon} i \quad (65)$$

and, if the terms  $kl/2\sigma h\epsilon$  and  $klU\alpha$  be interpreted as representing respectively a resistance

$$R = \frac{kl}{2\sigma h\epsilon} \tag{66}$$

and a potential difference

$$\Delta\bar{\varphi} = klU\alpha \tag{67}$$

there is obtained

$$\varphi^+ - \varphi^- + Ri = \Delta\bar{\varphi} \tag{68}$$

Thus, one is led to feed the electrodes as indicated in Fig. IX-4. Each pair of electrodes ( $e^+$ ,  $e^-$ ) is fed by an independent circuit so as to satisfy the condition  $i^+ = -i^-$  automatically. For this purpose, small identical transformers, T, are used, the primaries being in parallel and connected to the generator, G. The secondary of each transformer feeds one pair of electrodes only. A potentiometer, p, is connected to the terminals of the secondary and the potential difference,  $\Delta\bar{\varphi}$ , is read off here as indicated in the illustration.

It is of course necessary to establish a scale of potential differences for the measurements and potentials to be fixed. A calibrated potentiometer bridge, P, fed by another transformer, T<sub>1</sub>, is used. The measurement of a potential difference,  $\varphi^+ - \varphi^-$ , is always done by opposition. For example,  $e^-$  is connected to one of the extremities of the bridge and  $e^+$ , across a zero-reading oscilloscope, to the movable point of the bridge.

This set-up differs from that of the ordinary wing calculator only by the addition of the transformer; hence, the group of

graduated resistances and potentiometers described previously can be used in this new device. Also, the experimental procedure is exactly the same and it is not necessary to repeat this part of the discussion. Thus all the problems discussed for the straight line wing can be carried over to a more complicated lifting system.

This new analog set-up was first used for studies of biplanes and monoplane wings near the ground (Ref. 11). In this latter case, the cut representing the wing was a straight line placed near one of the insulating sides of the tank which represented the ground. Numerous other applications have since been undertaken. This set-up is useful for studying the effect of dihedral on the wing and for determining all the characteristics of a V-form empennage. The interacting effects of the vertical fins and horizontal stabilizer of an H-empennage can thus be analyzed for all deflections of the rudders or elevator. In this way useful information is obtainable on the hinge moments and load distributions over the various assemblies.

In certain problems of strut-supported wings the electrical analogy has been useful for studying wing-strut interaction in different flight conditions (low-speed flight with flaps deflected, high-speed flight with flaps retracted, etc.) and in guiding the choice of the most favorable angular setting to give to the strut so as to disturb as little as possible or even to improve the qualities of the wing.

A very complete, systematic study was undertaken in order to analyze the influence of end plates of circular or elliptic form on rectangular wings of various aspect ratios. The purpose was to determine formulas which would give the infinite aspect ratio characteristics of the airfoil section, starting from wind tunnel results on low aspect ratio wings tested between end plates (Ref. 62).

Some details on the corresponding analog set-up will be given as this constitutes a good example of the simplifications which may occasionally be adopted. The wing being symmetrically placed between the end plates, this symmetry was used to the maximum in reducing the field represented in the tank to a quarter-plane (Fig. IX-5).

The end plates being supposedly directed straight into the wind, their angle of attack,  $\alpha$ , is zero. It is therefore similar, in the analogy, to the potential difference  $\Delta\bar{\varphi}$ . The electrode pairs ( $e^+$ ,  $e^-$ ) of the end plates are simply joined together through the resistance,  $R$ . The transformers,  $T$ , are unnecessary on the end plates as well as the wing, provided that an electrode,  $E_0$ , at zero potential be placed in extended position as indicated in the figure (same set-up as that for the wing calculator).

The case of the annular wing, or of any wing forming a closed lifting line, can be treated, provided, of course, that the interaction effect of the bound vortices does not become preponderant. It is also possible to use the analogy for preliminary studies of interaction between wing and fuselage, or wing and streamlined body, when the object placed near the wing may be schematically represented by an infinite cylinder.

To illustrate the problem we may consider the case of a cylinder having its generating lines parallel to the wind, for which the analog representation is very simple. The cylinder is represented in the tank by an insulating object having the shape of the normal section of the cylinder ( $d\varphi/dn = 0$  on the contour). The wing is represented as before either by the electrode-carrying plate or the strip, according to whether there is an axis of symmetry or not.

Fig. IX-6 shows the arrangement of the analog model in the latter case. It is obviously easy to generalize to the case of

the lifting cylinder. It can be seen that a Neumann condition must be installed on the contour of the cylindrical section. This problem will be discussed in the next section.

(e) Problems of Optimum Lifting Systems

It is a known fact that for any lifting system the induced drag is a minimum when the component  $w_n$ , normal to the contour, of the induced velocity is related to the angle,  $\theta$ , between the normal,  $n$ , and the  $z$ -axis (Fig. IX-7) by the simple relation

$$w_n = \frac{W}{2} \cos \theta \tag{69}$$

where  $W$  is a constant depending on the incidence.

The determination of the distribution of circulation,  $\Gamma$ , which corresponds to this optimum can be made by considering the velocity potential,  $\varphi$ , defined in the Trefftz plane. Relation (69) becomes a condition on the normal derivative:

$$\frac{d\varphi}{dn} = -W \cos \theta \tag{70}$$

The corresponding boundary condition is therefore of the Neumann type. The values of the normal derivative are known on the boundaries of the field (here, on the cut  $C$ , representing the lifting line). It is known from what has gone before that this condition, in the electrical analogy, is equivalent to imposing current flows,  $i$ , in the small electrodes,  $e$ . They are given by

$$i = -\sigma h \epsilon \frac{d\varphi}{dn} = +\sigma h \epsilon W \cos \theta \tag{71}$$

The analog set-up can be that of Fig. IX-7 wherein the transformers are retained, since

in the case of a cut the relation  $i^+ = -i^-$  always holds. The potentiometer,  $p$ , is adjusted until the potential difference,  $\delta \psi$ , across the resistance,  $R$ , (which is of arbitrary value) is equal to

$$\delta \psi = R \sigma h \epsilon W \cos \theta. \quad (72)$$

There is no need to give further details on this set-up since there exists a much simpler analog method for solving this problem.

Let us add a uniform flow at velocity  $W$  parallel to the  $z$ -axis to the flow having potential  $\psi(y,z)$ . This total flow has the potential

$$\Phi(y, z) = Wz + \psi(y, z). \quad (73)$$

The boundary conditions which define this new potential are as follows:

(1) At infinity,  $\psi(y,z)$  being zero,  $\Phi(y,z)$  reduces to the uniform flow  $Wz$ .

(2) On the contour ( $\gamma$ ) representing the projection of the lifting system onto the Trefftz plane (Fig. IX-8), the normal derivative

$$\frac{d\Phi}{dn} = W \cos \theta + \frac{d\psi}{dn}$$

is zero, according to Eq. (70).

This auxiliary potential  $\Phi$  then corresponds to a uniform field disturbed by the presence of an object of which the contour represents the front view ( $\gamma$ ) of the lifting system. The analog representation of a field of this type is well known (see Section III(a)). The plane tank of large dimensions is electrically fed by two electrodes parallel

to the  $y$ -axis, and the model of the lifting system is constructed of insulating material.

In this way, the optimum distribution for any lifting system can be determined whether it consist of lifting lines or a wing-fuselage system like that shown in Fig. IX-8. The measurement of the electrical potential in the tank gives the function,  $\Phi$ , from which is obtained  $\psi$  on the contour ( $\gamma$ ) and thence the circulation,  $\Gamma$ , subtracting if required the appropriate values of  $Wz$  according to Eq. (73).

This analog set-up has been applied to various problems such as the determination of optimum conditions for wings with vertical fins, wings with lifting fuselage, etc. It can also be used when the geometric form of the lifting system is multiple connected. This was the case, in particular, for the determination of the optimum for the wing with lifting strut.

(f) Determination of Wind Tunnel Wall Corrections

The analog set-up used for the wing calculator can be adapted, with appropriate modifications, to the study of interaction problems of the most varied kinds. Examples have been cited in the preceding sections. In the same way it is possible to study the situation due to the finite size of the test section containing a wing model, thus calculating in a practical way the classical wind tunnel wall effects (Refs. 9, 11, and 14).

As is known, two principal cases are distinguishable, that of a test section having solid walls (closed section) and that of a section surrounded by fluid at rest (open section). The boundary conditions of the test section are obvious. The fluid velocity must be tangent to the solid wall for a closed

section, and the pressure is constant across the boundary of the open section.

Prandtl showed that these conditions imply the following for the free vortex field at infinity downstream:

(1) The velocity is tangent to the contour (C) of the normal section of the wind tunnel for the case of a closed test section.

(2) The velocity is normal to (C) in the case of an open section.

Let  $\varphi(y,z)$  represent, as previously, the vortex field potential in an infinite fluid, and let  $\varphi_1(y,z)$  be the potential of these vortices when the fluid is limited by the tunnel section contour (C). It can then be easily verified that

(1) Condition 1 imposes  $d\varphi_1/dn = 0$  on the contour (C) (closed test section).

(2) Condition 2 imposes  $\varphi_1 = \text{constant}$  on the contour (C) (open test section). (The constant, of little importance, may be taken as zero.)

Consider first, to make things concrete, a simple and typical case. Suppose that the test section (C) admits of an axis of symmetry,  $y$ , and that the wing (-L, +L) is located along this axis (Fig. IX-9). The distribution of circulation,  $\Gamma_1(y)$ , along the span is given, in the case of the closed section, by

$$\Gamma_1 = k\ell U \left( \alpha - \frac{w_1}{U} \right) \quad (74)$$

where  $w_1(y)$  represents, in this instance, the downwash velocity induced by the free vortices when the effect of the tunnel walls is taken into account, that is, when the images with respect to (C) of the free vortices are accounted for.

As previously, the following hold on (-L, +L):  $\Gamma_1 = 2\varphi_1$  and  $w_1 = -1/2(\partial\varphi_1/\partial z)$ .

The expression (74) can then be written

$$\varphi_1 = \frac{k\ell U}{2} \left( \alpha + \frac{1}{2U} \frac{\partial\varphi_1}{\partial z} \right) \quad (75)$$

which is analogous to Eq. (45).

The electrical analog interpretation is then immediate. It is only necessary to limit the electric tank field of the wing calculator by a partition having the form of the contour (C) of the test section. This will be taken insulating in the case of the closed test section (condition a) and conducting at zero potential, in the case of the open test section (condition b). The rest of the set-up remains unchanged and the determination of the distribution,  $\Gamma_1$ , is carried out as was explained above in section (b).

In this way the circulatory correction  $\Delta\Gamma = \Gamma(y) - \Gamma_1(y)$  for each point of the span is easily obtained by carrying out successively two experiments, one without tunnel wall (C) and the other with the model of this wall in the tank. Thereafter, it is possible to define an average correction without difficulty and to revert to the usual correction formulas affecting the angle of incidence,  $\alpha$ , and the drag coefficient,  $C_D$  (Ref. 11).

It is interesting to notice that the electrical method holds for any initial distribution of the circulation,  $\Gamma$ , and does not require any prior hypothesis concerning the distribution,  $\Gamma_1$ . In the usual calculation methods it is generally assumed that the distribution is rectangular or elliptic and remains so when the finite test section is present.

The method described above also applies without difficulty to the case of a mixed-type tunnel test section, i.e., a test section enclosed between solid walls or free surfaces along certain regions of its boundary. In this case the partition placed in the electric tank must be made up of conducting parts for the open regions of the test section and of insulating parts for the closed regions of the section (Fig. IX-10).

This set-up is particularly suited for solving the problem of the mixed-type test section having an average wall correction of zero (Ref. 11). This result is obtained through successive trials by shortening more or less the conducting portion of the partition with respect to the insulating portion. In the set-up of Fig. IX-10 it is merely necessary to cut back little by little the copper foil electrode  $\hat{AM}$  applied to the partition  $\hat{AB}$  to obtain the desired effect.

There is of course no special difficulty to be encountered in applying the method described here to the case of a wing oriented in any position. In this case the electrode-carrying plate, which forms a cut, and electrical feed by transformers (Section IX(d)) are used. Fig. IX-11 illustrates the case of a wing carrying vertical end plates placed in a wind tunnel with a test section of given shape.

Another analog possibility will be indicated, in closing, for the determination of wall corrections. When greater accuracy is sought, the potential difference  $\Phi = \varphi - \varphi_1$ , may be represented in the electric tank, thus obtaining directly the correction  $\Gamma - \Gamma_1 = 2\Phi$  along the lifting segment.

Let us first examine the simple example (easily generalized) of an open test section ( $\varphi_1 = 0$  on (C)) which is symmetrical about the y-axis, the segment  $(-L, +L)$  being

placed along this axis (Fig. IX-12). In a preliminary experiment, without tunnel walls, the values of the potential  $\varphi = \varphi_{(C)}$  along the future position of these walls (C) can be read off. An ensuing experiment is carried out with the walls (C) simulated.

The following conditions will determine  $\Phi(y,z)$ :

- (1) On (C),  $\Phi_{(C)} = \varphi_{(C)}$  . (Dirichlet condition).
- (2) On  $(-L, +L)$ ,  $\Phi = (kl/4)(\partial\Phi/\partial z)$ . (Mixed condition).
- (3) On the y-axis outside  $(-L, +L)$ ,  $\Phi = 0$ .

Fig. IX-12 presents the corresponding electrical set-up. The tunnel wall contour (C) is covered with little electrodes raised to the potentials  $\varphi_{(C)}$  (known from the first experiment) by means of the potentiometers,  $\pi$ . The lifting segment  $(-L, +L)$  continues to be represented by the electrode-carrying plate. The resistances, R, are known and calculated from Eq. (53). The potentiometers, p, of the wing calculator are not needed since the mixed condition (2) is simplified, and the resistances, R, are connected directly to zero potential.

The same holds for the electrodes  $E_0$  and  $E'_0$  which lie on either side of  $(-L, +L)$ . Measurement of the potential on the electrode-carrying plate provides the values of the difference which is being sought.

$$2\Phi(y) = \Gamma(y) - \Gamma_1(y).$$

In the case of a closed test section, a Neumann condition would have to be satisfied along (C):  $d\Phi/dn = (d\varphi/dn)_{(C)}$  where  $d\varphi/dn_{(C)}$  represents the normal gradient to the wall position (C) read off during the first experiment (without wall).

## X. ANALOG STUDY OF PROPELLER THEORY

In a very complete study of the analog interpretation of the problems dealing with the vortex theory of propellers, R. Siestrunk has developed the principles of the electric tank representation of the velocity field induced by the helicoidal vortex sheets leaving the trailing edges of the blades. (Ref. 36.) He developed an apparatus, based on this principle, which is called the "propeller calculator." This solves in a few minutes the practical problem of analyzing the operation of a propeller of given characteristics in different regimes.

For the details the reader is referred to the excellent paper of Siestrunk. It will suffice here to present only the essential aspects of the question which, apart from its general interest, constitutes a remarkable example of interpretation of the analytic conditions of the problem, and terminates by presenting a simple analog set-up which is particularly well adapted to the needs of the user.

### (a) Principles of the Propeller Calculator

It is known that the potential,  $\varphi$ , of the velocity induced by the trailing vortex sheets is a harmonic function of three variables and satisfies the equation

$$\frac{\partial^2 \varphi}{\partial \xi^2} + \frac{1}{\xi} \frac{\partial \varphi}{\partial \xi} + \frac{1}{\xi^2} \frac{\partial^2 \varphi}{\partial \theta^2} + \frac{\partial^2 \varphi}{\partial z^2} = 0 \quad (76)$$

when, in a system of axes fixed to the propeller, the semi-polar coordinates  $\xi$ ,  $\theta$ ,  $z$  are used (the  $z$ -axis coincides with the propeller axis).

In what follows, all lengths such as that of the radius vector,  $\xi$ , or the distance,  $z$ , will be measured in terms of the radius,  $R$ , of the propeller. On the blade which carries the  $x$ -axis, for example, this system of measurement gives  $\xi = x/R$ . If the propeller has  $p$  blades, the trailing vortex system is composed of  $p$  helicoids of geometric pitch  $h = 2\pi W/\omega$ , where  $W$  is the translation velocity along the  $z$ -axis and  $\omega$  is the angular speed of rotation.

The equation of these helicoidal surfaces is defined by

$$\theta - z/\lambda = \frac{2K\pi}{p} \quad (K = 0, 1, \dots, p-1), \quad 0 \leq \xi \leq 1 \quad (77)$$

where  $\lambda$  is the operating parameter  $\lambda = W/\omega R$ .

As in the wing problem, these vortex sheets constitute surfaces of discontinuity for  $\varphi$  which take on different values  $\varphi^+$  and  $\varphi^-$  at two points located on opposite sides of the surfaces (cuts). The difference  $\varphi^+ - \varphi^-$  is equal to the circulation,  $\Gamma$ , along a space curve which, emerging from a point on the upper side of the surface, comes back to point under this surface after having passed around the edge ( $\xi = 1$ ) of the sheet.

The expressions which define the semi-polar components of the induced velocities only employ the variables  $z$  and  $\theta$  in the combination  $\zeta = \theta - z/\lambda$ . This property exhibits the helicoidal symmetry of the field which Goldstein used to show that the velocity potential,  $\varphi$ , depends only on the two variables  $\xi$  and  $\zeta$  and therefore satisfies the equation

$$\frac{\partial^2 \varphi}{\partial \xi^2} + \frac{1}{\xi} \frac{\partial \varphi}{\partial \xi} + \left( \frac{1}{\lambda^2} + \frac{1}{\xi^2} \right) \frac{\partial^2 \varphi}{\partial \zeta^2} = 0 \quad (78)$$

which is obtained from Eq. (76).

With the variables  $\xi$  and  $\zeta$ , respectively interpreted as radius vector and polar angle, the surfaces (77) give a system of radiating segments in the  $(\xi, \zeta)$  plane

$$\zeta = \frac{2K\pi}{\rho} \quad (79)$$

which form cuts (Fig. X-1). The periodicity of the field with respect to  $\zeta$  (period  $2\pi/\rho$ ), together with the antisymmetry of  $\varphi$  with respect to the cut, allows the domain of definition of the potential  $\varphi$  to be reduced to the sector  $0 \leq \zeta \leq \pi/\rho$ .

Summing up, the boundary conditions, no matter what the propeller under discussion, are as follows:

(1)  $\varphi = 0$  on the axis  $\zeta = 0$  for  $\xi > 1$ .

(2)  $\varphi = 0$  on the straight line segment  $\zeta = \pi/\rho$ .

(3) On the edge of the cut ( $\zeta = 0$ ,  $0 \leq \xi \leq 1$ ) inside the domain

$$\varphi(\xi) = \varphi^+ = \frac{\Gamma(\xi)}{2} \quad (80)$$

The circulation,  $\Gamma(\xi)$ , is calculated as in the lifting line problem by supposing that the airfoil section  $\xi$  of the blade has the same properties as for infinite aspect ratio but is attacked by a wind of velocity  $\sqrt{W^2 + (\omega x)^2}$  at an effective angle of attack  $(\alpha - \delta\alpha)$ ,  $\alpha$  designating the geometric angle of attack and  $\delta\alpha$  the induced angle.

Thus there is obtained for the reduced circulation

$$\Gamma(\xi) = kt \sqrt{\lambda^2 + \xi^2} (\alpha - \delta\alpha) \quad (81)$$

(where  $t = l/R$  is the reduced chord).

It can be shown that the angle  $\delta\alpha$  is linked to the normal derivative  $(\partial\varphi/\partial\zeta)_{\zeta=0}$  to the cut ( $\zeta = 0$ ,  $0 \leq \xi \leq 1$ ) so that finally there is obtained from Eqs. (80) and (81) the following condition:

$$\varphi(\xi) = \frac{kt}{2} \sqrt{\lambda^2 + \xi^2} \left[ \alpha + \frac{1}{2\lambda\xi} \frac{\partial\varphi}{\partial\zeta} \right] \quad (82)$$

which must hold at every point  $\xi$  of the upper side of this cut.

Goldstein's equation (78) may be integrated by means of the rheoelectric analogy if a suitable change of variable be effected, this latter being determined only to within an arbitrary conformal transformation. Siestrunk's solution will be presented here, retaining the notation of his paper (Ref. 36, p. 30).

It should first be stated that Eq. (5) of Section II governing the distribution of electric potential,  $V$ , in a conductor of slowly variable thickness,  $h$ , may be written, in terms of polar coordinates,  $r$  and  $\theta$ , and for a conductor forming a body of revolution about the vertical axis  $z$  through 0 ( $h$  depending only on  $r$ ):

$$\frac{\partial}{\partial r} \left( hr \frac{\partial V}{\partial r} \right) + \frac{\partial}{\partial \theta} \left( \frac{h}{r} \frac{\partial V}{\partial \theta} \right) = 0 \quad (83)$$

or again

$$hr \frac{\partial^2 V}{\partial r^2} + (h'r + h) \frac{\partial V}{\partial r} + \frac{h}{r} \frac{\partial^2 V}{\partial \theta^2} = 0 \quad (84)$$

where  $h'$  is the derivative  $dh/dr$ .

Goldstein's equation (78) may be written,

if  $\mu = \xi/\lambda$ ,

$$\frac{\partial^2 \varphi}{\partial \mu^2} + \frac{1}{\mu} \frac{\partial \varphi}{\partial \mu} + (1 + \frac{1}{\mu^2}) \frac{\partial^2 \varphi}{\partial \zeta^2} = 0. \quad (85)$$

Let there be performed the transformation  $\mu = \mu(r)$ ,  $\theta = \zeta$ , on Eq. (85). If  $\dot{r}$ ,  $\ddot{r}$  represent the derivatives of  $r$  with respect to  $\mu$ , there is obtained:

$$\mu \dot{r}^2 \frac{\partial^2 \varphi}{\partial r^2} + (\dot{r} + \mu \ddot{r}) \frac{\partial \varphi}{\partial r} + \frac{1 + \mu^2}{\mu} \frac{\partial^2 \varphi}{\partial \theta^2} = 0. \quad (86)$$

If the velocity potential,  $\varphi$ , be identified with the electric potential,  $V$ , and Eqs. (84) and (86) be compared, there is obtained

$$\frac{\mu \dot{r}^2}{hr} = \frac{\dot{r} + \mu \ddot{r}}{h'r + r} = \frac{(1 + \mu^2)r}{h\mu}. \quad (87)$$

The transformation  $\mu(r)$  is defined by equating the first and third terms:

$$\frac{\dot{r}^2}{r^2} = \frac{1 + \mu^2}{\mu^2}$$

i.e.,

$$r = C_1 e^{\sqrt{1+\mu}} \sqrt{\frac{\sqrt{1+\mu^2}-1}{\sqrt{1+\mu^2}+1}} \quad (88)$$

where  $C_1$  is an arbitrary scale factor.

The depth,  $h$ , may be obtained, for example, by equating the first two terms of Eq. (87)

$$\frac{\mu \dot{r}^2}{hr} = \frac{\dot{r} + \mu \ddot{r}}{h'r + r}$$

and, using  $\dot{h} = dh/d\mu = h' \dot{r}$ ,

$$\frac{\dot{h}}{r} = -\frac{\dot{r}}{r} + \frac{\ddot{r}}{\dot{r}} + \frac{1}{\mu}$$

i.e.,

$$h = C_2 \frac{\mu \dot{r}}{r} = C_2 \sqrt{1 + \mu^2} \quad (89)$$

$C_2$  being a second scale factor.

The variable,  $\mu$ , can be eliminated between Eqs. (88) and (89) and there is thus obtained, if  $\rho = r/C_1$ ,  $H = h/C_2$

$$\rho = e^H \sqrt{\frac{H-1}{H+1}}. \quad (90)$$

The depth,  $H$ , of the liquid at the distance  $\rho$  from the origin is then defined by Eq. (90). The electric tank is circular about the vertical axis through the origin  $O$ , and the profile of the bottom must be shaped according to the law  $\rho(H)$ . Moreover, it is clear that for its construction, one may adopt all the meridian profiles obtainable from the preceding  $\rho(H)$  by any possible affined transformation of  $\rho$  or  $H$  (obtained by giving  $C_1$  and  $C_2$  arbitrary values).

Siestrunck used this fact as the basis for the construction of four independent tanks which differ by appropriate choices of  $C_1$  and  $C_2$  and which are usable each in a certain range of operation  $\lambda$ . A single basin would have been too large to be used conveniently. (It should be noted that the segment representing the blade has a length in the tank which depends on  $\lambda$ , since  $\mu = \xi/\lambda$ ).

The expression Eq. (82) defining the condition to be satisfied by the velocity potential,  $\varphi$ , on the upper side of the cut in the  $\xi, \zeta$ -plane allows the equivalent condition on the potential,  $V$ , to be stated. Let us first introduce the derivative of  $\varphi$  taken normal to the polar axis  $\zeta = 0$  but

in the  $(r, \zeta)$ -plane; this will be designated by

$$\left(\frac{d\varphi}{dN}\right) = \frac{1}{r} \left(\frac{\partial\varphi}{\partial\zeta}\right)_{\zeta=0}$$

Then, Eq. (82) can be written

$$\varphi(\xi) = \frac{kt}{2} \sqrt{\lambda^2 + \xi^2} \left[ \alpha + \frac{r}{2\lambda\xi} \frac{d\varphi}{dN} \right]$$

or again, with the variable,  $\mu$ , and considering now that it is a question of the electrical potential,  $V$ :

$$V(\mu) = \frac{kt}{2} \lambda \sqrt{1 + \mu^2} \left[ \alpha + \frac{kt}{4} \frac{r\sqrt{1 + \mu^2}}{\mu\lambda} \frac{dV}{dN} \right] \quad (91)$$

This last condition is of the mixed type (linear relation between the potential,  $V$ , and its normal derivative  $dV/dN$ ). In connection with the wing calculator, the type of electric set-up which served automatically to satisfy this condition was described (Section IX (a)).

In the electric tank (Fig. X-2) that part of the side  $\zeta = 0$  which represents the image of the blade, is provided with small electrodes,  $e$ , which are electrically fed through resistances,  $R$ , by means of potentiometers,  $p_1$ . According to Eq. (91) the resistances,  $R$ , should take on the values

$$R = \frac{kt}{4\sigma h\epsilon} \frac{r\sqrt{1 + \mu^2}}{\mu\lambda} \quad (92)$$

and the potentials,  $\bar{V}$ , should be adjusted through the potentiometers,  $p$ , to the values

$$\bar{V} = \frac{kt}{2} \lambda \sqrt{1 + \mu^2} \alpha \quad (93)$$

It should be remembered that the potential,  $V$ , must fall to zero on the same side outside the blade as well as on the straight line  $\zeta = \pi/p$ .

Once these adjustments have been made it is only necessary to read off the values of the potentials,  $V$ , at the electrodes,  $e$ , and thus obtain the distribution of circulation  $\Gamma(\xi)$  along the blade  $[\Gamma(\mu) = 2V(\mu)]$ .

The tanks which were built each represent a quadrant ( $0 \leq \zeta \leq \pi/2$ ) of the plane  $(\xi, \zeta)$ . This quadrant is used in its entirety for the study of two-blade propellers ( $p = 2$ ). When  $p > 2$ , a mobile electrode  $E'_0$  may be displaced so as to create an angle with the electrode-carrying plate of  $\pi/p$ . This electrode is kept at potential  $V = 0$ . It is possible with this movable electrode to analyze the effect of the number of blades by simple displacement, in the tank, of the boundary of the domain of definition for  $\varphi$ . With this movement it is unnecessary to change the adjustments of  $R$  and  $V$ .

The experiments are carried out in the same way as for a wing calculation (see Section IX (b)). As a matter of fact, for these experiments the general electrical feed panel of the wing calculator is used. It should be noted that with the tanks having variable depth bottoms like that in the propeller calculator, it is necessary to measure the conductivity and the liquid depth separately. The first of these two measurements is carried out using a resistivity-measuring cell which is introduced into the tank just before the main experiment and withdrawn immediately upon measurement of  $\sigma$ . To adjust the water level to the right height a micrometer screw with point is used. This is fixed permanently to one of the sides of the tank. The tank is filled until contact (identified electrically) is established between the point and the electrode.

(b) Examples

The electrical set-up which has just been described permits determination of a distribution of circulation with an accuracy of about 1 percent. This has been verified in treating optimum problems and by comparison of them with theoretical solutions given explicitly for particular values of the operational parameter,  $\lambda$ , and the number of blades,  $p$ .

It should be noted in this connection that the wing calculator can rapidly furnish the optimum distribution of circulation corresponding to a given problem of adaptation. It is known that in this case the distribution of the induced angles along the blade is determined beforehand and therefore also the values of the normal derivative,  $d\varphi/dN$ . The problem to be solved is thus of the Neumann type, that is, from the electrical point of view, one in which it is necessary to adjust the current flows from the electrodes,  $e$ , to known values. Thereafter, measurement of the potentials gives the optimum distribution of the circulation.

To solve the same problem, T. Theodorsen has employed a rheoelectric set-up based on a very different principle (Ref. 35). This principle is based on the well-known fact that in the optimum case the velocity potential,  $\varphi$ , corresponds to that of the flow about the helicoidal vortex sheets, supposed solid, and given a uniform motion of translation along their axis (the  $z$ -axis). It is clear that such a flow can easily be represented in a deep tank if the helicoidal surfaces be represented by insulating models and if there be established a uniform electric field parallel to the  $z$ -axis between two electrodes  $E_0$  and  $E_1$  which are perpendicular to that axis (Fig. X-3).

The potential difference ( $V^+ - V^-$ ) measured on either side of the helicoid along the

same horizontal generating line, gives the optimum distribution of circulation sought for. It will be noticed that the electrical set-up used here to solve the propeller optimum problem is very similar to that considered in Section IX (e) for treating the optimum lifting system. It is evidently necessary to construct as many models as there are values of the operating parameter,  $\lambda$ , and numbers of blades,  $p$ , to be considered. Also, the construction of these helicoidal sheets is quite difficult.

We will not dwell on the use of the propeller calculator as regards solution of operating problems which are handled without difficulty. It has been seen that it is only necessary to vary the resistances,  $R$ , and the potentials,  $V$ , when, for a propeller of given geometric characteristics, it is desired to vary the parameter,  $\lambda$ . The situation is the same when it is desired to undertake a systematic study of the variable pitch propeller.

The analog set-up can also be used to represent certain interactions due to devices limiting the extent of the flow. Thus, the presence of a spinner or hub, schematically represented by a cylinder of indefinite length along the  $z$ -axis, is easily reproduced by placing an insulating cylinder in the electric tank so as to fill up a suitable portion of the angular space at the origin, 0. In this way also the influence of a closed wind tunnel around the propeller can be analyzed, and, as a generalization, the problem of the operation of simple axial machines, fans, or blowers without fixed guide vanes can be examined.

It is interesting to note that R. Siestrunk and J. Bernard have generalized the principle of the propeller calculator to studies concerning coaxial contrarotating propellers (Ref. 41). They have also treated the problem of optimum operation of the double

propeller by setting up hypotheses analogous to those for the single propeller, basing their method upon the minimizing of the lost energy through a process of the calculus of variations. To solve the same problem, Theodorsen has used quite different hypotheses in which he supposes that, although the aerodynamic phenomenon ceases to be stationary, the helicoidal vortex sheets can still be considered as rigid. The flow about these sheets can then be studied in the electric tank as was described above.

## XI. ANALOG STUDY OF LIFTING SURFACE PROBLEMS

The aerodynamics of high-speed flight has led to the employment of new wing plan forms having high sweepback and low aspect ratios. In these cases the Prandtl lifting-line theory does not correctly predict performance, and it is necessary to utilize the linear theory of lifting surfaces, development and use of which have expanded considerably in the last few years. In this new domain, the rheoelectric analogy method is able to render appreciable service by facilitating the solution of the principal problems posed in practice.

### (a) Study of Two-Dimensional Problems

Before examining how the model of a lifting surface may be represented in the electric tank, a few simple examples relative to two-dimensional problems will be treated. Thereafter it will be seen how the principles of the analog set-ups used for these examples can be carried over without difficulty to the general three-dimensional case.

We will then take up the study of the perturbation caused in a uniform stream of velocity,  $U$ , parallel to the  $x$ -axis by a thin airfoil placed at small angle of attack when the classical hypothesis of linearization of the boundary conditions is assumed.

Two problems may be distinguished:

- (1) The lifting problem, corresponding to the study of an airfoil section considered as being infinitely thin, of very little camber, and of low inclination to the relative wind  $U$ .
- (2) The symmetrical (or thickness) problem, which corresponds to the study of a symmetrical airfoil section of low thickness placed at zero lift.

### Lifting Problem

We will first consider the perturbation velocity potential,  $\varphi(x,y)$ , caused in the uniform stream,  $U$ , by the presence of an infinitely thin airfoil. This airfoil may be reduced to a curve  $(c)$  defined by the equation

$$y = f(x) \tag{94}$$

The properties of this potential,  $\varphi(x,y)$ , and its boundary conditions are well known. They are rapidly summarized below (Fig. XI-1).

(1)  $\varphi$  is harmonic and defined in the  $x,y$ -plane, which has a cut along the  $x$  axis from the leading edge of the airfoil ( $x = -l/2$ ) to infinity downstream.

(2)  $\varphi$  is an odd function of  $y$  and takes on values of opposite sign on either side of the cut. It vanishes at infinity.

(3) On the segment  $(-l/2, +l/2)$  of the  $x$ -axis, which represents the projection of the airfoil of chord  $l$  onto this axis, the normal derivative  $\partial\varphi/\partial y$  satisfies the condition

$$\left(\frac{\partial\varphi}{\partial y}\right)_{y=0} = U(\partial f/\partial x) \tag{95}$$

which expresses (within the limits of the linearizing assumptions) the fact that the fluid filaments are tangent to the airfoil. This normal derivative remains continuous across the cut.

(4) On the segment  $(+\ell/2, +\infty)$  of the  $x$ -axis, which corresponds to the streamline emerging from the trailing edge of the airfoil, the potential  $\varphi$  is constant and takes on values of opposite sign,  $+\varphi$ , and  $-\varphi$ , on the upper and lower edges of the cut, respectively. The value of the constant  $\varphi$  if defined by the Joukowski condition which requires that  $\partial\varphi/\partial x$  be zero at the trailing edge, i.e. that the potential  $\varphi$  be continuous at this point.

The representation of  $\varphi$ , identified with the electric potential, on the electric tank is easy. Since it is an odd function of  $y$ , the representation can be limited to a half-plane, that for positive  $y$ , for example. The  $x$ -axis can then be taken along one of the sides of a tank of large dimensions. Along the middle of this side an electrode-carrying plate is placed (electrodes  $e$ ). This represents the segment  $(-\ell/2, +\ell/2)$ . On either side of this are placed two large electrodes,  $E_0$  and  $E_1$  (Fig. XI-1), the first corresponding to the segment  $(-\infty, -\ell/2)$ , the second to the segment  $(+\ell/2, +\infty)$ .

It can be seen that the electrode arrangement here is exactly the same as that used in the wing calculator tank (Section IX (b), Fig. IX-2). This apparatus can therefore be used in the present problem.

To take account of the antisymmetry of  $\varphi$ , the electrode  $E_0$  is held at potential zero. Condition (3) is of the Neumann type. To satisfy it each electrode,  $e$ , must be made to pass an electric current,  $i$ , having a value proportional to its width,  $\epsilon$ , and to the slope  $df/dx$  calculated from Eq. (94)

for  $x$  taken at its midpoint

$$i = -\sigma h \epsilon U (df/dx) \tag{96}$$

To satisfy condition (4) (Joukowski condition) the potential  $\varphi_1$  at first unknown, is adjusted on the downstream electrode  $E_1$  so as to insure that, at the trailing edge ( $x = +\ell/2$ ) the potential remains the same in passing from  $E_1$  to the electrode carrying plate. In practice, if the number of electrodes,  $e$ , is sufficient (10 to 20 for example),  $\varphi_1$  is adjusted so as to achieve equality of the potential between  $E_1$  and the final electrode  $e_F$  of the airfoil (usually this last electrode  $e_F$  is given an interval,  $\epsilon$ , which is half as large as the others).

A short description will be given of the method for imposing the intensities,  $i$ , at the electrodes,  $e$ . Various set-ups can be used. If the feed section of the wing calculator (Section IX (b)) is used, the potentiometers,  $p$ , are adjusted so as to obtain a potential drop,  $\delta V$ , across the resistances  $R$  (which are chosen arbitrarily at some hundreds or thousands of ohms),  $\delta V$  being given by

$$\delta V = \bar{V} - V = -R\sigma h \epsilon U (df/dx) \tag{97}$$

according to Eq. (96).

This set-up (Fig. XI-2a) has the disadvantage of requiring a fairly high number of trial adjustments because these latter interact on each other, the potentials,  $V$ , of the electrodes undergoing considerable modification.

To eliminate this difficulty, the set-up used by R. Duquenne (Ref. 45) can be used. This has the advantage of retaining a fixed value of the potentials,  $V$ , though not of course that of the electrode which is being

adjusted. A special device is used which functions like an ammeter having zero resistance.

This device uses a method of opposition (Fig. XI-2b). In order to measure the current,  $i$ , in the wire between the potentiometer,  $p$ , and the corresponding electrode,  $e$ , without disturbing it, a circuit is introduced between the points A and B of this wire. This circuit consists of a known reactance,  $r$ , the secondary of a transformer,  $T$ , and an oscilloscope,  $O$ , which acts as a null meter with practically infinite impedance. The potential difference,  $\delta V'$ , applied to the terminals of the primary by means of the voltage divider,  $P'$ , is regulated so as to balance exactly the voltage drop  $\delta V' = ri$  in the resistance,  $r$ , by the potential rise across the terminals of the secondary. Under these conditions the potentials of points A and B are identical. This is easily verified on the oscilloscope,  $O$ . The characteristics of the circuit ATB are such that the current flowing through it is directly proportional to the indication of  $\delta V'$  on the voltage divider.

To fix the current passing through an electrode,  $e$ , at a given value, the movable point of  $P'$  is placed opposite the corresponding graduation (obtained by previous calibration of the apparatus), and the potentiometer,  $p$ , is adjusted until zero is read on the oscilloscope. Once the adjustment is made, the points A and B are short-circuited, which has no effect on the values of current or voltage of the electrode,  $e$ . The current-measuring device is then disconnected to pass on to another one of the electrodes,  $e$ .

A third type of set-up may also be used (Ref. 18). This has the advantage of rendering the imposition of currents,  $i$ , semi-automatic, but it has the disadvantage of reducing the useful range of potentials in the tank. If, for example, all the currents,  $i$ , have the

same sign, the electrodes,  $e$ , may all be joined to the +100 terminal of the generator through the intermediary of very large resistances,  $R$ , (from 500,000 ohms to 1 megohm or more) (Fig. XI-2c). The tank potentials and those of the electrodes are then very low, and, as a first approximation, they can be neglected with respect to the potential drop across the resistances,  $R$ . The relation then holds,  $Ri \approx 100$ .

If it is desired to impose currents,  $i$ , of known value, as given by Eq. (96) for example, the magnitudes of the resistances,  $R$ , must then be taken proportional to

$$\frac{100}{\sigma h \epsilon U (df/dx)} \quad (98)$$

The proportionality constant can evidently be chosen at will for it enters only in the final reduction of the results wherein the scale used for defining the slopes  $df/dx$  is established.

If necessary afterward, the values set up can be readjusted, taking into account the potentials measured at the electrodes. Usually, the first approximation is sufficient, this giving satisfactory results if the resistances,  $R$ , are really large. The tank potentials are of course defined within a very narrow range (2 to 3 in the 0 to 100 scale used), and the quality of the results depends on the accuracy possible in the measurements. The first decimal place, i.e. 1/10,000 of the scale of 0 to 100, must be readable.

When, through use of one of the three above-mentioned set-ups, the currents,  $i$ , have been set at appropriate values while the Joukowsky condition is also satisfied, the adjustments are finished. The measurement of the potential  $\varphi_1$  of  $E_1$  then gives the circulation about the thin airfoil

(since  $\Gamma = 2\varphi_1$ ). To obtain the pressure distribution over the airfoil the potentials of the electrodes must be measured and the distribution thus obtained differentiated to get  $u = \partial\varphi/\partial x$ . It can in fact, be seen that the pressure difference,  $\Delta p$ , between upper and lower surfaces is given by,

$$\Delta p = 2\rho U u \tag{99}$$

where  $\rho$  is the fluid density.

The methods just described permit the rapid determination of the pressure distribution over any thin airfoil of prescribed form. Also, the solution of the inverse problem is at least equally straightforward when use is made of the electrical analogy. In this case, the starting point is the pressure distribution curve over the chord. This being given, the airfoil shape which will produce this distribution is sought.

In this case the potential  $\varphi_1$  is known for the electrode  $E_1$ . By integration of the known pressure distribution the curve for the potential  $\varphi(x)$  along the chord is obtained, i.e., the electrical potential needed for each of the electrodes,  $e$ . These potentials are fixed using the potentiometers,  $p$ . The currents,  $i$ , are then measured. Use being made of Eq. (96), the corresponding slopes,  $df/dx$ , are obtained, from which finally the airfoil form  $y = f(x)$  is deduced by integration.

Use of the perturbation potential,  $\varphi(x,y)$ , is not the only method which can lead to a solution of the lifting problem. The acceleration potential  $u(x,y) = \partial\varphi/\partial x$  can also be employed. Its determination by electrical analogy is occasionally advantageous.

The conditions defining the acceleration (or pressure) potential,  $u(x,y)$ , can easily be obtained from those given above for the

velocity potential,  $\varphi(x,y)$ :

(1) The function  $u$  is zero at infinity as well as on the  $x$ -axis outside the segment  $(-\ell/2, +\ell/2)$ . In the corresponding analog representation the electrodes  $E_0$  and  $E_1$  on either side of  $(-\ell/2, +\ell/2)$  are therefore both held at zero potential.

(2) On the segment  $(-\ell/2, +\ell/2)$  condition (95) gives

$$\frac{\partial u}{\partial y} = U (d^2f/dx^2) \tag{100}$$

or the equivalent integrated form

$$\int_{-\infty}^x \frac{\partial u}{\partial y} dx = U (df/dx). \tag{101}$$

(3) Finally, the value of  $u$  on the airfoil tends toward zero at the trailing edge.

Condition (100) for the normal derivative  $\partial u/\partial y$  is again a Neumann type condition. As is known, to represent it in the electrical analogy, an elementary current,  $di$ , must pass through the element,  $dx$ , of the segment  $(-\ell/2, +\ell/2)$ , this current being proportional to  $d^2f/dx^2$ , i.e. to the value of the curvature at the point  $x$  considered

$$di = \sigma h U (d^2f/dx^2) dx. \tag{102}$$

Once more then, one of the previous analog set-ups will be used to feed the small electrodes of the system.

It should now be pointed out that condition (100) alone is not sufficient to define the problem because it cannot show the effect of a change of incidence of the airfoil. To

bring this out clearly it is only necessary to consider the straight-line airfoil. Here the slope  $df/dx$  is constant, and, according to Eq. (102), there would be no current flow into the tank since the electrodes  $E_0$  and  $E_1$  are both at potential zero. Therefore it must be required that condition (101) be satisfied at the same time.

From the electrical standpoint this condition expresses the fact that the sum of the currents flowing into the tank along the  $x$ -axis between infinity upstream and the point  $x$  of the airfoil is equal to a certain value,  $I$ , not zero, which is proportional to the angle of attack  $\alpha = - (df/dx)$ , given by

$$I = \int_{-\infty}^x di = -\sigma h \int_{-\infty}^x \frac{du}{dy} dx = -\sigma h U(df/dx) = \sigma h U \alpha. \quad (103)$$

Therefore, to avoid the trivial solution  $I = 0$ ,  $\alpha = 0$ , a current source must be placed at the leading edge. This current source corresponds in the theoretical analogy to a singularity (as a matter of fact, the theoretical pressure distribution generally has an infinity at the leading edge of a thin airfoil). The nature of this singularity has been studied in detail by W. F. Campbell (Ref. 39), and for the analog interpretation it is only necessary to know that in its immediate neighborhood the equipotential lines (curves  $U = \text{constant}$ ) and their orthogonal trajectories have the form of cardioids.

An arc of each of these lines may be represented in the electric tank, one by a conducting contour ( $u = \text{constant}$ ), the other by an insulating contour (Fig. XI-3). The conducting contour will thus serve as a feed electrode,  $E_2$ , the current of which will be adjusted so as to satisfy Eq. (103). Aside from this singularity, the rest of the straight line airfoil is represented by an insulating segment.

If, in addition, a flap is hinged on the straight profile at B and given an additional deflection angle,  $\beta$ , the slope,  $df/dx$ , will undergo a discontinuity at B which corresponds to an infinity of the normal derivative,  $\partial u / \partial y$ . A new singularity must then be envisaged at this point. It is easy to verify that this is of logarithmic type. It can be represented in the analogy by a small semicircular electrode,  $E_3$ . Its current flow will be adjusted so that the total current from the three electrodes  $E_3$ ,  $E_2$ , and  $E_0$  is equal to  $\sigma h U (\alpha + \beta)$ . Reading off the electric potential along the insulating part will then give the pressure distribution sought ( $\Delta p = 2\rho U u$ ).

In the general case of a cambered airfoil, the installation of an electrode-singularity at the leading edge and the usual electrodes,  $e$ , will have to be envisaged, the latter in order to satisfy Eq. (100). If a flap exists (or any break whatever in the line) there will also be required a small semicircular electrode at the hinge point (or break).

Finally, it should be remarked that, for all cambered profiles there exists a certain incidence called the "adaptation incidence" at which the infinite pressure rise at the leading edge disappears. In this case, the electrode-singularity  $E_2$  is not necessary. A method for finding the adaptation incidence for a cambered profile can be based on this fact. What is more interesting is that it is also possible to solve the inverse problem, i.e. to determine the form of the airfoil necessary to produce a given pressure distribution which has no infinite peak at the leading edge. In this case, the potentials of the electrodes,  $e$ , are chosen proportional to the pressures, and the current flows are measured. From these the slopes and the airfoil orientation are deduced by the first integration of Eq. (101). The form of the airfoil is obtained by a second integration of Eq. (101).

### Symmetric Problem

In this problem, the pressure distribution over a symmetric airfoil is sought, the airfoil being placed at zero incidence and having thickness  $y$  defined by

$$y = \pm g(x) \cdot \tag{104}$$

To solve this problem a distribution of sources and sinks of varying density can be made along the axis of the airfoil, the value of the density being taken proportional to the slope  $dg(x)/dx$  at the point  $x$  of the segment  $(-l/2, + l/2)$ . The potential  $\varphi(x,y)$  of these sources and sinks can easily be represented in the electric tank. Its defining conditions are simple:

(1) The function  $\varphi$  is zero at infinity and even in  $y$ . It may therefore be defined in the half-plane  $y > 0$ .

(2) On the segment  $(-l/2, + l/2)$  the normal derivative of  $\varphi$  must be proportional to the slope  $dg(x)/dx$  so that the condition of tangency of the fluid at the contour of the object be satisfied:

$$\left(\frac{\partial \varphi}{\partial y}\right)_{y=0} = U(dg/dx) \cdot \tag{105}$$

The arrangement of the small electrodes,  $e$ , is the same as that used for the lifting problem, but, since the field is symmetric about the  $x$ -axis, the edge of the tank which represents this axis is insulating outside the segment  $(-l/2, + l/2)$ . The electrical adjustments are evidently similar to those considered earlier. Once the currents,  $i$ , are fixed, the potentials of the electrodes,  $e$ , are measured, and, as before, the pressures are calculated by differentiation of the potential distribution curve.

One may also consider the acceleration potential  $u = \partial \varphi / \partial x$ . This analysis is similar to that given above for the lifting problem. In this case, it becomes apparent that two singularities are to be represented, one for the leading edge and the other for the trailing edge.

Moreover, the electric tank representation of the function  $\psi(x,y)$  conjugate to  $\varphi(x,y)$  can be envisaged. The problem to be treated is then of the Dirichlet type. According to Eq. (105),  $\psi$  is proportional to the thickness, and it is then only necessary to set up in terms of electric potential, the thickness distribution (Eq. (104)). Along the  $x$ -axis outside of  $(-l/2, + l/2)$ , the potential  $\psi$  is zero, and therefore the arrangement of the tank electrodes is exactly the same as in the wing calculator (see Fig. IX-2). The measurement of the currents flowing through the small electrodes,  $e$ , gives the normal derivative  $\partial \psi / \partial y$  and hence  $\partial \varphi / \partial x$ , i.e. the pressure distribution along the airfoil contour.

#### (b) Principles of the Rheoelectric Analogy for Lifting Surfaces

##### (1) Statement of the Problem

We restate the lifting surface problem here very briefly. The wing, supposed infinitely thin (lifting surface), is placed in a uniform stream of velocity  $U$  parallel to the  $x$ -axis. The span  $2L$  lies along the  $y$ -axis, and the  $z$ -axis is directed vertically, upward being positive. The fluid is supposed incompressible; steady-state potential flow is assumed.

The theory of the lifting surface deals with the case of a thin wing of very small curvature and low inclination to the relative wind. Therefore, from the point of view of defining the velocity potential field, the wing

can be identified with the area  $S$  of its projection on the  $x,y$ -plane. The free vortices occupy the wake region,  $\Sigma$ , which is the projection of  $S$  downstream and is bounded by the two lines parallel to the  $x$ -axis which pass through the wing tips (Fig. XI-4).

The perturbation velocity potential  $\varphi(x,y,z)$  is harmonic and regular in the space surrounding the cut produced by  $S$  and  $\Sigma$ . It can easily be shown that it is an odd function of  $z$  and hence is zero for  $z = 0$  in the region "A" of the  $x,y$ -plane outside  $S$  and  $\Sigma$ . Within  $S$  and  $\Sigma$  it takes on values of opposite sign on either side of this plane. This is also true of its derivatives  $\partial\varphi/\partial x$  and  $\partial\varphi/\partial y$ . On the other hand, the derivative  $\partial\varphi/\partial z$  which is even in  $z$  takes on the same values on either side; it is continuous across the  $x,y$ -plane within the points of  $S$  and  $\Sigma$ .

These preliminary remarks allow the boundary conditions which determine the perturbation potential  $\varphi(x,y,z)$  to be detailed as follows:

a. Since  $\varphi$  is an odd function of  $z$ , it is sufficient to determine it in the half-space  $z > 0$  above the  $x,y$ -plane.

b. The potential,  $\varphi$ , is zero at infinity and zero at every point of the region "A" of the  $x,y$ -plane outside  $S$  and  $\Sigma$ .

c. At every point of  $S$ ,  $\partial\varphi(x,y,0)/\partial z$  takes on values determined by the shape of the lifting surface. Let

$$z = f(x, y) \tag{106}$$

be the equation of the lifting surface. At all points of this surface, the fluid velocity must be tangent to the surface. This gives, with the standard linearizing assumptions:

$$\left(\frac{\partial\varphi}{\partial z}\right)_{z=0} = U \frac{\partial f(x, y)}{\partial x} \tag{107}$$

d. In the wake region,  $\Sigma$ , since the pressure is continuous across  $z=0$ , the function  $\partial\varphi/\partial x$  which is odd in  $z$ , must be zero. Therefore, the potential therein depends only on  $y$  and will be noted by  $\varphi(y)$ .

e. Finally, according to the Joukowski condition,  $\varphi$  is continuous at the trailing edge of  $S$  and the derivative,  $\partial\varphi/\partial x$ , becomes zero there.

It may be recalled also that the circulation about a curve leaving a point  $M$  of  $S$  or  $\Sigma$  and reentering it after having crossed the  $x,y$ -plane at a point of "A", is given by

$$\Gamma(x, y) = 2\varphi(x, y). \tag{108}$$

At a point within the wake,  $\Sigma$ , the circulation, like the potential, depends only on  $y$ . It will be noted by  $\Gamma(y)$ .  $[\Gamma(y) = 2\varphi(y)]$ .

As in the two-dimensional case, the acceleration potential  $u(x,y,z) = \partial\varphi(x,y,z)/\partial x$  can be employed. The boundary conditions which define this potential  $u$  are obtained directly from the preceding ones:

I. Like  $\varphi$ , the function  $u$  is an odd function of  $z$ .

II. The function  $u$  is zero at infinity. It is zero at all points of the area "A" of the  $x,y$ -plane outside  $S$ . It will be noticed that, according to subparagraph d, it is now zero within the wake  $\Sigma$ .

III. The condition of tangent flow of the fluid along the surface gives, from Eq. (107),

$$\left(\frac{\partial u}{\partial z}\right)_{z=0} = U \frac{\partial^2 f(x, y)}{\partial x^2} \tag{109}$$

to which could be added, in view of the necessity of defining the angle of attack of each section (see the remarks on this topic, in the two-dimensional case),

$$\int_{-\infty}^x \left( \frac{\partial u}{\partial z} \right)_{z=0} dx = U \frac{\partial f(x)}{\partial x} \quad (110)$$

the integration being along a line  $y = \text{constant}$  (which is the ordinate of the section considered) up to an arbitrary point  $x$  of the wing section where the slope is defined by  $\partial f(x)/\partial x$ .

Finally, the Joukowsky condition requires that  $u(S)$  tend toward zero at the trailing edge.

(2) Principles of the Analogy  
for the Velocity Potential  
 $\varphi(x,y,z)$

The harmonic perturbation potential  $\varphi(x,y,z)$  is identified in the half-space  $x,y,z$  ( $z > 0$ ), with the electrical potential,  $V$ , in a deep tank of large dimensions. The  $x,y$ -plane can be represented by the free surface of the liquid, and the electrical potential,  $V$ , is thus defined (condition (1)) in a conducting half-space wherein the positive  $z$ -axis corresponds to the downward-pointing vertical.

The analog interpretation of the boundary conditions leads to the following representations (Fig. XI-5).

a. In accordance with condition (2), the area,  $A$ , of the  $x,y$ -plane outside ( $S+\Sigma$ ), is represented by a large conducting plate  $E_0$  covering the corresponding surface of the liquid. This electrode,  $E_0$ , is connected directly to one terminal of the generator,  $G$ , and its potential is conventionally taken as the zero of the electrical potential scale.

b. To satisfy condition (107), the area,  $S$ , is represented by a sort of checkerboard consisting of a large number of small electrodes,  $e$ , each of which represents an element,  $\delta S$ , of the area,  $S$ , of the wing. Each electrode is electrically fed so that it passes a current,  $i$ , proportional to the local slope of the lifting surface, this slope being measured in the  $x$ -direction and calculated at point  $(x,y)$  (midpoint of electrode  $e$ ) by the formula

$$i = -\sigma U \delta S \left( \frac{\partial f(x,y)}{\partial x} \right). \quad (111)$$

c. In accordance with condition (4) the wake region,  $\Sigma$ , is represented by a certain number of electrodes,  $E_\Sigma$ , which form narrow conducting bands parallel to the  $x$ -axis. Thus the electrical potential,  $V$ , is constant along each band, and its value at a point  $(x,y)$  of  $\Sigma$  can only be a function of the ordinate  $y$ . This is, in fact, the requirement imposed on  $\varphi$  at any point of the wake.

d. The value of the potential  $V(y)$  of an arbitrary one of these bands is at first unknown. To determine it, it is necessary to take into account the Joukowsky condition (5) for which the analog interpretation may be translated as the continuity of the electrical potential between the wing and its wake. The values  $V(y)$  are regulated so as to achieve equality between the potentials of  $E_\Sigma$  and those of the last line of wing electrodes (this is a generalization of the two-dimensional case of Section XI(a)(1)).

(3) Description and Operation  
of an Analog Installation

In the most recent installations made in France, at ONERA (Office National d'Etudes et de Recherches Aéronautiques)

and the CNRS (Centre National de la Recherche Scientifique), the tank used is of slate and has interior dimensions 200 x 100 x 80 cm. The large surface electrode,  $E_0$ , covering the tank, is composed of several rectangular panels fitted together. The method of attachment of these panels is such that one or several can easily be removed and replaced by another which carries the analog model of the wing,  $S$ , and its wake,  $\Sigma$ .

It may immediately be remarked, in this connection, that the wing plan form is symmetric about the  $x$ -axis in the most typical applications. The representation is then limited to half the field. A vertical side of the tank is taken to represent the  $x,z$ -plane. In the case of perfect symmetry of the wing slopes (on either side of this plane), this tank wall is left insulating. In the case of perfect antisymmetry, (aileron study, for example), this wall is covered by an electrode connected to  $E_0$  along the  $x$ -axis and held, therefore, at zero potential.

The model representing only half the total wing,  $S$ , and its wake,  $\Sigma$ , the panel which carries it is placed on the surface ( $x,y$ -plane) and has one edge (the  $x$ -axis) against the side of the tank representing the  $x,z$ -plane. If the flow under study presents no symmetry with respect to  $y$ , the model-carrying panel is placed horizontally near the middle of the tank surface. In this case the whole wing is represented. Wing plan forms being almost always symmetric, this unsymmetric study is practically never used except for the case of a wing flying at an angle of yaw.

The panel which carries the wing model is made of plexiglass. The electrodes,  $e$ , on it are made as follows. At the center of each electrode a hole is drilled and threaded so as to take a screw, the head of which is flush with the surface that is

later to be in contact with the water surface of the tank. The other end of the screw, coming out of the upper side of the plate, takes a fastener to accommodate an electrical wire lead. The electrode is then painted over the screw head, silver-base electrically conducting paint being used. This is applied to all the electrodes at once, usually by gun spraying of the entire surface, after attachment to the plate of narrow bands of paper which represent the separating strips between electrodes. When these strips are pulled off later, they leave the insulating spaces which define the checkerboard of electrodes  $e$ . The preparation of these models is fast and cheap. The wake electrodes,  $E_\Sigma$ , may be prepared in the same fashion on the same plexiglass panel.

The geometric arrangement of the electrodes may be chosen so that the semi-span  $L$  is divided into 11 strips, the midpoints of which correspond to the nondimensional spanwise coordinates  $y/L = 0, 0.1, 0.2, \dots, 0.9, 0.975$ . The way in which  $S$  is divided up into elementary areas  $\delta S$  depends on the wing plan form. It may, depending on the case, be carried out according to rectangular, parallelogram, or trapezoidal patterns. In Fig. XI-6, a system of wing elements is shown for the simple case of a sweptback wing with constant chord (all dimensions are given in millimeters).

The electrical feed circuits and controls may be grouped in a separate installation which forms, together with the tank set-up, an analog calculating machine which has been called the "lifting surface calculator." In those machines which are presently in service, the feed unit is able to handle 120 electrodes,  $e$ . It can establish either 120 electrical potential values or impose 120 current values by any one of the methods outlined in Section XI (a) (1).

The calculations preparatory to the tank tests are usually very rapid. They consist

of the determination of the coordinates of the center of each electrode,  $e$ , the calculation of the slope,  $\partial f/\partial x$ , at each corresponding point, the calculation of the elementary areas,  $\delta S$ , which are determined by the way in which the wing is divided up geometrically into electrodes. (Note that  $\delta S$  is not calculated as the electrode area alone but rather the entirety of one of the elemental subareas into which the wing is divided).

The electrode-carrying panel must be placed in position with some care in order to avoid formation of small air bubbles between the liquid and the electrodes. The time required to fix the current flows,  $i$ , depends on the electrical set-up used. When the large resistances,  $R$ , are used the settings are automatically made as soon as the resistance values are chosen on the electrical feed panel. In this case it remains necessary only to manipulate the potentiometers,  $\pi$ , controlling the wake electrodes,  $E_{\Sigma}$ , so as to satisfy the Joukowski condition by bringing the potentials of these electrodes into coincidence with the potentials of the corresponding electrodes,  $e$ , at the trailing edge.

Once these adjustments have been made, the measuring potentiometer  $P$  is used to read off the potentials at all the electrodes  $e$  and  $E_{\Sigma}$ . The conductivity,  $\sigma$ , of the tank water is also obtained by means of the special resistivity-measuring cell described in Section IV (a).

The length of time necessary for an experiment of this type does not exceed two hours, even in the most complicated cases. In general, a great number of tests are run off on a given wing. The various effects of incidence, camber, flaps, ailerons, etc., are determined separately. During such systematic investigations, certain tests require only a few minutes (for example, determination of the effect of flaps or ailerons).

The reduction of test results is carried out without special difficulty since the circulation  $\Gamma$  and the electrical potential are simply linked by a proportionality factor. To take a specific example, let us consider the wing of Fig. XI-6, which will enable the reader to grasp the order of magnitude of the quantities involved.

The problem selected is that of defining the effect of incidence ( $\partial f/\partial x = \text{constant} = -\alpha$ ,  $\alpha$  being the angle of attack). The model of this wing has a semispan of 20 cm, the wing chord is  $l = L/2$ , one of the elementary areas is  $\delta S = L/10$  ( $l/10$ ) =  $L^2/200$  (half this value for the electrode  $e$  on the midsection  $y/L = 0$  and at the tip  $y/L = 0.975$ ). Large resistances,  $R$ , of 500,000 ohms are used (with 1 megohm for  $y/L = 0$  and 0.975).

It is always convenient to determine the circulation in reduced form, taking for example

$$\gamma = \frac{\Gamma}{UL\alpha} \quad (112)$$

From this the following formula will result, as can easily be verified from Eqs. (111) and (98) wherein the product,  $\epsilon h$ , is replaced by  $\delta S$ :

$$\gamma = \frac{2V}{100} R \sigma \frac{\delta S}{L} \quad (113)$$

Since the conductivity measurement yields, let us say,  $1/\sigma = 2500$  ohm cm, Eq. (113) yields simply

$$\gamma = \frac{V}{2.5} \quad (114)$$

where  $V$  is taken as usual within the 0 to 100 scale. The maximum value of  $\gamma$  is obtained

here for a trailing edge electrode for which  $y/L = 0.4$ ,  $V$  being measured at  $V = 2.122$ , i.e. from Eq. (114),  $\gamma = 0.8488$  ( $\alpha$  being measured in radians).

The measurement of the wake electrode potentials gives the  $\gamma(y)$  distribution directly throughout the span. The  $\gamma(y)$  distribution in the chordwise direction for each section  $y = \text{constant}$  must be differentiated to give the pressure coefficient distributions. It is interesting to note that this differentiation is unnecessary if only the center of lift be required at each section.

It may be shown that the distance,  $X$ , of the center of lift from the leading edge of a given section,  $y$ , of chord,  $l$ , is given by

$$\frac{X}{l} = 1 - \frac{1}{\gamma(y)} \int_0^l \gamma \frac{dx}{l} \quad (115)$$

where  $\gamma(y)$  is the total circulation about the section (obtained directly from the measurement of the electric potential of the corresponding wake electrode). The numerical calculation of the integral Eq. (115) is carried out easily, given the curve of distribution  $\gamma(x/l)$ .

#### (4) Examples

The most common application evidently concerns the load distribution over a plane wing when  $\partial f/\partial x = \text{constant} = -\alpha$  (incidence effect). There is no need to discuss this case in detail, for a particularly simple analog representation of it will be presented in the next section.

The lifting surface calculator is practical for evaluating effects of curvature and, particularly, of flaps (or ailerons). In the latter problem, the effect due to a flap deflection,  $\beta$ , is determined when  $\partial f/\partial x = 0$  all over

the wing except at the flap and  $\partial f/\partial x = \text{constant} = \beta$  in the flap region. The electrodes,  $e$ , for which  $\partial f/\partial x$  is zero are therefore not electrically connected. It is therefore easy, after having run off the experiment for determining incidence effects ( $\partial f/\partial x = \text{constant}$  all over  $S$ ), to disconnect those electrodes outside the flap region. The effects of flaps which are successively reduced in dimensions can thus easily be ascertained.

When greater accuracy is desired, a special model can be prepared which concentrates a large number of electrodes (up to 120 with the aforementioned installation) in the flap (or aileron) region, leaving the rest of the surface,  $S$ , insulating. This type of model has been used to determine as completely as possible the loads on a flap. Fig. XI-7 gives an example of this.

The division of the wing into elementary areas  $\delta S$  corresponding to the electrodes,  $e$ , lends itself particularly well to the determination of aerodynamic influence coefficients. R. H. Scanlan has used this fact to develop an elegant method of calculation for steady-state aeroelastic phenomena (Ref. 55). The aerodynamic influence coefficients are determined by using only one electrode,  $e$ , at once, the Joukowski condition being satisfied along the trailing edge. (It is of course necessary to make as many test runs as there are electrodes in order to define all the elementary effects.) On occasion, it may be sufficient to determine the elementary effects only for each chordwise strip  $y = \text{constant}$  or each of several small groups of electrodes.

When the aerodynamic influence coefficients are known it is possible to calculate the lift distribution corresponding to any distribution of twist by linear superposition

of elementary effects. However, the constitution of the tables of influence coefficients necessitates a very large number of test manipulations and measurements and thus represents a large amount of work. Therefore, in the case where overall wing characteristics are sufficient, use is made of the well-known reverse-flow properties of the wing. It is a known fact that the total lift, as well as the total pitching and rolling moments, can easily be obtained for a given wing (no matter what twist distribution or flap and aileron dispositions it may have) from certain results obtained on the wing of the same plan form placed in a stream of reversed direction (velocity =  $-U$ ) and studied for certain special twist distribution.

In such studies, it is obviously advantageous to have to build only a single model of the given plan form. Therefore, the analogy provides for representation of the two wakes,  $\Sigma$  and  $\Sigma'$ , one behind the trailing edge for forward flight, and the other ahead of the wing for reverse-flow studies. (Fig. XI-8). According to the case under examination, either the electrodes  $E_{\Sigma'}$ , or the electrodes  $E_{\Sigma}$  (for reverse flow) are short-circuited to zero by connecting them to  $E_0$ .

In the study of the two-dimensional case it was seen that the electrical analogy could serve to define the camber distribution required over an airfoil to give a prescribed pressure distribution. The solution of this problem presents no special difficulty in the case of the lifting surface (Ref. 67). Knowledge of the pressure distribution gives the value of  $\partial\varphi/\partial x$  at each point of  $S$ , and, by integration, the perturbation potential  $\varphi(x,y)$ . It is then necessary to establish a known potential at each electrode,  $e$ , as well as at each of the wake electrodes  $E_{\Sigma}$ .

This operation is very easy to carry out by means of the potentiometers  $p$  and  $\pi$  of the general electrical feed panel.

Once these adjustments have been made the currents,  $i$ , flowing through the electrodes are measured. In this way, the slopes  $\partial f/\partial x$  are obtained, and finally, the equation of the surface  $z = f(x,y)$ , by integration.

This analog procedure is used especially in adaptation problems, determination of the camber to be given to a wing of given plan form in order to avoid an infinite pressure rise at the leading edge. There are clearly an infinity of possible solutions, among which the ones appearing more favorable can be chosen quite rapidly through use of the electrical analogy.

As another application, the possibility of studying various lifting-surface interaction problems in the electric tank can be mentioned. The remarks in Chapter IX concerning the lifting line suggest how the effect of wind tunnel walls may be taken into account. Wall corrections of closed or open test sections can be studied in this way. It is only necessary to limit the electric tank by insulating or conducting boundaries according to the case under consideration.

In a very similar way, the effect of a central body (representing a fuselage, for example) can be studied. If, for instance, this body is a cylinder of indefinite length having the  $x$ -axis for centerline, it can be represented in the tank by an insulating model as shown in Fig. XI-9.

Cases of configurations which are unsymmetrical about the  $x,y$ -plane can also be treated, but then it is necessary to represent physically the cut ( $S+\Sigma$ ) with pairs of opposed electrodes ( $e^+$ ,  $e^-$ ) and ( $E_{\Sigma}^+$ ,  $E_{\Sigma}^-$ ) on the upper and lower cut surfaces, and to feed these electrode pairs by means of transformers as in the lifting line problems (see Section IX (d)). In these cases the construction of the model is much more complicated.

(5) Analog Study of Plane Wings

R. Duquenne has developed the principles of a very interesting analog method for studying plane wings (Ref. 47). In this case, the slope  $\partial f/\partial x$  being constant and equal to  $-\alpha$  ( $\alpha$  being the angle of attack), the preceding condition (107) which must be satisfied throughout the wing area,  $S$ , reduces to

$$\left(\frac{\partial \varphi}{\partial z}\right)_{z=0} = -U\alpha. \tag{116}$$

For the electric tank representation it is then advantageous to consider a new potential,  $\varphi_1(x,y,z)$ , such that

$$\varphi_1(x,y,z) = \varphi(x,y,z) + U\alpha z. \tag{117}$$

In the  $x,y$ -plane this potential  $\varphi_1$  is equal to  $\varphi$  (since  $z = 0$ ). It is therefore zero outside  $S+\Sigma$  and takes on the same values as  $\varphi$  on the wing,  $S$ , and wake,  $\Sigma$ . The condition of tangent flow (116) is simplified for  $\varphi_1$  because, in view of Eq. (117), the following must hold:

$$\left(\frac{\partial \varphi_1}{\partial z}\right)_{z=0} = 0 \tag{118}$$

this condition indicating that the normal derivative of  $\varphi_1$  must vanish at the surface.

From the electrical standpoint this condition is particularly easy to satisfy since it corresponds, in the tank, to representing the area occupied by the wing model by an insulating surface. The construction of the analog model is thus very much simplified and the construction of the checker-board of electrodes needed in the general method described above is avoided, as are the corresponding current-flow adjustments. It may further be noted that the potential

distribution throughout  $S$ , i.e., the circulation  $\Gamma(x,y)$ , is then a continuous one.

The boundary condition at infinity must evidently be observed also. Far from the model, at the bottom of the tank, for example, it was previously considered that the potential,  $\varphi$ , vanished. As a result, according to Eq. (117),  $\varphi_1$  is reduced to that for a uniform flow  $U\alpha z$ . Therefore, if  $H$  is the depth of the tank, the difference  $\Delta\varphi_1$  in  $\varphi_1$  between  $z=0$  and  $z = H$  must be given by

$$\Delta\varphi_1 = U\alpha H. \tag{119}$$

Hence the bottom of the tank is fed electrically by means of a horizontal electrode,  $E_1$ , raised to a potential proportional to  $U\alpha H$ .

The electrical set-up is shown in Fig. XI-10. The electric tank is fed through the two electrodes  $E_0$  and  $E_1$  and by the wake electrodes  $E_\Sigma$ . Far from the object a uniform electric current parallel to the  $z$ -axis is established between the electrodes  $E_0$  and  $E_1$ . This corresponds to a flow normal to the wing of velocity  $U\alpha$ .

The only adjustments necessary are in connection with the Joukowski condition. Continuity of the electric potential must be assured between the trailing edge of the wing and the wake. To accomplish this, a tiny probe is placed in the immediate neighborhood of (and aligned with) each wake electrode  $E_\Sigma$ . The potentiometers,  $\pi$ , are then manipulated so as to equalize the potential between the probe and the corresponding electrode,  $E_\Sigma$ .

The strength of the circulation  $\Gamma(x,y)$  at a point of the wing is calculated by measuring the electric potential  $V_1 = m\varphi_1$ . The

reduced circulation,  $\gamma$ , is then given by

$$\gamma = \Gamma / UL = 2V_1 / mUL$$

If  $\Delta V_1$  is the potential difference between the electrodes  $E_0$  and  $E_1$ , then  $\Delta V_1 = mU\alpha H$ , from which

$$\gamma(x,y) = 2\alpha \frac{H}{L} \frac{V_1(x,y)}{\Delta V_1} \quad (120)$$

This method is extremely valuable for determining the effect of angle of attack change for a lifting surface of arbitrary plan form. The accuracy of results obtained is of the order of  $\pm 1.5\%$ , which is satisfactory for applications. As may be imagined, the test runs are very rapid. This set-up is now in everyday use for all lifting surface calculations. The studies of Ref. 60 were carried out in this way.

Since the model of the wing surface,  $S$ , is insulating, the free surface of the liquid can be used to represent it if the plan form of  $S$  be cut out of the electrode  $E_0$  covering the tank water surface. In this case, certain precautions must be taken to adjust the water level correctly. The adjustment of the Joukowsky condition is in fact quite sensitive to small depth changes. Hence, to satisfy this condition, it is preferable to cover the open hole with an insulating plexiglass plate, leaving tiny holes in the plate for passage of the probe. Once these precautions have been followed and the Joukowsky condition satisfied, the insulating cover plate may be removed for purposes of tracing out the complete, continuous field of surface equipotential lines.

In this way, the locations of the vortex filaments are traced out (Fig. XI-11). Also, if the double probe is used with an orientation parallel to the  $x$ -axis, the electric gradient at each point can be obtained and

even the curves of  $(\partial V_1 / \partial x)_{z=0} = \text{constant}$  traced out, these latter defining the isobars of the lifting surface.

It is interesting to remark that the traces of the equipotential lines over the wing may be used, if the uniform field,  $U_x$ , is added, to define the potential lines of the whole flow. If thereafter the orthogonal trajectories of these curves are traced, an image of the streamlines over the wing surface is produced. This picture is useful for obtaining information on the general aspect of the flow at various angles of attack. Fig. XI-12 is an example of the streamlines traced in this way over the upper and lower sides of a delta wing at 18 degrees incidence.

Finally, it may be noted that R. Duquenne's method is particularly well suited to the analysis of reverse flow. The upstream and downstream wake electrodes are easily visualized. The equipotential field in reverse flow, traced out as has been described above, is very useful for rapid prediction of any lift variation brought about by a change in wing camber and particularly the increase in lift due to deflection of a flap occupying any part of the wing surface,  $S$ . Examples of this are given in Ref. 63.

#### (6) Principles of the Acceleration Potential Analogy

The boundary conditions for the acceleration potential,  $u(x,y,z)$ , have already been discussed above in Section XI (b) (1). It was seen for the two-dimensional case, that the condition (110) implied the existence of a singularity on the leading edge of the airfoil. In the case of the lifting surface there will exist, then, a line of singularities along the leading edge (Ref. 39).

To make this more concrete, let us first consider the simple case of a plane wing

( $\partial f / \partial x = -U\alpha$ ,  $\partial^2 f / \partial x^2 = 0$ ). According to Eq. (109) the surface,  $S$ , is represented by an insulating plate. Along the leading edge must be placed a row of projecting electrodes, shaped in the form of arcs of cardioids according to the form indicated in the two-dimensional case. The conducting parts of these singularities are separated from each other and constitute independent electrodes  $E_2^1$ ,  $E_2^2$ ,  $E_2^3$ , . . . (Fig. XI-13).

According to condition II the potential,  $u$ , is zero in the  $xy$ -plane outside the wing,  $S$ ; therefore a large electrode  $E_0$  will again be used to cover the remainder of the liquid surface, its potential being zero as before. To satisfy condition (110), it is necessary to divide  $E_0$  into independent strips  $E_0^1$ ,  $E_0^2$ ,  $E_0^3$ , located respectively across from the projecting electrodes  $E_2^1$ ,  $E_2^2$ ,  $E_2^3$ , . . . so as to assure that the difference  $I^n$  between the electric current  $I_2^n$  entering the tank through  $E_0^n$ , for example, and that,  $I_0^n$ , leaving by way of  $E^1$ , actually satisfies the condition

$$I^n = I_2^n - I_0^n = \sigma h U \alpha. \quad (121)$$

This electrical set-up thus allows adjustment of the current flows through the projecting electrodes so as to be able correctly to represent the slope,  $\alpha$ , of each section. It will also be noticed that the analog model is not modified if the wing, while retaining straight-line airfoil sections, has a twist distribution  $\alpha(y)$ . It is only necessary, in this case, to adjust the values of  $I(y)$  according to the given distribution  $\alpha(y)$ .

If the wing is equipped with a flap (or aileron), it is also necessary to attach another line of semicircular singularities to  $S$ . (See the two-dimensional case.) These singularities will correspond to new projecting electrodes  $E_3^1$ ,  $E_3^2$ ,  $E_3^3$ , . . . the current flows  $I_3^1$ ,  $I_3^2$ ,  $I_3^3$ , . . . of which will

be adjusted proportional to the deflection angle of the control surface.

Finally, in the general case of a cambered lifting surface, the standard small electrodes,  $e$ , must be provided, each one representing an element,  $\delta S$ , of the surface. According to Eq. (109) these electrodes will emit currents proportional to the curvatures  $\partial^2 f / \partial x^2$ .

The construction of the projecting electrodes at the leading edge is not always easy; therefore this analogy, even though very attractive because it gives wing pressure distributions directly, is less used than that of the velocity potential.

On the other hand, for questions of adaptation, the acceleration potential analogy is quite useful. In this case, the inverse problem is involved. A pressure distribution is given over the wing and the corresponding form to be given to the wing surface is sought. In the adaptation case (finite velocity at the leading edge) the singularities disappear and the problem reduces to a Dirichlet problem on the wing. Setting of the potentials of the electrodes,  $e$ , on the wing to values proportional to the known pressures (if the pressure distribution is uniform, these potentials are constant over  $S$ ) (Ref. 67).

Subsequent measurement of the current flows gives, from Eq. (109), the curvature  $\partial^2 f / \partial x^2$ . The upstream electrodes  $E_0^1$ ,  $E_0^2$ ,  $E_0^3$ , . . . must again be used, the current flow through each being measured in order to permit calculation by Eq. (110), of the slope  $\partial f / \partial x$  at any point of the section under consideration. In this way there may be ascertained the angle of attack setting of each section  $y = \text{constant}$ , which cannot be defined by the knowledge of  $\partial^2 f / \partial x^2$  alone at the point  $(x, y)$ .

The analog experiments can be carried out using the model described in Section XI (b) (4) which serves for the study of forward and reverse flows. This model contains, in fact, upstream and downstream electrodes,  $E_{\Sigma'}$  and  $E_{\Sigma}$ ; the former,  $E_{\Sigma'}$ , may play the role of the electrodes  $E_0^n$  of the present problem. The others,  $E_{\Sigma}$ , are then all shortcircuited to  $E_0$ .

(c) Analog Study of Thin Wings  
 (Symmetric Problem)

The study described in Section XI (a) (2) for the two-dimensional case is easily generalized to the case of a wing of any form (Ref. 58). The wing is supposed very thin, at zero lift, and made up of symmetric airfoil sections.

The thickness distribution is defined by the equation

$$z = \pm g(x, y). \quad (122)$$

Here the perturbation potential,  $\varphi(x, y, z)$ , is an even function of  $z$ ; therefore, in the  $xy$ -plane outside  $S$ , the normal derivative  $(\partial \varphi / \partial z)_{z=0}$  is zero. The corresponding boundary of the electric tank will be insulating and this may be taken as the free surface of the liquid.

The condition of tangent flow of the fluid over the wing implies that on  $S$

$$\left(\frac{\partial \varphi}{\partial z}\right)_{z=0} = U \frac{\partial g(x, y)}{\partial x}. \quad (123)$$

From the electrical standpoint, current flows,  $i$ , will again be required, passing through electrodes,  $e$ . The currents will be taken proportional to the slopes

$\partial g(x, y) / \partial x$ :

$$i = -\sigma U S S (\partial g(x, y) / \partial x). \quad (124)$$

The analog model of the wing,  $S$ , is identical to that for the lifting problem. In general the electrical method based on the large resistances,  $R$ , is used in these experiments. For a given wing section ( $y = \text{const.}$ ) the slopes  $\partial g / \partial x$  have opposite signs near the leading and trailing edges. The current flows,  $i$ , should also satisfy this requirement. The electric currents then enter the tank through the electrodes,  $e$ , near the leading edge and leave by those near the trailing edge, the sum of these currents over a section of fixed chord being zero.

According to the sign of the current,  $i$ , the resistance,  $R$ , will be connected to the positive or negative terminal of the generator,  $G$ . The measurement of the potentials at the electrodes,  $e$ , will give the perturbation potential  $\varphi(x, y, 0)$  on the wing. Differentiation in the  $x$ -direction will finally yield the pressure distribution over each section.

This method has been employed for various wing plan forms and thickness distributions. It is very rapid and convenient when, for a given plan form, the changes in pressure distribution due to local modifications of the thickness are sought. In this manner certain regions of the wing can be shaped to obtain desired changes in the pressure distribution.

The inverse problem can also be handled. Here, again, is sought the thickness distribution required over a wing to give a desired pressure distribution. One starts in this case from a distribution of  $\partial \varphi / \partial x$  for each section  $y = \text{constant}$ . Upon integrating in the  $x$ -direction,  $\varphi(x, y)$  is obtained, and the

problem is reduced to one of Dirichlet type. However, the distribution,  $\partial \varphi / \partial x$ , which is adopted must be compatible with a thickness distribution which goes to zero at the leading and trailing edges.

This condition can automatically be imposed if all the potentiometers,  $p$ , of a single section are fed by an independent generator, that is, in practice, by a transformer. One can thus be sure that the algebraic sum of the current flows in the section is actually zero. In this case, if the chosen distribution,  $\partial \varphi / \partial x$ , is incompatible it becomes immediately apparent, because it will not then be possible to adjust the potentials,  $\varphi$ , to the values which have been chosen.

## XII. ANALOG STUDY OF COMPRESSIBLE FLOWS

### (a) Representation of Subsonic Compressible Flow Fields

The principle of the electric tank representation of plane compressible flow fields was given by G. I. Taylor (Refs. 3 and 4) in 1928. A brief review will be given of this method.

The velocity potential,  $\varphi(x,y)$ , of a plane steady-state flow of a compressible fluid satisfies the equation

$$\frac{\partial}{\partial x} \left( \rho \frac{\partial \varphi}{\partial x} \right) + \frac{\partial}{\partial y} \left( \rho \frac{\partial \varphi}{\partial y} \right) = 0 \quad (125)$$

wherein  $\rho(x,y)$  is the density which varies from point to point.

The stream function,  $\psi(x,y)$ , of such a flow is governed by the equation

$$\frac{\partial}{\partial x} \left( \frac{1}{\rho} \frac{\partial \psi}{\partial x} \right) + \frac{\partial}{\partial y} \left( \frac{1}{\rho} \frac{\partial \psi}{\partial y} \right) = 0. \quad (126)$$

Eq. (125), when compared to the expression Eq. (5) defining the distribution of electrical potential,  $V(x,y)$ , in a conducting plate of slowly varying thickness, shows that the velocity potential,  $\varphi(x,y)$ , may be identified with  $V(x,y)$  provided that the bottom of the electric tank is so constructed that the depth,  $h(x,y)$ , at each point is proportional to the density,  $\rho(x,y)$ . In the same way, using Eq. (126), it is seen that the stream function,  $\psi(x,y)$ , may be obtained in a tank wherein the depth,  $h(x,y)$ , is inversely proportional to  $\rho(x,y)$ .

It should be noticed, however, that in this type of problem the density,  $\rho(x,y)$ , is a priori unknown and is only determined in terms of the velocity of the flow at the same point  $(x,y)$  through use of the characteristic equation of the fluid and Bernoulli's equation. The electric tank solution of Eqs. (125) or (126) can therefore be effected only through a process of successive approximations. The following is the method used.

An approximate distribution for  $\rho(x,y)$  is used to start with. From this a first approximation,  $h_1(x,y)$ , is obtained for the depth of the electric tank. Often this first approximation is simply taken as the incompressible value, i.e.  $\rho = \rho_1 = \text{constant}$ . The analog experiment then being carried out in the standard way, the electrical gradient at each point of the field is measured, and from this the fluid velocity at each point is determined. Using this velocity distribution, a new, closer approximation is calculated for the density, say  $\rho_2$ .

The experiment is redone with the corresponding new depths,  $h_2$ . The velocity field is once more determined, and a third approximation ( $\rho_3, h_3$ ) is thus obtained. This process is continued until the measurements of the  $n^{\text{th}}$  experiment coincide with those of the  $(n-1)^{\text{st}}$  experiment. The applications of

this method which have been carried out have shown that convergence was satisfactory as long as the Mach number was less than one, and the flow showed no extreme local velocity peaks.

In practice the bottom of the tank is constructed of materials which are easily cut and sculptured. For this, paraffin or hard beeswax or a mixture of the two is used. The velocity at a point is measured from the electrical gradient by means of the double probe as was indicated in Section III (f). It is obviously convenient to use the set-up described later in the same section which directly traces the constant velocity lines corresponding to lines of constant density.

These correspond also to the lines of constant depth ( $h_n = \text{constant}$ ) of the surface of the bottom of the tank for the next experiment. The graphical trace of these lines can then be used to guide a small rotary cutter which is supported (in place of the probe) by the traveling carriage Section III (d). This cutter mills out in the wax bottom the trace of each contour line of constant depth at the proper level. It only remains necessary to scratch or file off the surplus material located between the lines of constant depth. This modeling of the bottom remains a rather long and painstaking process, particularly in the neighborhood of a body such as a wing section where the velocities, and as a result, the depths, vary rapidly.

The analog representation of the circulation is accomplished in the same way as in the case of an incompressible fluid. A conducting model of the body serving as an auxiliary electrode in the case of analogy B (Section IV (a)) and an insulating model of the body, with a material cut provided, in the case of analogy A (Section IV (a)). For a wing section the Joukowski

trailing edge condition is satisfied in the same way as was described in Section III (b).

This method was applied by G. I. Taylor in the determination of the compressible flow about a circular cylinder and in the study of certain wing sections. It is quite convenient to use for analyzing the flow in a plane convergent channel. An example of this is given in Fig. XII-1 wherein the orthogonal network of equipotential lines and streamlines is given for a flow having a Mach number which varies practically from 0 to 1 in passing from upstream to downstream positions. Certain studies of this type also have been carried out on compressible flows through cascades of airfoils, using the special set-up described in Section VI (b).

It should finally be mentioned that the method is applicable to axially symmetric flows as well. Here the velocity potential,  $\varphi(x,y)$ , defined in a meridian plane,  $x,y$ , through the origin, 0, (where  $x$  is the axis of revolution) satisfies the equation

$$\frac{\partial}{\partial x} (\rho y \frac{\partial \varphi}{\partial x}) + \frac{\partial}{\partial y} (\rho y \frac{\partial \varphi}{\partial y}) = 0. \tag{127}$$

In the electric tank set-up it is then necessary to choose the depth,  $h(x,y)$ , proportional to the product,  $\rho y$ , of the density,  $\rho$ , by the ordinate,  $y$ , of the point under consideration. Therefore the tank bottom must be inclined and sculpted. It is seen, analogously, that for representation of the stream function,  $\psi(x,y)$ , the depth must be made inversely proportional to  $\rho y$ .

#### (b) Hodograph Tank

The determination of the velocity potential,  $\varphi$ , or the stream function,  $\psi$ , can also be carried out by replacing the space coordinates

(x,y) by the independent variables (q,θ) which are the modulus and argument of the velocity. The flow is then defined in the hodograph plane. It is evidently possible to envisage an analogy in which the tank represents the (q,θ) plane and in which the electric potential, V, represents either φ or ψ. The principle of this analogy is based on the following considerations.

In the hodograph plane the velocity potential, φ, and the stream function, ψ, of a compressible fluid are related by the following classical equations:

$$\begin{aligned} \frac{\partial \varphi}{\partial q} &= -\frac{\rho_0}{\rho q} (1 - M^2) \frac{\partial \psi}{\partial \theta} \\ \frac{\partial \varphi}{\partial \theta} &= q \frac{\rho_0}{\rho} \frac{\partial \psi}{\partial q} \end{aligned} \quad (128)$$

where M is the local Mach number and ρ<sub>0</sub> is the density for q = 0.

From these relations it is immediately possible to obtain the partial differential equations which govern φ and ψ:

$$\frac{\partial}{\partial q} \left[ \frac{1}{\frac{\rho_0}{\rho q} (1 - M^2)} \frac{\partial \varphi}{\partial q} \right] + \frac{\partial}{\partial \theta} \left[ \frac{\rho}{q \rho_0} \frac{\partial \varphi}{\partial \theta} \right] = 0 \quad (129)$$

$$\frac{\partial}{\partial q} \left[ q \frac{\rho_0}{\rho} \frac{\partial \psi}{\partial q} \right] + \frac{\partial}{\partial \theta} \left[ \frac{\rho_0}{\rho q} (1 - M^2) \frac{\partial \psi}{\partial \theta} \right] = 0 \quad (130)$$

These expressions may be compared to the expression Eq. (83) which defines, in polar coordinates (r,θ), the distribution of electric potential, V, in a solid conductor of revolution having thickness h(r):

$$\frac{\partial}{\partial r} \left( hr \frac{\partial V}{\partial r} \right) + \frac{\partial}{\partial \theta} \left( \frac{h}{r} \frac{\partial V}{\partial \theta} \right) = 0 \quad (83)$$

By identifying Eqs. (129) or (130) with Eq. (83) it is possible to establish the correspondence, r(q), as well as the function,

h(q), (i.e., h(r)) for the depth of the electric tank.

This latter point may be made clear by taking, for example, the case where V represents φ. It is convenient to set:

$$\tau = \frac{q^2}{2a_0^2} (\gamma - 1)$$

$$\beta = \frac{1}{\gamma - 1}$$

$$\delta = \frac{\gamma + 1}{\gamma - 1}$$

(where γ is the ratio of specific heats and a<sub>0</sub> is the velocity of sound for q = 0). Eq. (129) may then be written:

$$\begin{aligned} \frac{\partial}{\partial \tau} \left[ \frac{2\tau(1-\tau)^{\beta+1}}{1-(2\beta+1)\tau} \frac{\partial \varphi}{\partial \tau} \right] \\ + \frac{\partial}{\partial \theta} \left[ \frac{1}{2\tau(1-\tau)^\beta} \frac{\partial \varphi}{\partial \theta} \right] = 0. \end{aligned} \quad (131)$$

In order to define the transformation τ = τ(r), the partial derivatives of V with respect to τ are introduced into Eq. (83) and the result is identified term by term with Eq. (131). The result is

$$\begin{aligned} \frac{h}{r} \cdot 2\tau(1-\tau)^{-\beta} &= hr \left( \frac{dr}{d\tau} \right)^2 \frac{1-(2\beta+1)\tau}{2\tau(1-\tau)^{\beta+1}} \\ &= \frac{\frac{\partial}{\partial r} \left( hr \frac{\partial \tau}{\partial r} \right)}{\frac{\partial}{\partial \tau} \left[ \frac{2\tau(1-\tau)^{\beta+1}}{1-(2\beta+1)\tau} \right]} \end{aligned} \quad (132)$$

From the first equation, r(τ) is given by

$$\begin{aligned} r &= C_1 \sqrt{\frac{2 [1 - \sqrt{(1-\tau)(1-\delta\tau)} - \tau(1+\delta)]}{\tau(\delta-1)}} \\ &\times \left[ \frac{1 + \delta - 2(\delta\tau - \sqrt{\delta(1-\tau)(1-\delta\tau)})}{\delta - 1} \right]. \end{aligned} \quad (133)$$

From the first and last terms, the depth,  $h(\tau)$ , is given by

$$h = C_2 (1 - \tau)^\beta \sqrt{\frac{1 - \tau}{1 - \delta\tau}} \quad (134)$$

The factors  $C_1$  and  $C_2$  are constants defined by the geometrical dimensions used for the tank. In the practical case of Ref. 32,  $C_1$  was chosen so that a length  $r$  of 300 mm corresponded to a Mach number of 0.976. The constant  $C_2$  represented the depth of water,  $h$ , corresponding to  $M = 0$ , this being taken at 15 mm.

The electric tank was taken in circular form (Fig. XII-2), the center, 0, corresponding to the origin of the  $(q, \theta)$  plane. The bottom was a surface of revolution about the vertical axis through the origin, 0. The form of the meridian contour was given by the function  $h(r)$  obtained from Eqs. (133) and (134). Several values of  $h$  are given in the following table:

$r$ (mm)	$h$ (mm)
0	15
100	15
150	15.1
200	15.4
220	15.6
240	16
280	18.9
290	21.9
295	25.5
298	30.9
300	44.5

For Mach number 1, the depth is infinite. For this reason the tank radius was limited to a value corresponding to  $M = 0.976$ , slightly less than 1.

This tank was used to study symmetric wing sections at zero lift. The streamline  $x'AEPx$  (Fig. XII-2) in the physical plane, which is identified with the axis  $x'x$  and the contour of the object, is found in the velocity plane to follow a closed curve which defines the limit of the hodograph domain and represents the insulating tank wall in the analogy considered ( $\varphi$  identified with  $V$ ).

In the hodograph plane the two straight line parts,  $Ax'$  and  $xP$ , occupy the same place and define the two sides of a cut which extends from the origin (velocity zero, points A and P on the airfoil section) to a point  $(x, x')$  the distance of which from 0 corresponds to the magnitude of the velocity of the uniform stream at infinity.

The image of this uniform flow is given by a singularity placed at this point. The nature of this singularity is easy to define, it being represented in the tank by portions of equipotential lines (arcs of a cardioid) which form electrodes  $e_0$  and  $e_1$ , and portions of streamlines (insulating arcs of cardioids). (Note that a singularity of this type has already been described in Section XI(a)(1). Another application will be examined in Section XII(c) hereunder.)

In the experiment the circular tank described above is limited to the contour AEP modeled in paraffin. The cut  $Ax'xP$  is made from a thin wall of insulating material built in at the bottom of the tank so as to avoid any leakage underneath. The two electrodes  $e_0, e_1$ , cut to the correct form and separated by a small insulating piece, are directly connected to the output terminals of the generator and thus take care of the electrical feed to the tank.

The study is carried out in the following way. At first, the hodograph is given, i.e., the form of the contour  $x'AEPx$  in the tank. During the experiment the electric potential,

$V$ , is read off along this contour, and from this is obtained, to within a proportionality factor, the distribution law for  $\psi(q, \theta)$  on the contour.

It is then easy to determine the form of the wing section which corresponds to the hodograph chosen, the following relation obtaining:

$$dz = \frac{e^{i\theta}}{q} (d\psi + i \frac{\rho_0}{\rho} d\psi).$$

(135)

Now, on the contour  $d\psi = 0$ , and hence:

$$dx = \frac{\cos \theta}{q} d\psi$$

$$dy = \frac{\sin \theta}{q} d\psi$$

(136)

From this the coordinates  $x, y$  are obtained by simple integration.

This method has been employed to estimate the exactness of certain approximate formulas used in subsonic compressibility studies (Ref. 32). In regard to other problems, the hodographic tank may be found useful for the study of plane jets and, in general, for any study of compressible fluid having a free surface. In the latter case, the contour of the hodograph is circular, and the above-mentioned experimental method can be used to determine the form of the jet or of the free surface.

### (c) Study of Certain Linearized Supersonic Flows

The rheoelectric analogy method can also be used in the practical solution of certain linearized supersonic flow problems if it is possible, by an appropriate change of

variables, to convert the problem to one in the determination of a harmonic function. As examples, there will be considered two cases of this type. The first concerns the analysis of conical flows and the second deals with the calculation of the wave drag of very slender bodies.

#### (1) Analog Representation of Conical Flows

It is known that in a linearized supersonic flow the perturbation velocity components satisfy the equation

$$\beta^2 \frac{\partial^2 f}{\partial x^2} = \frac{\partial^2 f}{\partial y^2} + \frac{\partial^2 f}{\partial z^2}$$

(137)

where  $\beta^2 = M^2 - 1$ . ( $M$  is the Mach number at infinity.)

When the flow is "conical" Eq. (137) is simplified since the vector velocity remains parallel to itself along any line,  $\Delta$ , passing through the origin,  $O$ , and therefore depends on only two variables (Fig. XII-3).

To show the conical character of the flow we take

$$y = r \cos \theta$$

$$z = r \sin \theta$$

$$x = \beta r \chi$$

so that  $f$  (i.e., any one of the three components  $u, v, w$ ) is a function of only  $\chi$  and  $\theta$ .

It can then be shown from Eq. (137) that for  $\chi < 1$  (which corresponds to the interior of the Mach cone) and for  $\chi = \cosh \xi$ ,  $f$  satisfies the Laplace equation in the  $(\theta, \xi)$  plane:

$$\frac{\partial^2 f}{\partial \theta^2} + \frac{\partial^2 f}{\partial \xi^2} = 0.$$

(138)

Furthermore, for  $\chi > 1$  (exterior of the Mach cone), if we take  $\chi = \cos \eta$ ,  $f$  satisfies the wave equation in the  $(\theta, \eta)$  plane:

$$\frac{\partial^2 f}{\partial \theta^2} - \frac{\partial^2 f}{\partial \eta^2} = 0. \quad (139)$$

For studying the flow inside the Mach cone, it is often convenient to use the conformal transformation  $Z = e^i \zeta$  where  $\zeta$  is the complex variable of the  $(\theta, \xi)$  plane. If we take  $Z = \rho e^{i\theta}$  it can be seen that the locus of the point  $Z$  is the image of half a straight line emerging from the origin in  $(x, y, z)$  space and characterized by the angle,  $\theta$ , and the radius vector,  $\rho$ , given by the ratio

$$\frac{x}{\beta r} = \chi = \frac{1 + \rho^2}{2\rho}. \quad (140)$$

The origin of the  $Z$ -plane corresponds to the axis of the Mach cone, and the circle  $(C_0)$  of unit radius, to this cone itself. The components  $u, v, w$ , of the perturbation velocity can thus be defined inside this circle  $(C_0)$ . In view of the fact that they are harmonic functions of the coordinates  $(x, y)$  they can also be considered the real parts of three analytic functions of the complex variable  $Z = X + iY$  which can be indicated respectively by  $U(Z), V(Z), W(Z)$ .

These three analytic functions are in fact linked by compatibility relations which express the fact that the flow is irrotational. It can be verified that these relations have the form, in the  $Z$ -plane:

$$-\beta dU = \frac{2Z}{Z^2 + 1} dV = \frac{2iZ}{Z^2 - 1} dW. \quad (141)$$

It should finally be recalled that the pressure at each point is proportional to  $u$  and that the boundary conditions on the object

establish the normal component of the perturbation velocity. According to the application either  $u, v$ , or  $w$  may be identified with the electrical potential,  $V$ , in a plane circular tank the contour of which represents the circle  $(C_0)$ .

In his work on the general theory of conical flows (Ref. 37), Paul Germain has analyzed in detail the principle of this analog representation and has described various cases of practical application studied in the electric tank. In what follows, we present two examples of such studies.

Consider a very flat cone of any section situated inside the Mach cone. The image of this cone in the  $Z$ -plane is given by the segment  $AA'$  of the  $X$ -axis which forms a cut (Fig. XII-4). When the section of the cone is given,  $w$  is known along this segment. On the circle  $(C_0)$ , image of the Mach cone, the perturbation velocity becomes zero and hence  $w = 0$ . The function,  $w$ , can be identified with the electric potential,  $V$ , of a semicircular tank,  $ABA'$ , in view of the symmetry of the problem. Separate treatments are given the symmetric problem (thickness effect,  $w$  an odd function of  $Y$ ) and the lifting problem (infinitely thin delta wing,  $w$  an even function of  $Y$ ).

In the case of the symmetric problem,  $w$  is zero on the portions of the  $X$ -axis outside the cut  $(C, C')$ . The corresponding boundaries in the tank will then be represented by electrodes at zero potential and hence connected to the semicircular electrode  $E_0$  which represents the Mach cone. On the cut  $(C, C')$ ,  $w$  is given (Dirichlet problem). Therefore an electrode-carrying plate is used whereon each small electrode,  $e$ , is brought to the correct potential,  $V$ , by means of a potentiometer,  $p$ . The unknown of the problem is the value of the pressure along the segment  $(C, C')$ , i.e. the values of the velocity component,  $u$ .

Now  $u$  is related to  $w$  through the first compatibility equation, which is written on the  $X$  axis as

$$\beta \frac{\partial u}{\partial X} = \frac{2X}{1-X^2} \frac{\partial w}{\partial Y} . \tag{142}$$

The factor  $\partial w / \partial Y$  is proportional to the electric current which enters the tank through each electrode,  $e$ . This quantity can easily be measured by an appropriate device. With  $\partial u / \partial X$  known from these considerations, it is also necessary, for determination of the desired pressure distribution, to establish a value of  $u$  along  $(C, C')$ , for example at the point 0.

On the  $Y$ -axis we can write

$$\beta \frac{\partial u}{\partial Y} = - \frac{2Y}{1+Y^2} \frac{\partial w}{\partial Y} . \tag{143}$$

Since  $u$  is zero at the point  $B(0,1)$  we obtain

$$\beta u(0) = \int_0^1 \frac{2Y}{1+Y^2} \frac{\partial w}{\partial Y} dY = -2 \int_0^1 w(0,Y) \frac{1-Y^2}{(1+Y^2)^2} dY . \tag{144}$$

Thus  $u(0)$  will be known through calculation of this latter integral;  $w(0,Y)$  is obtained by reading off the electric potential distribution  $V$  along the  $Y$ -axis.

In the case of the lifting problem the boundary conditions to be set up on the semicircle  $A'BA$  and on the cut  $(C, C')$  are the same as for the symmetric problem. On the other hand, along the segments  $AC$  and  $A'C'$ ,  $\partial w / \partial Y$  must be zero; therefore it follows that the corresponding boundaries of the tank must be insulating. Furthermore,

theoretical study of the aerodynamic problem shows that there exist two singularities at the ends of the cut  $(C, C')$ . At point  $C$  (of abscissa  $c$ ), for example, the analytic function  $W(Z)$  has a singularity in  $(C - Z)^{-1/2}$ , and  $w(X, Y)$  becomes infinite at the points  $C$  and  $C'$ .

It is evidently necessary to take this particular fact into account in making the electrical set-up. Singularities of this type have already been encountered (see Section XI (a)(1)). It has been pointed out that in the neighborhood of singular points it is necessary to construct a model which is partly conducting and partly insulating so as to represent an arc of an equipotential line and an arc of a streamline. These lines are in this case portions of cardioids. In the present problem the intensities of these singularities are determined by the condition that the gradients of  $w$  be zero on the circle  $(C_0)$  at the points  $A$  and  $A'$ .

Finally, the analog experiment is carried out in the following way. After having brought the circumference  $(C_0)$  to zero and having adjusted the potentials of the electrodes,  $e$ , of  $(C, C')$  to the imposed values, the operator brings the conducting part of the two singularities to those potentials required to insure zero current density at points  $A$  and  $A'$ . From a practical standpoint this condition is satisfied by separating off at  $A$  and  $A'$  on  $(C_0)$ , a small electrode,  $e_0$ , which is not electrically fed and the potential of which is opposed to that of the remainder of the circumference across a null indicator. The potentials of the singularities are then adjusted to obtain equal values on  $e_0$  and  $E_0$ .

The experiment then continues as in the symmetric case. The current flows through the electrode,  $e$ , of the cut  $(C, C')$  are measured. This gives  $\partial u / \partial X$ . Finally, the value of  $u$  is determined at point 0 by reading off the series of values for  $w$  along the  $Y$ -axis from 0 and applying Eq. (144).

In a similar fashion the case of an object passing outside the Mach cone can be treated. For details of this procedure, the reader is referred to the paper of P. Germain (Ref. 37, page 100).

Let us now consider another application wherein it is required to determine the pressure distribution over a lifting delta wing with dihedral (Fig. XII-5). The wing is inside the Mach cone and the dihedral is characterized by the angle  $\theta_0$  of the figure. The defining conditions of the problem are as follows:

a. On the Mach cone ( $C_0$ ),  $u, v, w$ , are zero.

b. On the segment OC, which represents in the Z-plane the image of a half-wing (we are considering here the particular case of a configuration which is symmetrical with respect to OY), the condition that the velocity be tangent to the object gives

$$w \cos \theta_0 - v \sin \theta_0 = \alpha \tag{145}$$

( $\alpha$ , the angle of attack of the wing, is here a constant).

This latter condition (145) implies that on OC the real part of the expression

$$\left[ Z \frac{dW}{dZ} \cos \theta_0 - Z \frac{dV}{dZ} \sin \theta_0 \right]$$

is zero. From this it is deduced that the imaginary part of  $[Z(dU/dZ)]$  is zero, i.e., finally that the normal derivative of  $u$  is zero along OC.

If the function  $u$  be identified with the electric potential  $V(u = mV)$  of a circular tank and if the set-up be reduced to one-half by

taking the symmetry about the Y-axis into account, the preceding conditions show that the half circumference  $BAB_1$  must be made of conducting material and brought to zero potential while  $BOCOB_1$  must be insulating with a cut OC. As in the previous example, there is a singularity at the point C of the form  $U(Z) \approx K(Z - Z_c)^{-1/2}$  which can be physically represented in the tank by a piece of conducting cardioid arc (electrode  $E_1$ ) and a piece of insulating cardioid arc. The tank is thus fed electrically through the half circumference ( $C_0$ ) and the small electrode  $E_1$ .

Reading off the potential,  $V$ , along the two sides of the cut OC gives, to within the factor  $m$  of proportionality, the value of  $u$  and therefore the pressure at each point of the wing. To determine the factor  $m$ , the following facts are used.

The compatibility formula

$$-\beta \frac{dU}{dZ} = \frac{2iZ}{Z^2 - 1} dW$$

gives, on the Y-axis:

$$\beta \frac{\partial u}{\partial Y} = - \frac{2Y}{1 + Y^2} \frac{\partial w}{\partial Y} \tag{146}$$

from which the value of  $w$  at the point 0 may be obtained, the electrical potential  $V = u/m$  being introduced:

$$w(0) = m \frac{\beta}{2} \int_0^1 \frac{1 + Y^2}{Y} \frac{\partial V}{\partial Y} dY. \tag{147}$$

Now, condition (145) gives, for point 0 (the component  $v$  being zero):

$$w(0) \cos \theta_0 = \alpha. \tag{148}$$

If Eqs. (147) and (148) be compared, the value of the factor  $m$  may be obtained immediately when the distribution of potential,  $V$ , along the  $Y$ -axis has been measured and the integral in Eq. (147) calculated.

The case of a wing with dihedral emerging from the Mach cone would be treated with the same facility by rheoelectric analogy even in the case where  $\alpha$  varies spanwise.

Numerous other applications of this analog method to conical or homogeneous flow studies can be imagined. For the details we refer the reader to the work of P. Germain.

(2) Calculation of the Supersonic Drag of a Thin Body

The linearized theory of supersonic flows shows that the drag,  $T$ , of a very thin streamlined body placed at zero lift angle in a stream of velocity  $U$  at infinity and directed along the  $x$ -axis is given by the expression

$$T = \frac{\rho U^2}{4\pi} \int_{-L}^{+L} \int_{-L}^{+L} S''(x) S''(\xi) \text{Log} |x - \xi| dx d\xi \quad (149)$$

when the distribution law  $S(x)$  of the right sections of the body is given ( $2L$  is the length of the body:  $-L \leq x \leq +L$ ) and provided that the derivative  $S'(x)$  remains continuous in the interval  $(-L, +L)$  and becomes zero at the ends of the body ( $S'(-L) = S'(L) = 0$ ).

Even though the expression (149) is simple since it uses only the function  $S(x)$  describing the variation of the sections with  $x$ , the numerical calculation of this integral is generally long and tedious if an electronic calculating machine is not available. In a recent report (Ref. 59) P. J. Pocock has presented an interesting method for the analog solution of Eq. (149) which is based on the use of the electrical set-up of the wing calculator.

The principle of the method proposed by Pocock depends on the remark, made as early as 1935 at the Volta Congress by Th. von Karman, concerning the analogy which exists between the wave drag for slender bodies (as it is given by Eq. (149)) and the induced drag,  $T_i$ , of the Prandtl lifting line.

In the wing theory of Prandtl the induced drag,  $T_i$ , of a wing of span  $2L$  having a spanwise distribution of circulation  $\Gamma(x)$  ( $x$  and  $\xi$  being spanwise coordinates\*) is given by

$$T_i = \rho \int_{-L}^{+L} w(x) \Gamma(x) dx \quad (150)$$

The distribution of induced velocities,  $w(x)$ , along the span is given by

$$w(x) = \frac{1}{4\pi} \int_{-L}^{+L} \frac{\Gamma'(\xi)}{x - \xi} d\xi \quad (41)$$

Therefore the induced drag,  $T_i$ , can be written in the form

$$T_i = \frac{\rho}{4\pi} \int_{-L}^{+L} \Gamma(x) \left\{ \int_{-L}^{+L} \frac{\Gamma'(\xi)}{x - \xi} d\xi \right\} dx \quad (151)$$

which can also be transformed by integration by parts and use of the fact that the circulation becomes zero at the wing tips ( $\Gamma(-L) = \Gamma(+L) = 0$ ).

---

\*In Section IX, the span was in the  $y$ -direction. Here  $x$  and  $\xi$  replace respectively the notations  $y$  and  $\eta$  which are found in the formulas of Section IX.

Finally there is obtained

$$T_i = - \frac{\rho}{4\pi} \int_{-L}^{+L} \int_{-L}^{+L} \Gamma'(x) \Gamma'(\xi) \text{Log}|x-\xi| dx d\xi. \quad (152)$$

The expressions (149) and (152) are clearly identical if we take  $\Gamma'(x) = U S''(x)$  or  $\Gamma(x) = U S'(x)$ . The condition  $\Gamma(-L) = \Gamma(+L) = 0$  also corresponds to the condition  $S'(-L) = S'(L) = 0$ . In other words, the resistance of a slender body in supersonic flow where the body sections follow the distribution  $S(x)$  is identical to the induced drag of incompressible flow for a lifting line along which the distribution of circulation is  $\Gamma(x) = US'(x)$ . This correspondence makes possible the easy calculation of  $T$  by identity with  $T_i$ , the integral of Eq. (150) being evaluated from results obtainable by rheoelectric analogy.

When the circulatory distribution  $\Gamma(x)$  is known, it is in fact easy to determine the corresponding distribution of induced velocities  $w(x)$ . It has already been seen in Section IX (Eqs. (43) and (44)) that  $\Gamma(x)$  is equal to twice the potential  $\Psi(x)$  and that  $-w(x)$  is equal to half the normal derivative of  $\Psi$  taken at the point  $x$ . When the potential  $\Psi$  is identified with the electric potential of the plane tank used in the wing calculator the values of this normal derivative are proportional to the current intensities passing through the small electrodes of the segment  $(-L, +L)$ . The distribution  $w(x)$  can then be obtained in the electric tank by measuring the currents of the electrodes,  $e$ , which have been previously brought to the known values,  $\Gamma(x)$ .

To sum up, to obtain the value of the wave drag,  $T$ , of a slender body the following procedure is followed:

a. A distribution of electric potential  $US'(x)$  is set up along the electrode-carrying plate of the wing calculator

(Dirichlet problem, adjustment by potentiometers,  $p$ ).

b. The current flow through each electrode is measured. This gives, to within a proportionality factor, the distribution of  $w(x)$  corresponding to that of  $US'(x)$ .

c. The product  $w(x) S'(x)$  is calculated and integrated graphically or numerically over the interval  $(-L, +L)$  to obtain finally the value of the drag,  $T$ .

Pocock carried out check experiments on theoretical cases easy to calculate (body of revolution with parabolic meridian contour and Sears-Haack body with minimum drag). Using an analog set-up with 50 small electrodes he was able to show that the error in  $T$  obtained by this procedure did not exceed one percent. The time necessary for obtaining the final result was about two or three hours.

It may finally be remarked that this method is useful for the direct and convenient calculation of the difference between the drags of two bodies, and, in particular, for studying the variation of drag of a body produced by changes in parts of its section  $S(x)$ .

### XIII CONCLUSION

The practical solution of numerous and varied problems in aerodynamics can be accomplished by means of the rheoelectric analogy method. This method may be profitably employed for the tracing out of a plane flow field, an axially symmetric field, and a three-dimensional field, as well as for those cases wherein the principal aerodynamics characteristics of wing sections and lattices of blades, streamlined bodies, air intakes,

lifting lines, propellers, lifting surfaces, etc. are sought.

In this AGARDograph the various possible applications of the method have been analyzed, the theoretical bases of the analogy and the accompanying techniques for model construction, physical establishment of the problem data, and for reading the results of experiment being given in each case. The equipment necessary for carrying out this work is relatively modest and its cost remains quite low compared to that of large calculating machines and wind tunnels. Set-up and operation are generally rapid with this method, and the experimental work itself permits of a certain flexibility which is inherent in all analog processes wherein an easily modified model is employed.

The present report covers only the more classic and important applications, but from these examples it is easy to imagine other

uses of the method. Numerous other problems can, in fact, be solved in an interesting fashion by the analogy. For example, there may be mentioned certain unsteady flows about profiles or lifting surfaces and the determination of jet lines in plane and axial symmetric flows. In icing problems the electric tank may be used to obtain the ice trajectories and in the calculation of the ice capturing coefficient of an object in the airstream.

Lastly, it should be noted that, besides aerodynamic applications, various other questions pertaining to aeronautics may be treated by the rheoelectric analogy method. Examples are heat transfer and temperature field studies, problems in elasticity, electronics, meteorology, etc. The various pieces of equipment set up for the solution of aerodynamic problems can thus be utilized directly in many other domains of science and technology.

## REFERENCES

1. Relf, E. F., "An Electrical Method of Tracing Stream Lines for the Two-Dimensional Motion of a Perfect Fluid," ARC R and M 905, 1924.
2. Hahn, E., "Méthode expérimentale pour la résolution des équations du mouvement des fluides," Revue Gén. d'Electricité, t. 21, 1927.
3. Taylor, G. I., and Sharman, C. F., "A Mechanical Method for Solving Problems of Flow in Compressible Fluids," ARC R and M 1195, 1928.
4. Taylor, G. I., and Sharman, C. F., "Problems of Flow in Compressible Fluids," Proc. Roy. Soc. of London, Série A, t. 121, 1928.
5. Ferrari, C., "Sull'analogia fra i campi elettrici e i campi aerodinamici," Atti dell'Accademia d. Scienze di Torino, vol. LXIV, 1929.
6. Ferrari, C., "La determinazione sperimentale dei campi aerodinamici a due e tre dimensioni per mezzo delle loro analogie coi campi elettrici," Aerotecnica, Vol. X, n° 6, 1930.
7. Pérès, J., et Malavard, L., "Application de la méthode électrique à un problème concernant l'aile d'envergure finie," C. R. Acad. Sc., 10 octobre 1932.
8. Malavard, L., "Application de l'analogie électrique à la solution de quelques problèmes d'hydrodynamique," Publ. Scient. et Techn. du Ministère de l'Air, fasc. n° 57, 18 décembre 1934.
9. Malavard, L., "La méthode des analogies électrique pour le calcul des corrections de parois," C. R. Acad. Sc. 5 avril 1937.
10. Pérès, J., "Les méthodes d'analogies en Mécanique Appliquée," 5ème Congrès Int. de Mécanique Appliquée, Cambridge, Mass., septembre 1938.
11. Malavard, L., "Etude de quelques problèmes techniques relevant de la théorie des ailes. Application à leur solution de la méthode rhéoelectrique," Publ. Scient. et Techn. du Ministère de l'Air, n° 1953, juillet 1939.
12. Malavard, L., "Pour le calcul des effets du fuselage et des fuseaux-moteurs sur la répartition en envergure des efforts aérodynamiques," C. R. Acad. Sc., 5 octobre 1942.
13. Pérès, J., Malavard, L., et Romani, L., "Tables numériques pour la répartition des charges aérodynamiques suivant l'envergure d'une aile," Rapport technique G. R. A. n°9, 1943.

14. Bazjanac Davorin, "Untersuchungen mit Hilfe der elektrischen Analogie über den Einfluss der Luftstrahlbegrenzung in Windkanälen auf Tragflügelmessungen," Institut für Aerodynamik, Zurich 1943.
15. Malavard, L., "Sur la solution rhéoelectrique de questions de representation conforme et application à la théorie des profils d'ailes," C. R. Acad. Sc., 17 janvier 1944.
16. Siestrunk, R., "Sur un mode de solution rhéoelectrique des problèmes de l'hélice propulsive," C. R. Acad. Sc., 30 octobre 1944.
17. Cheers, F., Raymer, W. G., Fowler, R. G., "Preliminary Test on Electrical Potential Flow Apparatus," ARC R and M 2205, 1945.
18. Malavard, L., "La Technique des analogies électriques" 1945, un chapitre du volume "Techniques générales du Laboratoire de Physique," éditions CNRS, vol. II, chap. XV, juin 1950. ("The Technique of Electrical Analogies," translation of the Aeronautics Department, Rensselaer Polytechnic Institute, Troy, N. Y., 1953, by J. Bègue and W. B. Brower).
19. Malavard, L., "Applications aérodynamiques du calcul expérimental analogique," 1er Congrès de l'Aviation Française, mai 1945.
20. Malavard, L., et Siestrunk, R., "Méthode d'étude des grilles rectilignes indéfinies de profils quelconques," 1er Congrès de l'Aviation Française, mai 1945.
21. Pérès, J., et Malavard, L., "Sur la détermination des corrections de soufflerie," C. R. Acad. Sc., 24 septembre 1945.
22. Malavard, L., "The Use of Rheoelectrical Analogies in certain Aerodynamical Problems," 25 September 1945 (The Journal of the Royal Aeronautical Society, no. 441, vol. 51, September 1947).
23. Pérès, J., Malavard, L., et Romani, L., "Problème non linéaire de la théorie de l'aile. Application à la détermination du maximum de portance," Rapport technique G. R. A., n° 20, 1946.
24. Legras, J., Malavard, L., "Etude au bassin électrique du problème de la surface portante," 6<sup>o</sup> Congrès Int. de Mécanique Appliquée, septembre 1946.
25. Romani, L., et Revuz, J., "Sur la détermination des systèmes portants optima," 6<sup>o</sup> Congrès Int. de Mécanique Appliquée, septembre 1946.
26. Malavard, L., et Siestrunk, R., "Diverses méthodes analogiques pour le calcul des grilles d'aubes," 6<sup>o</sup> Congrès Int. de Mécanique Appliquée, septembre 1946.
27. Poisson-Quinton, Ph., "Recherches théoriques et expérimentales sur le contrôle de la couche limite," 6<sup>o</sup> Congrès International de Mécanique Appliquée, Londres, septembre 1946.

28. Lewis, W. T. D., "Potential Flow Apparatus," *Aeronautics*, December 1946.
29. de Haller, Pierre, "Application of Electrical Analogy to Investigations of Cascades," *Sulzer Technical Review*, no. 3/4, 1947.
30. Kelk, G. F., Misener, W. S., d'Arcy, D. F., "An Electrolytic Tank for Potential Plotting," A. V. Roe Canada Ltd., Gas Turbine Engineering Division, rep. no. 17, November 1947 and no. 20, July 1948.
31. Pizer, H. I., Wallis, R. A., Warden, M. C., "An Electrolytic Tank Simulator," *Aerodynamic Note 76*, Council for Scientific and Industrial Research, Australia, February, 1948.
32. Malavard, L., "Quelques récentes applications de la méthode d'analogies électriques," avril 1948, (Colloque Int. du CNRS sur "Les méthodes de calcul dans les problèmes de Mécanique," éditions du CNRS, 1949).
33. Malavard, L., Siestrunk, R., Germain, P., "Calcul des répartitions de vitesse sur les profils des grilles planes," *La Recherche Aéronautique*, n° 4, juillet 1948.
34. Green, Paul E., "Automatic Plotting of Electrostatic Fields," *The Review of Scientific Instruments*, October 1948.
35. Theodorsen, Th., "Theory of Propellers," McGraw-Hill, 1948.
36. Siestrunk, R., "Ecoulements à potentiel dans les machines hélicoidales simples," ONERA, Publication n° 32, 1949, chap. 2.
37. Germain, P., "La théorie générale des mouvements coniques et ses applications à l'Aérodynamique supersonique," (voir par. 3,1.3.2., "Utilisation des analogies électriques," Publication ONERA, n° 34, 1949).
38. Hargest, T. J., "An Electric Tank for the Determination of Theoretical Velocity Distributions," *ARC R and M 2699*, April 1949.
39. Campbell, W. F., "Two Electrical Analogies for the Pressure Distribution on a Lifting Surface," Report no. MA-219, National Research Council of Canada, 18 October 1949.
40. Malavard, L., "Aperçu sur la méthode d'analogie rhéoelectrique," *Publ. Scient. et Techn. du Ministère de l'Air*, n° 261, avril 1950.
41. Bernard, J. J., et Siestrunk, R., "Sur l'utilisation d'approximations successives dans la détermination de certains potentiels aérodynamiques," *La Recherche Aéronautique*, n° 17, septembre 1950.
42. Malavard, L., "Sur une nouvelle technique dans le calcul expérimental par analogies rhéoelectriques," *La Recherche Aeronautique*, n° 20, mars 1951.

43. Babister, A. W., Marshall, W. S. D., Lilley, G. M., Sills, E. C., and Deards, S. R., "The Use of a Potential Flow Tank for Testing Axi-symmetric Contraction Shapes Suitable for Wind Tunnels," The College of Aeronautics Cranfield, Report no. 46, April 1951.
44. Malavard, L., "Use of Electrolytic Plotting Tank," Art. H.2, vol. IX, of "High Speed Aerodynamics and Jet Propulsion," Princeton University, May 1951, published in 1954.
45. Malavard, L., et Duquenne, R., "Etude des surfaces portantes par analogies rhéoelectriques," La Recherche Aéronautique, n° 23, septembre 1951. (Translated in TIB/T3989 and ARC 15108).
46. Stenstrom, Lennart, "The SAAB Gradient Tank and Aid to Aeroplane Design," abstract from SAAB Sonics no. 12, Sweden.
47. Duquenne, R., "Sur le calcul analogique des surfaces portantes," C. R. Acad. Sc. 26 mai 1952.
48. Germain, P., "Un procédé analogique pour la résolution de l'équation de Laplace," Bulletin Technique n° 5 de l'A.I.Br. (Université Libre de Bruxelles), 1952.
49. Miroux, J., "Sur la mesure des gradients en analogies rhéoelectriques. Appareil pour le relevé direct des isovitesse," La Recherche Aéronautique, n° 29, septembre-octobre 1952.
50. Revuz, J., "Profil d'ailette pour compresseur axial," La Recherche Aéronautique, n° 31, janvier-février 1953.
51. Borden, A., Shelton, G. L., Ball, W. E., "An Electrolytic Tank Developed for Obtaining Velocity and Pressure Distributions about Hydrodynamics Forms," Report 824, April 1953, Navy Dept., The David Taylor Model Basin.
52. Sander, K. F., Yates, J. G., "The Accurate Mapping of Electric Fields in an Electrolytic Tank," The Proceedings of the Institution of Electrical Engineers, Vol. 100, Part II, no. 74, April 1953.
53. Landahl, M. T., Stark, V. J. E., "An Electrical Analogy for Solving the Oscillating Surface Problem for Incompressible Nonviscid Flow," K. T. H. Aero TN 34, Sweden, July, 1953.
54. Castagno, Aldo, "Sulle trasformazioni conformi eseguite sperimentalmente con la vasca elettrica," Atti dell'Accademia delle Sc. di Torino, Luglio 1953.
55. Scanlan, R. H., "A Steady-Flow Aeroelastic Study by Electrical Analogy," J. A. S., vol. 20, no. 10, October 1953.

56. Revuz, J., "Familles de profils d'ailettes pour compresseurs axiaux," La Recherche Aéronautique, n° 37, 20 octobre 1953.
57. Castagno, Aldo, "Determinazione del campo di moto attorno ad una schiera di profili alari mediante la vasca elettrica," Atti dell'Accademia delle Scienze di Torino, Gennaio 1954.
58. Duquenne, R., et Grandjean, C., "Calcul par analogie rhéoelectrique de l'effet d'épaisseur sur des ailes symétriques à la portance nulle," C. R. Acad. Sc., 12 avril 1954.
59. Pocock, P. J., "The Calculation of the Wave Drag of an Arbitrary Slender Body by Means of an Electrical Analogy Tank," Laboratory Report, LR-27, March 17th, 1955, National Aeronautical Establishment, Canada.
60. Malavard, L., Duquenne, R., Enselme, M., Grandjean, C., "Propriétés calculées d'ailes en delta échancré ou non. Calcul par analogies électriques," Note Technique n° 25 1955.

#### ONERA INTERNAL TECHNICAL NOTES

61. Marchet, P., "Détermination des lignes de jet dans les mouvements plans et de révolution," N. T. D-359-A, juin 1949.
62. Revuz, J., "Mise au point d'une méthode de réduction des essais sur une aile munie de plaques de garde: 1ère partie: résolution par analogie électrique," N. T. 2/1358.A, janvier 1950 - 2ème partie: "Résultats des expériences," N. T. 4/1358.A, novembre 1951.
63. Vincent, J., "L'écoulement inverse en analogie rhéoelectrique," N. T. 3/1101.A, avril 1953.
64. Duquenne, R., Grandjean, C., "Application de l'analogie rhéoelectrique au calcul de trois ailes de même forme en plan," N. T. 9/1292.A, septembre 1953.
65. Duquenne, R., Grandjean, C., "Calcul d'effets de volets par analogie rhéoelectrique," P. V. n° 11/1292.A, juillet 1954.
66. Malavard, L., "Contribution à l'étude théorique du soufflage au bord de fuite d'un profil d'aile (résolution par analogie rhéoelectrique)," N. T. 4/1727.A, décembre 1954.
67. Enselme, M., "Calcul par analogies électriques d'ailes minces supportant une répartition de pression donnée," N. T. 5/1101, septembre 1955.

## CLASSIFICATION OF THE BIBLIOGRAPHY BY SUBJECT MATTER

1. Works of General Nature on the Rheoelectric Analogy Method and its Use in Aerodynamics  
Refs. (8), (10), (11), (22), (40), (44).
2. Principles of the Rheoelectric Analogy Method  
Refs. (4), (5), (8), (11), (18), (40), (44).
3. Technique of the Electric Tank  
General Technique, Refs. (11), (18), (29), (34), (52).  
Gradient Measurement, Refs. (18), (38), (46), (49).
4. Technique of Graphite Conducting Paper  
Refs. (42), (48).
5. Plane Flows and Airfoil Section Studies  
Refs. (1), (2), (5), (6), (8), (11), (27), (61), (66).
6. Rheoelectric Conformal Mapping  
Refs. (15), (19), (21), (26), (40), (54), (57).
7. Airfoils in Cascade  
Refs. (20), (26), (29), (30), (33), (38), (50), (56), (57).
8. Axially Symmetric Flows  
Refs. (8), (28), (32), (43), (61).
9. Three-Dimensional Flows  
Refs. (6), (46).

10. Lifting Line Problems

Refs. (7), (8), (9), (11), (12), (13), (14), (19), (21), (23), (25), (61).

11. Propellers

Refs. (16), (35), (36), (41).

12. Lifting Surface Problems

Refs. (24), (39), (41), (45), (47), (53), (55), (58), (60), (63), (64), (65), (67).

13. Compressible Flows

Refs. (3), (4), (32), (37), (59).



97

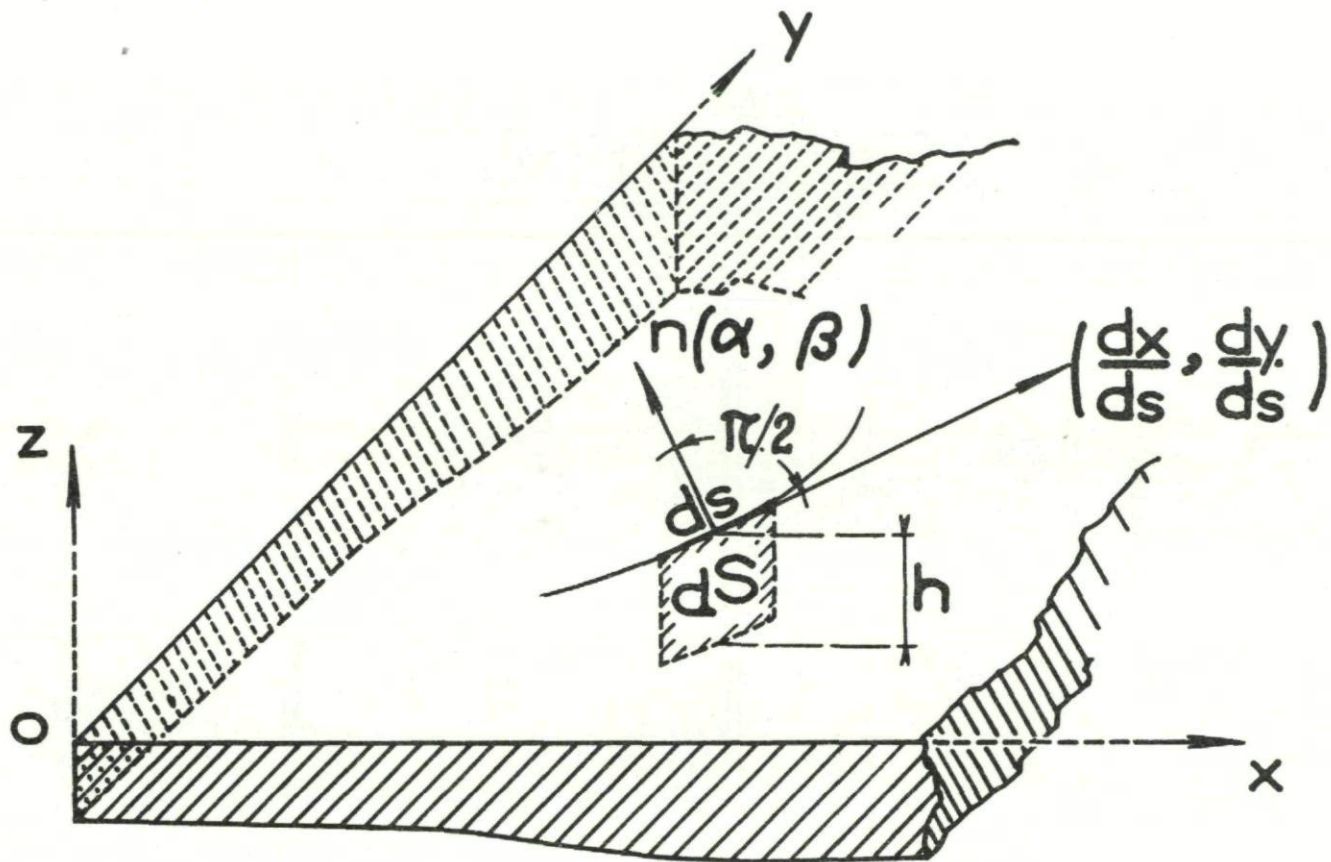


Fig. II-1. Conducting plate of slowly varying thickness.

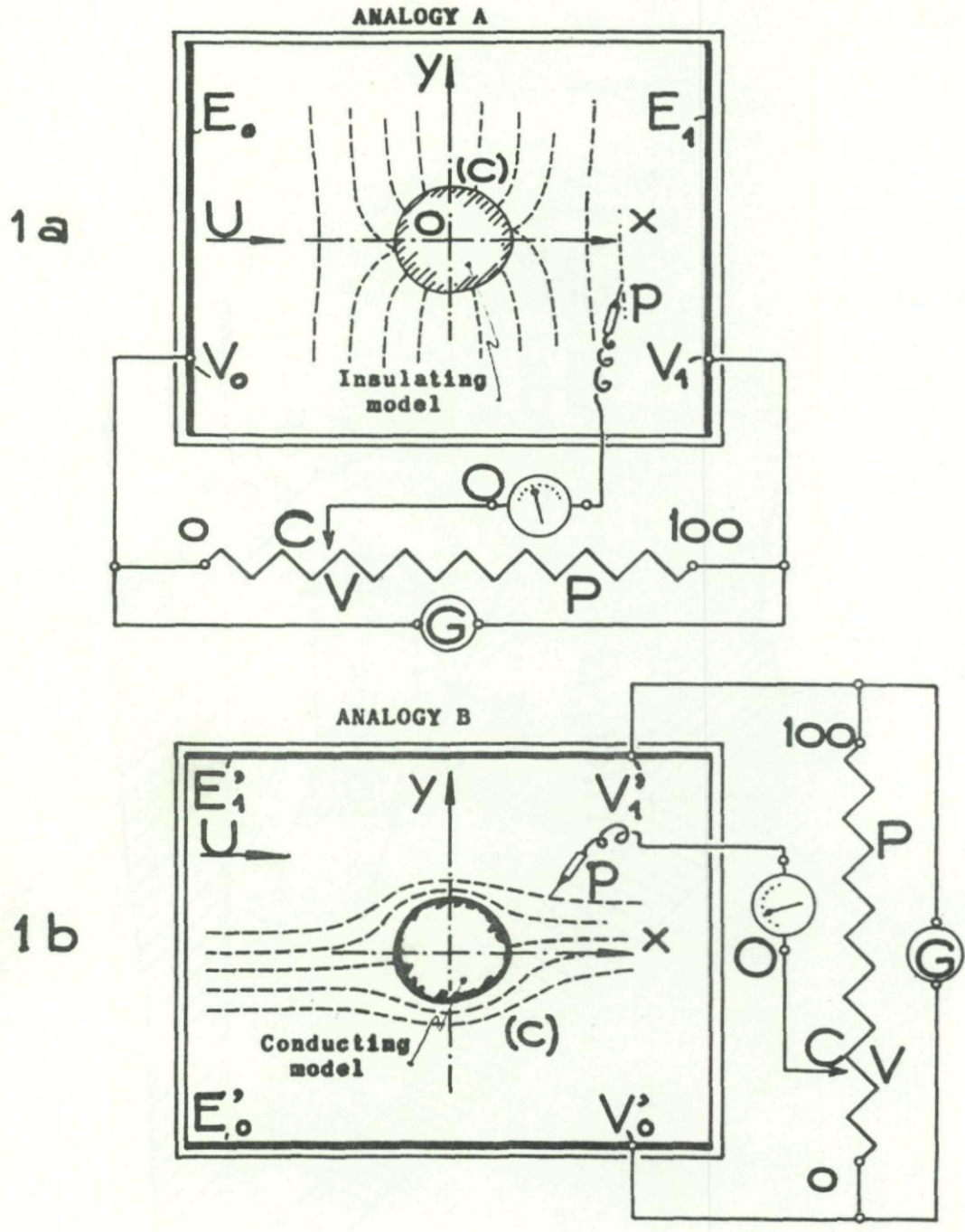


Fig. III-1. Representation of the velocity potential (Analogy A) and the stream function (Analogy B) of a flow about a plane object.



100

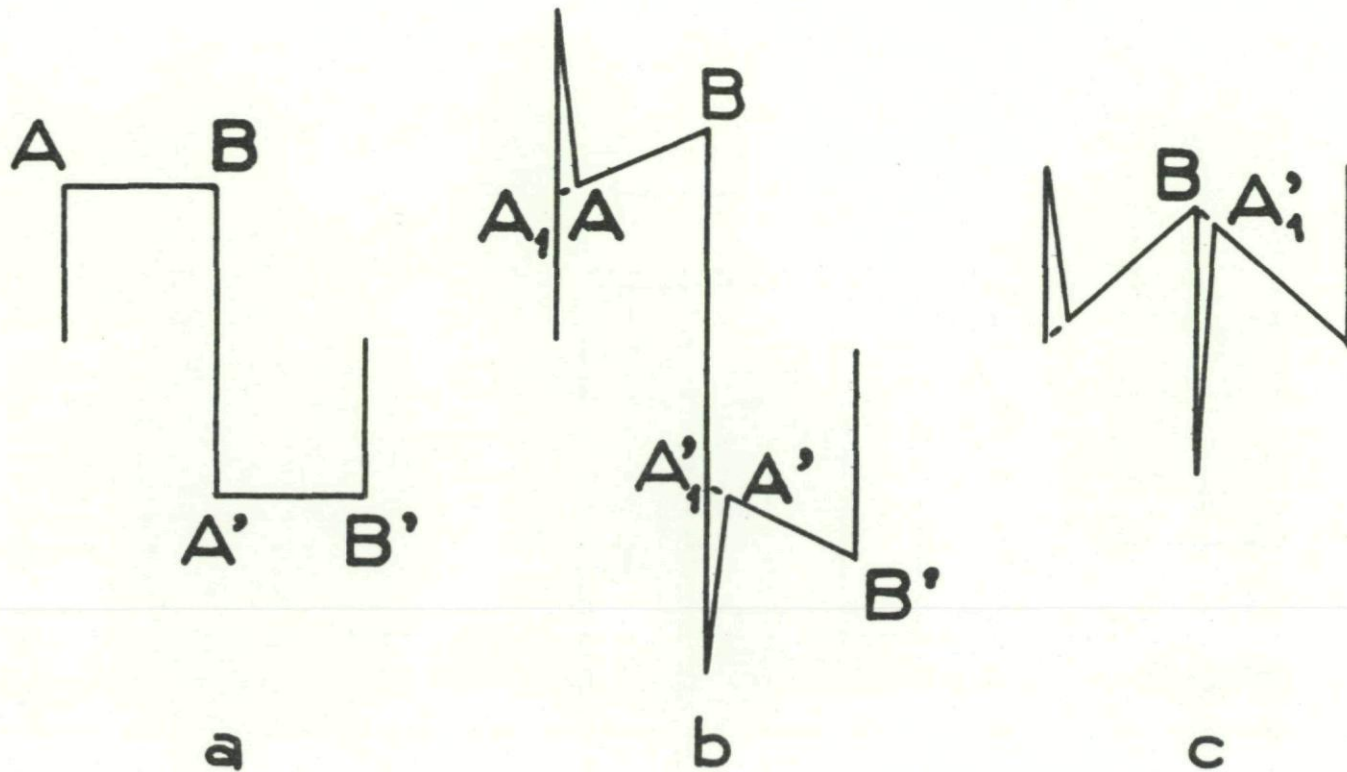


Fig. III-3. Square wave signal and zero adjustment.

101

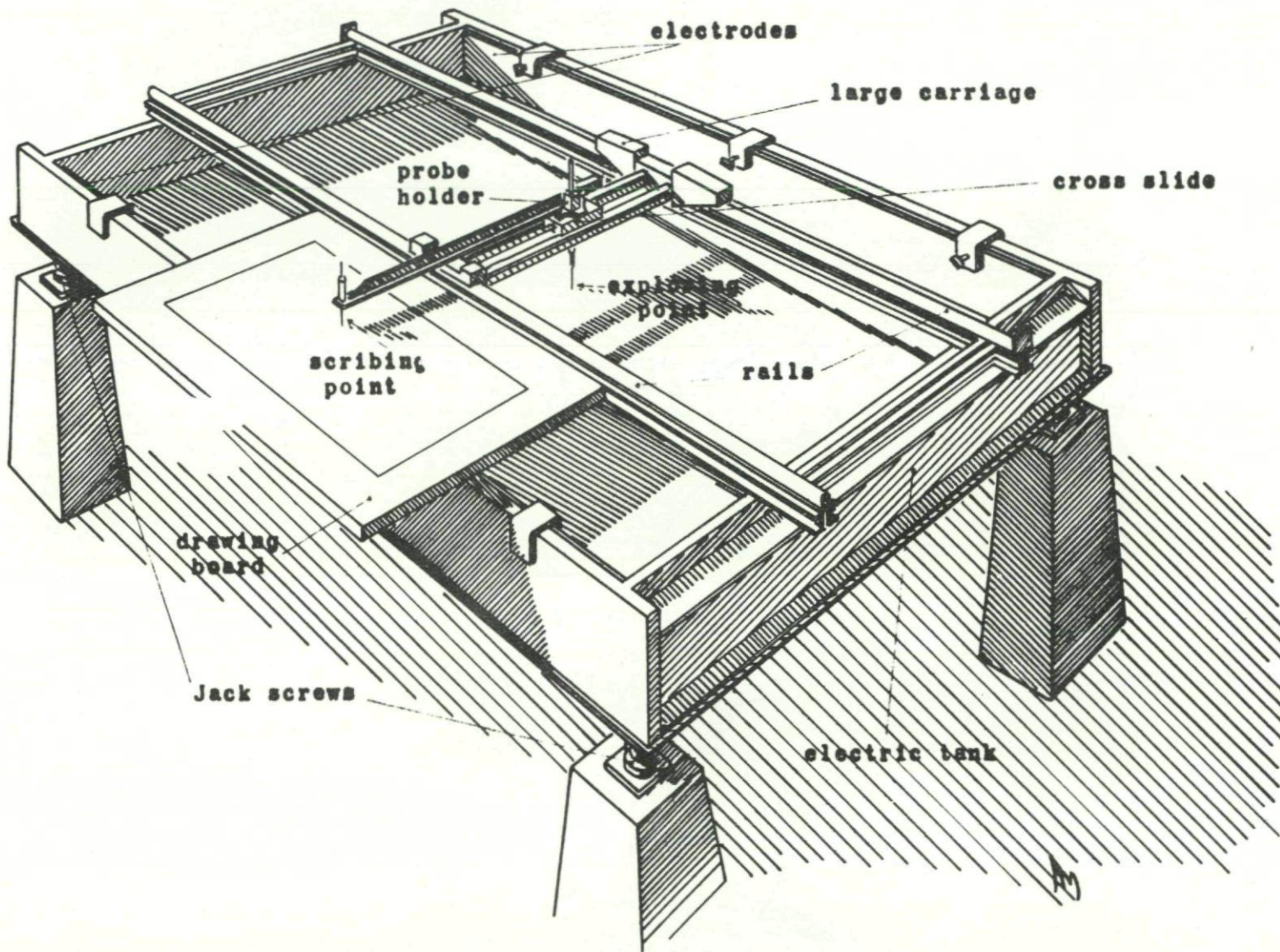


Fig. III-4. Electric tank and exploring device.

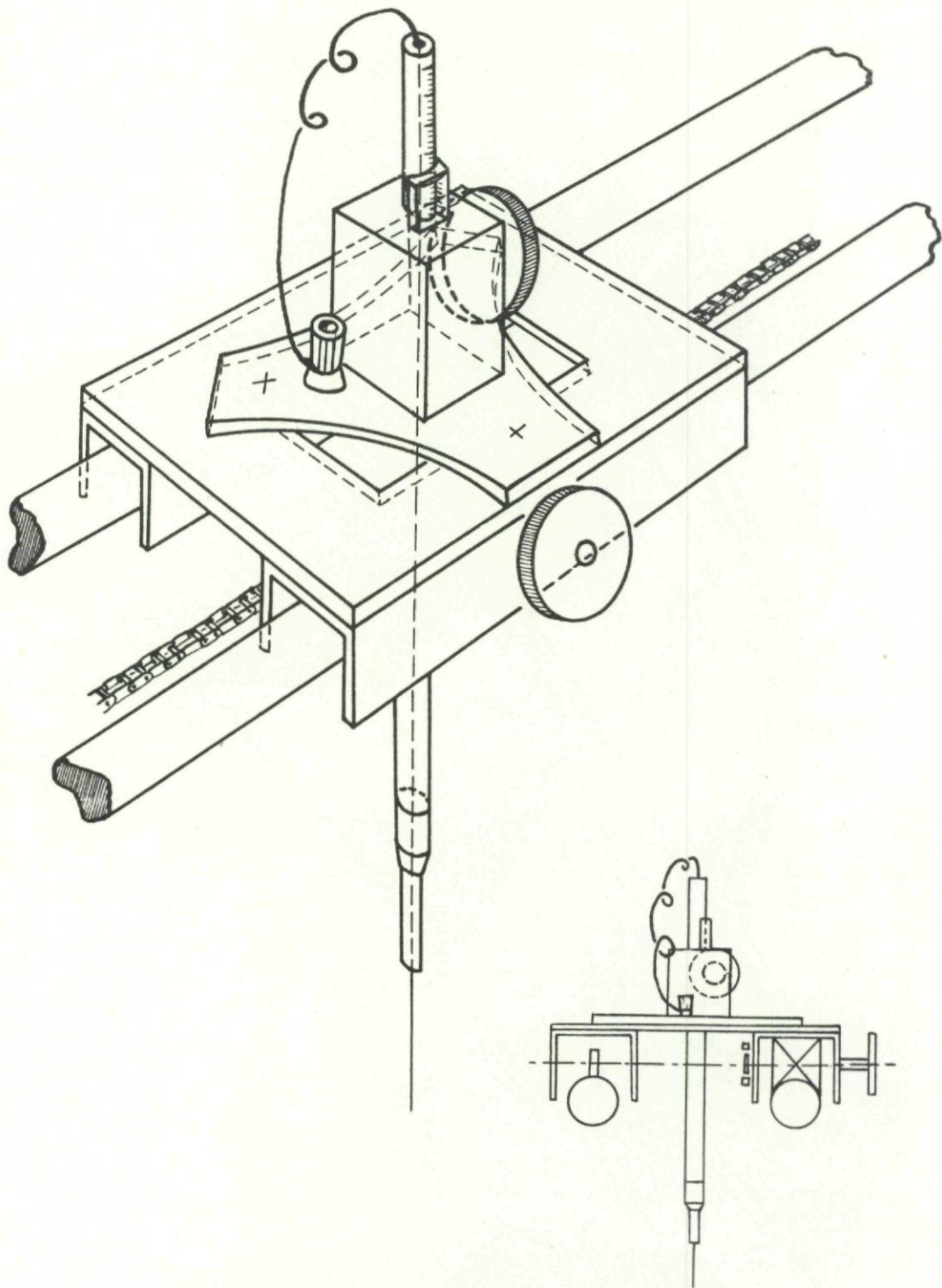


Fig. III-5. Probe holder.

103

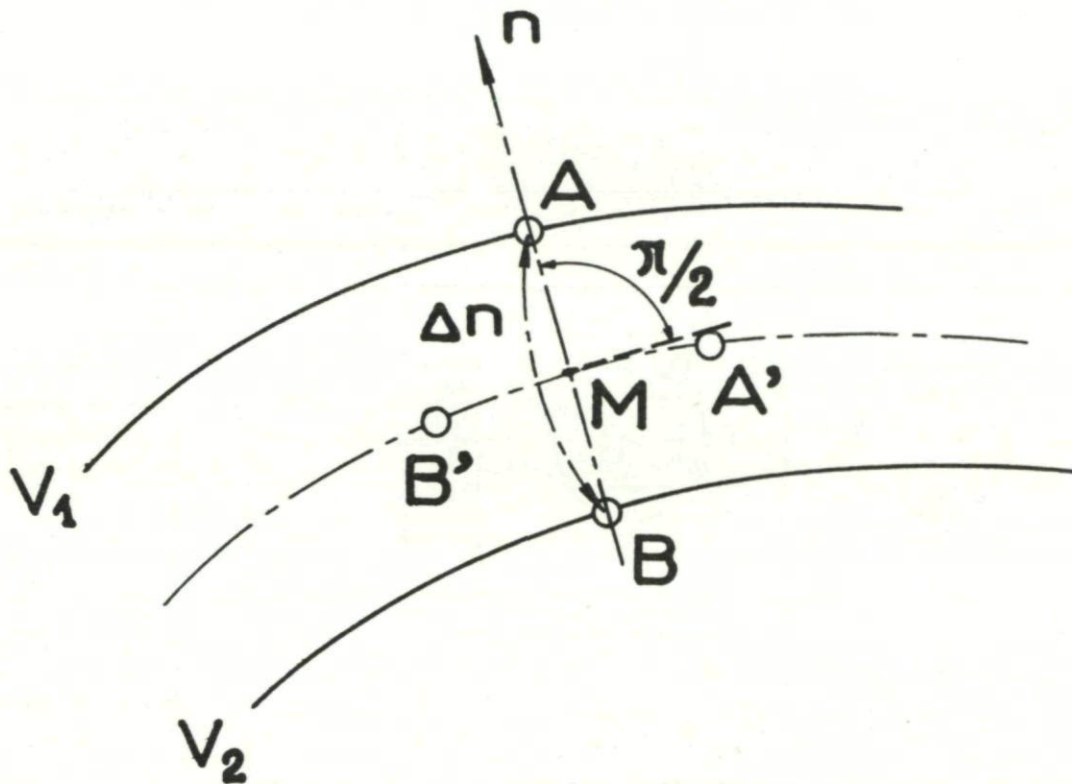


Fig. III-6. Gradient measurement.

104

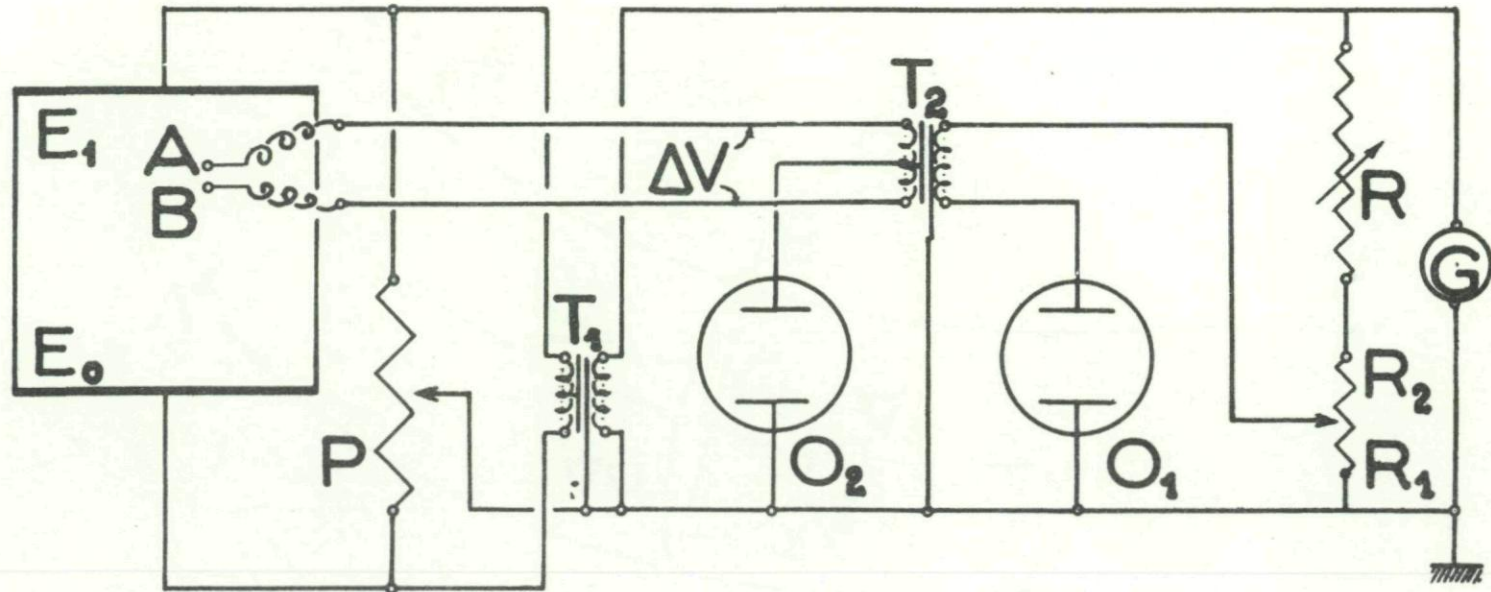


Fig. III-7. Electric circuit for gradient measurement.

105

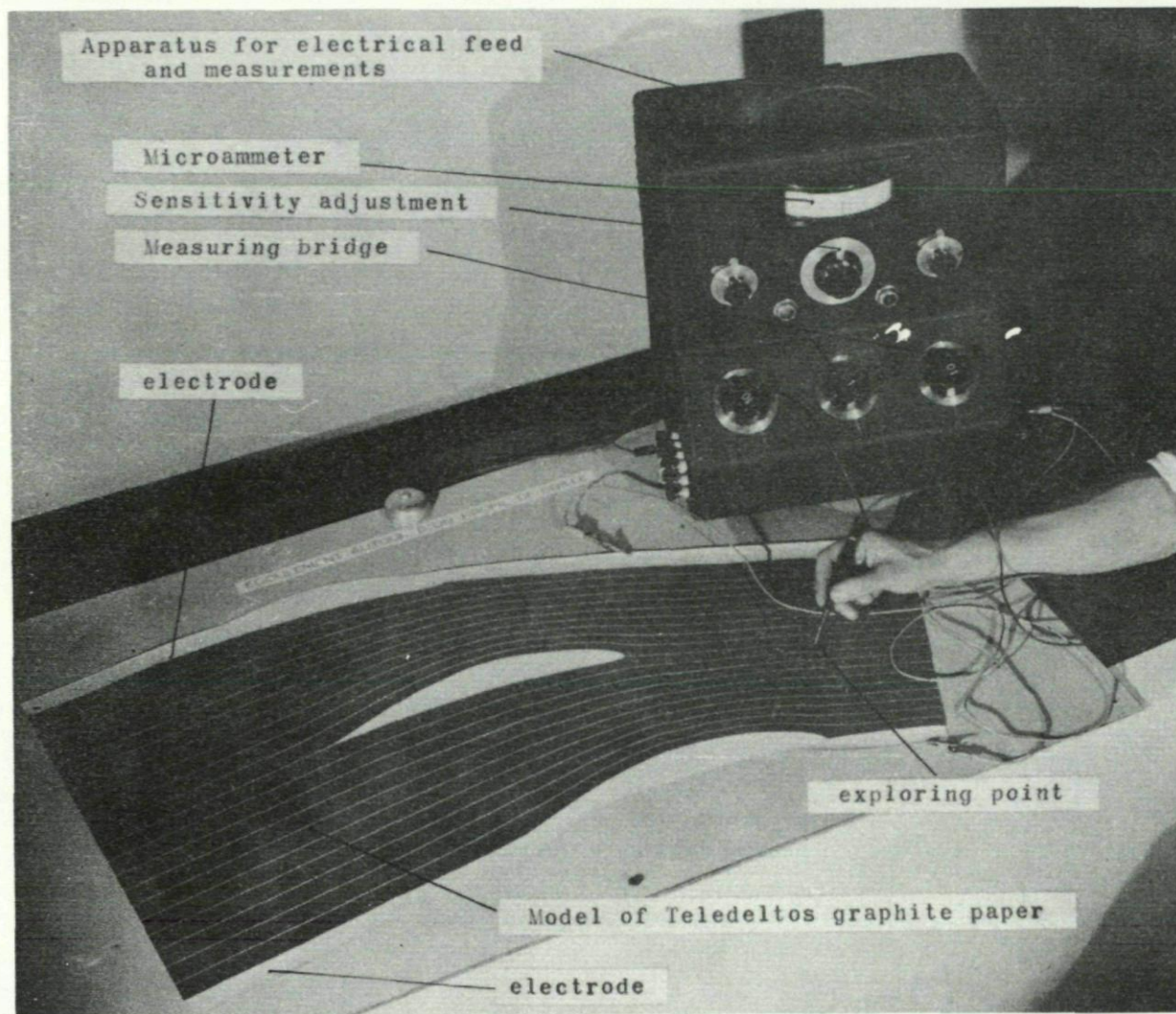


Fig. III-8. Set-up for exploring electric fields by means of Teledeltos graphite conducting paper.

106

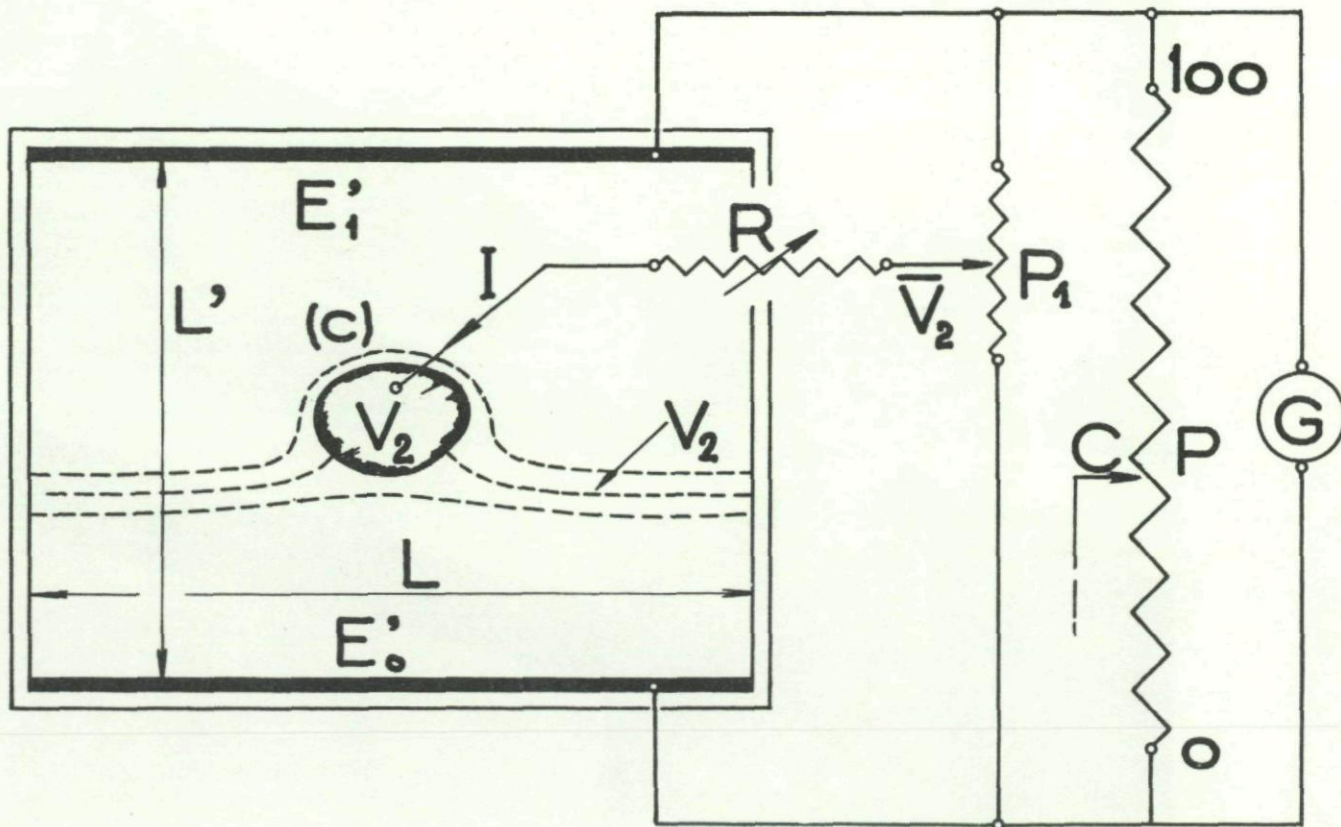


Fig. IV-1. Set-up for analog representation of circulation (Analogy B).

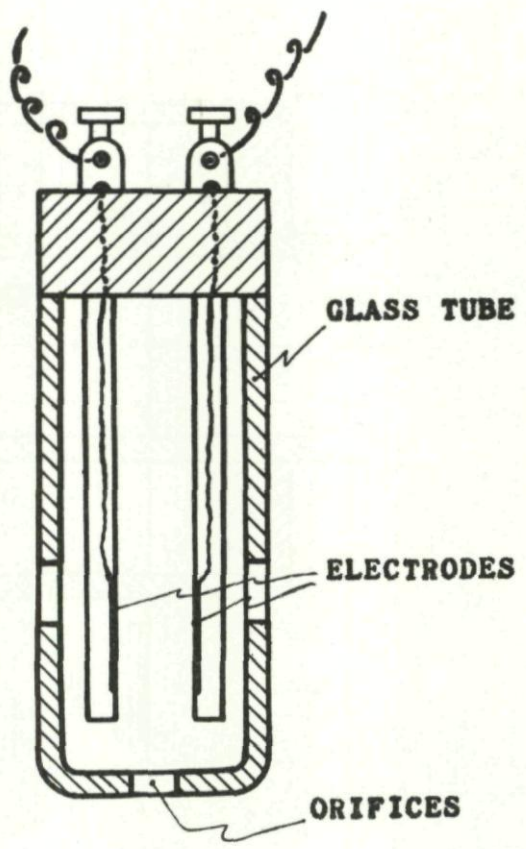


Fig. IV-2. Cell for measuring liquid resistivity  $1/\sigma$ .

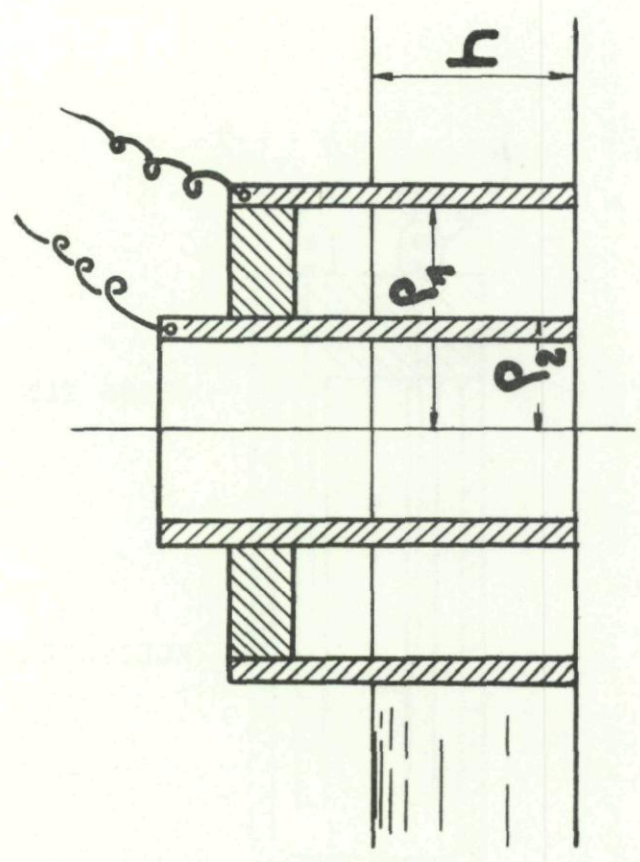


Fig. IV-3. Cell for measuring the ratio  $\sigma/h$ .

601

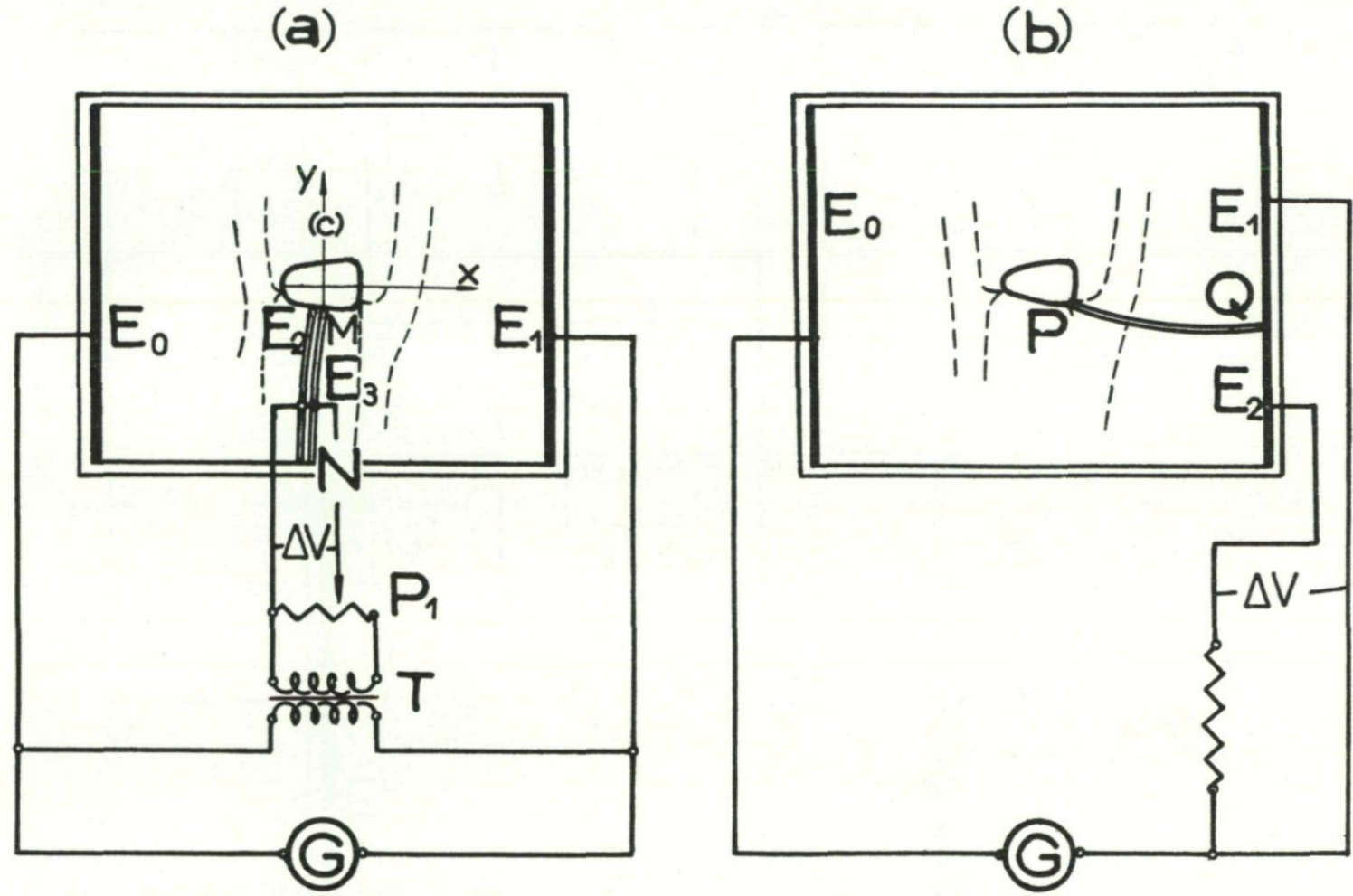


Fig. IV-4. Circulation about an object (Analogy A). 1st set-up (a), 2nd set-up (b).

(c)

110

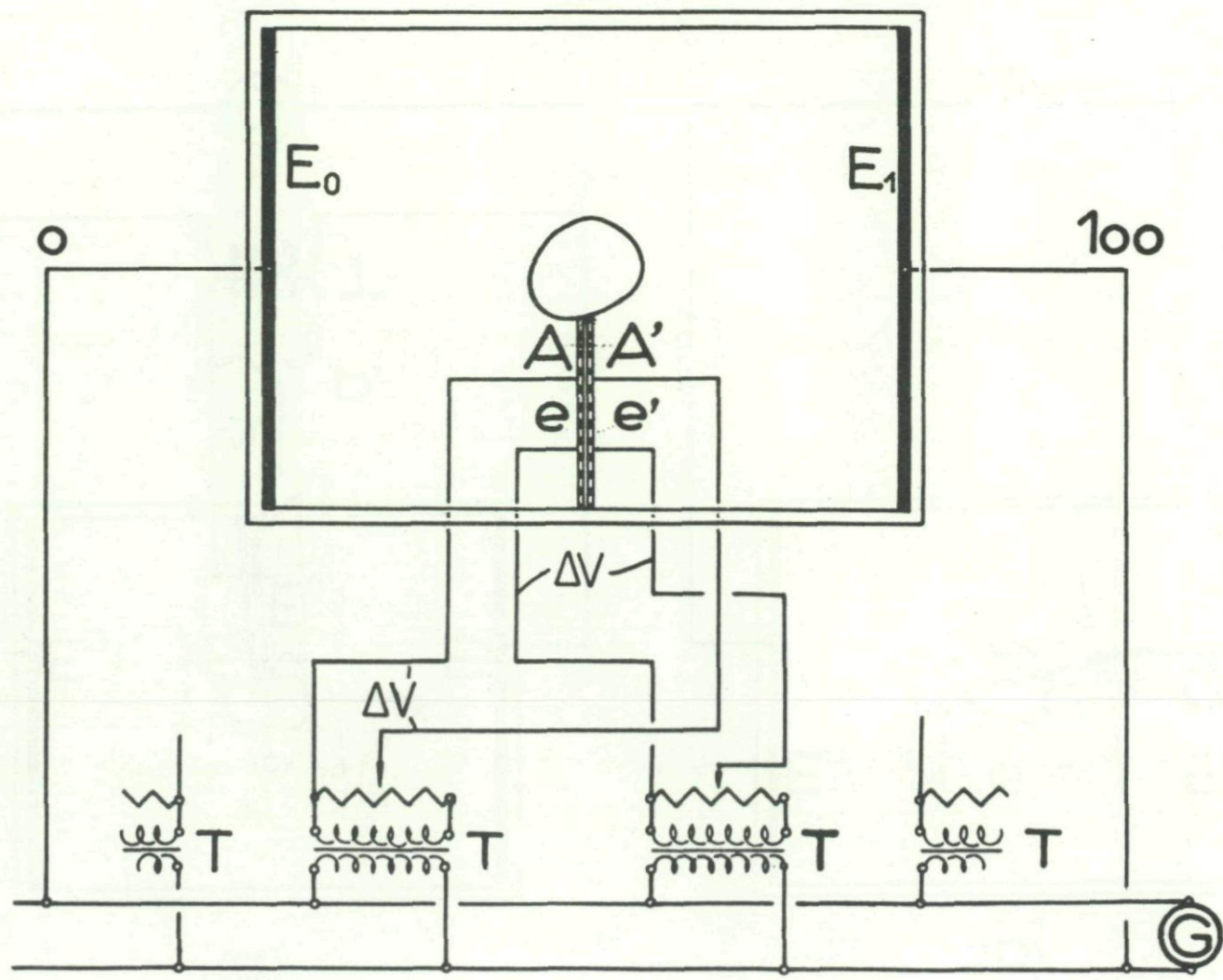


Fig. IV-4c. Circulation about an object (Analogy A). 3rd set-up.

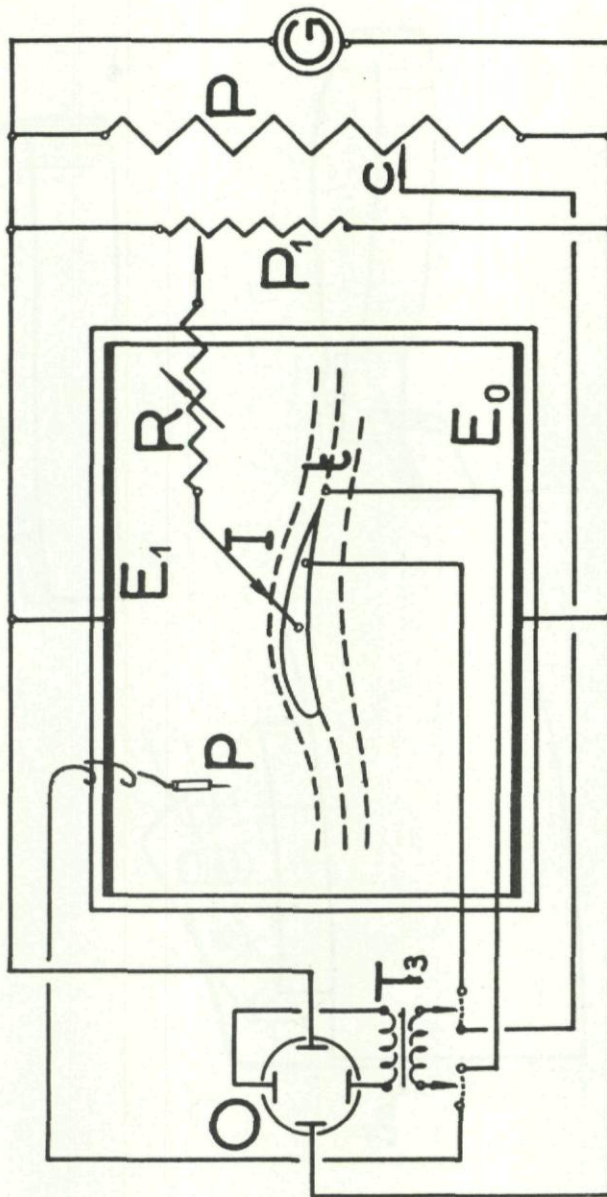


Fig. IV-5. Study of a wing section in the electric tank (Analogy B).

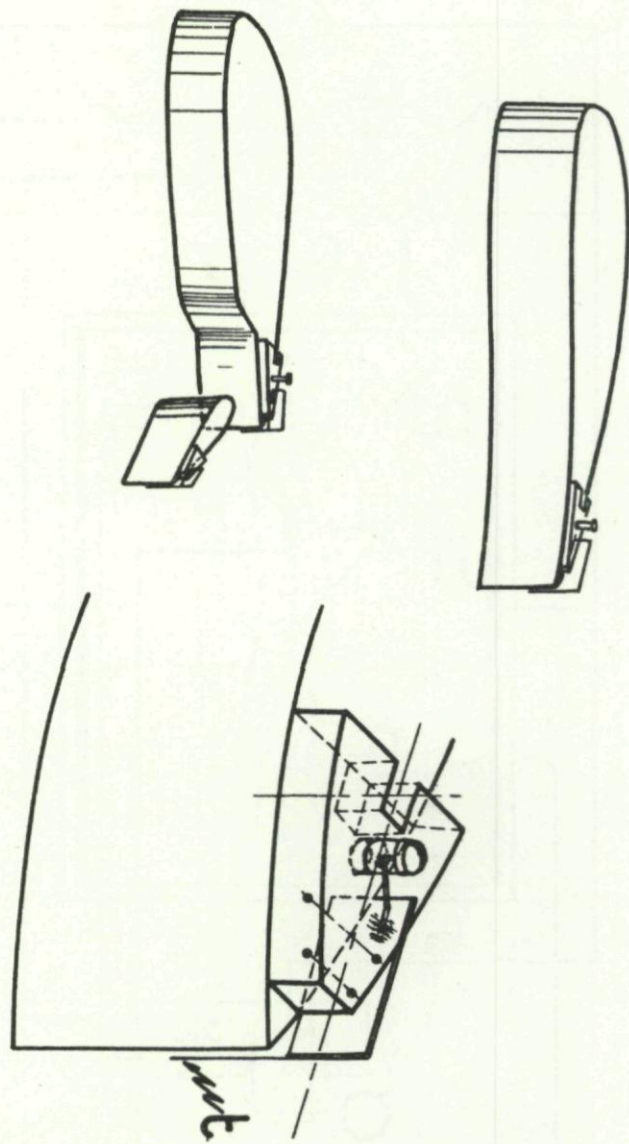
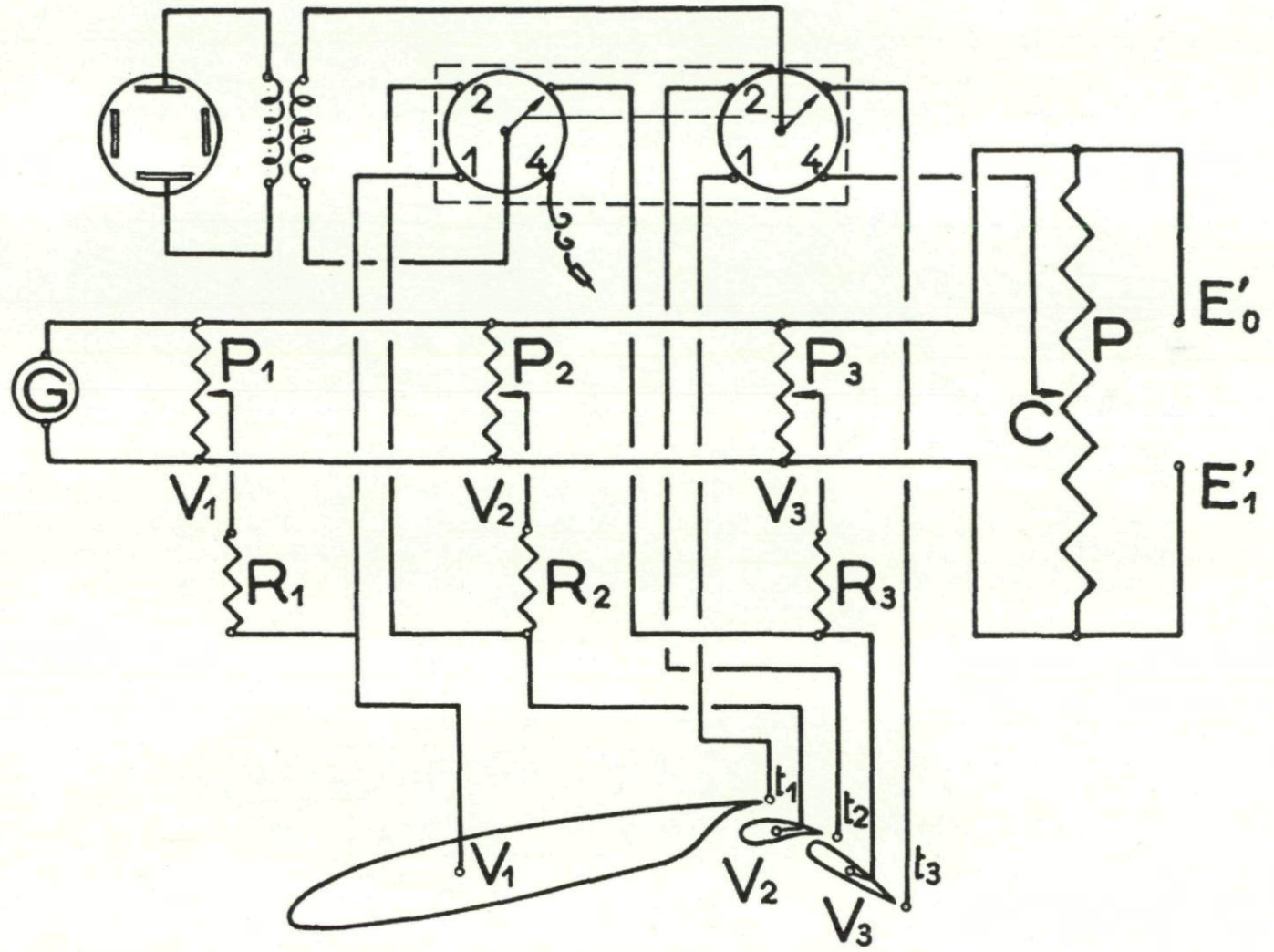


Fig. IV-6. Models of airfoil sections and details of the trailing edge probe used in establishing the Joukowsky condition.



113

Fig. IV-7. Electrical circuit for several airfoil sections in series.

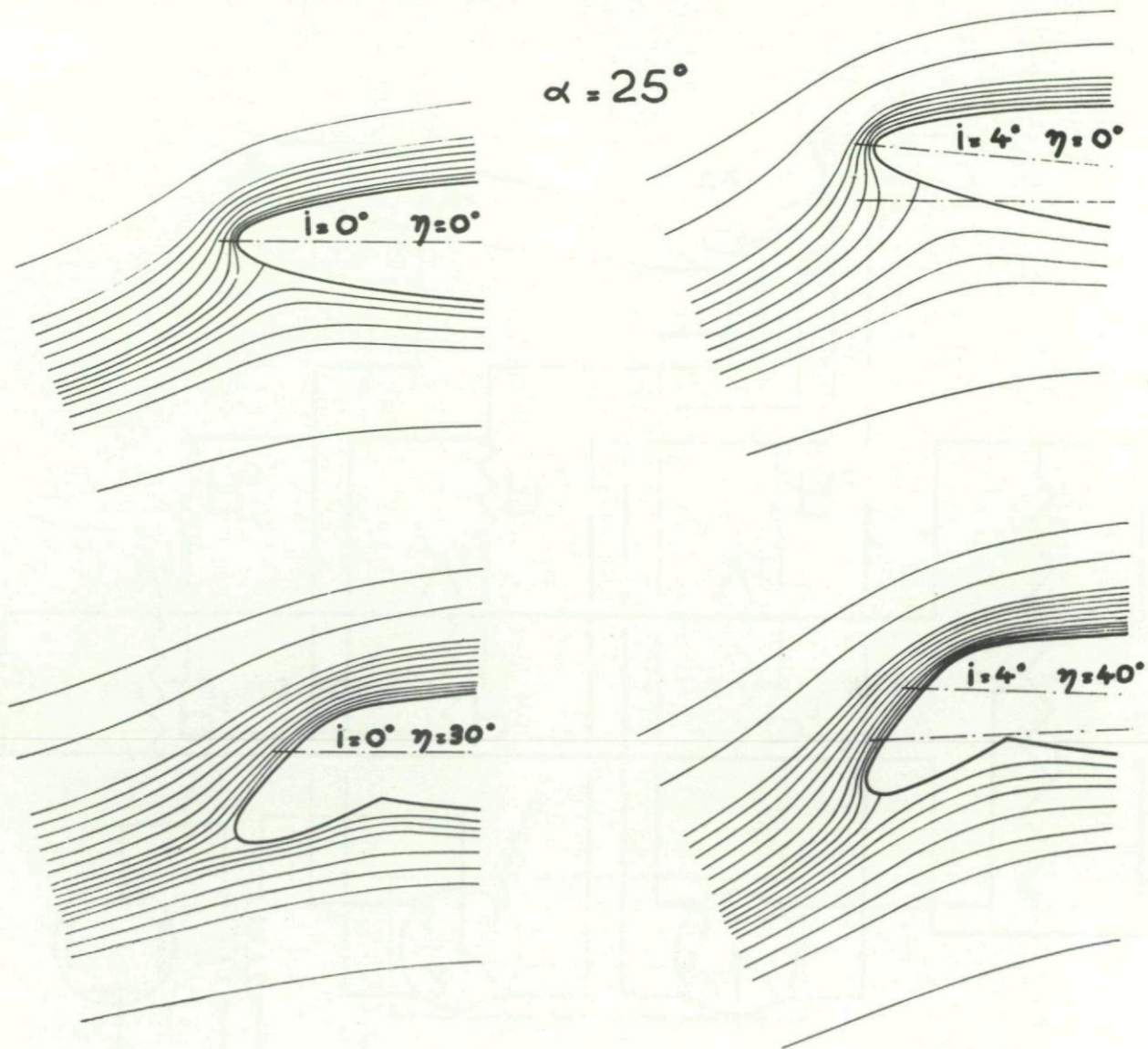


Fig. IV-8. Streamlines in the neighborhood of a wing leading edge.

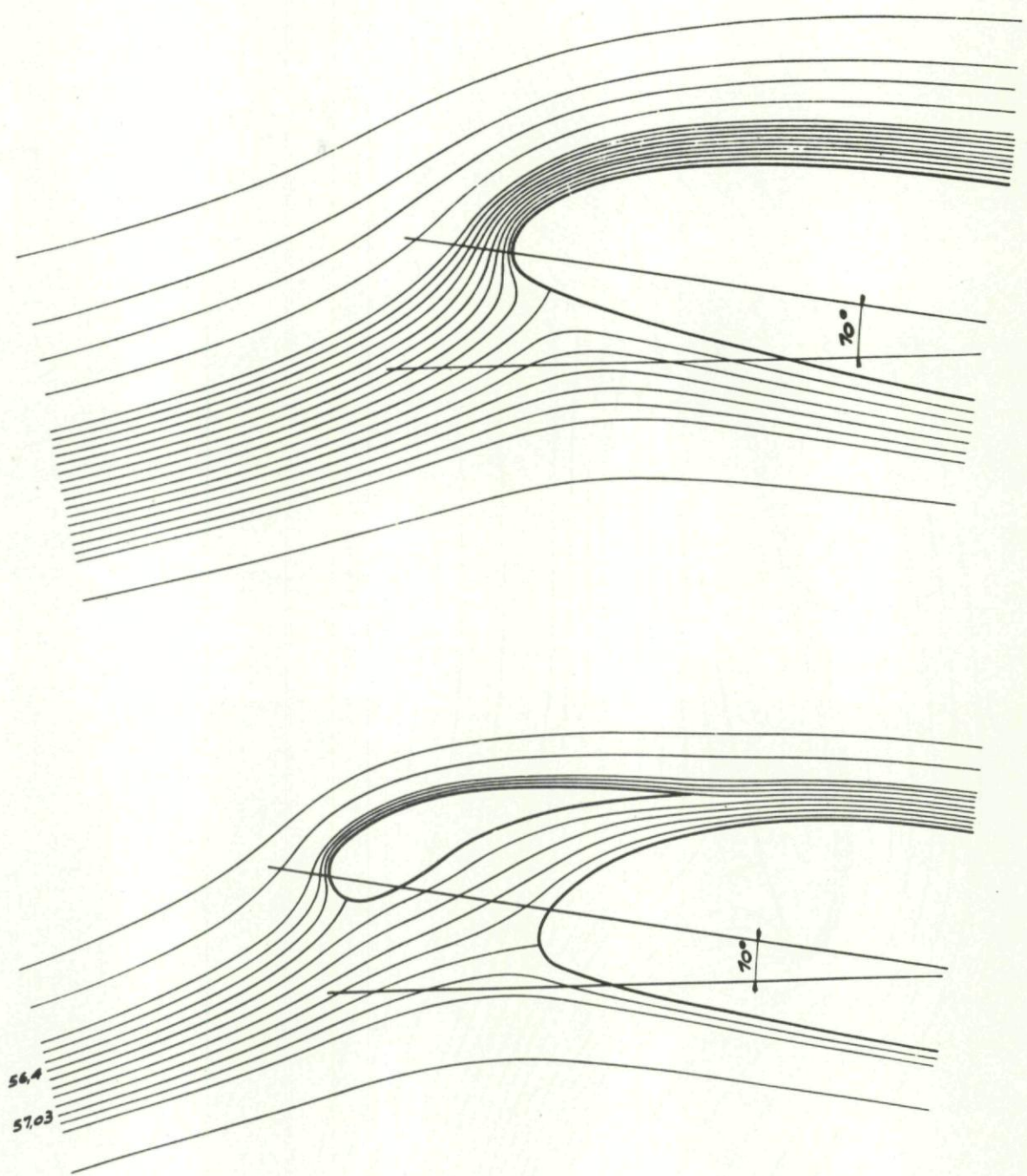


Fig. IV-9. Flow lines in the neighborhood of the leading edge of an airfoil section with and without leading edge slat.

116

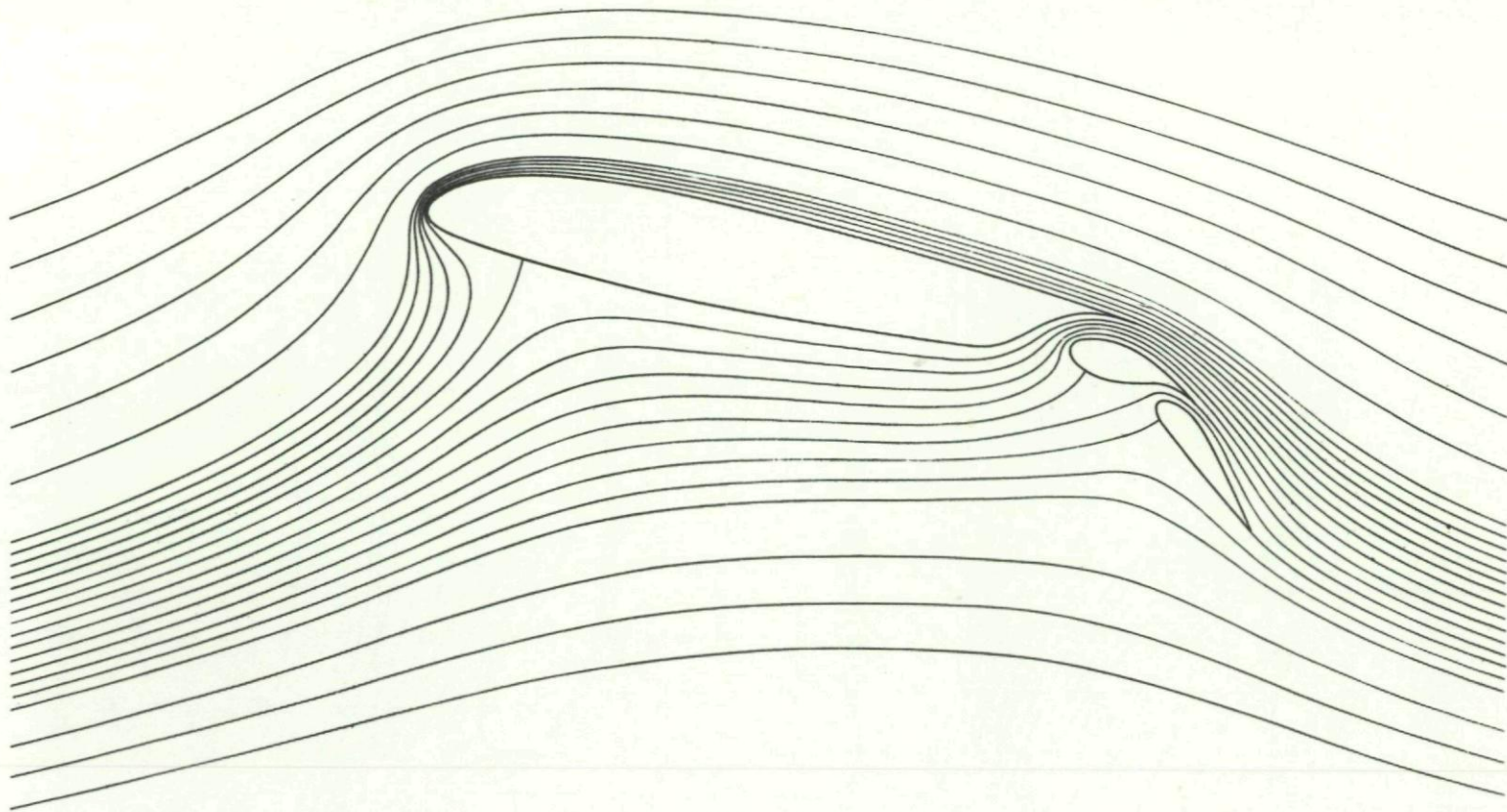


Fig. IV-10. Flow around an airfoil section with double, slotted flap.

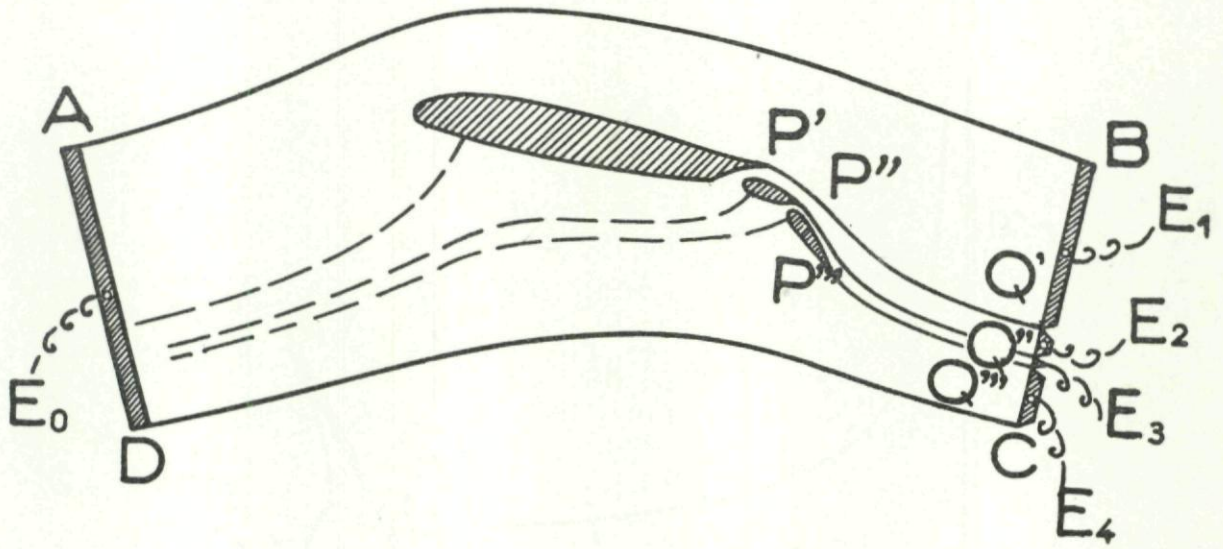


Fig. IV-11. Model in graphite conducting paper for Analogy A.

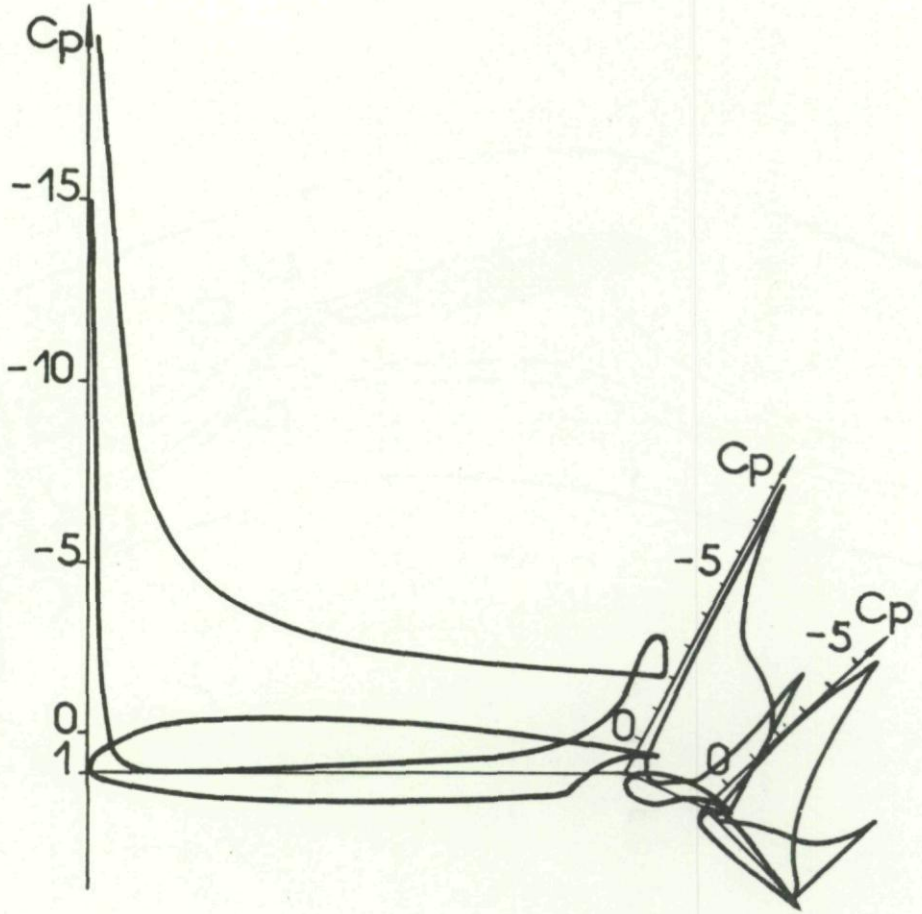


Fig. IV-12. Pressure coefficient over an airfoil with double flap.

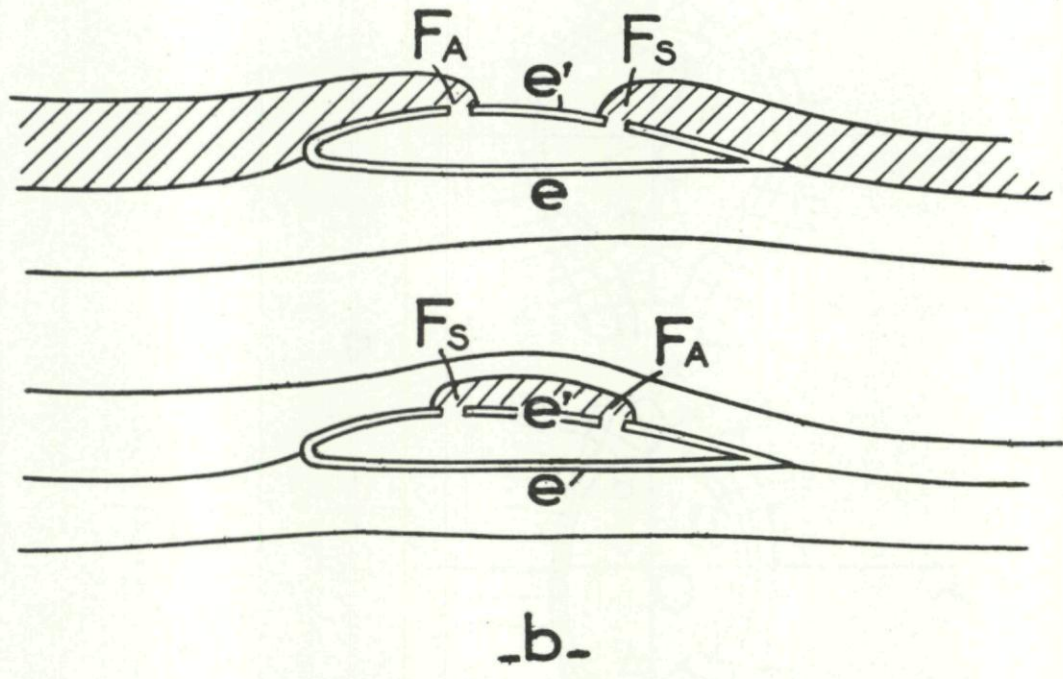
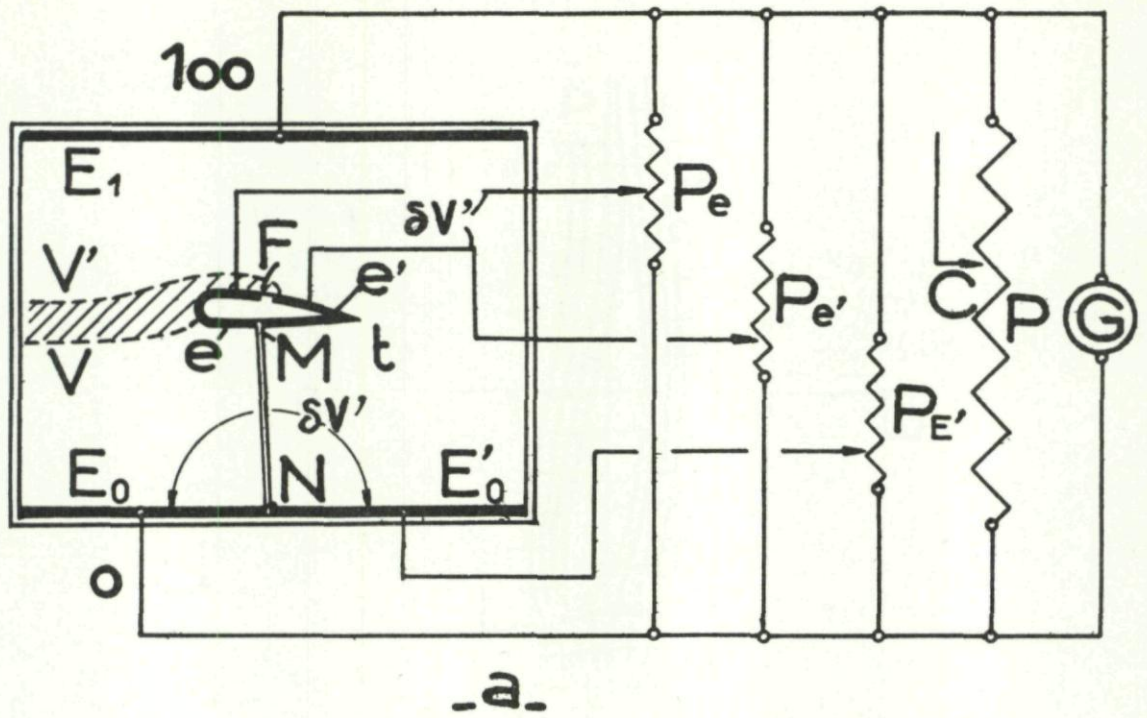


Fig. IV-13. Analog set-up for representing a source and a sink (aspiration) on an airfoil section.

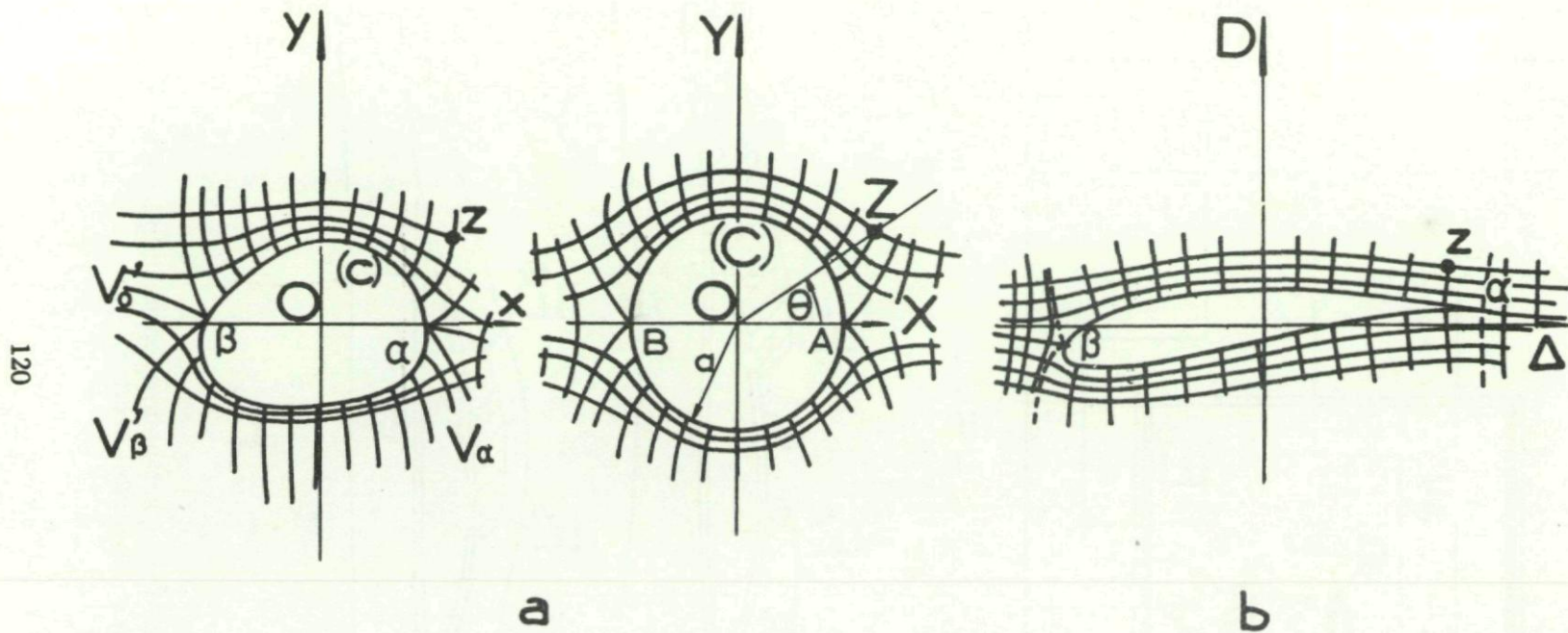


Fig. V-1. Conformal mapping of the outside of an arbitrary contour (a) or an airfoil section (b) on the outside of a circle.

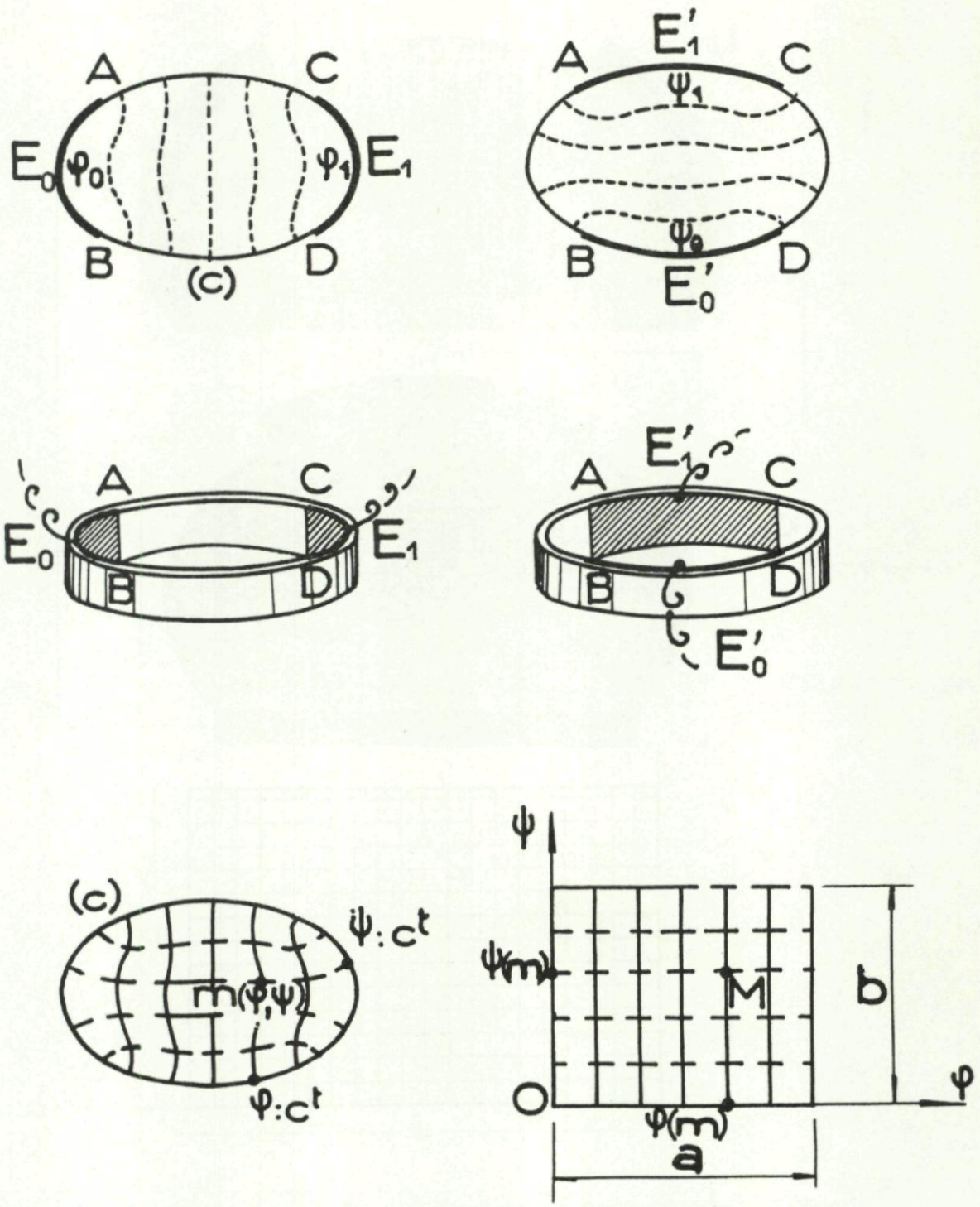
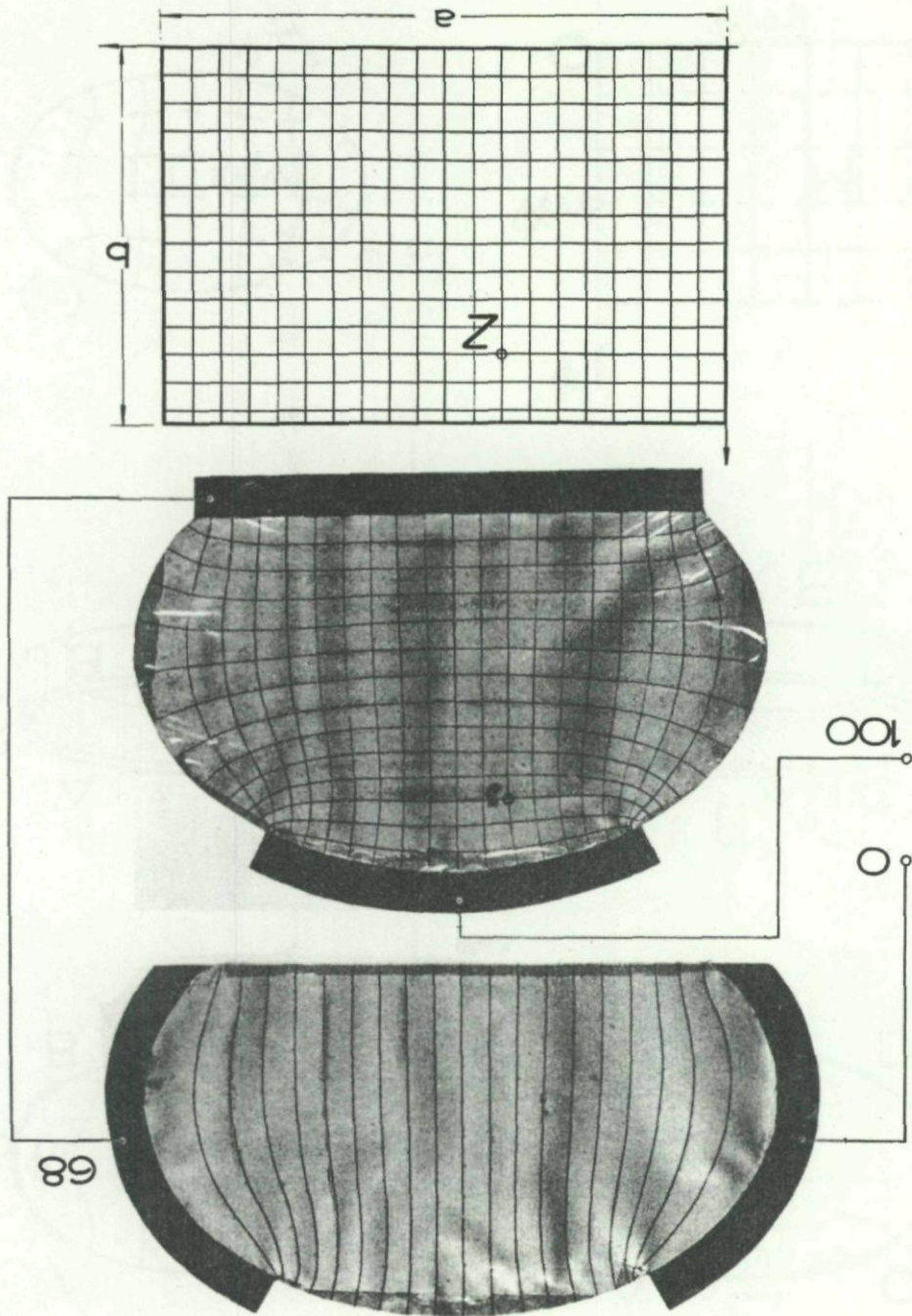
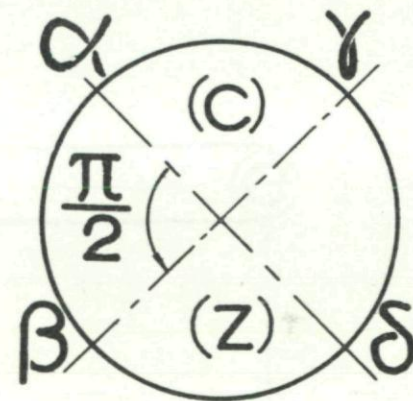
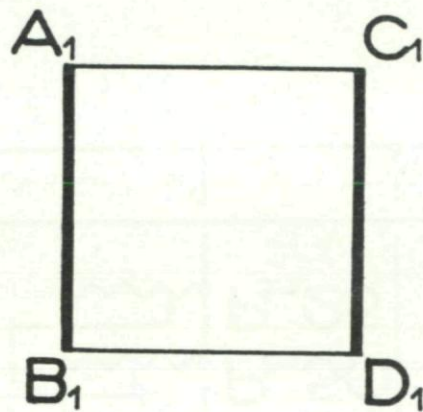
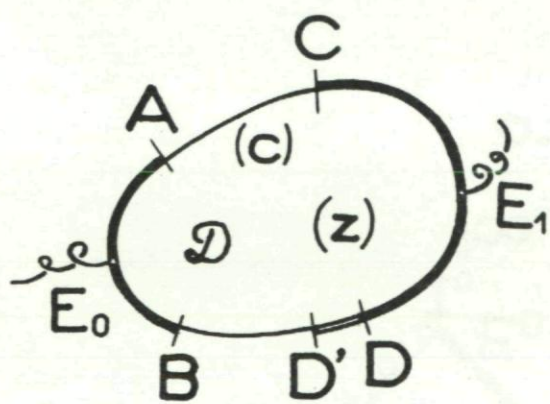


Fig. V-2. Conformal mapping of an area on the inside of a rectangle.

122

Fig. V-3. Conducting paper models used in defining a conformal transformation.





123

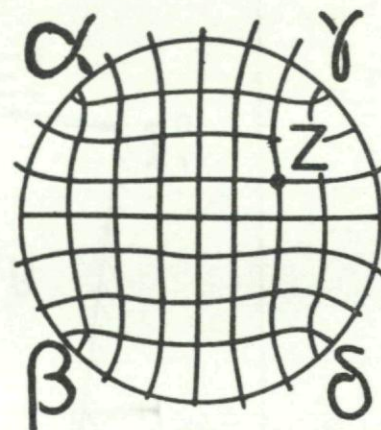
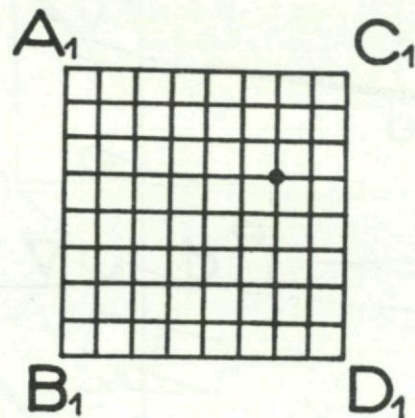
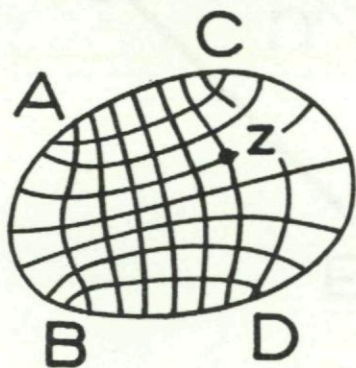


Fig. V-4. Conformal mapping of an area on a circle.

124

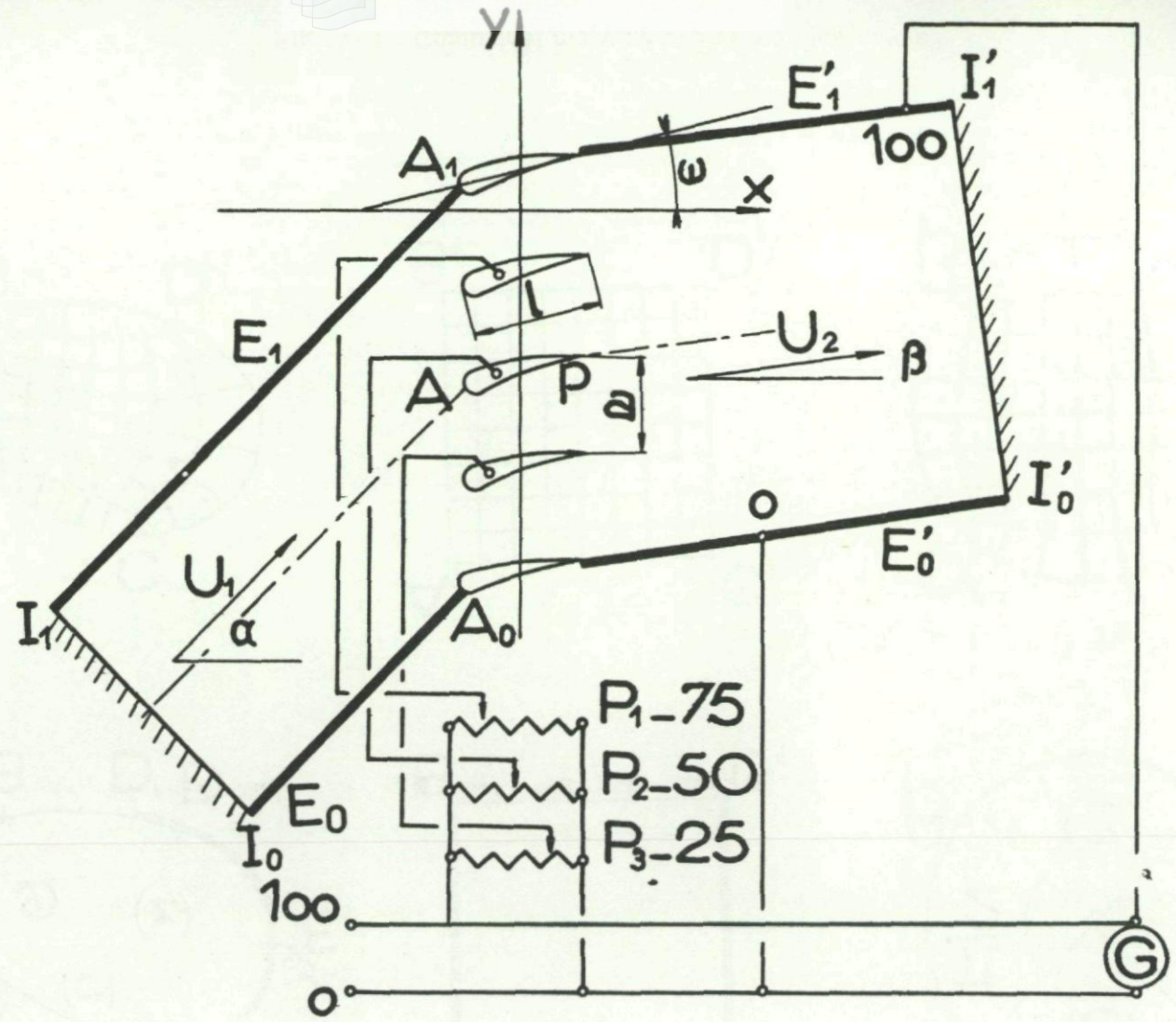


Fig. VI-1. Set-up in the electric tank for studying an airfoil cascade (Analogy B).

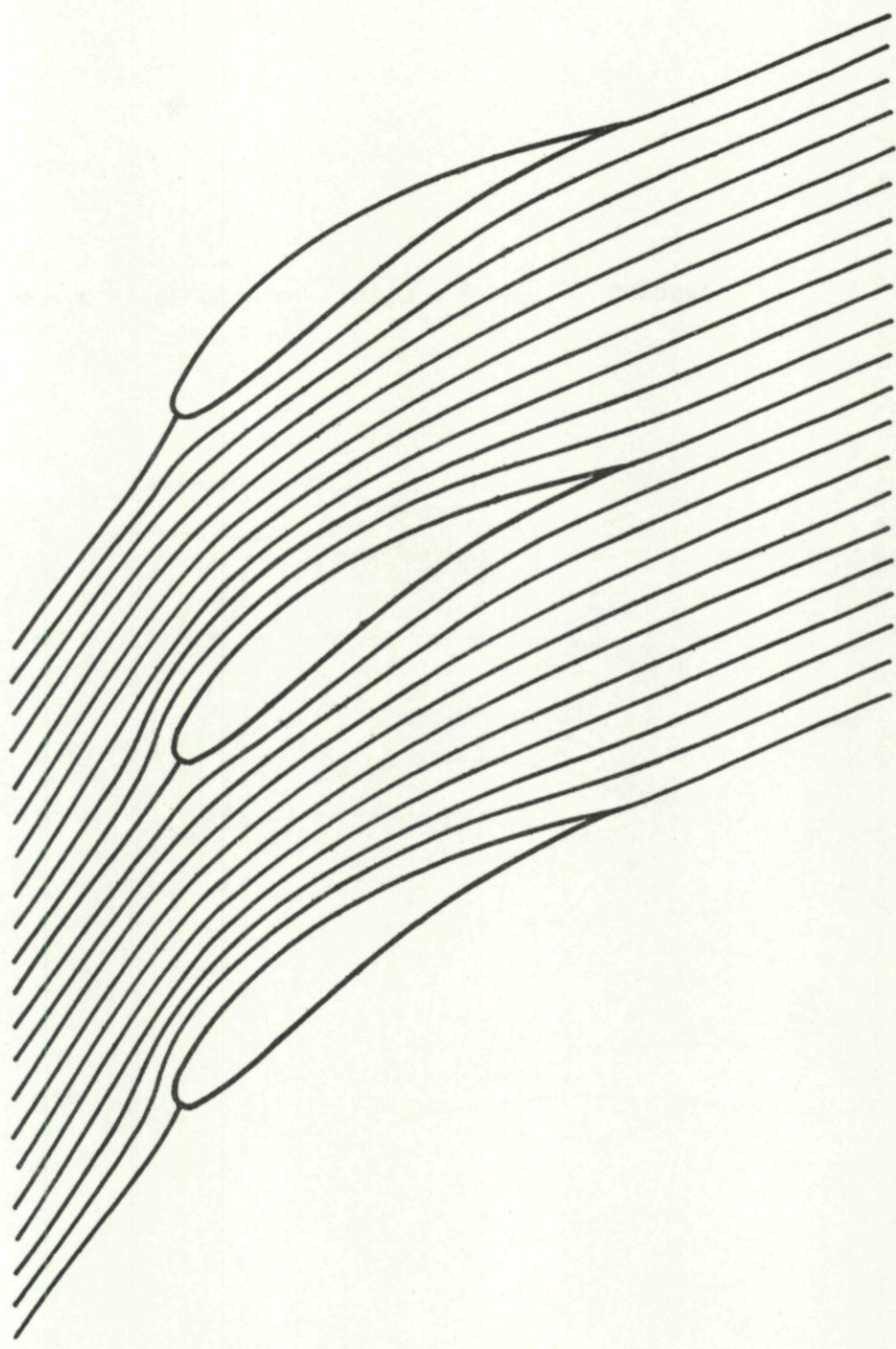


Fig. VI-2. Example of the streamlines traced around a cascade.

CASCADE ;  $\epsilon = \frac{a}{t} = 0,784 - \omega = 36^{\circ}36' - \alpha = 55^{\circ}21'$

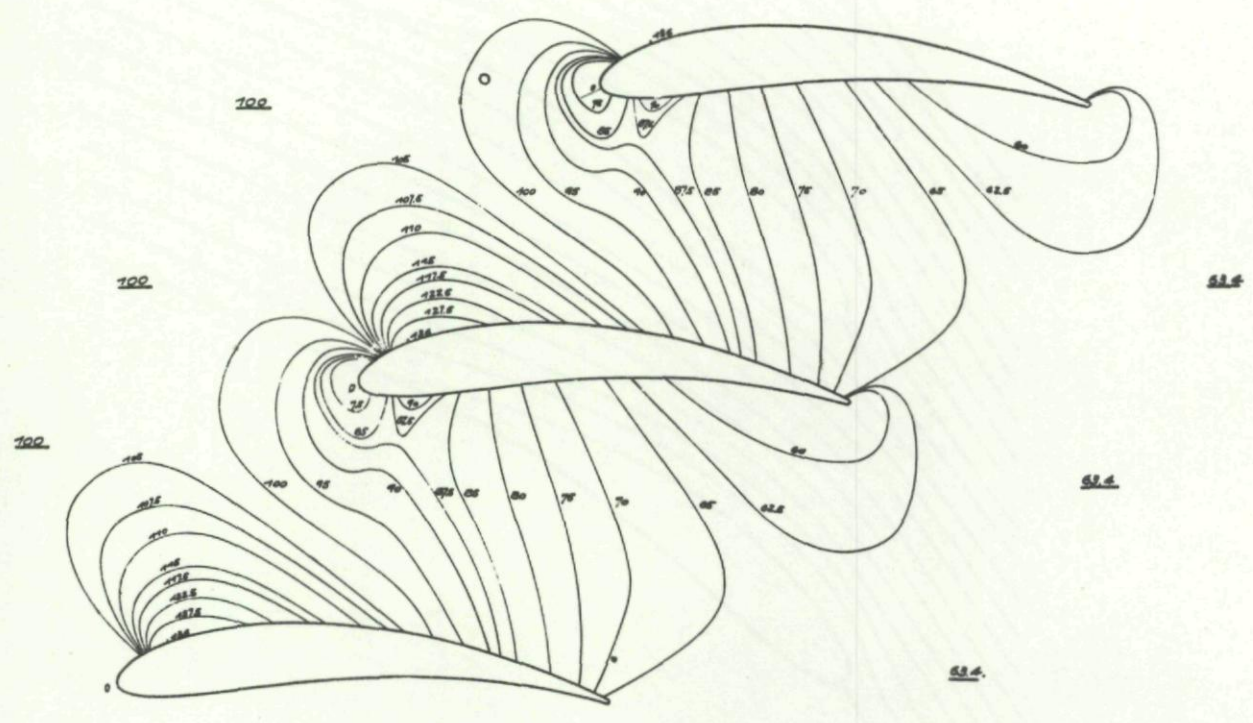


Fig. VI-3. Lines of constant velocity through a cascade.

127

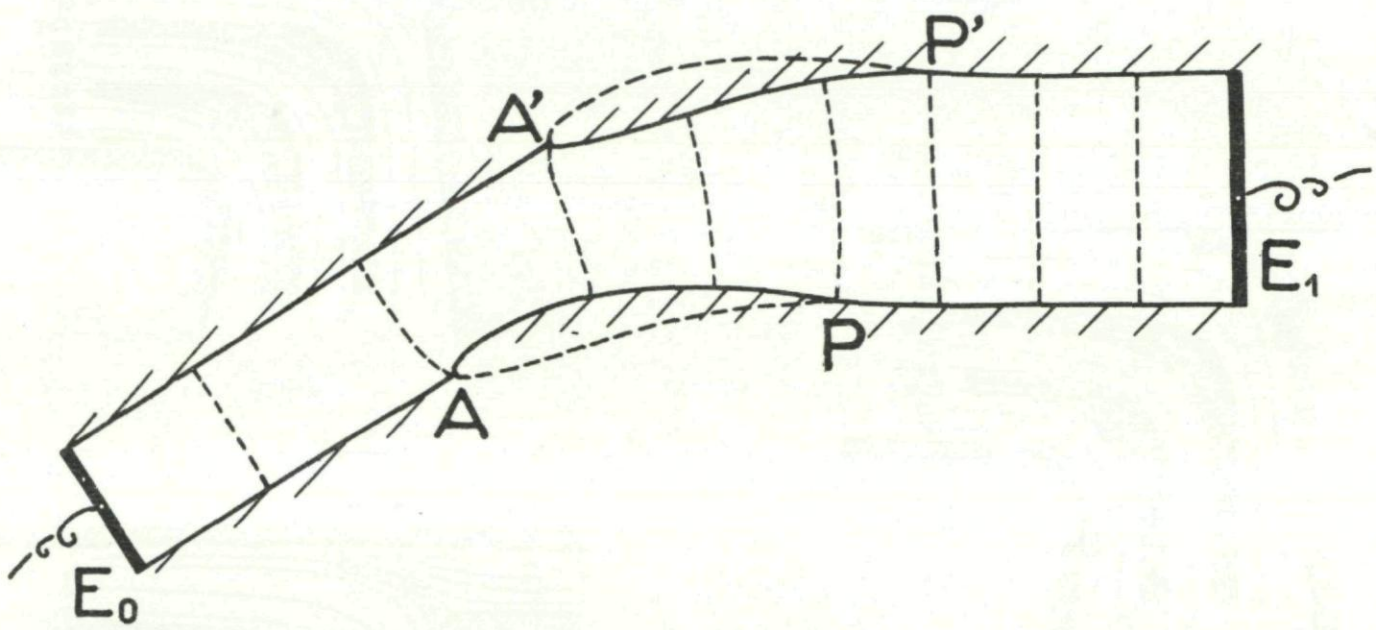
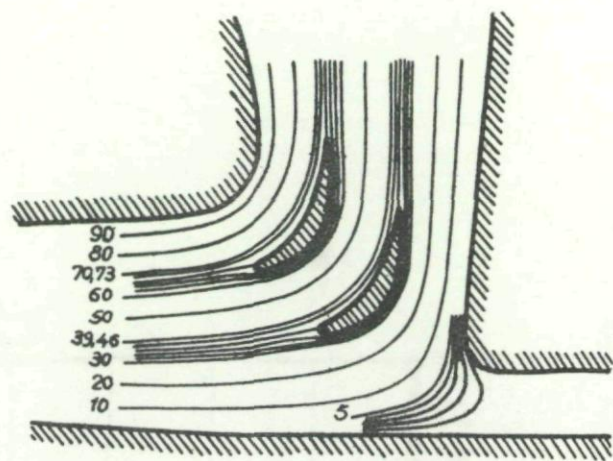
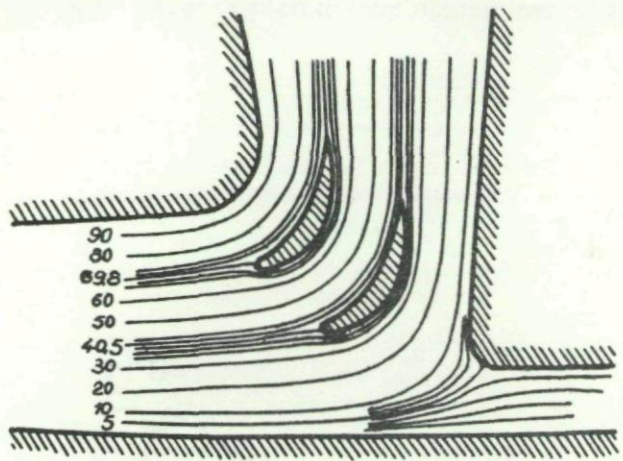


Fig. VI-4. Electric tank determination of the velocity potential about blades in cascade (Analogy A).



128

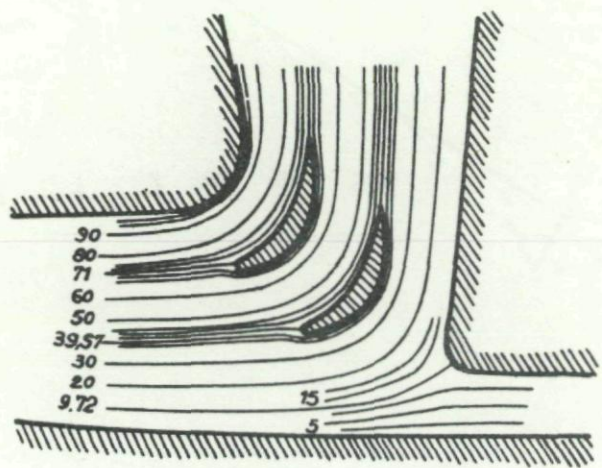


Fig. VI-5. Flow in an elbow with turning vanes.

129

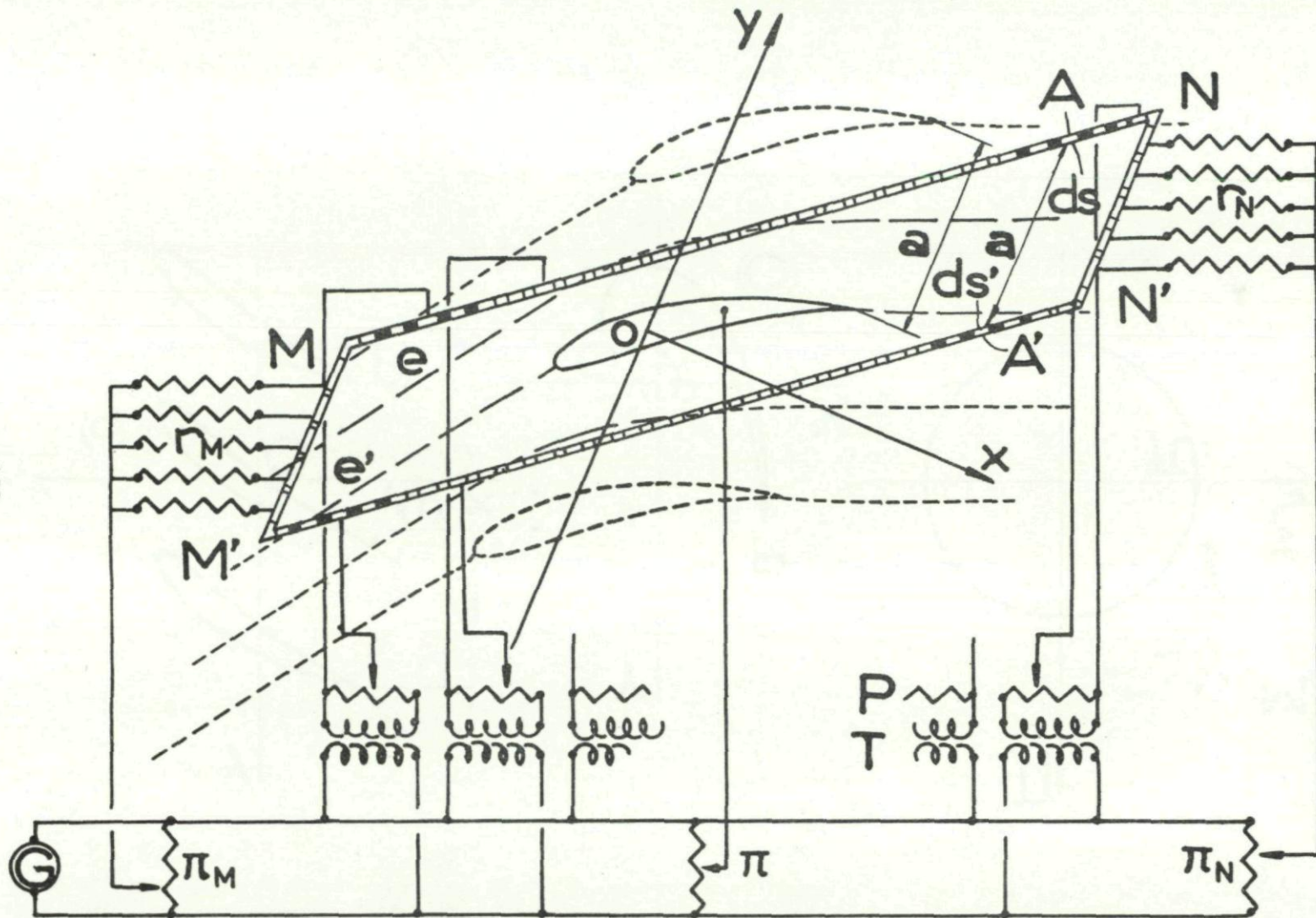


Fig. VI-6. Analog study of a cascade. Rheoelectric set-up based on periodicity of the field.

130

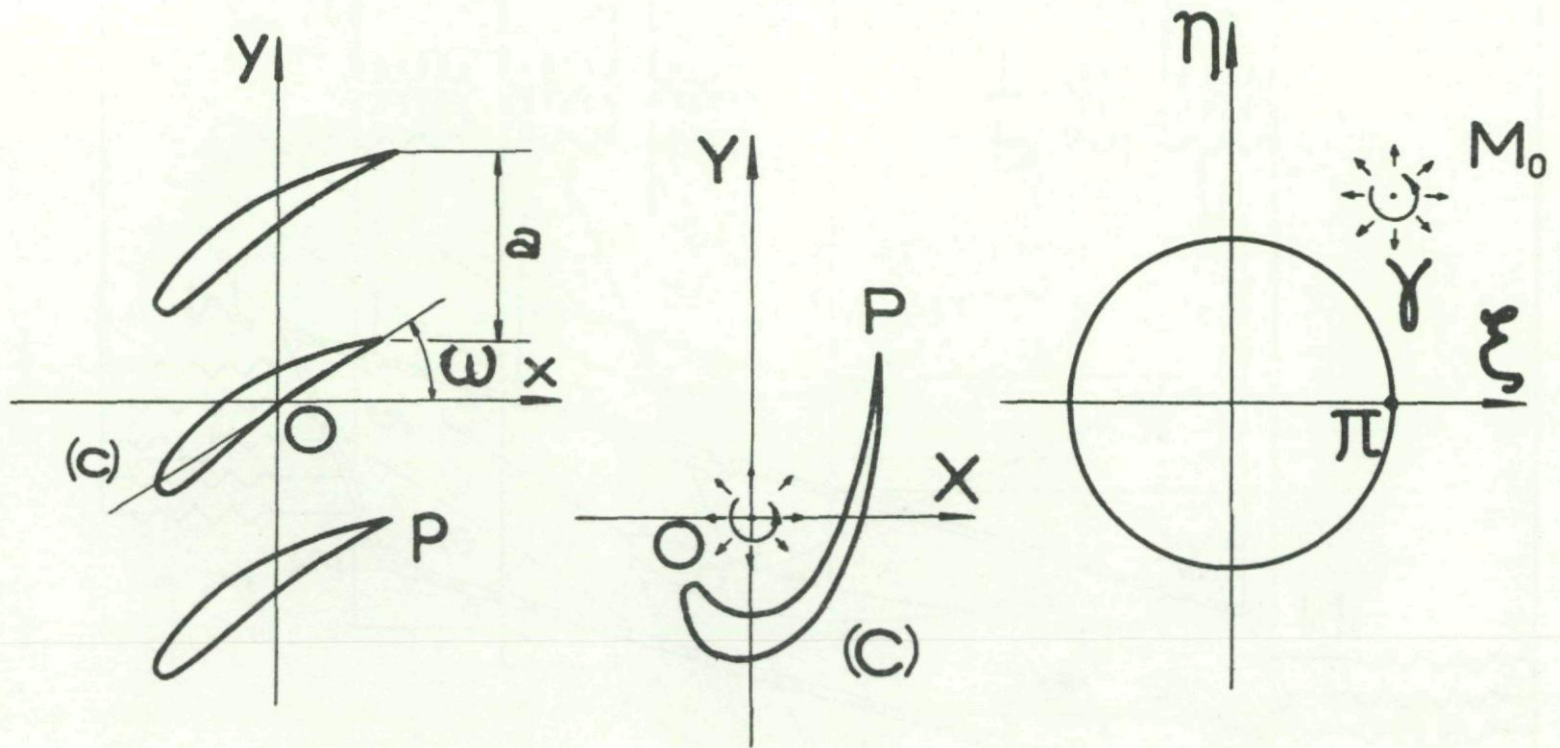


Fig. VI-7. Conformal mapping of a cascade onto a circle.

131

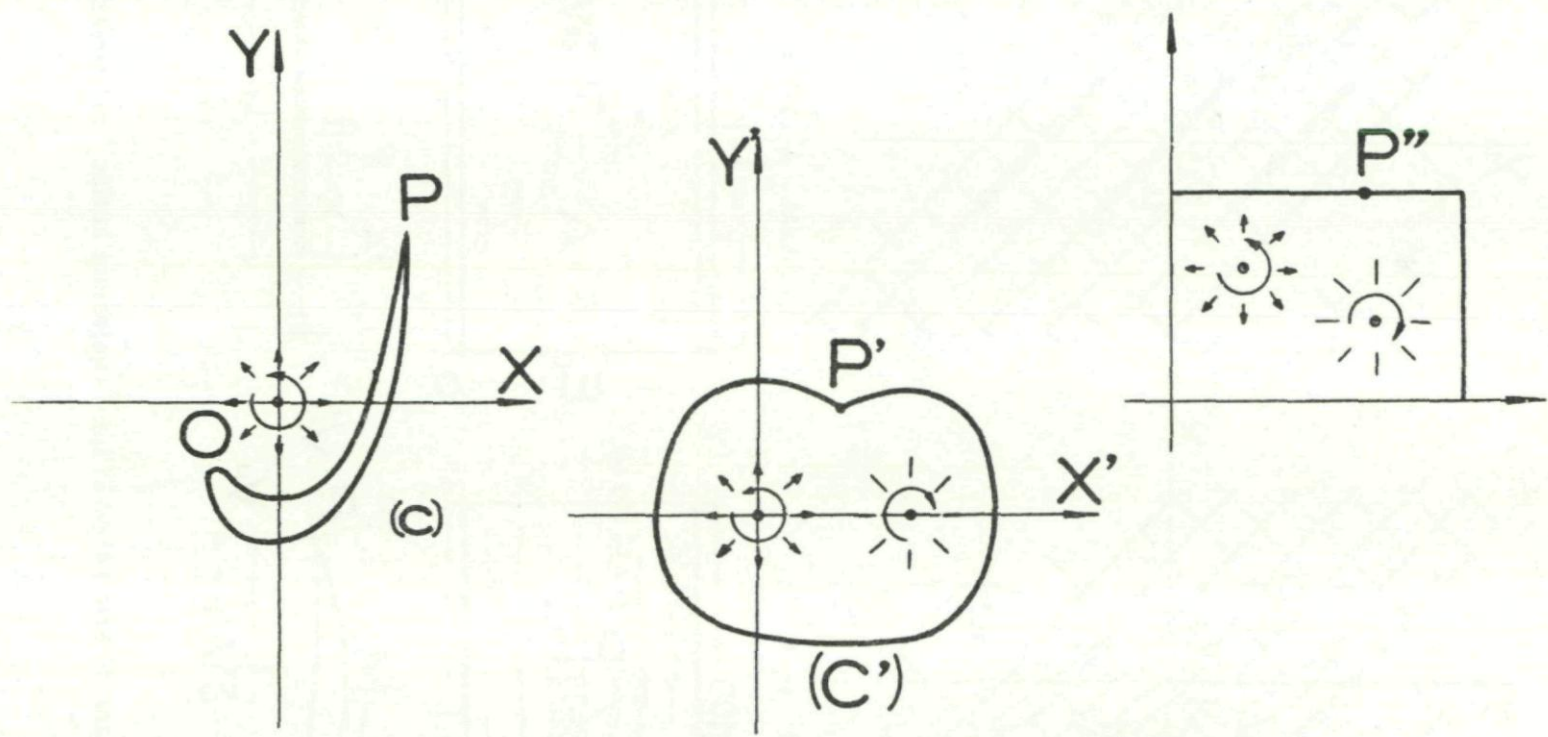


Fig. VI-8. Conformal mapping of a cascade onto a rectangle.

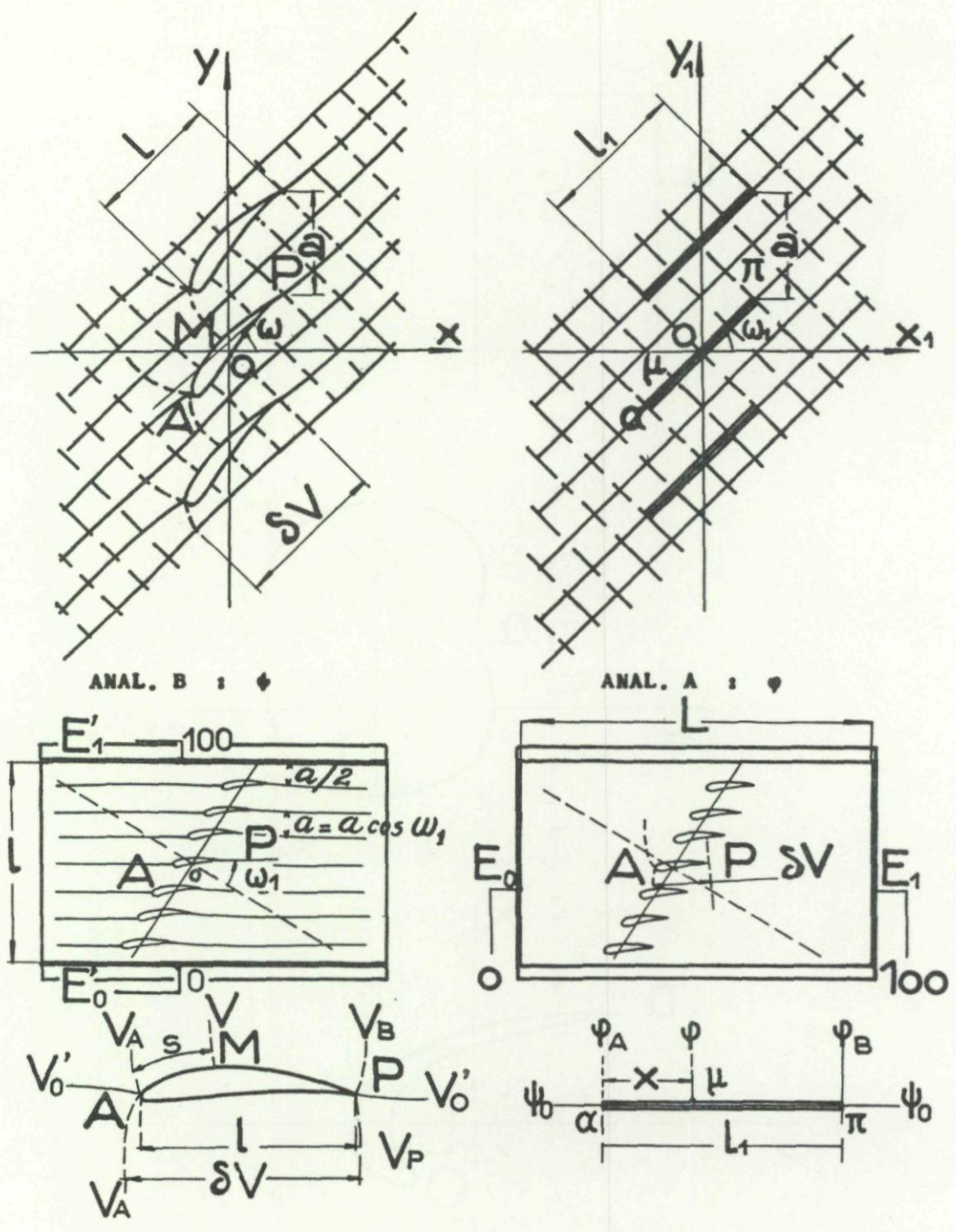
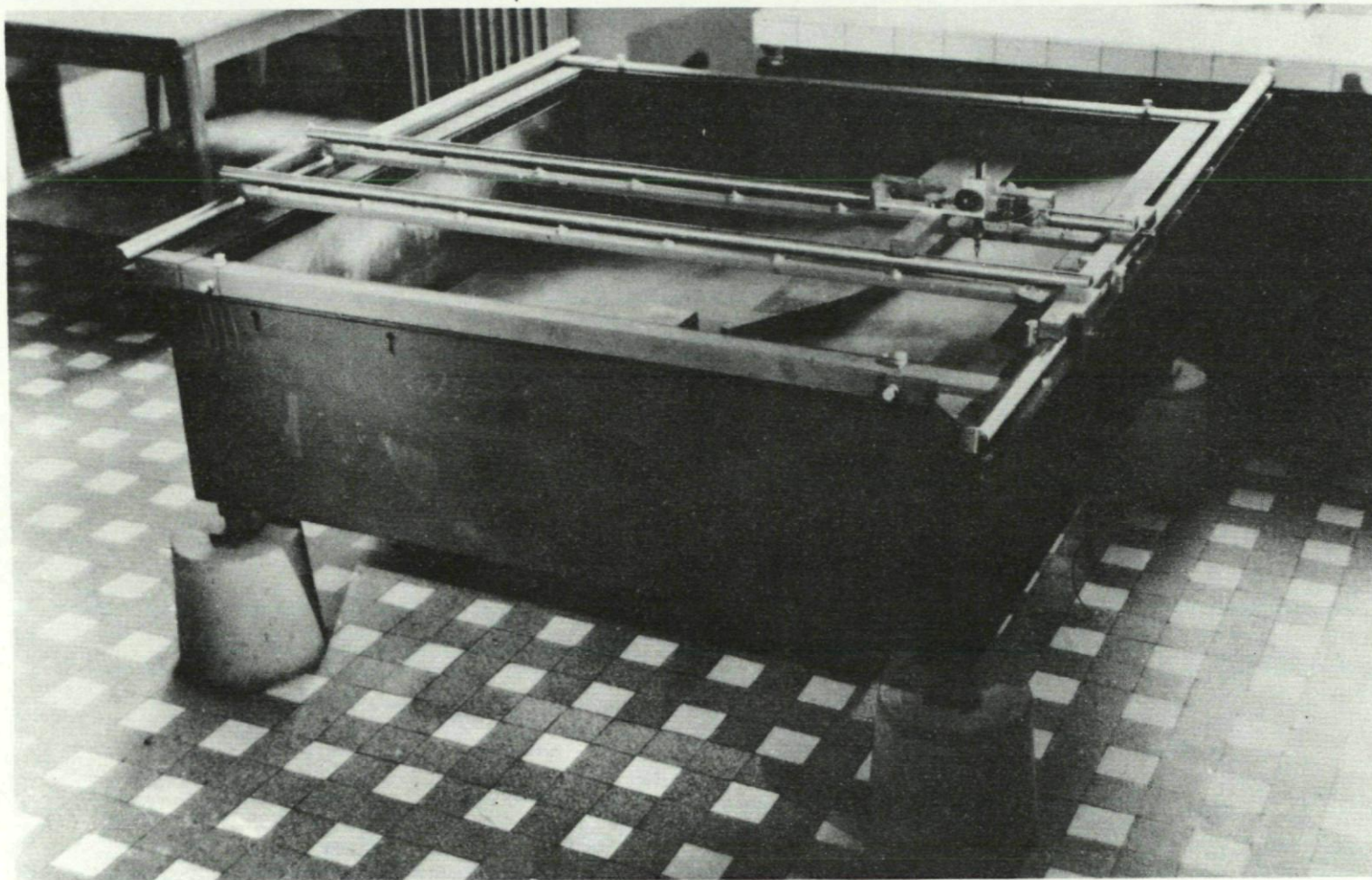


Fig. VI-9. Electric tank determination of the "equivalent lattice" to a given lattice.



133

Fig. VII-1. Inclined tank for the study of axially symmetric flows (Analogy A).

134

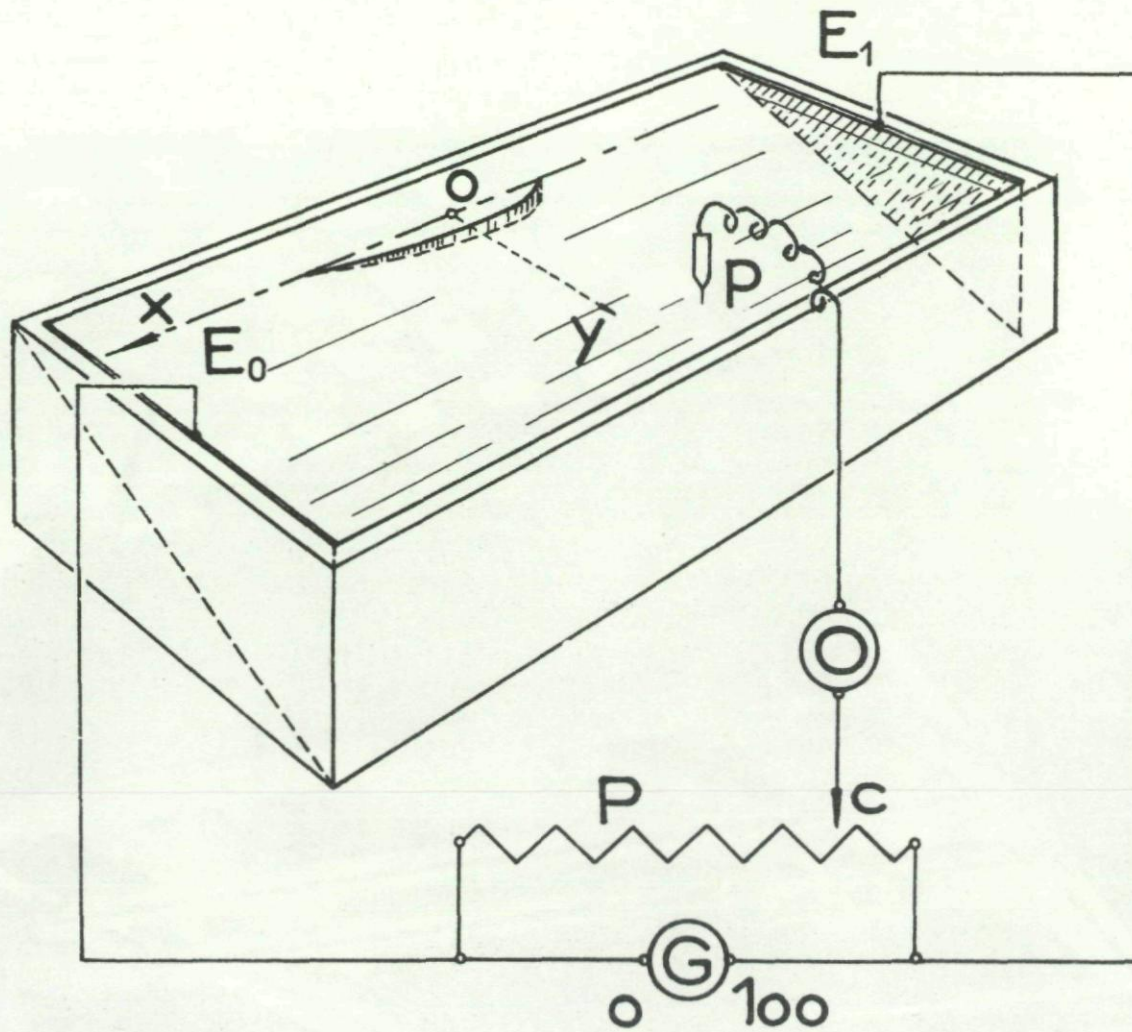


Fig. VII-2. Electrical circuit for an inclined tank.

135

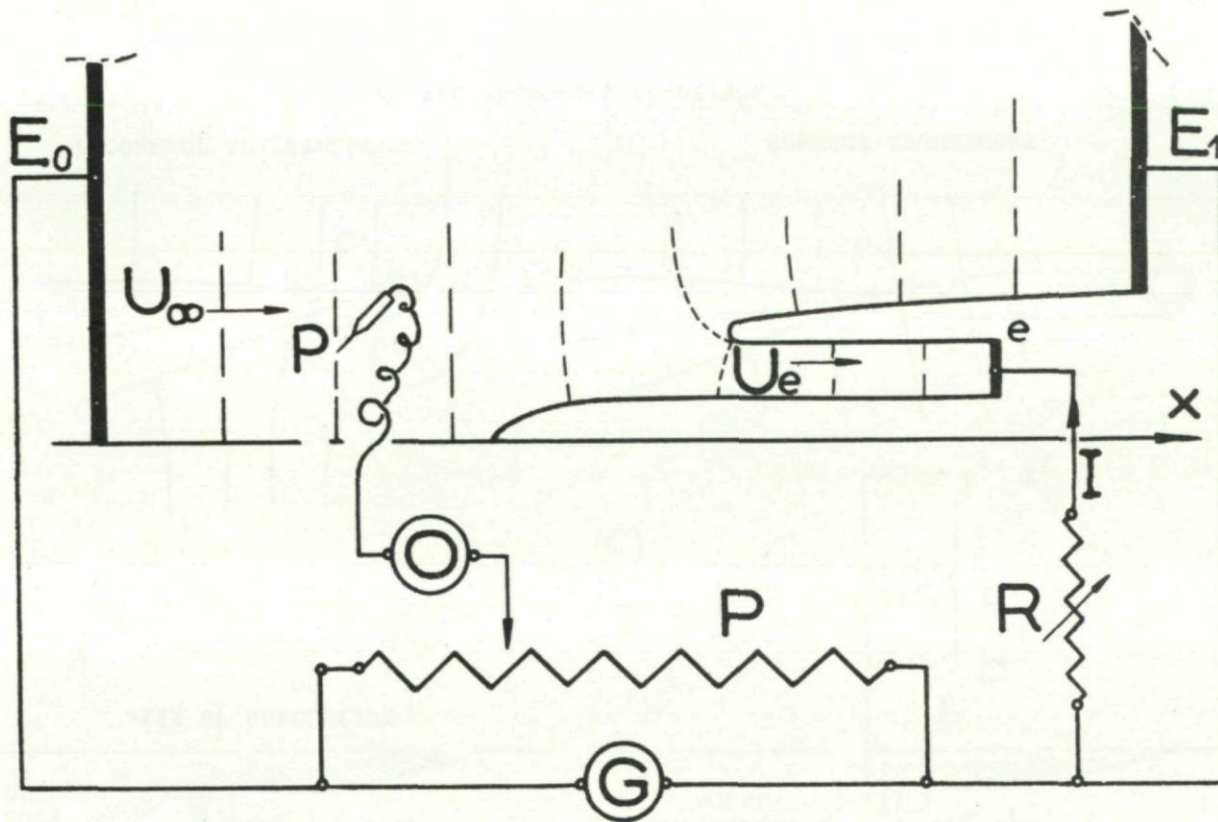


Fig. VII-3. Electric set-up for studying an air intake in the inclined tank.

136

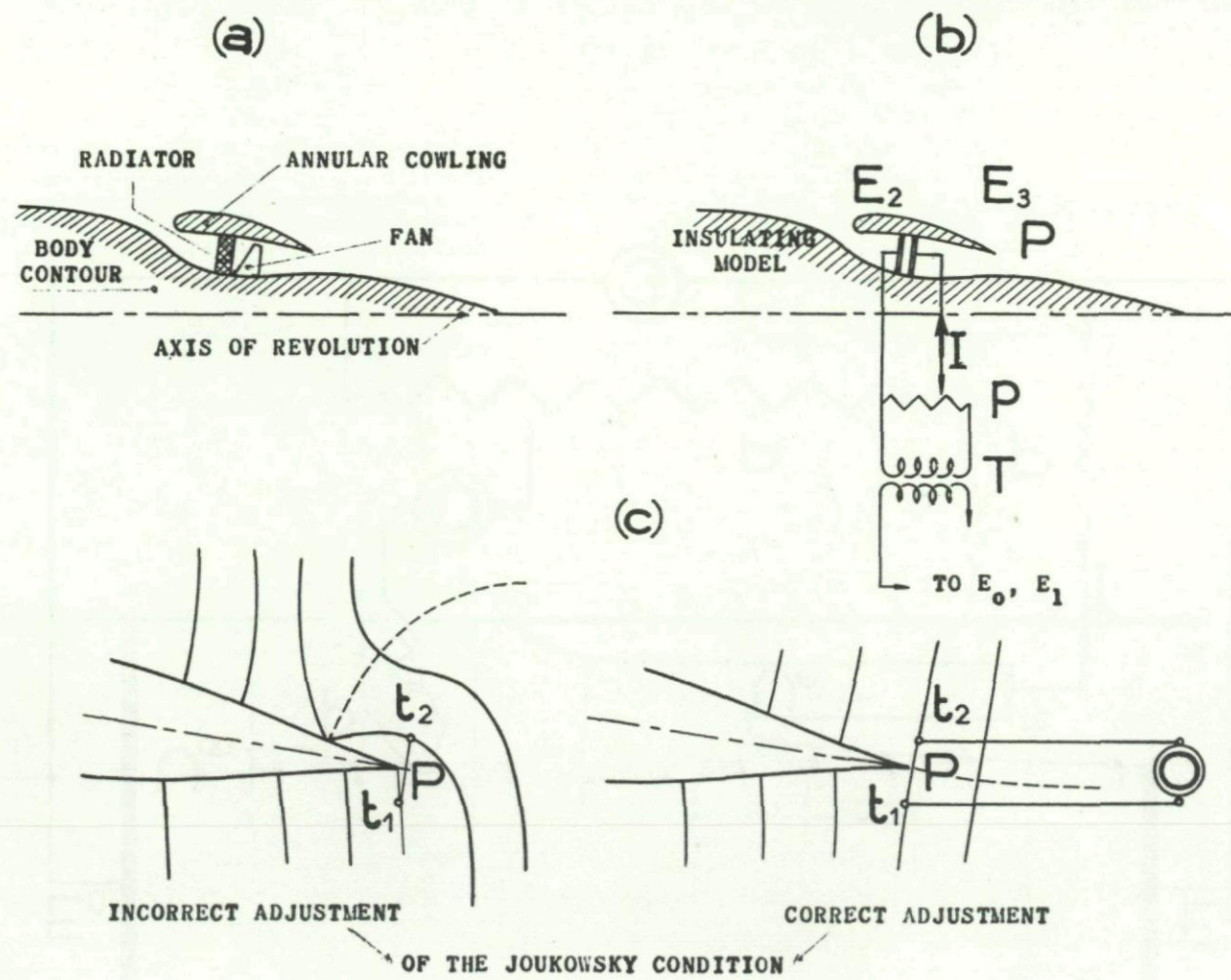


Fig. VII-4. Analog study of the flow about an annular cowling.

- (a) Arrangement of the cowling and streamlined body.
- (b) Electric circuit for establishing the circulation.
- (c) Adjustment of the Joukowski condition.

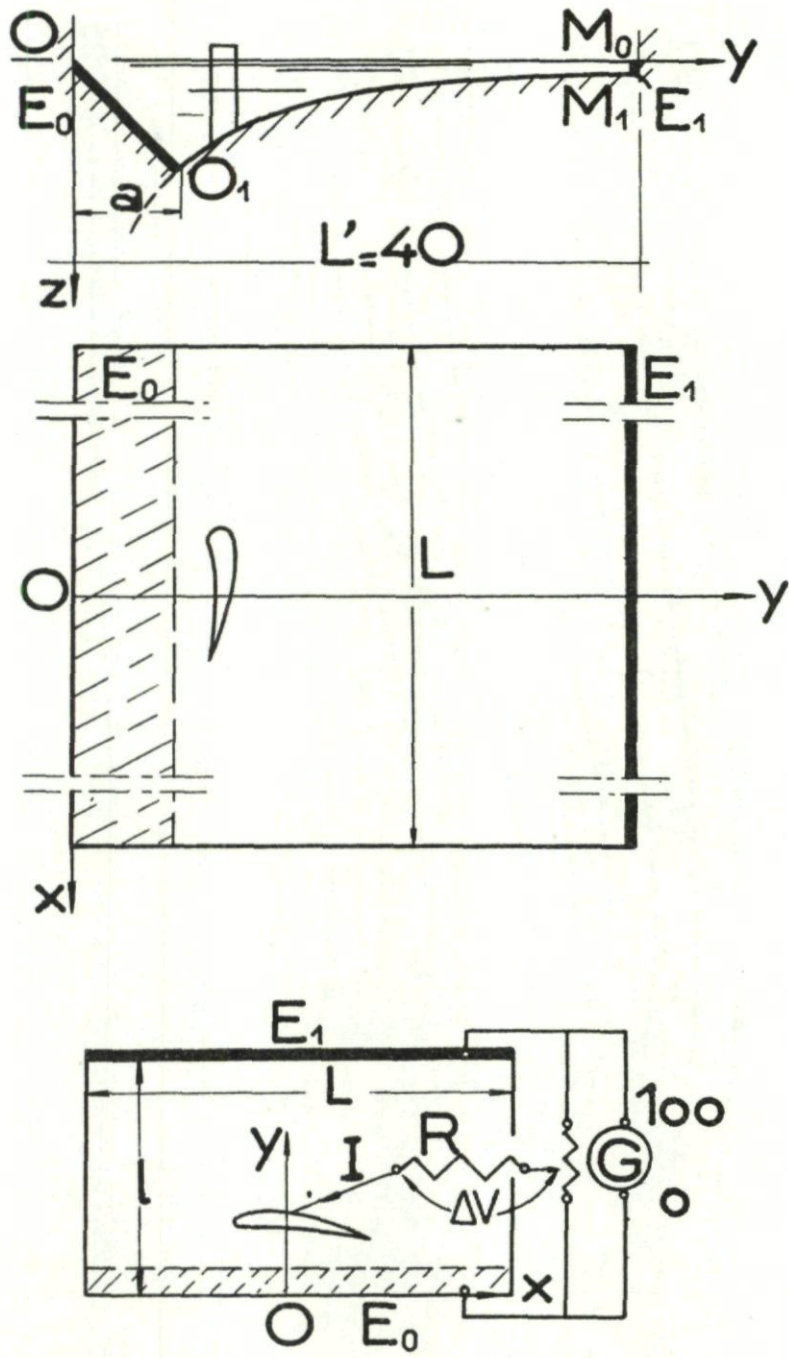


Fig. VII-5. Tank with hyperbolic bottom for tracing the streamlines of an axially symmetric flow. Electrical set-up for establishing the circulation about an airfoil.

138

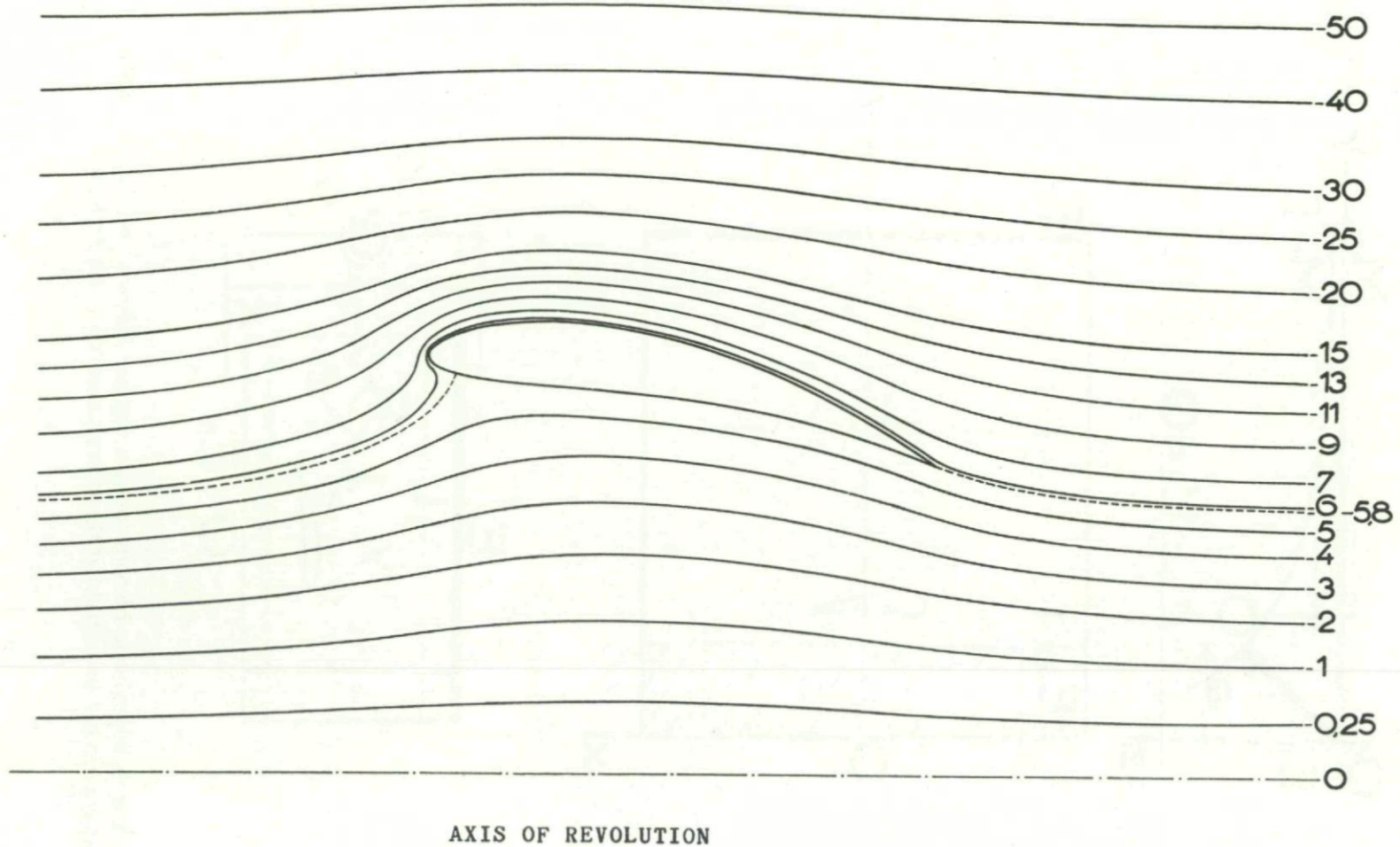


Fig. VII-6. Streamlines about section of an annular wing.

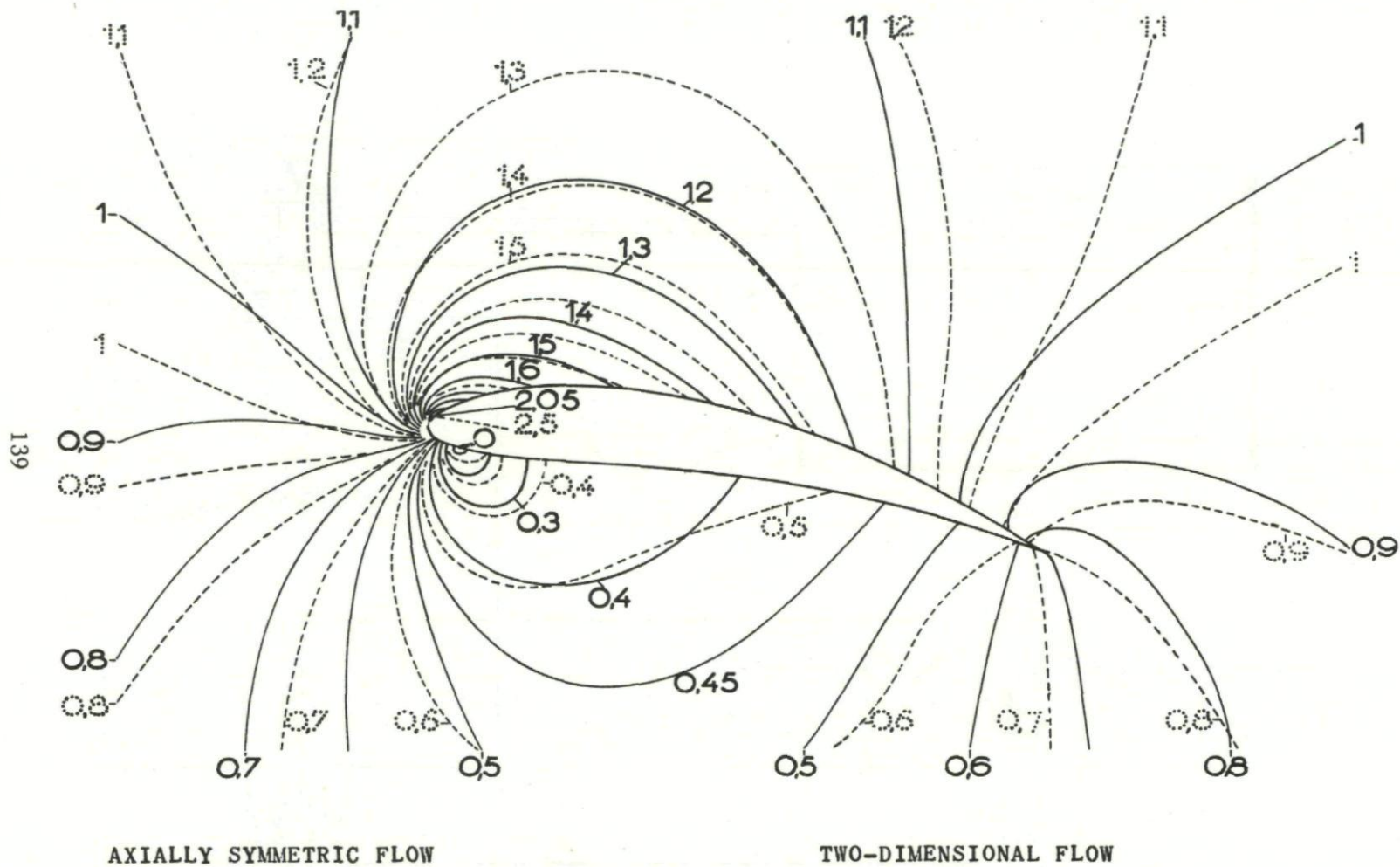


Fig. VII-7. Comparison between the constant velocity lines about an airfoil for plane and axially symmetric flows.

140

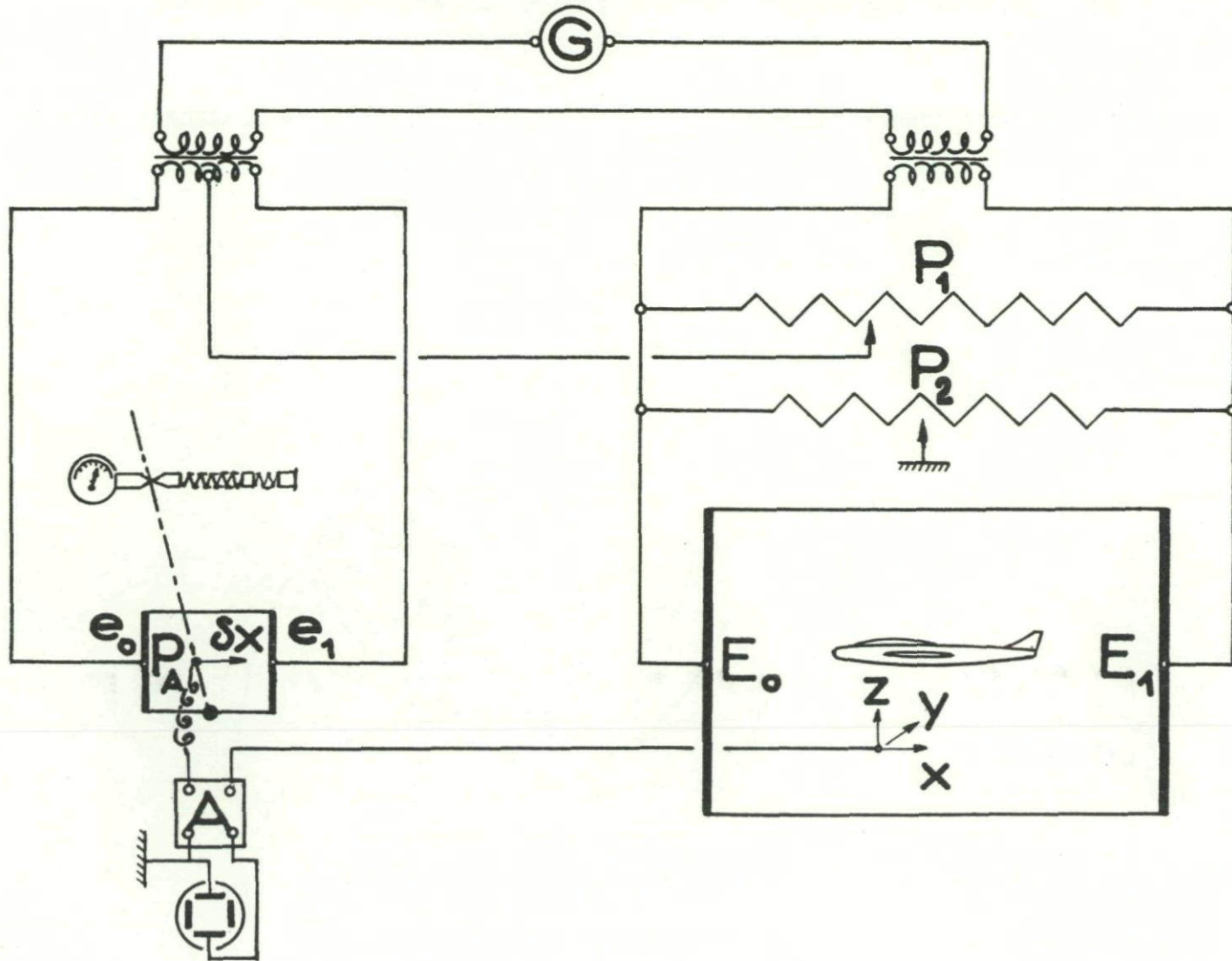
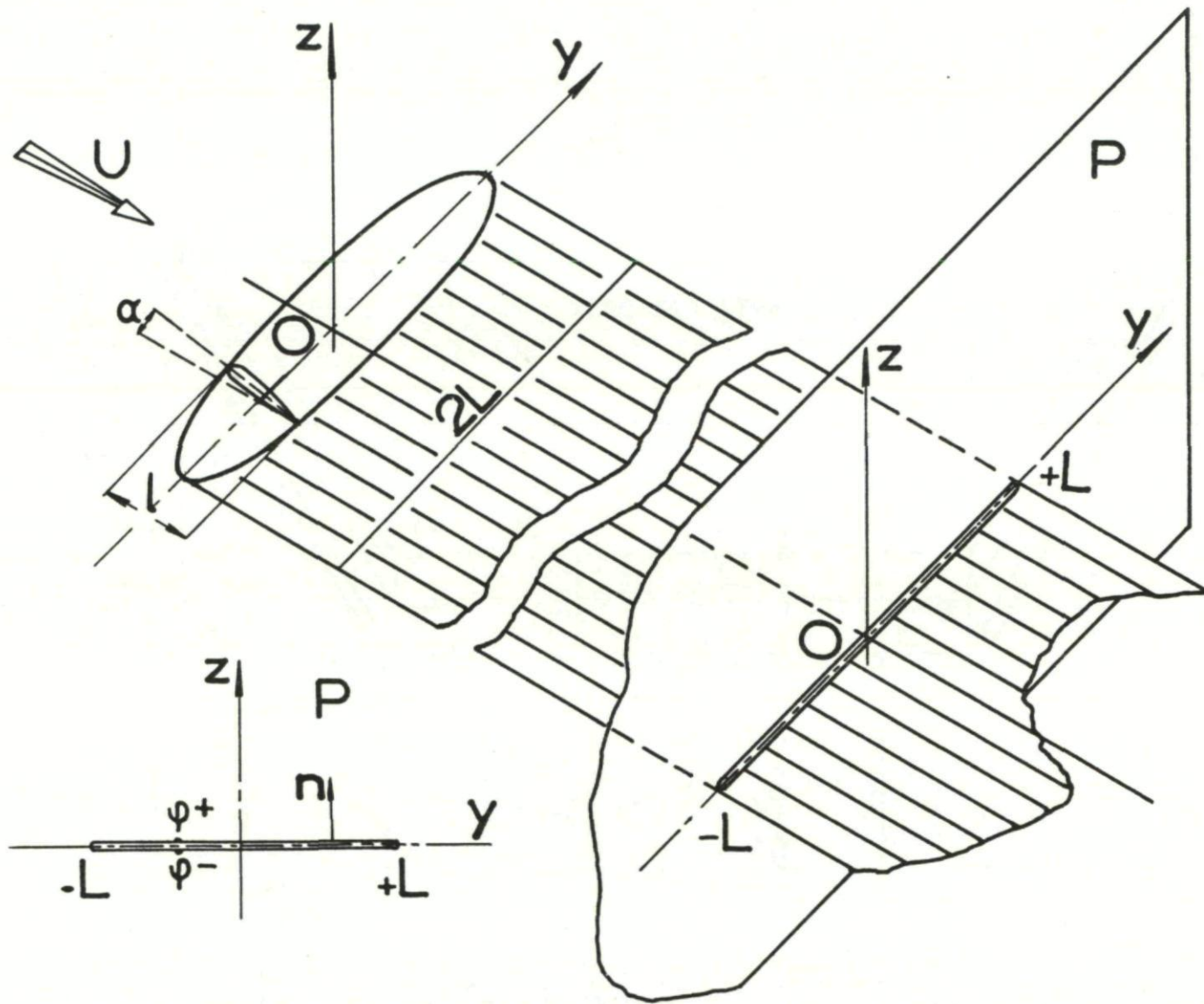
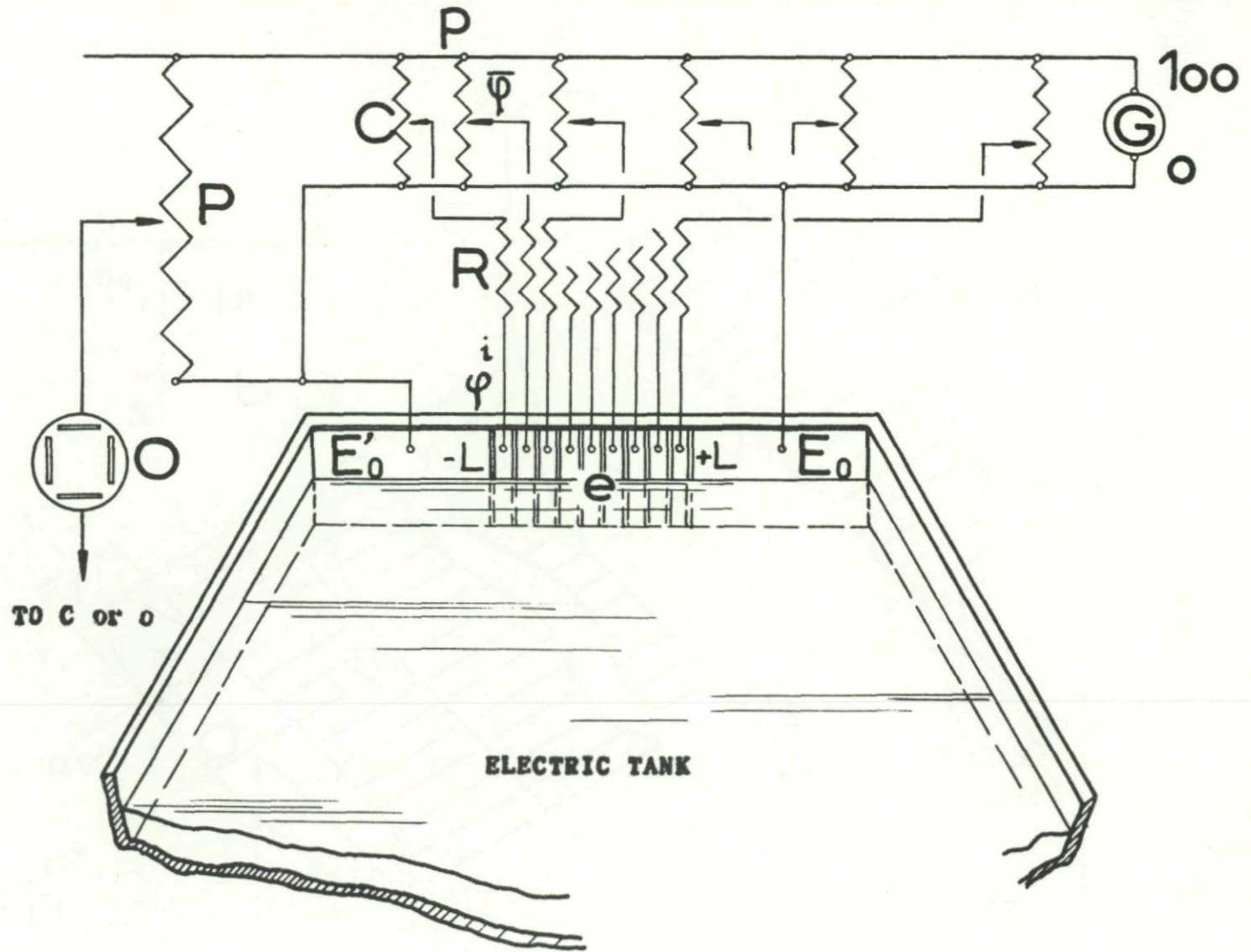


Fig. VIII-1. Determination of the gradient in the three-dimensional tank.



141

Fig. IX-1. Sketch of the vortex system behind a wing. Trefftz plane.



142

Fig. IX-2. Set-up for the "wing calculator."

143

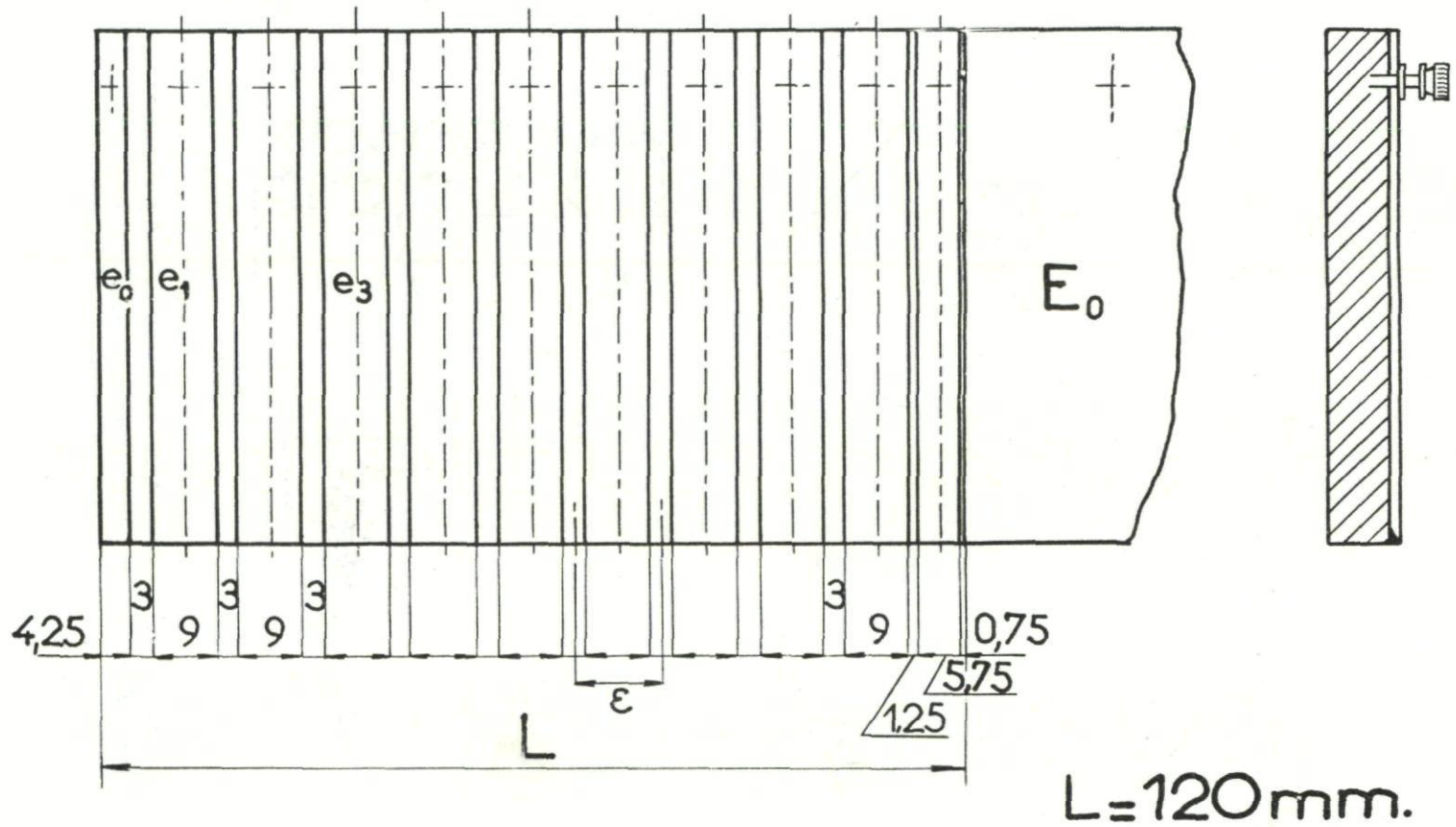


Fig. IX-3. Electrode carrying-plate for the wing calculator.

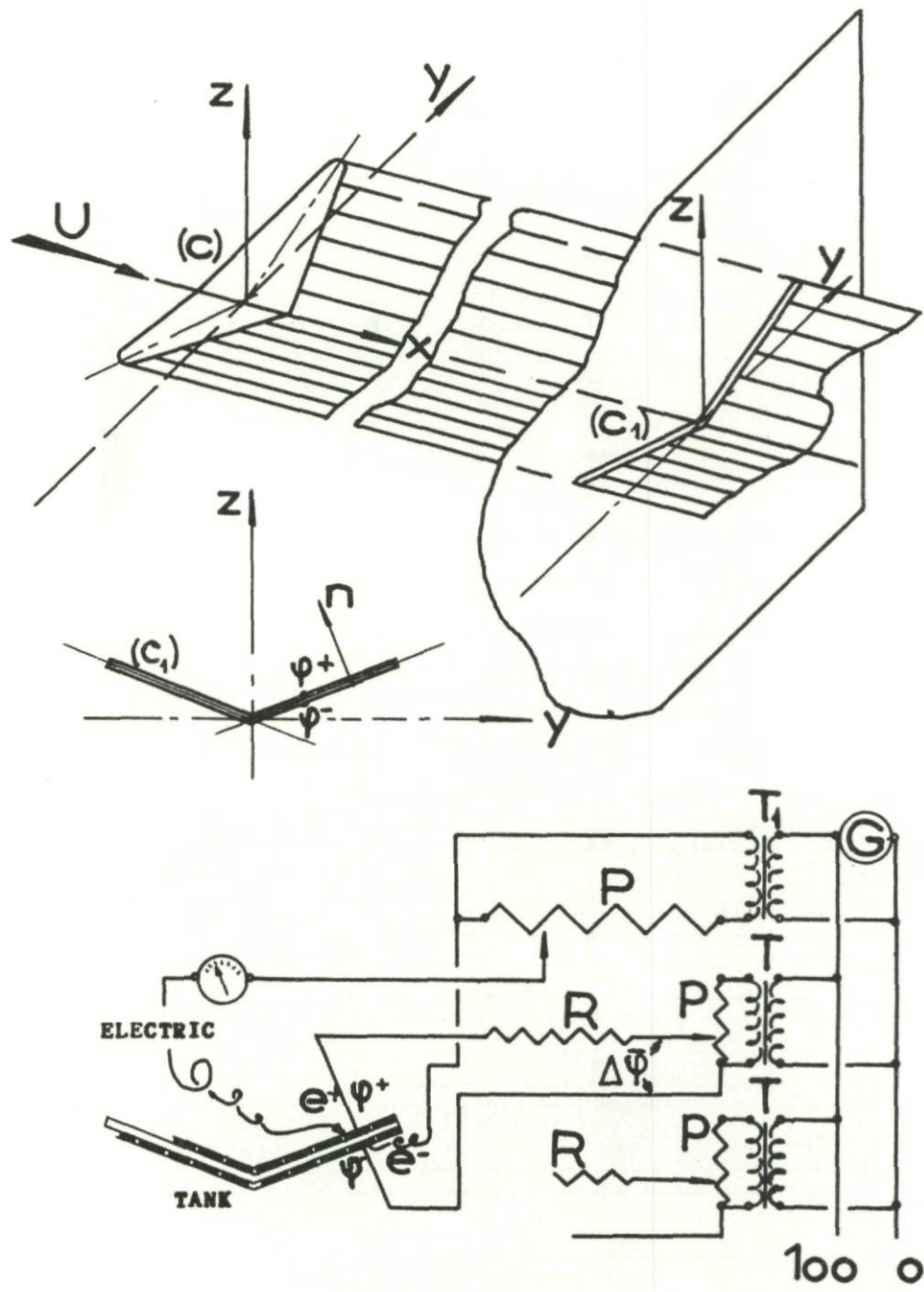


Fig. IX-4. Study of a nonstraight lifting line. Analog model of the lifting line. Electrical set-up for feeding the tank at the electrode holding strip.

145

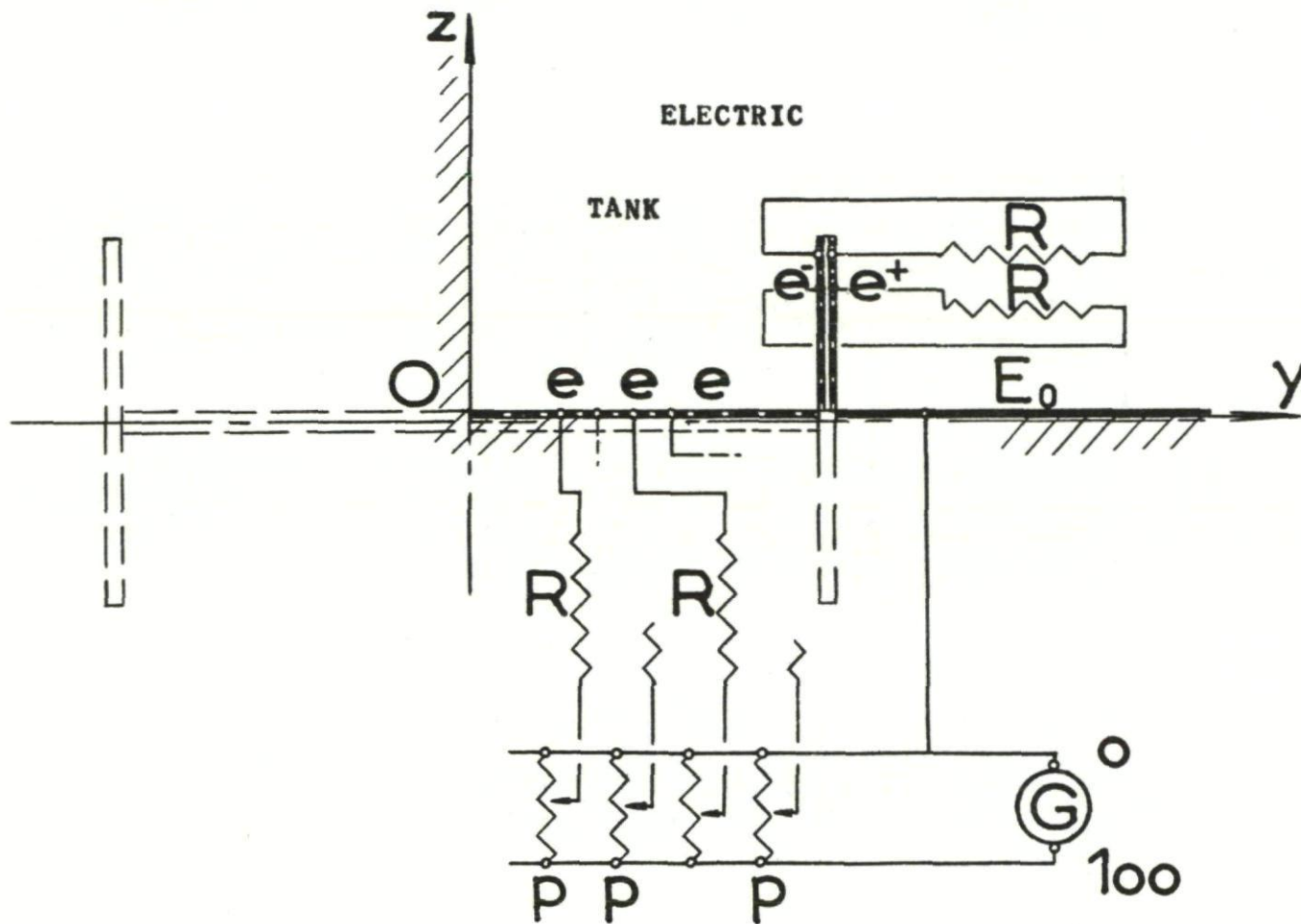


Fig. IX-5. Electrical model for studying a wing carrying vertical end plates.

146

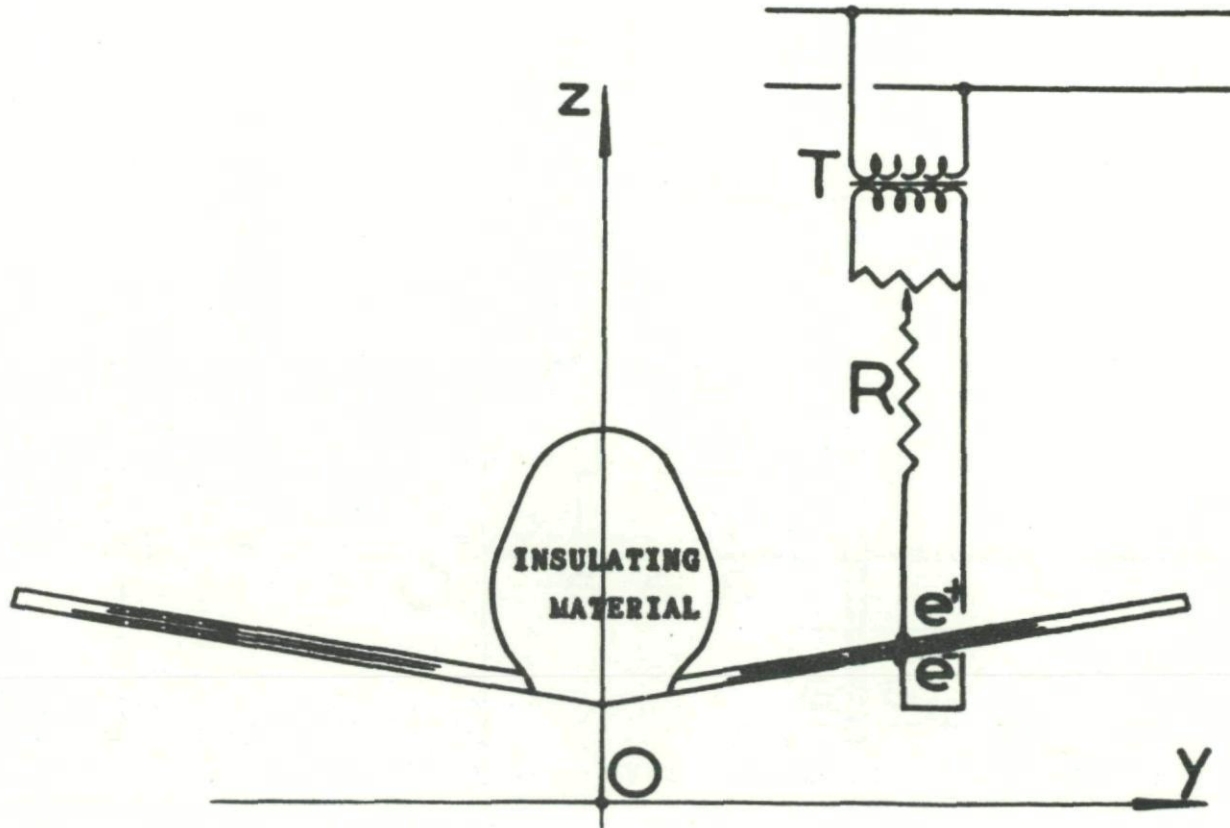


Fig. IX-6. Analog model of a lifting line in the presence of a fuselage.

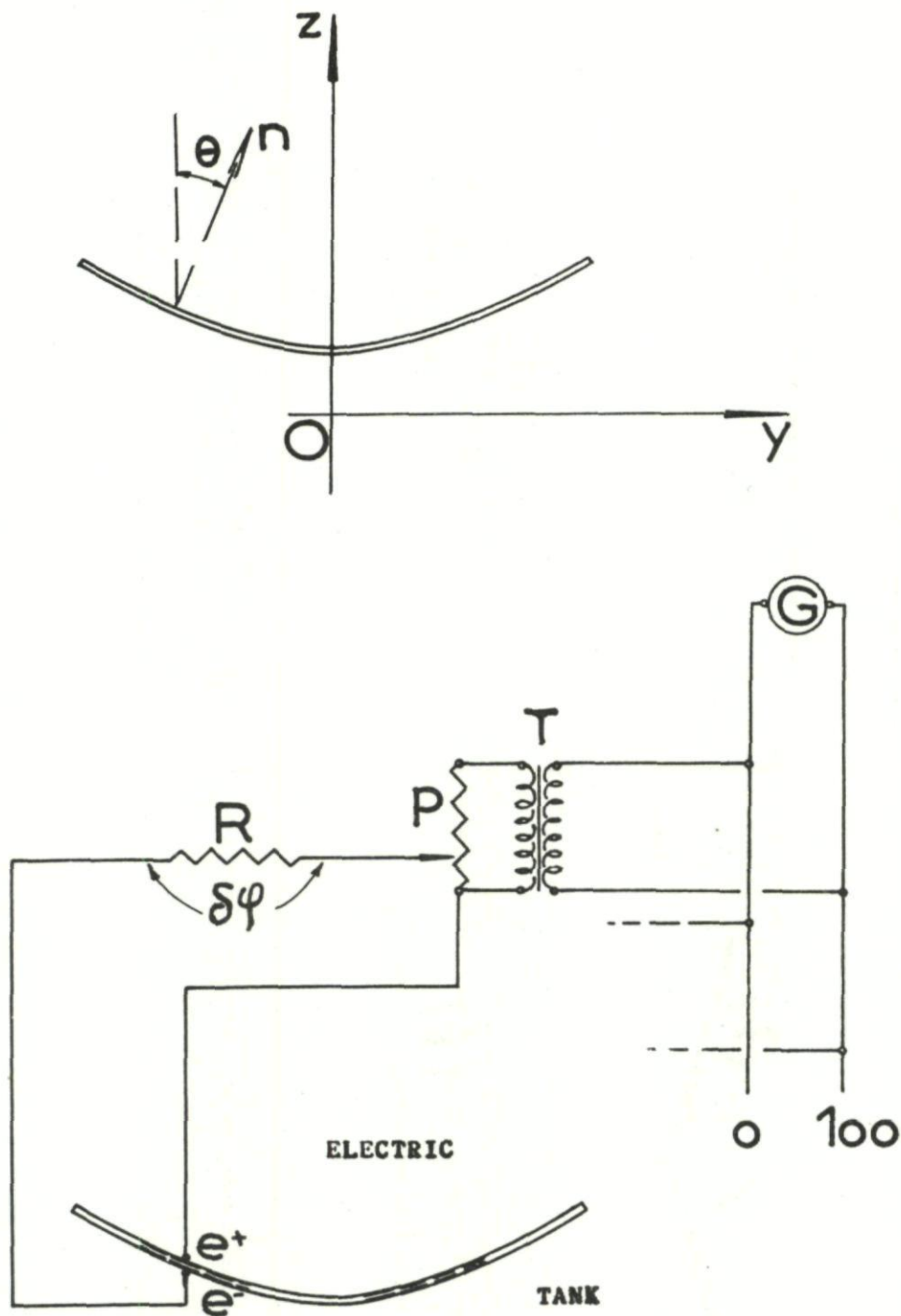


Fig. IX-7. Electrical model for determining optimum characteristics of a lifting line (1st analog set-up).

148

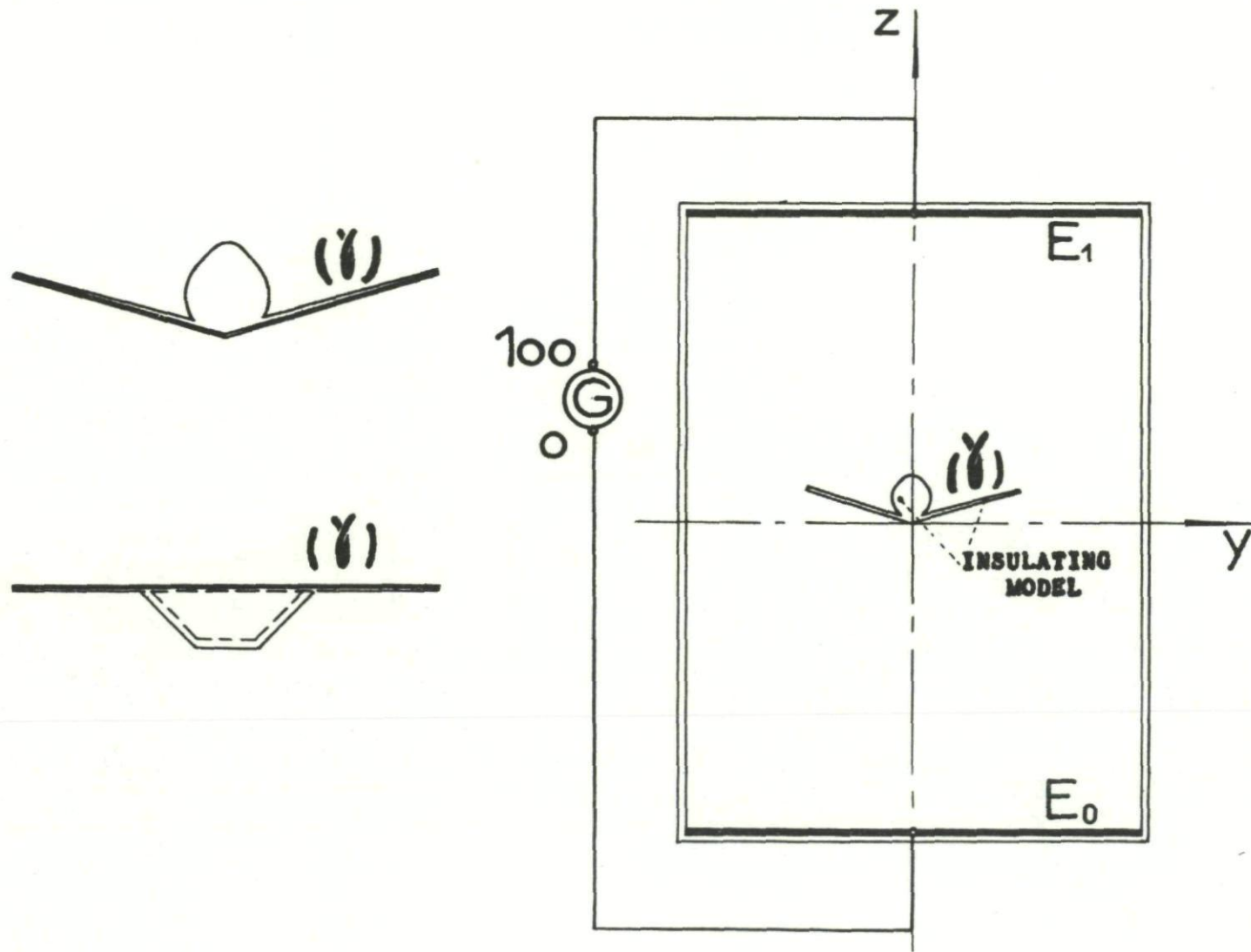
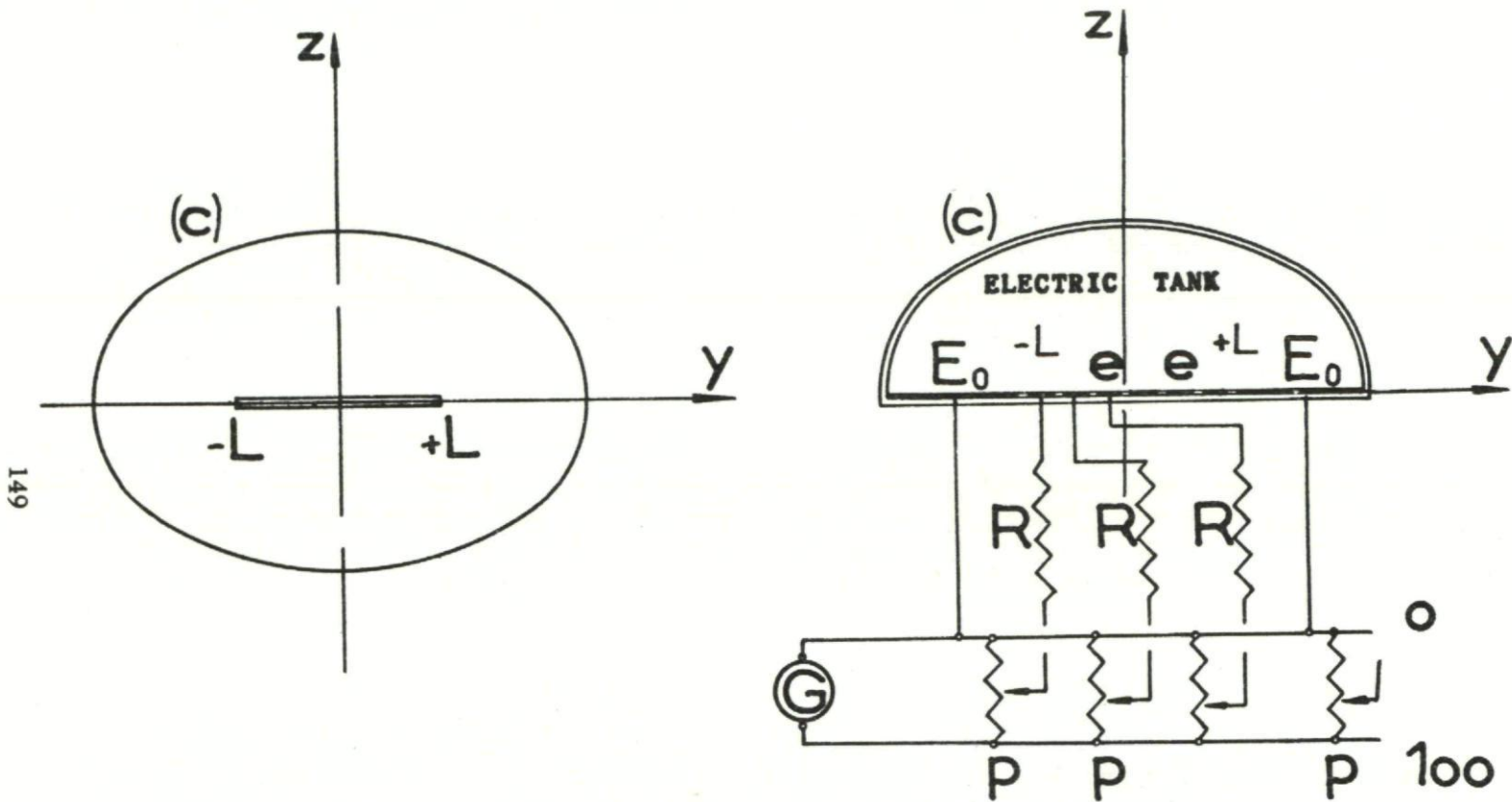


Fig. IX-8. Electrical model for determining optimum characteristics of a lifting line (2nd analog set-up).



149

Fig. IX-9. Analog representation of a wing placed in a wind tunnel test section.

150

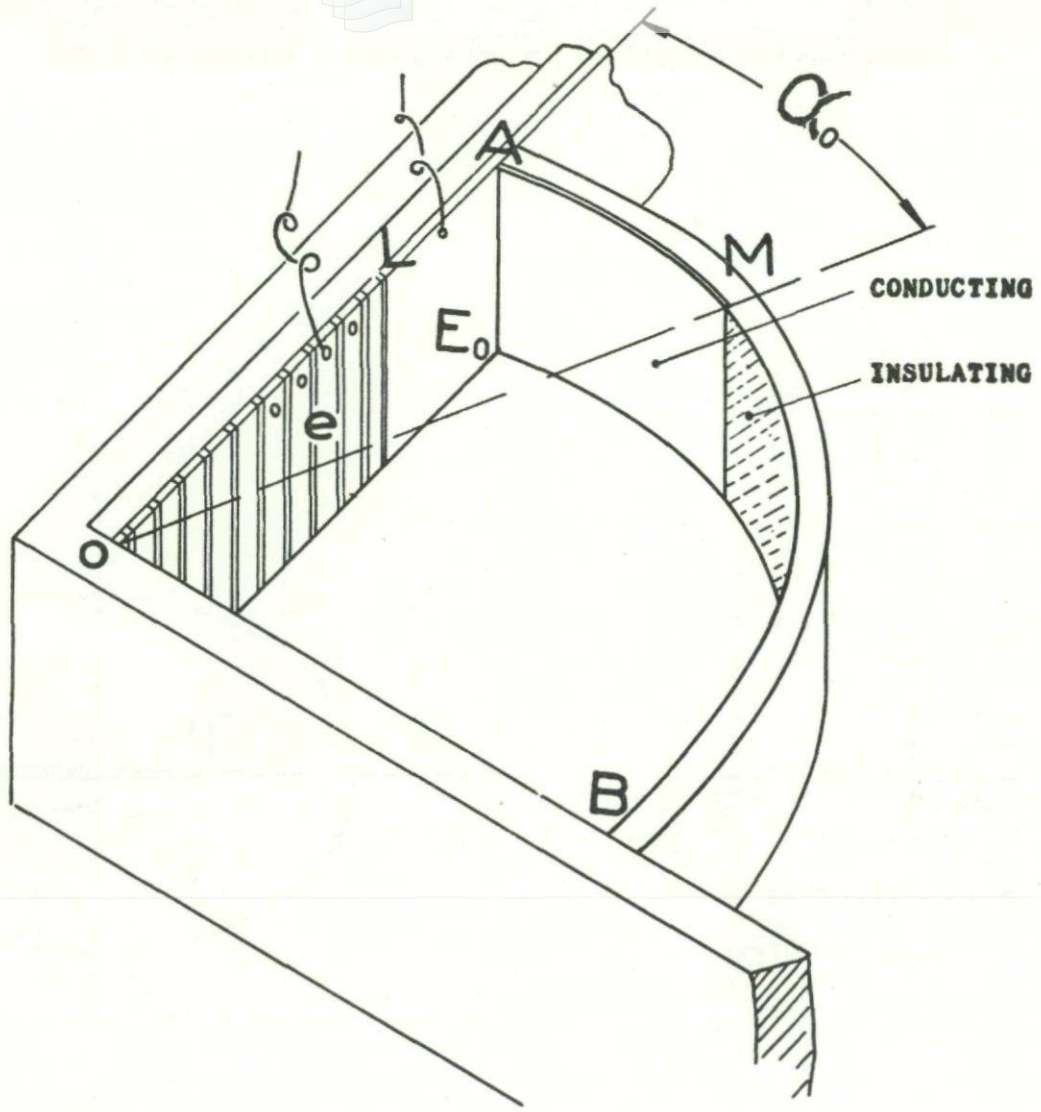


Fig. IX-10. Analog model of a wing in a wind tunnel test section having mixed (open and closed) boundaries. Search for a condition of zero wall correction.

151

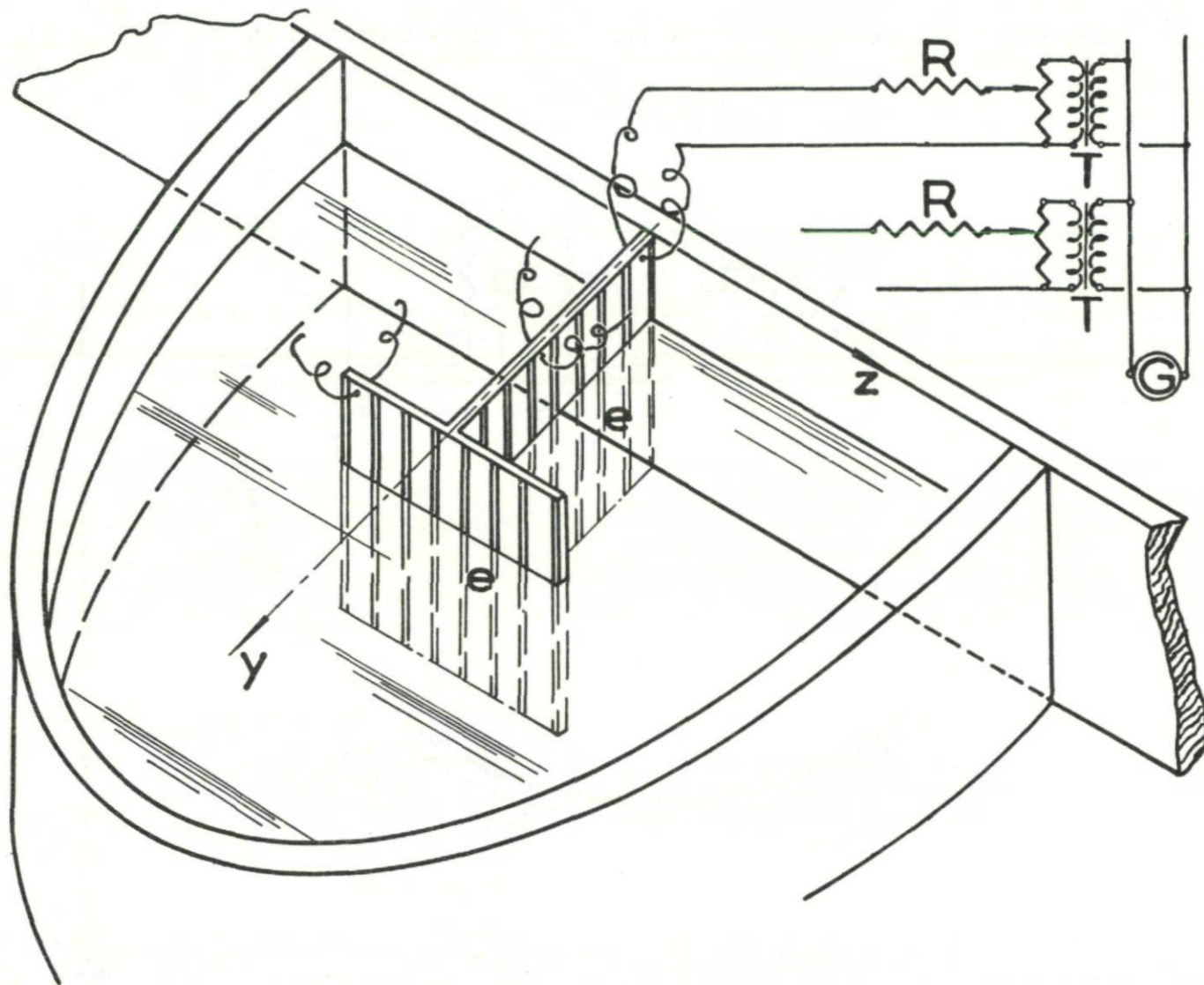
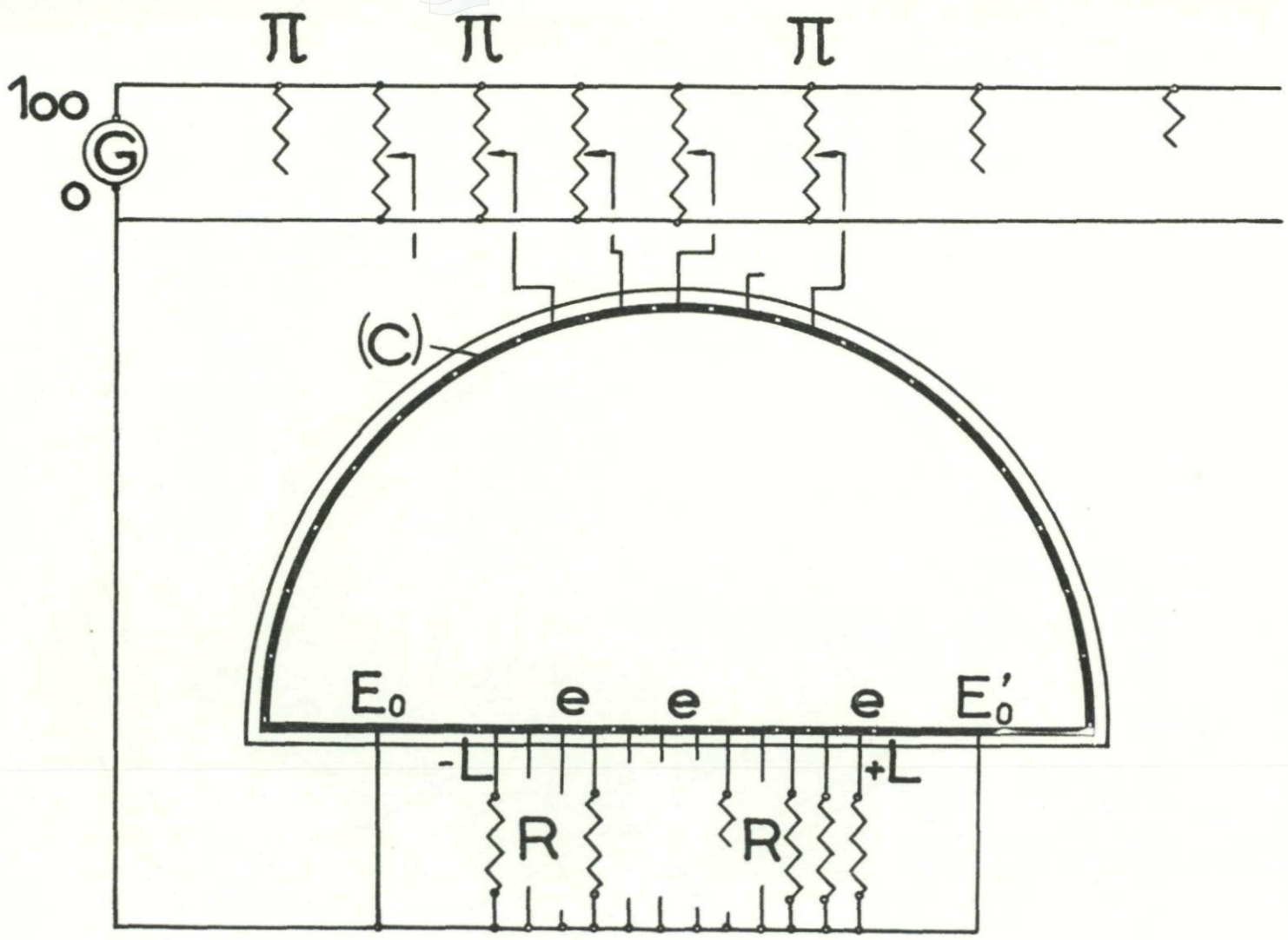


Fig. IX-11. Analog model of a wing with end plates in a closed test section.



152

Fig. IX-12. Electric tank determination of the perturbation field about a wing in the presence of wind tunnel walls.

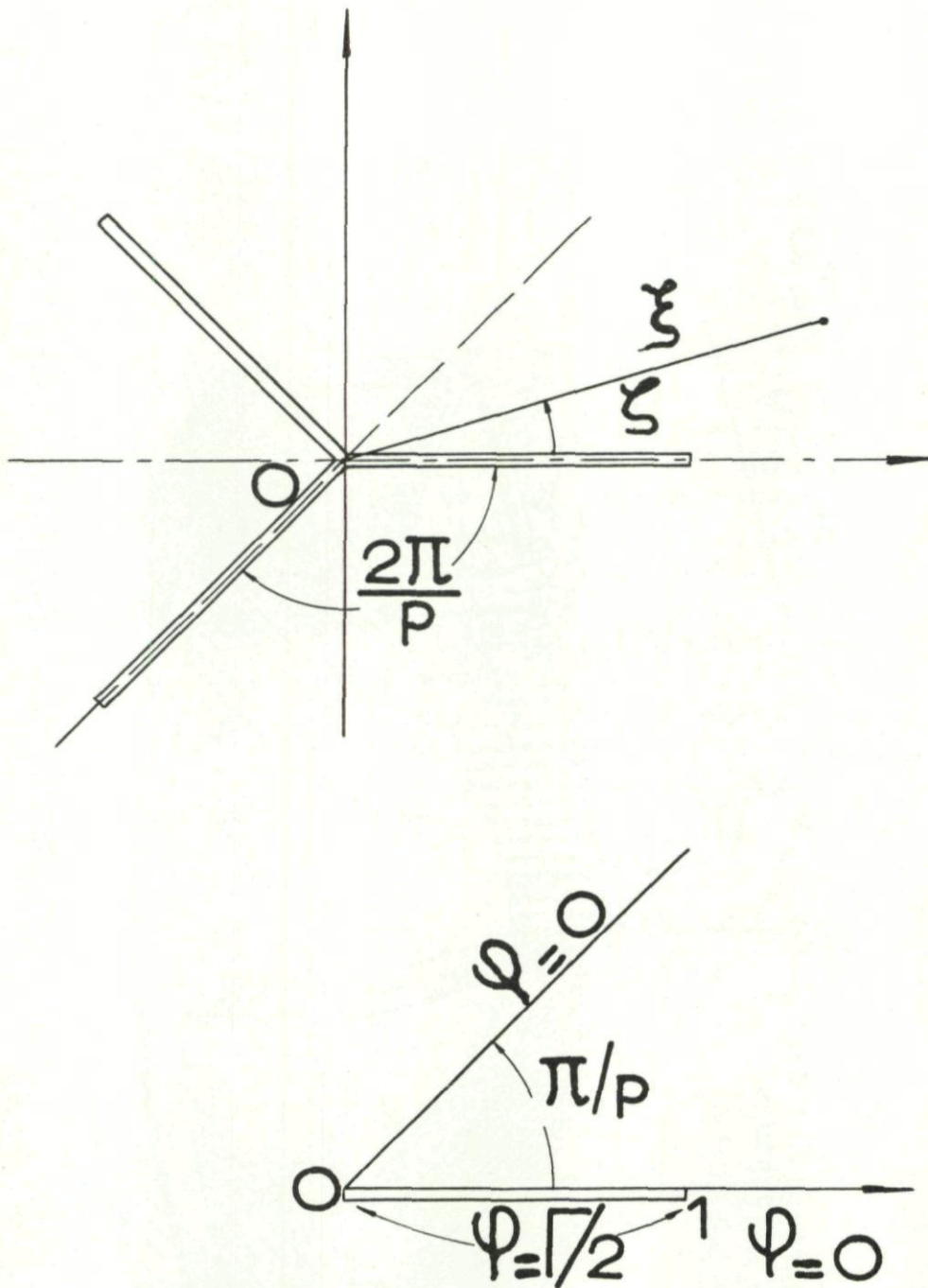


Fig. X-1. Image in the  $(\xi, \zeta)$  plane of the helicoidal vortex sheets for a three-bladed propeller. Domain of definition of the induced velocity potential.

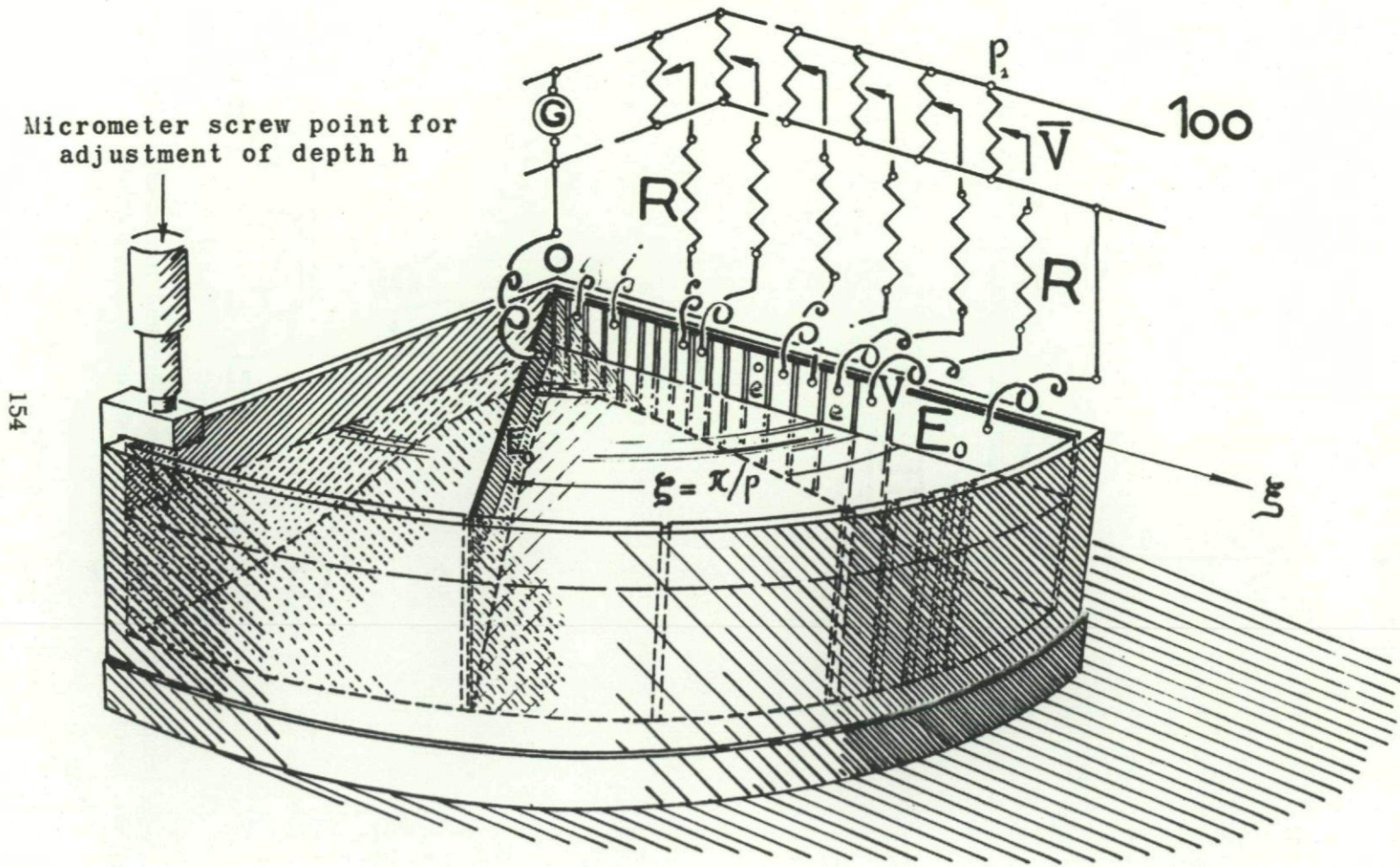


Fig. X-2. Sketch of the set-up for the "propeller calculator."

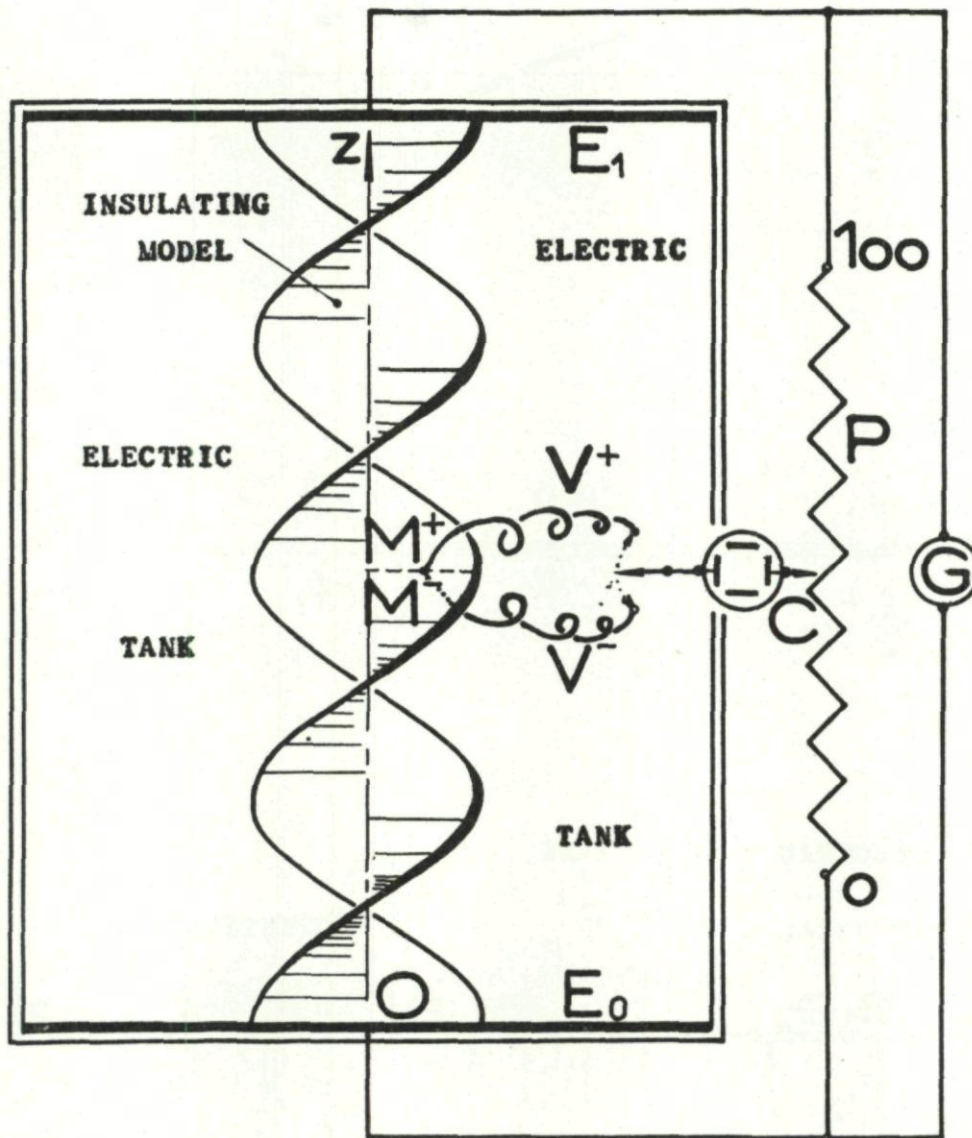


Fig. X-3. Electrical model for studying optimum operation of a propeller.

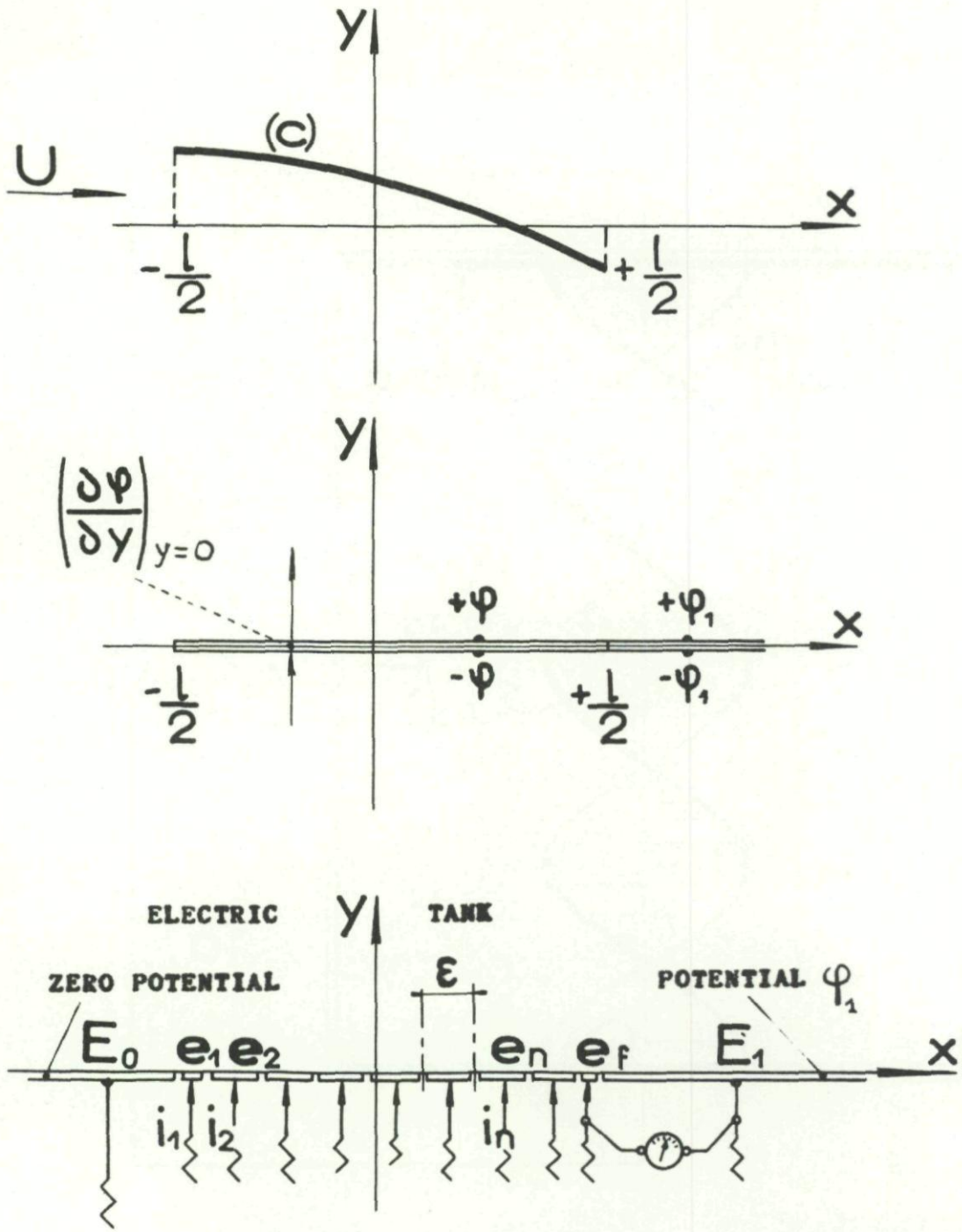


Fig. XI-1. Rheoelectric study of a thin airfoil. Determination of the perturbation potential in the electric tank.

157

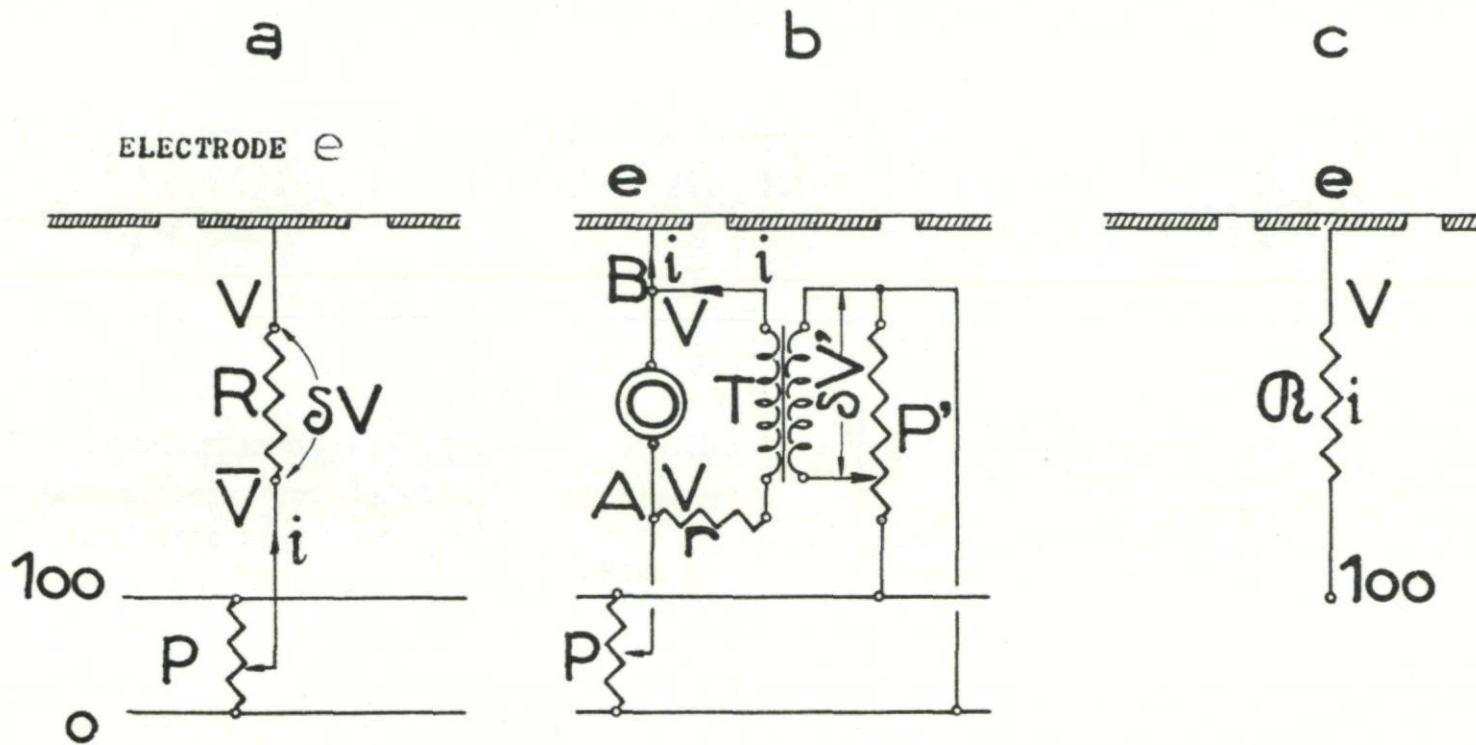
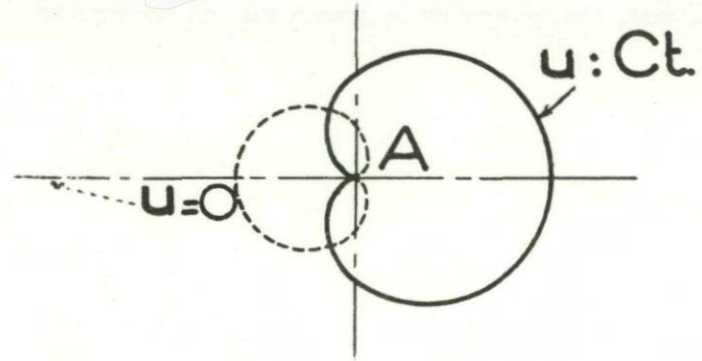
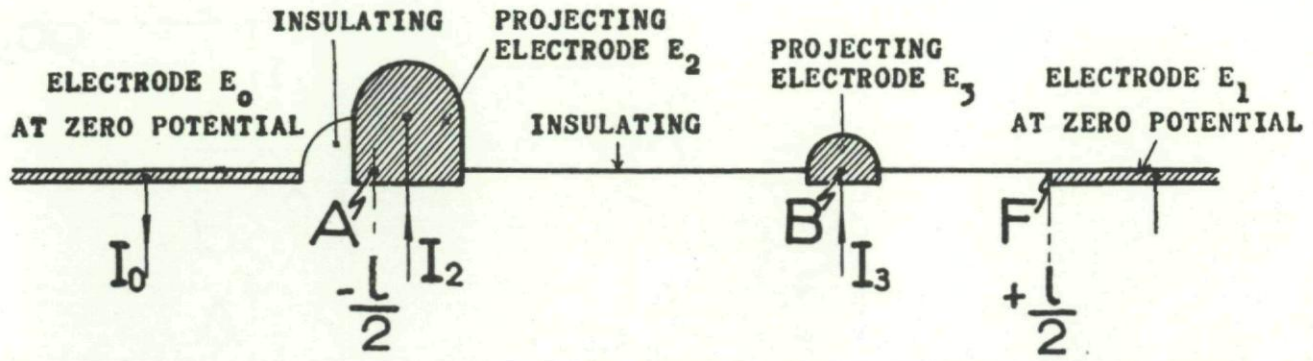


Fig. XI-2. Various set-ups for establishing a Neumann-type condition in the electric tank.



158



$$I_0 + I_2 = \sigma h U \alpha.$$

$$I_0 + I_2 + I_3 = \sigma h U (\alpha + \beta).$$

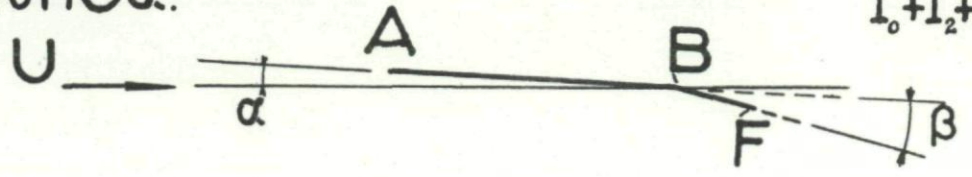


Fig. XI-3. Arrangement of electrodes along the tank side for the analog representation of the acceleration potential.

159

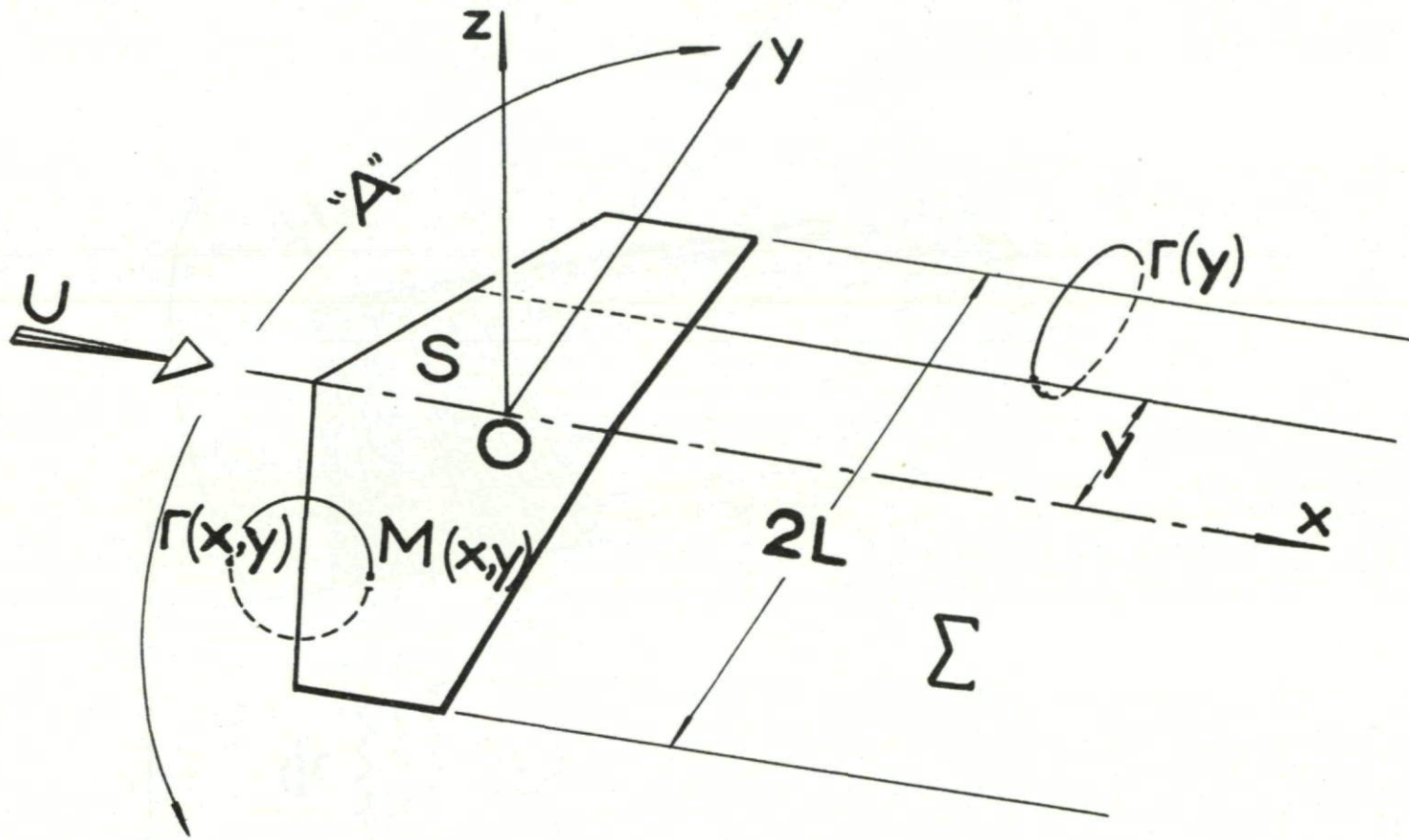


Fig. XI-4. Lifting surface. Coordinates system and regions of the plane  $z = 0$ .

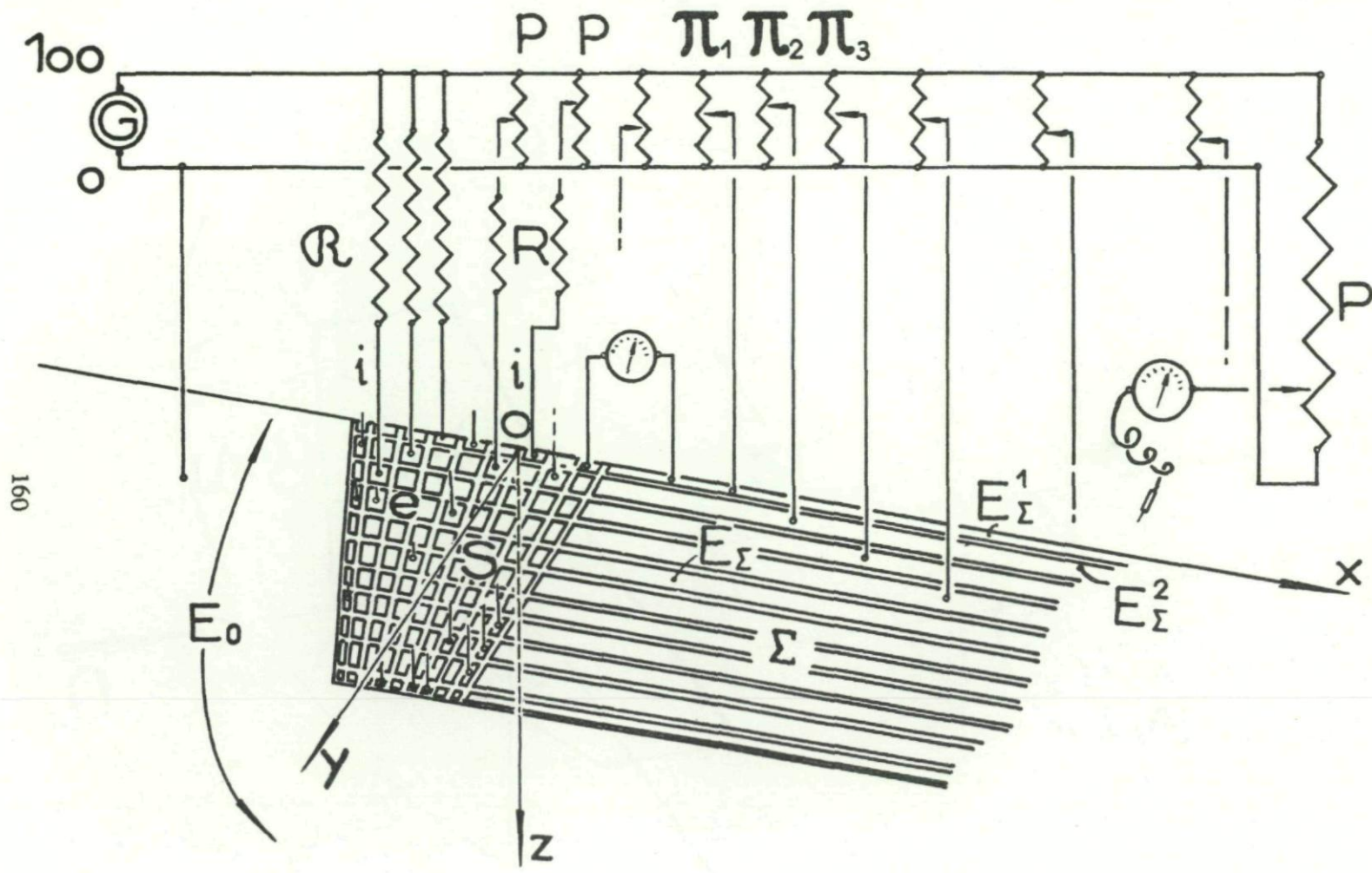


Fig. XI-5. Sketch of the set-up for the "lifting surface calculator." Electric circuits for wing and wake electrodes.

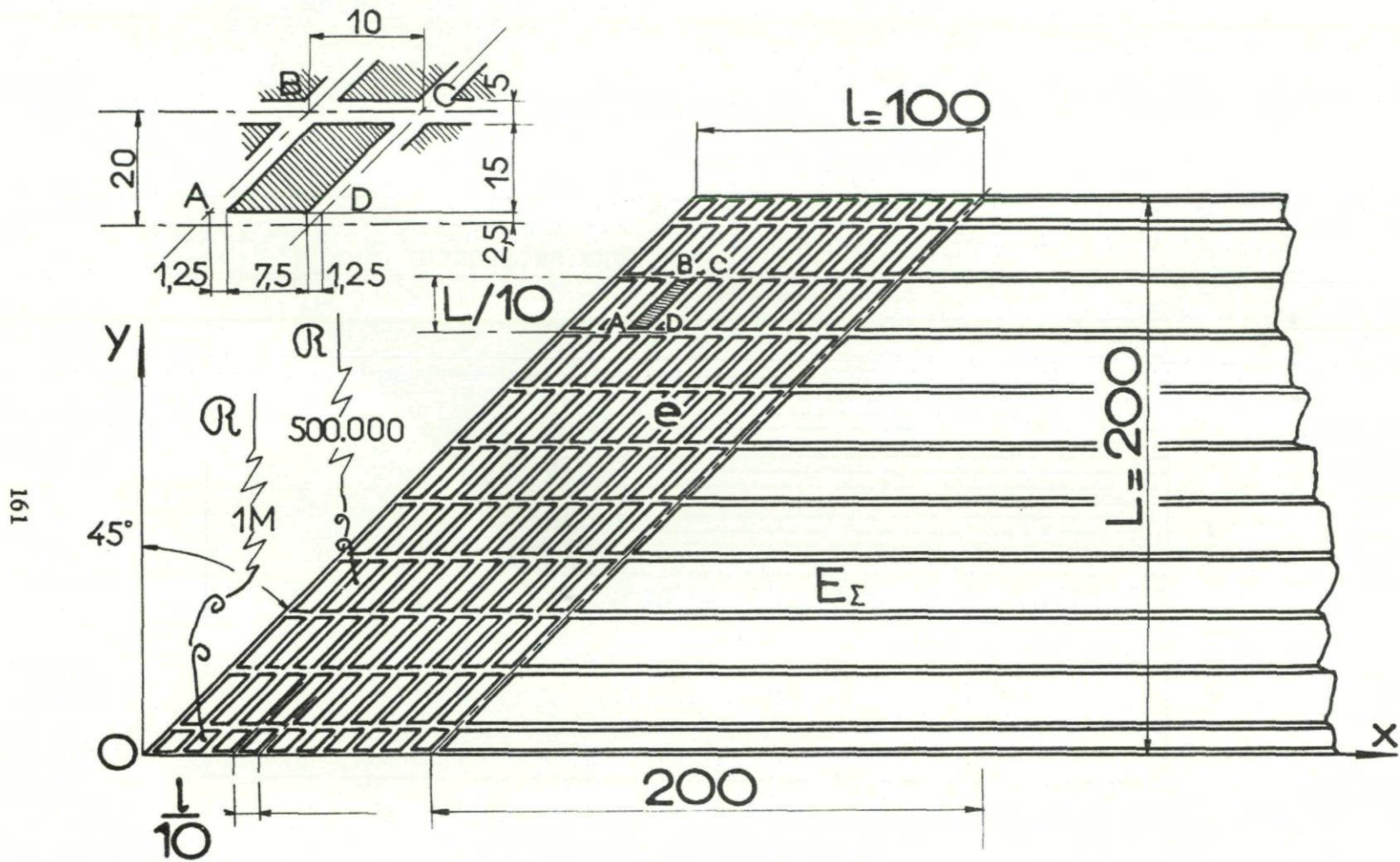


Fig. XI-6. Electrical model for a swept wing of constant chord. Electrode arrangement.

162

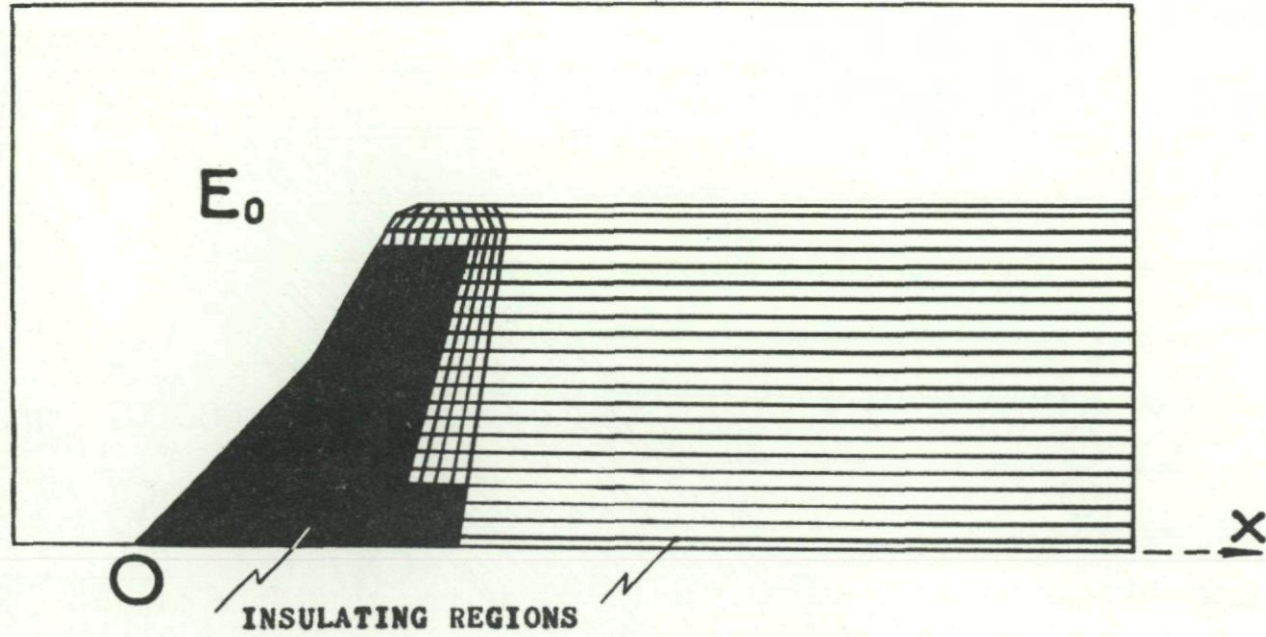


Fig. XI-7. Example of an electrode-carrying panel for the special study of flaps and ailerons.

163

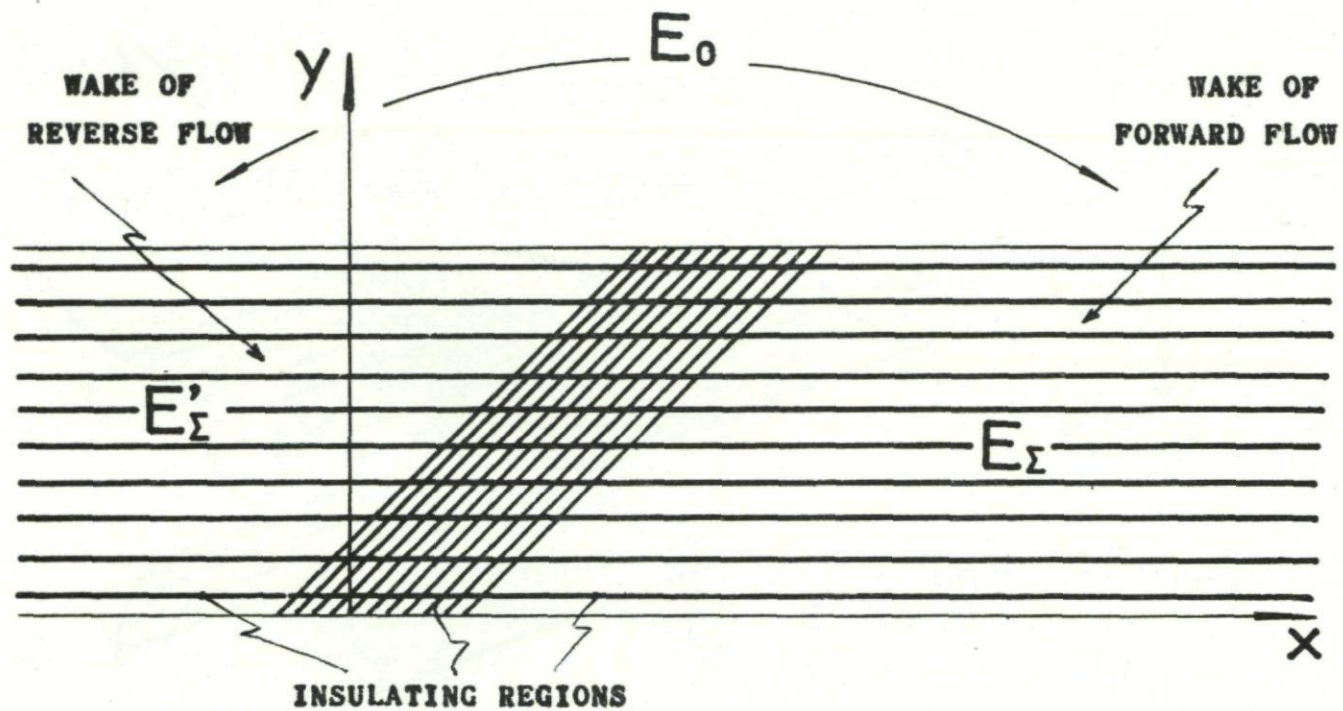


Fig. XI-8. Wing model for the study of forward and reverse flows.

164

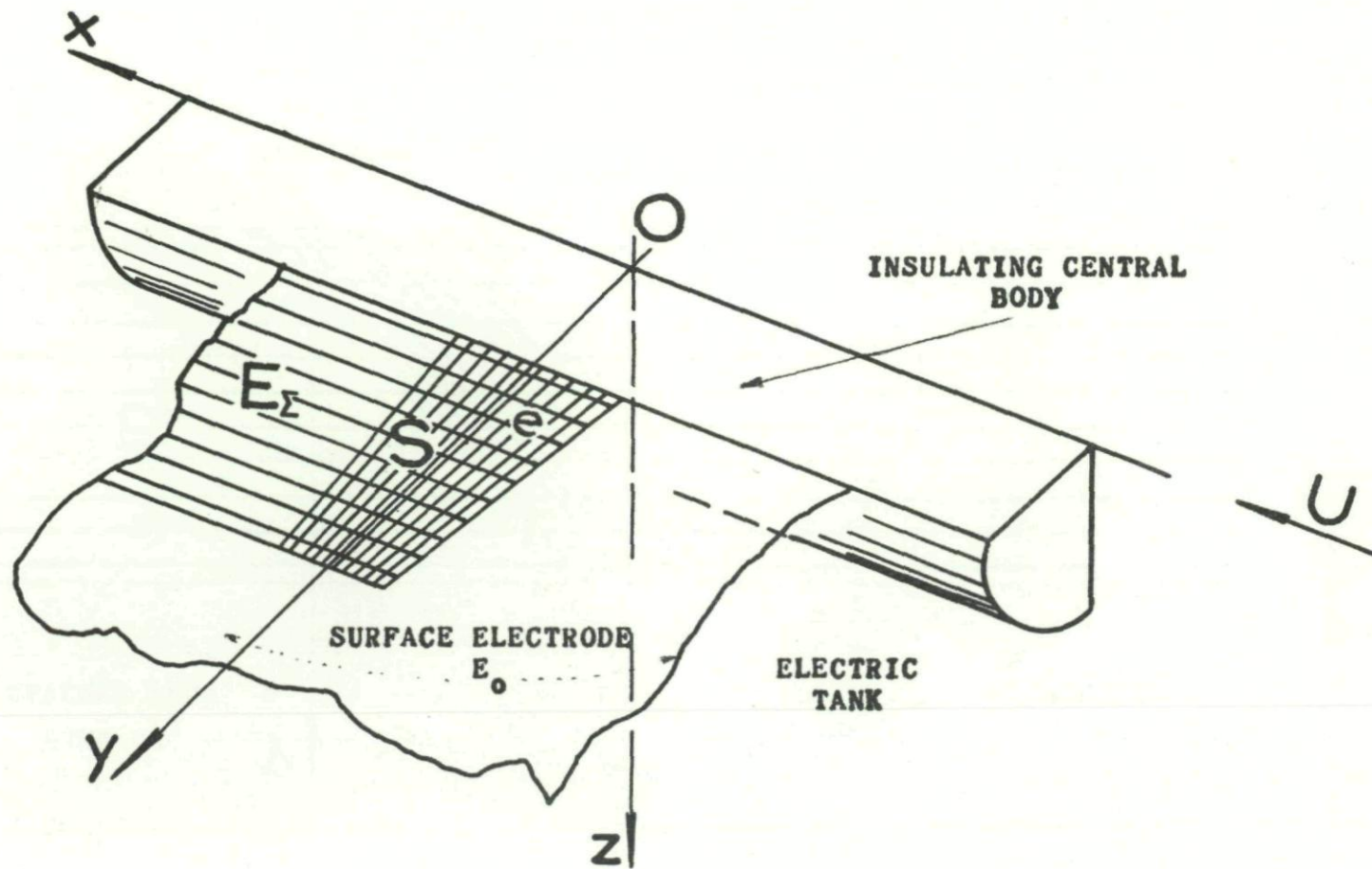
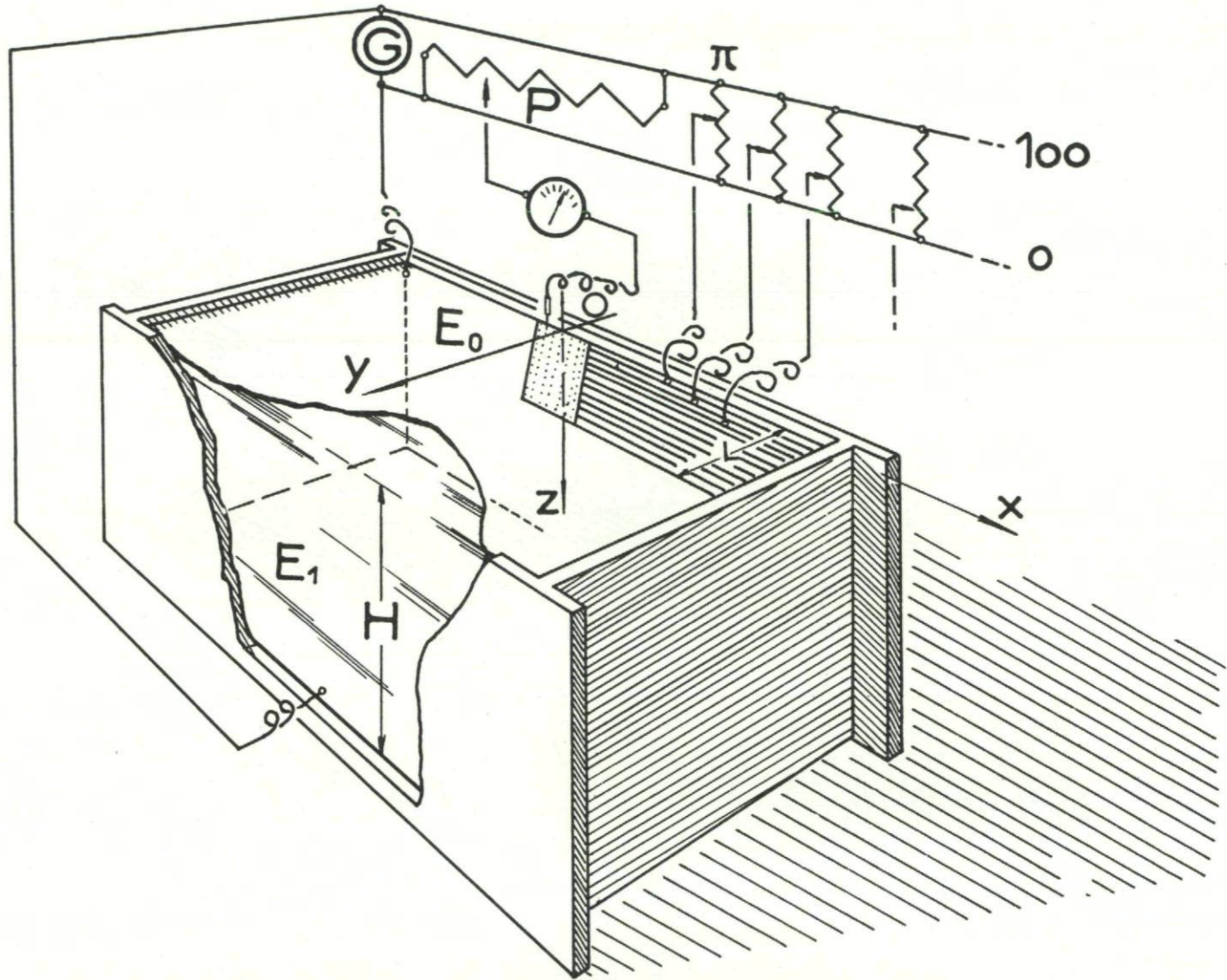


Fig. XI-9. Wing model in the presence of a central body.



165

Fig. XI-10. Analog study of plane wings.

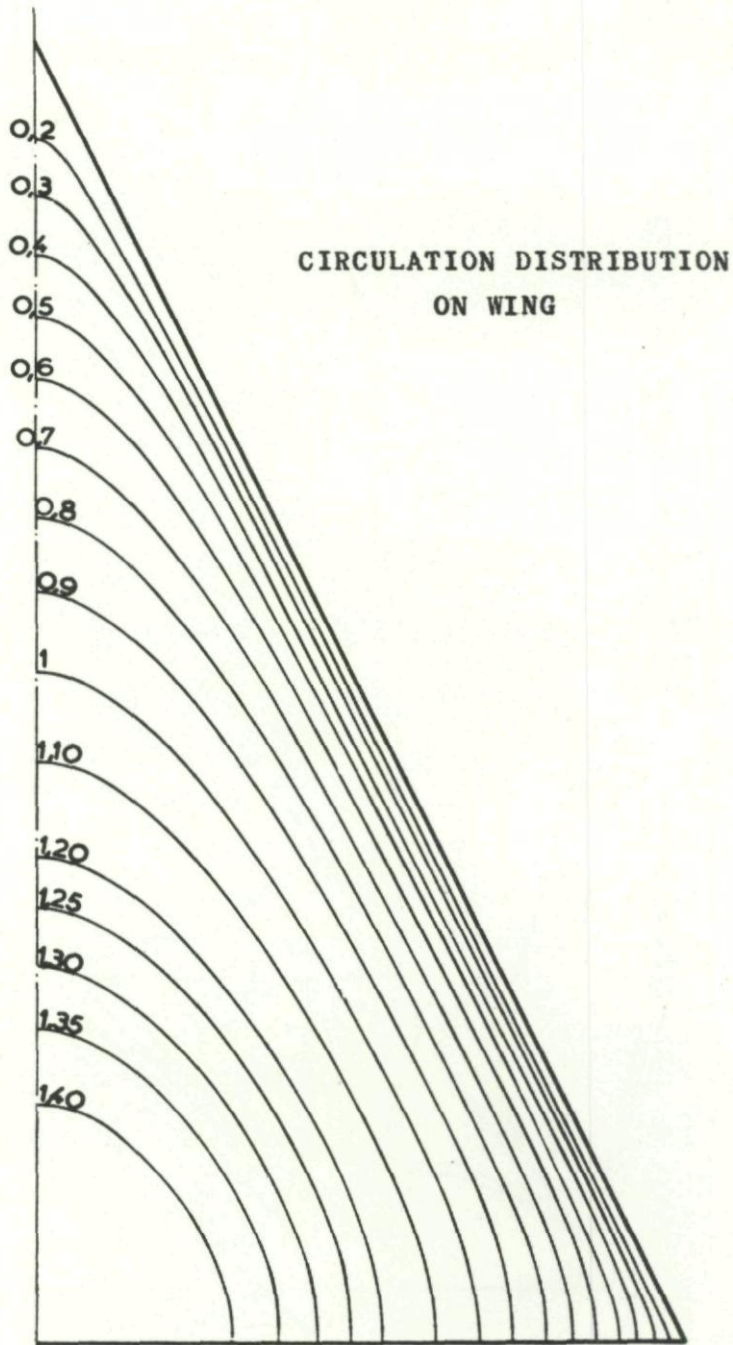


Fig. XI-11. Bound vortex lines on a delta wing.

167

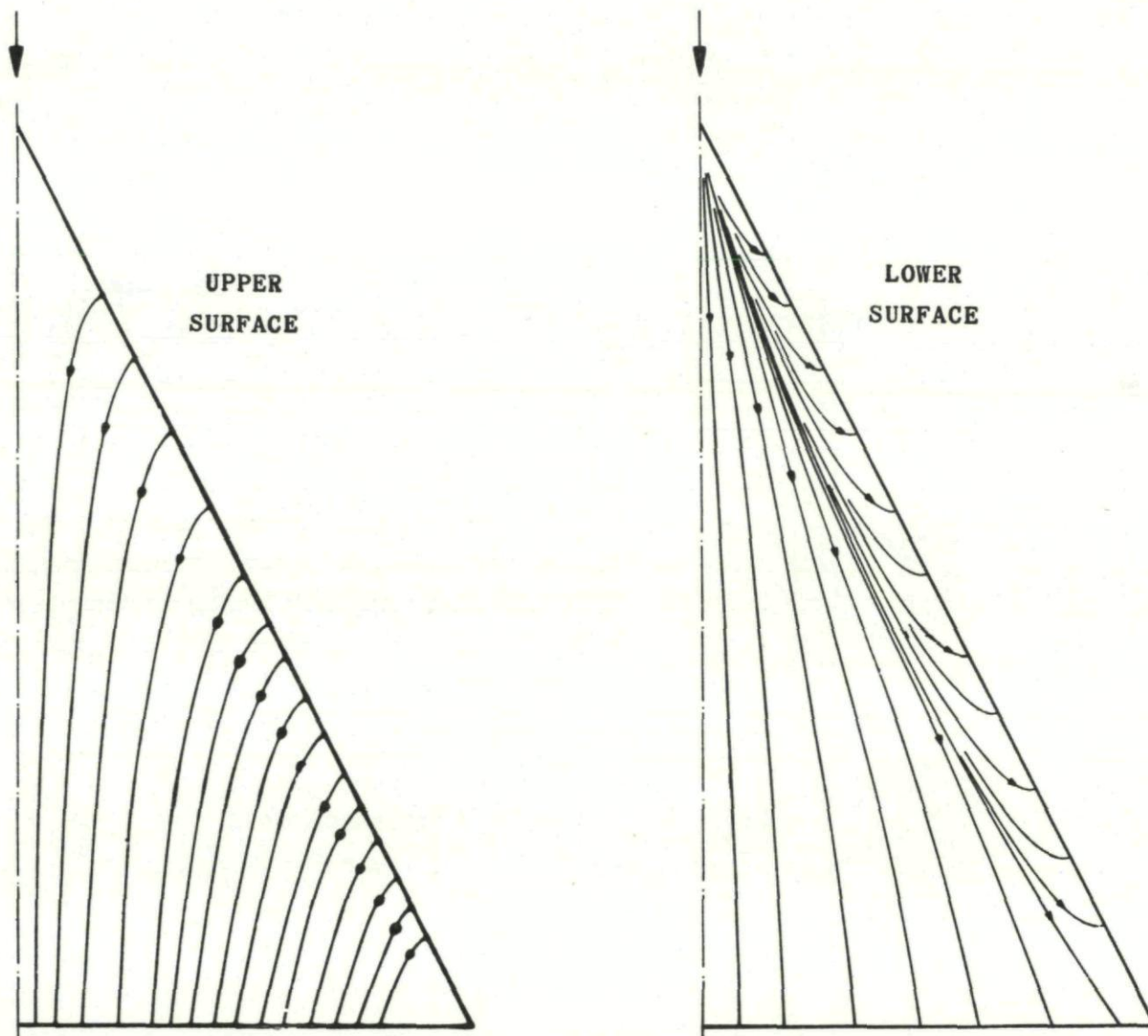


Fig. XI-12. Surface streamlines on a delta wing ( $18^\circ$  angle of attack).

168

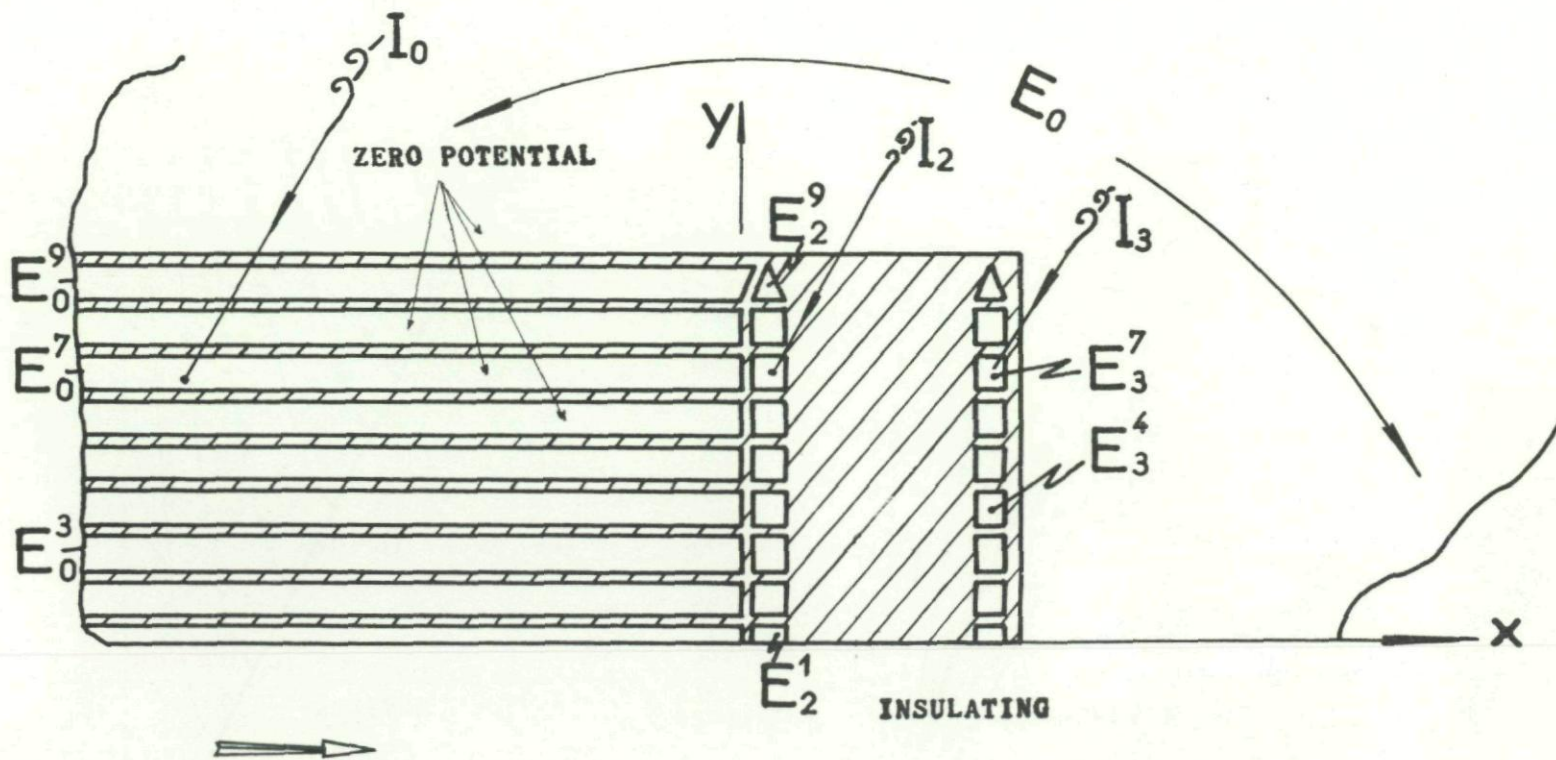


Fig. XI-13. Electrode arrangement over a lifting surface in the analogy for the acceleration potential (case of a plane wing with flap).

169

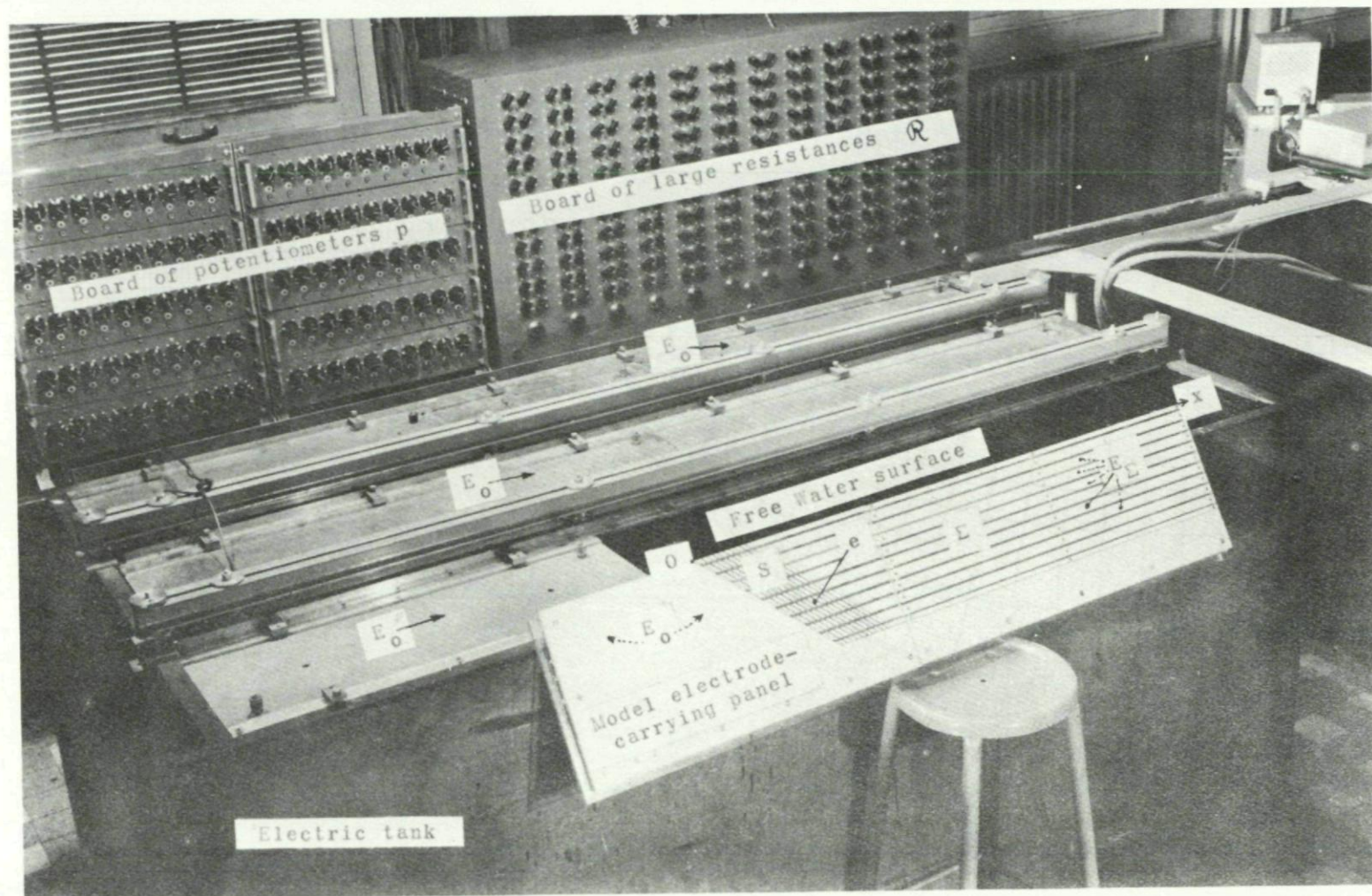


Fig. XI-14. View of a "lifting surface calculator."

170

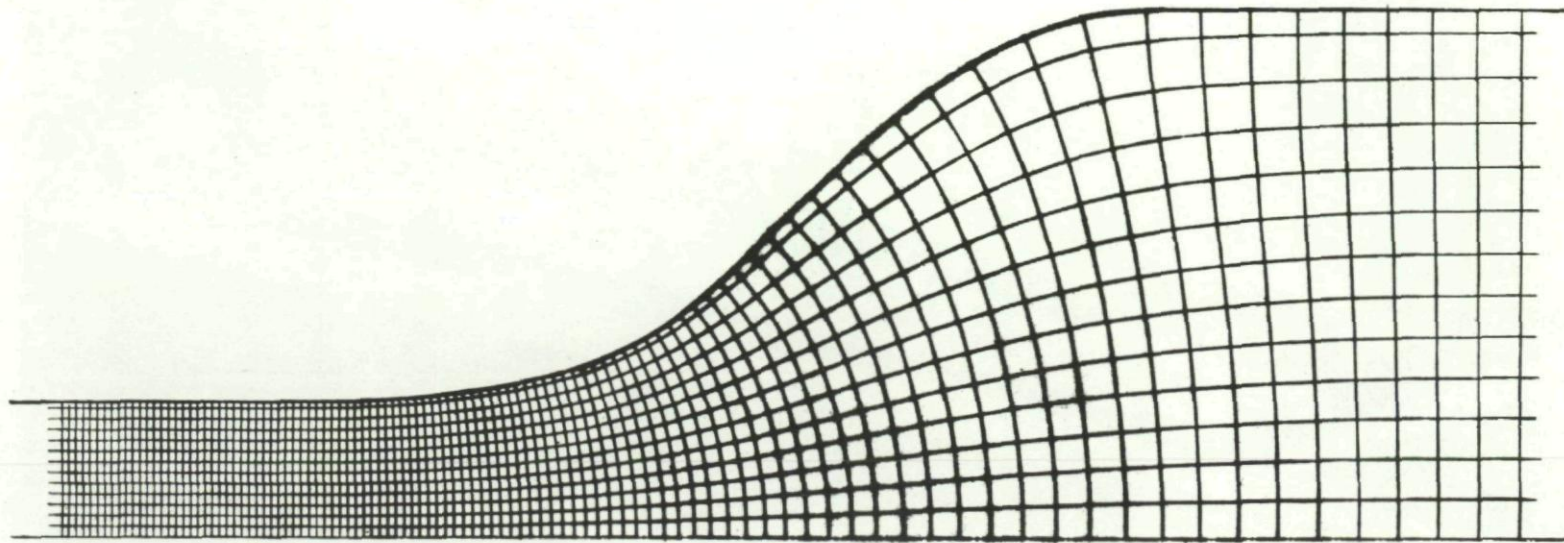


Fig. XII-1. Compressible flow in a plane convergent channel.

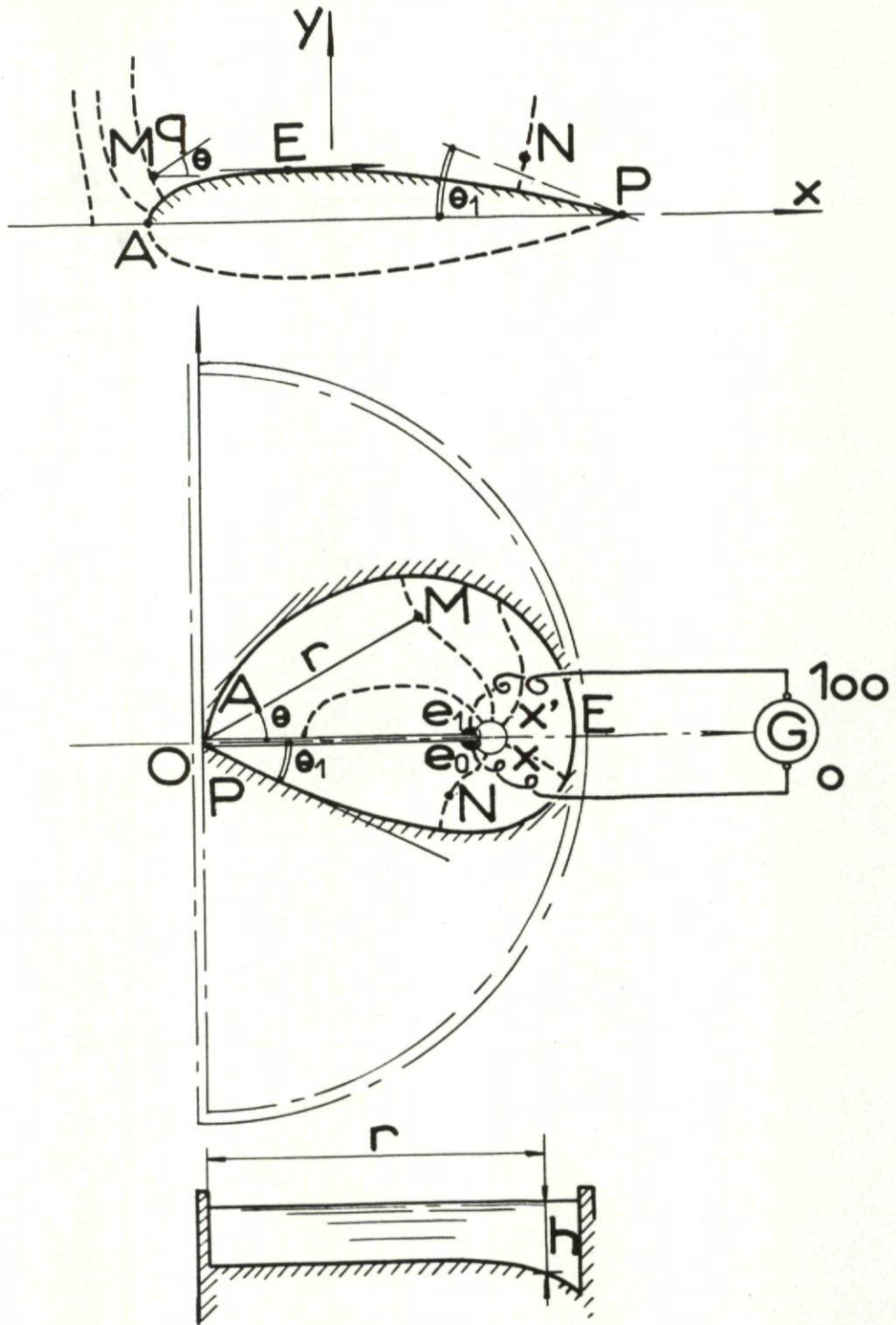


Fig. XII-2. Hodograph tank.

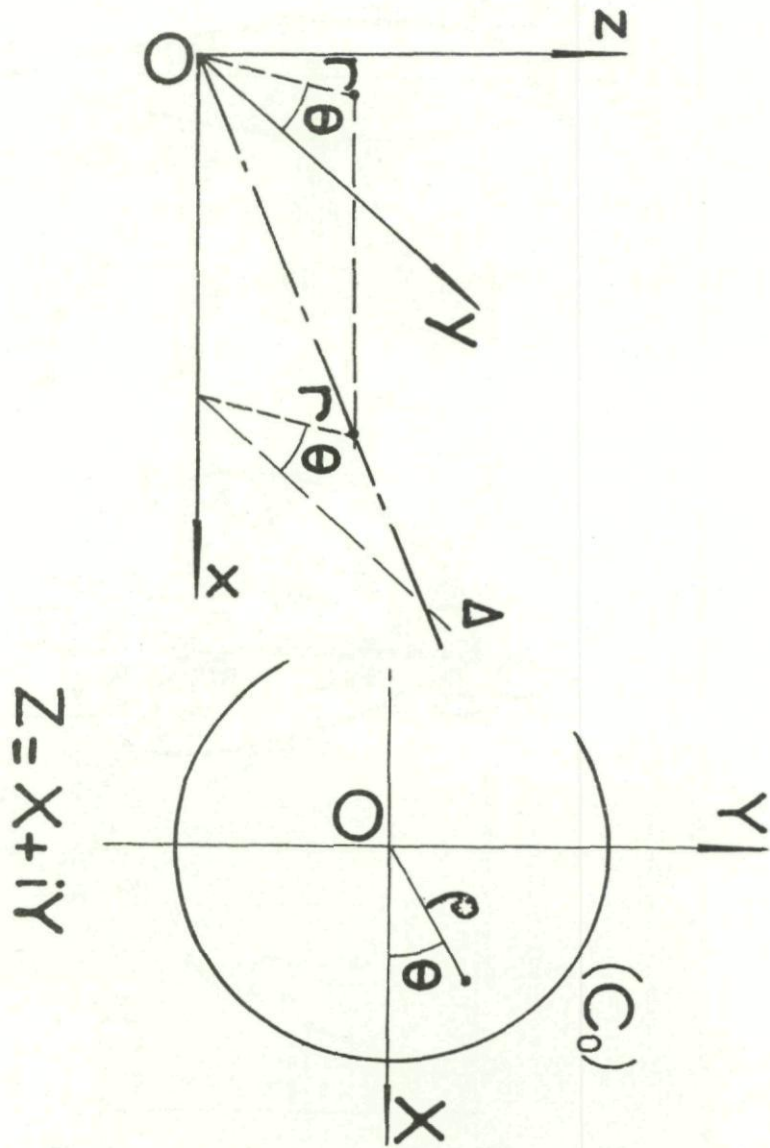


Fig. XII-3. Conical flow.

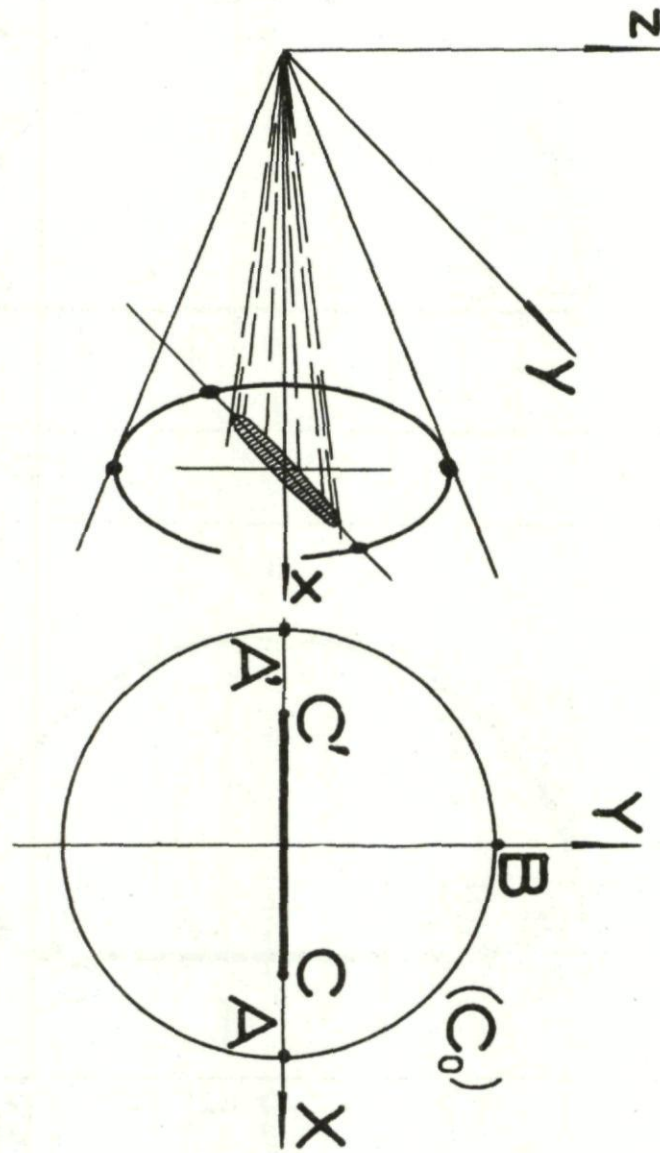
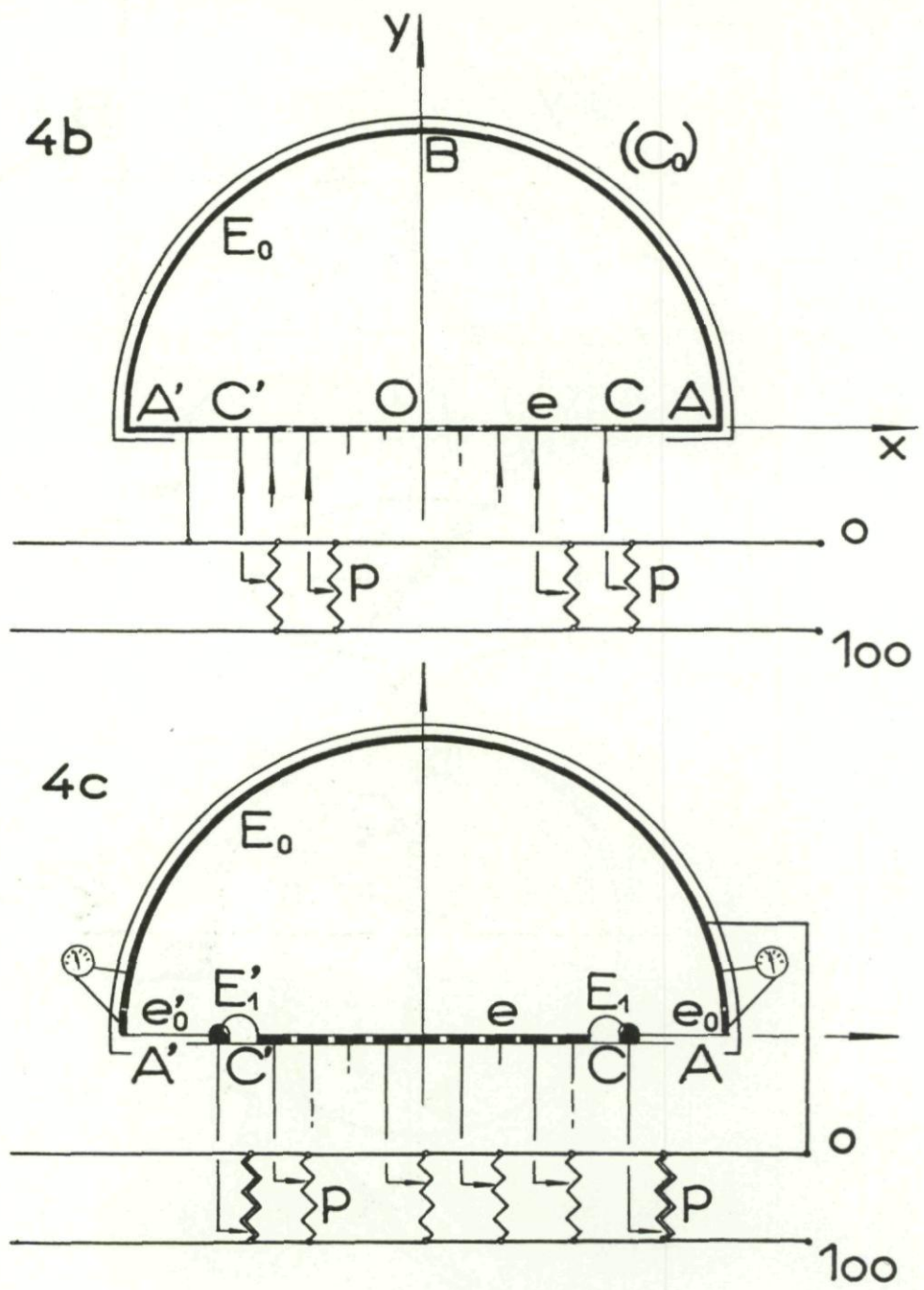


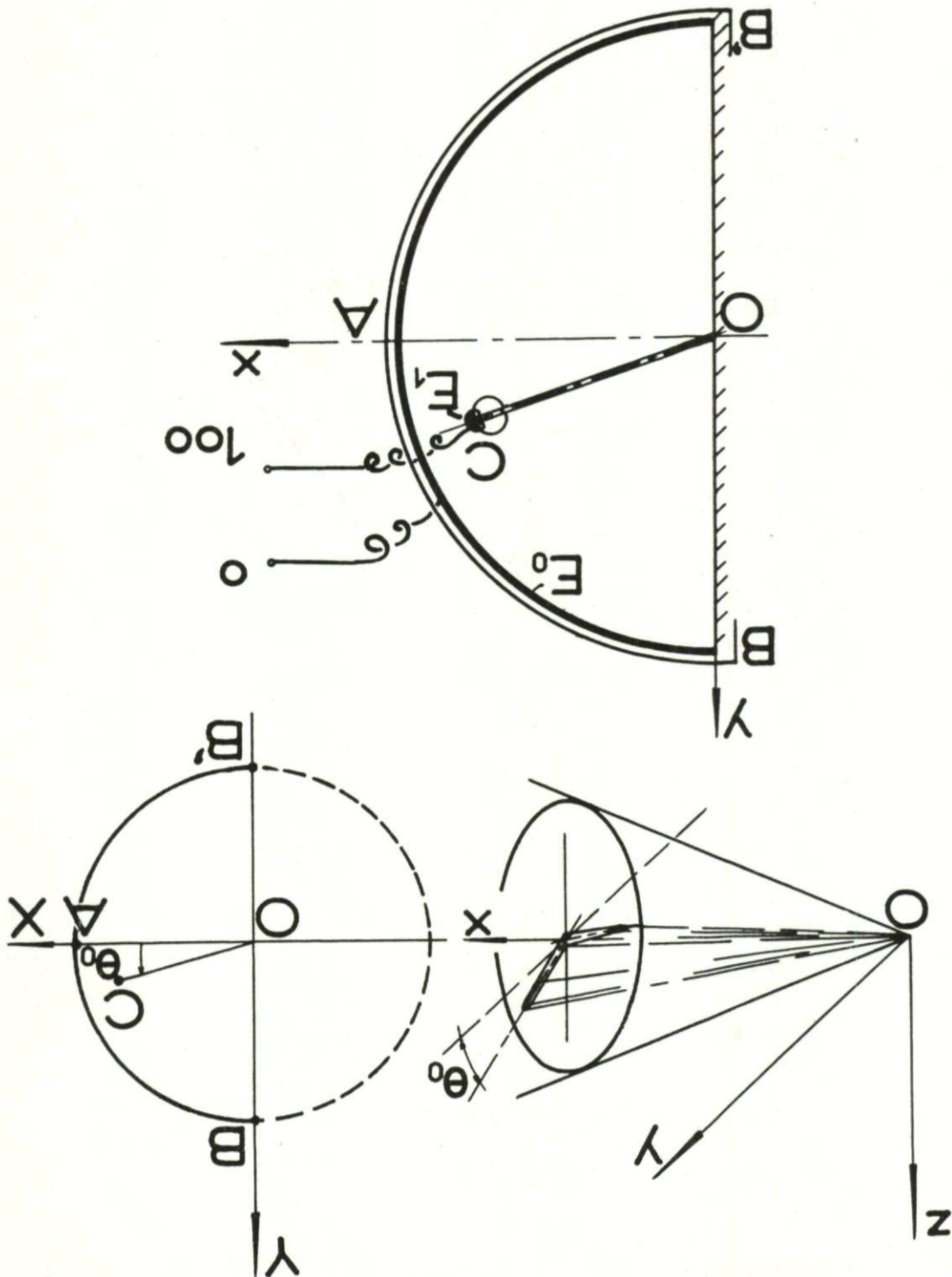
Fig. XII-4(a). Flattened cone in supersonic flow.

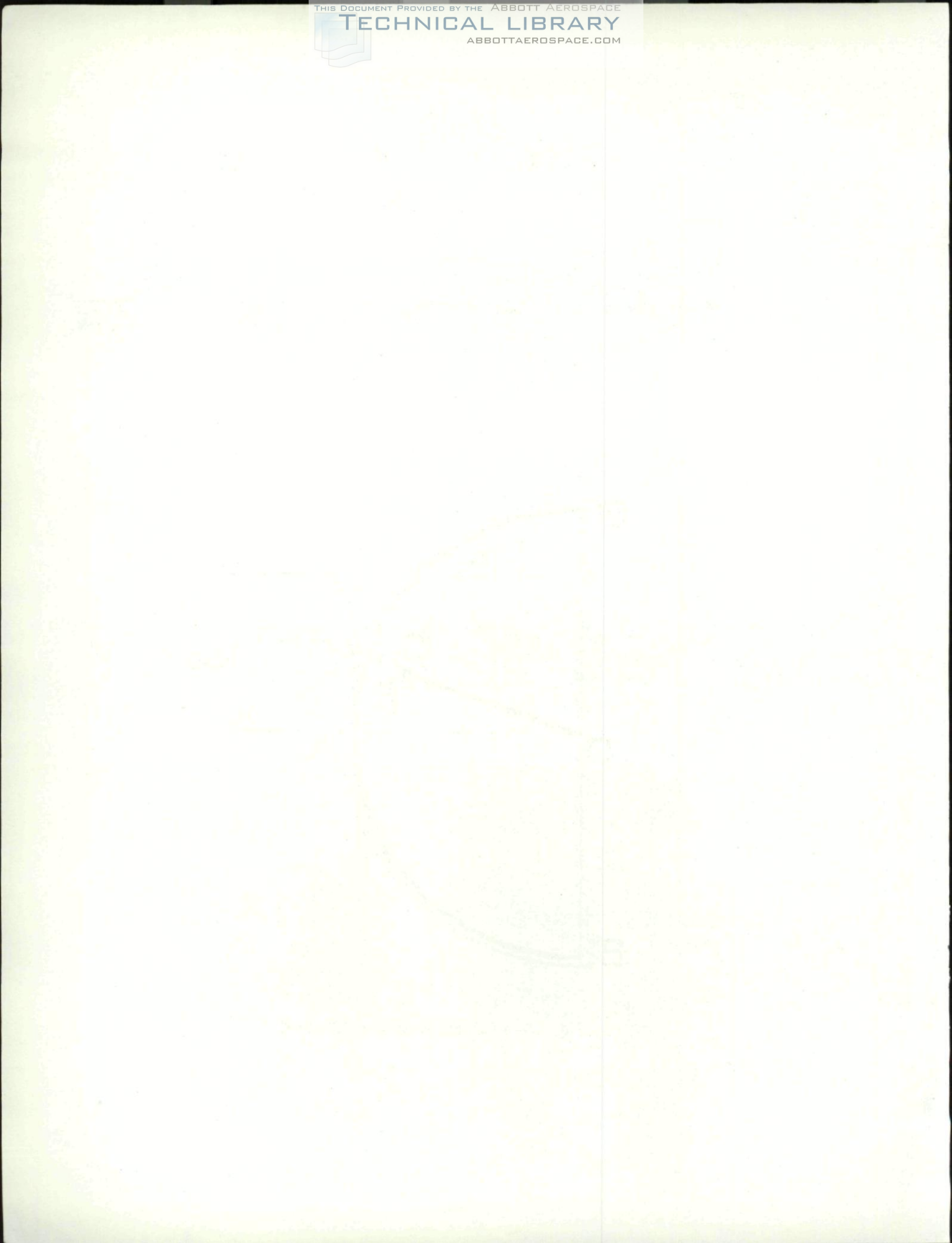


Lifting problem

Fig. XII-4(b)(c). Analog model of delta wing.

Fig. XII-5. Delta wing with dihedral.





## DISTRIBUTION

Copies of AGARD publications may be obtained in the various countries at the addresses given herewith.

BELGIUM	Centre National d'Etudes et de Recherches Aéronautiques 11, rue d'Egmont, Bruxelles, Belgique
CANADA	Director of Scientific Information Service Defence Research Board Department of National Defence "A" Building, Ottawa, Ontario, Canada
DENMARK	Military Research Board Defence Staff Kastellet, Copenhagen Ø, Denmark
FRANCE	ONERA (Direction) 25, avenue de la Division-Leclerc Châtillon-sous-Bagneux, Seine, France
GERMANY	Wissenschaftliche Gessellschaft für Luftfahrt Zentralstelle der Luftfahrtdokumentation München 64, Flughafen, Germany Attention: Dr. Ing. H. J. Rautenberg
GREECE	Greek Nat. Def. Gen. Staff B. MEO Athens, Greece
ICELAND	Iceland Delegation to NATO Palais de Chaillot Paris 16, France
ITALY	Centro Consultivo Studi e Ricerche Ministero Difesa Aeronautica Via Salaria 336, Roma, Italy
LUXEMBOURG	Luxembourg Delegation to NATO Palais de Chaillot Paris 16, France  Major Th. Melchers Chef de la Délégation Militaire du Luxembourg auprès du SHAPE SHAPE - Paris, France

NETHERLANDS

Netherlands Delegation to AGARD  
Kanaalstraat 10  
Delft, Holland

NORWAY

Chief Engineering Division  
Royal Norwegian Air Force  
Deputy Chief of Staff/Materiel  
Myntgaten 2  
Oslo, Norway  
Attention: Lt. Col. S. Heglund

PORTUGAL

Subsecretariado da Estado da Aeronautica  
Av. da Liberdade 252  
Lisbon, Portugal  
Attention: Lt. Col. Jose Pereira do Nascimento

TURKEY

M. M. Vekaleti  
Erkaniharbiyei Umumiye Riyaseti  
Ilmi Istisare Kurulu Mudurlugu  
Ankara, Turkey  
Attention: Colonel Fuat Ulug

UNITED KINGDOM

Ministry of Supply  
T.I.L., Room 009A  
First Avenue House  
High Holborn  
London W.C.1, England

UNITED STATES

National Advisory Committee for Aeronautics  
1512 H Street, N. W.  
Washington 25, D. C., U. S. A.

<p>North Atlantic Treaty Organization Advisory Group for Aeronautical Research and Development THE USE OF RHEOELECTRICAL ANALOGIES IN AERODYNAMICS L. C. Malavard, August 1956 (Wind Tunnel AGARDograph Series)</p> <p>After a review of the principle of the rheoelectric analogy method, the equipment and experimental techniques are described, followed by an examination of the aerodynamic applications.</p>		<p>North Atlantic Treaty Organization Advisory Group for Aeronautical Research and Development THE USE OF RHEOELECTRICAL ANALOGIES IN AERODYNAMICS L. C. Malavard, August 1956 (Wind Tunnel AGARDograph Series)</p> <p>After a review of the principle of the rheoelectric analogy method, the equipment and experimental techniques are described, followed by an examination of the aerodynamic applications.</p>	
<p>North Atlantic Treaty Organization Advisory Group for Aeronautical Research and Development THE USE OF RHEOELECTRICAL ANALOGIES IN AERODYNAMICS L. C. Malavard, August 1956 (Wind Tunnel AGARDograph Series)</p> <p>After a review of the principle of the rheoelectric analogy method, the equipment and experimental techniques are described, followed by an examination of the aerodynamic applications.</p>		<p>North Atlantic Treaty Organization Advisory Group for Aeronautical Research and Development THE USE OF RHEOELECTRICAL ANALOGIES IN AERODYNAMICS L. C. Malavard, August 1956 (Wind Tunnel AGARDograph Series)</p> <p>After a review of the principle of the rheoelectric analogy method, the equipment and experimental techniques are described, followed by an examination of the aerodynamic applications.</p>	





100  
↓

*Handwritten scribble or signature*

